ΓΕΩΠΟΝΙΚΟ ΠΑΝΕΠΙΣΤΗΜΙΟ ΑΘΗΝΩΝ

Τμήμα Επιστήμης Τροφίμων και Διατροφής του Ανθρώπου

Εργαστήριο Μηχανικής Τροφίμων, Επεξεργασίας και Συντήρησης Γεωργικών Προϊόντων

Χρήση διαφορετικών διεργασιών για την παρασκευή γαλακτωμάτων με σκοπό τον μικροεγκλεισμό βιοενεργών συστατικών

Διδακτορική Διατριβή

Παρασκευή Σ. Παξιμαδά

Επιβλέπουσα

Ιωάννα Μαντάλα

Αθήνα, 2017

ΓΕΩΠΟΝΙΚΟ ΠΑΝΕΠΙΣΤΗΜΙΟ ΑΘΗΝΩΝ

Τμήμα Επιστήμης Τροφίμων και Διατροφής του Ανθρώπου

Εργαστήριο Μηχανικής Τροφίμων, Επεξεργασίας και Συντήρησης Γεωργικών Προϊόντων

Χρήση διαφορετικών διεργασιών για την παρασκευή γαλακτωμάτων με σκοπό τον μικροεγκλεισμό βιοενεργών συστατικών

Διδακτορική Διατριβή

Παρασκευή Σ. Παξιμαδά

Επιβλέπουσα

Ιωάννα Μαντάλα

Αθήνα, 2017

AGRICULTURAL UNIVERSITY OF ATHENS

Department of Food Science and Human Nutrition

Laboratory of Food Process Engineering

Designing emulsions and nanostructures for the encapsulation of bioactive compounds

Ph. D. Thesis

Paraskevi S. Paximada

Supervisor:

Ioanna Mandala

Athens, 2017

Χρήση διαφορετικών διεργασιών για την παρασκευή γαλακτωμάτων με σκοπό τον μικροεγκλεισμό βιοενεργών συστατικών

Διδακτορική Διατριβή

Παρασκευή Σ. Παξιμαδά

Επιβλέπουσα

Ιωάννα Μαντάλα

Συμβουλευτική επιτροπή

Στοφόρος Νικόλαος
Ευαγγελίου Βασιλική

Λοιπά μέλη

Scholten Elke
Κουτίνας Απόλοστολος
Μοάτσου Γκόλφω
Φασσέας Κωνσταντίνος

Επιβλέπουσα

Ιωάννα Μαντάλα

Επίκουρη Καθηγήτρια, Εργαστήριο Μηχανικής Τροφίμων, Επεξεργασίας & Συντήρησης Γ. Προϊόντων, Γεωπονικό Πανεπιστήμιο Αθηνών

Συμβουλευτική επιτροπή

Νικόλαος Στοφόρος

Καθηγητής, Εργαστήριο Μηχανικής Τροφίμων, Επεξεργασίας & Συντήρησης Γ. Προϊόντων, Γεωπονικό Πανεπιστήμιο Αθηνών

Βασιλική Ευαγγελίου

Επίκουρη Καθηγήτρια, Εργαστήριο Χημείας & Ανάλυσης Τροφίμων, Γεωπονικό Πανεπιστήμιο Αθηνών

Λοιπά μέλη

Elke Scholten

Associate professor, Physics and Physical Chemistry of Foods, Wageningen University

Κουτίνας Απόστολος

Επίκουρος Καθηγητής, Εργαστήριο Μηχανικής Τροφίμων, Επεξεργασίας & Συντήρησης Γ. Προϊόντων, Γεωπονικό Πανεπιστήμιο Αθηνών

Μοάτσου Γκόλφω

Αναπληρώτρια Καθηγήτρια, Εργαστήριο Γαλακτοκομίας, Γεωπονικό Πανεπιστήμιο Αθηνών

Φασσέας Κωνσταντίνος

Καθηγητής, Εργαστήριο Ηλεκτρονικής Μικροσκοπίας, Γεωπονικό Πανεπιστήμιο Αθηνών

Designing emulsions and nanostructures for the encapsulation of bioactive compounds

Περίληψη

Η παρούσα διατριβή εξετάζει την δυνατότητα παρασκευής γαλακτωμάτων ως φορέων εγκλεισμού της επιγαλλικής γαλοκατεχίνης (EGCG). Το κίνητρο αυτής της εργασίας βασίστηκε σε πρόσφατες έρευνες που υπογραμμίζουν τη στροφή των καταναλωτών σε επιλογές καινοτόμων τροφίμων για τη διατροφή τους. Για το λόγο αυτό χρησιμοποιήθηκαν συστατικά όπως η πρωτεΐνη ορού γάλακτος και η βακτηριακή κυτταρίνη (BC) και επεξεργασίες όπως οι υπέρηχοι και ο ηλεκτροψεκασμός.

Το πρώτο μέρος αυτής της μελέτης αφορούσε την εξέταση της επίδρασης της προεπεξεργασίας με υπερήχους και όξινης υδρόλυσης στις φυσικές ιδιότητες υδατικών διασπορών ενός λιγότερο γνωστού πηκτικού παράγοντα, της βακτηριακής κυτταρίνης. Τα υδατικά αιωρήματα της BC υποβλήθηκαν σε επεξεργασία με υπέρηχους για διάφορες χρονικές περιόδους (0-5 λεπτά). Επίσης οι διασπορές της BC υδρολύθηκαν με διάφορα οξέα και χρόνους επεξεργασίας (0-72 ώρες). Ο χρόνος της επεξεργασίας ήταν κρίσιμος παράγοντας. Στη περίπτωση της επεξεργασίας με υπερήχους, δεν συνιστώνται μεγάλοι χρόνοι εφαρμογής υπερήχων, επειδή αυτό αυξάνει την κρυσταλλικότητα της κυτταρίνης και δημιουργεί συσσωματώματα ινιδίων. Ωστόσο, η παρατεταμένη όξινη υδρόλυση οδήγησε σε αιωρήματα με διαφορετική δομή και ρεολογικές ιδιότητες.

Το δεύτερο μέρος αυτής της εργασίας αποσκοπούσε στην κατανόηση της δυνατότητας της BC να λειτουργήσει ως υποκατάστατο των εμπορικών σταθεροποιητών. Γι αυτό το λόγο, παρασκευάσθηκαν γαλακτώματα σε pH 3,8 σταθεροποιημένα με διαφορετικούς τύπους κυτταρίνης (HPMC, CMC, BC) σε διάφορες τελικές συγκεντρώσεις. Τα γαλακτώματα που περιείχαν BC εμφάνισαν το μεγαλύτερο μέσο μέγεθος λιποσφαιρίων ($d_{3,2}$ = 26 μm) και την υψηλότερη σταθερότητα (SI = 3%), φαινόμενο το οποίο είναι χαρακτηριστικό γαλακτωμάτων σταθεροποιημένων με σωματίδια. Παράλληλα, αξιολογήθηκαν οι ρεολογικές ιδιότητες των γαλακτωμάτων με ξανθάνη, κόμμι χαρουπιού ή BC. Χαμηλότερη συγκέντρωση BC (0,1%) χρειάζεται σε σχέση με τη ξανθάνη (0,7%) ή το κόμμι χαρουπιού (1%) για να ληφθεί η ίδια αρχική τάση. Τα γαλακτώματα που περιείχαν BC ήταν αποτελεσματικότερα στην αύξηση της αρχικής τάσης διάτμησης με πιθανό ενδιαφέρον την αντικατάσταση κοινά χρησιμοποιούμενων πολυσακχαριτών.

Το τρίτο μέρος αυτής της εργασίας αποσκοπούσε στην εύρεση της βέλτιστης μεθόδου ομογενοποίησης. Γαλακτώματα παρασκευάστηκαν χρησιμοποιώντας πρωτεΐνη ορρού γάλακτος (WPI) και BC σε διάφορες συγκεντρώσεις και ομογενοποιήθηκαν είτε με υπερήχους είτε με ομογενοποιητή υψηλής πίεσης. Το χαμηλότερο μέγεθος λιποσφαιρίων βρέθηκε για τα γαλακτώματα που υποβλήθηκαν σε επεξεργασία με υπερήχους (D_{50} = 600 nm). Σε χαμηλότερες συγκεντρώσεις BC,

εκτεταμένη συσσωμάτωση μεταξύ των λιποσφαιρίων οδήγησε σε ασταθή γαλακτώματα. Η υψηλότερη συγκέντρωση της BC είχε ως αποτέλεσμα σταθερά γαλακτώματα, πιθανώς λόγω του σχηματισμού ενός δικτύου BC με αυξημένο ιξώδες, το οποίο απαγόρευσε τη συνάθροιση των λιποσφαιρίων. Αυτά τα αποτελέσματα επιβεβαιώνουν την μεγαλύτερη αποτελεσματικότητα της ομογενοποίησης με υπερήχους σε σύγκριση με την κατεργασία με ομογενοποιητή υψηλής πίεσης για τη λήψη σταθερών γαλακτωμάτων.

Το τέταρτο μέρος της παρούσας εργασίας, στοχεύει στην ενθυλάκωση της EGCG σε διάφορους φορείς. Αρχικά, παρήχθησαν γαλακτώματα που περιέχουν WPI και BC. Δύο διαφορετικές κατεχίνες: υδρόφιλη (H-EGCG) ή λιπόφιλη (L-EGCG) ενσωματώθηκαν στην υδατική ή ελαιώδη φάση των γαλακτωμάτων. Στα γαλακτώματα στα οποία ενσωματώθηκε η L-EGCG στην ελαιώδη φάση, επιτεύχθηκε η μεγαλύτερη απόδοση ενσωμάτωσης, 85 ± 2%, η μικρότερη διάμετρος λιποσφαιρίων (680 ± 10 nm) και ο μικρότερος δείκτης αποσταθεροποίησης (0%).

Ως δεύτερο βήμα, αξιολογήθηκε ο ηλεκτροψεκασμός διαλύματος ως μέθοδος για την ενθυλάκωση της EGCG. Διαλύματα WPI-BC σε διάφορες συγκεντρώσεις μελετήθηκαν για την ικανότητά τους να ηλεκτροψεκάζονται. Η επιφανειακή τάση και η ηλεκτρική αγωγιμότητα βρέθηκαν να αυξάνονται καθώς αυξάνεται η συγκέντρωση BC. Ένας καλός συσχετισμός (0,83) βρέθηκε μεταξύ των τιμών επιφανειακού ιξώδους του διαλύματος και της κατανομής των παραγόμενων νανοσωματιδίων. Τα παραγόμενα νανοσωματίδια ποίκιλλαν σε μέγεθος (120 έως 380 nm) και πολυδιασπορά (PDI = 0,8-3). Η απόδοση ενθυλάκωσης της κατεχίνης έδωσε μέτριες τιμές έως 51%. Επίσης μελετήθηκε η αποδόμηση της EGCG από τα σωματίδια που αποθηκεύτηκαν σε διάφορες συνθήκες. Η EGCG στα σωματίδια ήταν πιο σταθερή όταν αποθηκεύτηκε σε χαμηλή σχετική υγρασία. Τα σωματίδια WPI-BC προστατεύουν την EGCG από την υγρασία, τη θέρμανση και τη διάλυση σε διάφορα pH, οδηγώντας στην πιθανή χρήση τους ως αντικαταστάτη, προκειμένου να αυξηθεί η διάρκεια αποθήκευσης της κατεχίνης όταν ενσωματωθεί σε διάφορα τρόφιμα.

Τέλος, εξετάστηκε η μέθοδος ηλεκτροψεκασμού γαλακτώματος που περιείχε BC και WPI για τον εγκλεισμό της EGCG. Και πάλι, δύο διαφορετικές κατεχίνες, H-EGCG ή L-EGCG, ενθυλακώθηκαν είτε στην υδατική είτε στην ελαιώδη φάση των γαλακτωμάτων. Οι ιδιότητες του γαλακτώματος αναφορικά με τη σταθερότητα, το μέγεθος των λιποσφαιρίων και το ιξώδες μελετήθηκαν σε συνδυασμό με την αξιολόγηση των ιδιοτήτων των παραγόμενων σωματιδίων, δηλαδή της μορφολογίας και του μεγέθους των σωματιδίων, της αποτελεσματικότητας της ενθυλάκωσης της κατεχίνης και της σταθερότητας της EGCG εντός των σωματιδίων υπό διαφορετικές συνθήκες αποθήκευσης: υγρασίας, pH και θερμοκρασίας. Το χαμηλό ιξώδες του γαλακτώματος σε συνδυασμό με το χαμηλό μέγεθος λιποσφαιρίων και την υψηλή σταθερότητα έδωσε σωματίδια με τις μικρότερες

διαμέτρους. Η ομογενοποίηση με υπερήχους σε συνδυασμό με L-EGCG αποδείχθηκε ο πλέον κατάλληλος συνδυασμός, φθάνοντας σε απόδοση ενθυλάκωσης έως 97%. Η χρήση χαμηλής σχετικής υγρασίας (RH) (26-53%) και ουδέτερου ή αλκαλικού pH (6-9) είναι απαραίτητες για την προστασία της EGCG εντός των σωματιδίων. Ο ηλεκτροψεκασμός γαλακτώματος μπορεί να χρησιμοποιηθεί ως μια πολλά υποσχόμενη τεχνολογία για την ενθυλάκωση συστατικών.

Η ενσωμάτωση της EGCG στα συστήματα τροφίμων θα μπορούσε ενδεχομένως να οδηγήσει στην εμπορευματοποίηση προϊόντων με βελτιωμένες ιδιότητες, δηλαδή τρόφιμα που μπορούν να προωθήσουν έναν πιο υγιεινό τρόπο ζωής.

Επιστημονική περιοχή: Μηχανική Τροφίμων

Λέξεις κλειδιά: Γαλάκτωμα; Ενθυλάκωση; Κατεχίνη; Ρεολογία; Βακτηριακή κυτταρίνη; Ηλεκτροψεκασμός

Abstract

This thesis aims to advance the understanding of emulsion production for the encapsulation of epigallocatechin gallate (EGCG). The motivation of this work was based on recent research, highlighting the significant consumer shift to healthier food products with different food structures. Therefore, ingredients such as whey protein and bacterial cellulose were used and processes like ultrasonication and electrospraying were applied

The first part of this study dealt with the investigation of the effect of ultrasonic and acid hydrolysis pre-treatment on the physical properties of aqueous suspensions of a lesser- known thickener- bacterial cellulose (BC) - aqueous suspensions. BC suspensions were treated with ultrasounds under various periods of time (0-5 min) or with various acids and processing times (0-72 h). The time of treatment was critical. Longer ultrasonication times are not recommended, because the crystallinity of cellulose was increased and entangled fibrils were created. However, prolonged acid hydrolysis led to suspensions with different nanostructure and rheological properties.

The second part of this thesis, aimed the understanding of the possibility of BC acting as substitute for commercial thickeners. O/w emulsions (10% wt olive oil) were prepared at pH 3.8 stabilized by different types of cellulose: hydroxyl propyl methylcelluloseHPMC), carboxy methylcellulose (CMC) and BC at varying total concentrations. BC emulsions exhibited the largest droplet size ($d_{3,2}$= 26μm) and the highest stability (SI=3%), which is typical for particle-stabilized emulsions. Rheological properties of emulsions with xanthan gum (XG), locust bean gum (LBG) or BC were assessed; a lower BC concentration (0.1%) than that of XG (0.7%) or LBG (1%) was required to obtain the same yield stress. BC showed a greater shear thinning behavior than XG and LBG. BC was more efficient to increase the zero-shear viscosity, showing that BC has great potential in substituting the commercial thickeners.

The third part of this thesis, aimed at finding the optimal emulsification procedure for emulsions containing BC and whey protein isolate (WPI). Emulsions were prepared using WPI and BC in various concentrations and were homogenized either by ultrasounds or by high pressure homogenizer. The lowest droplet size was found for the emulsions treated by ultrasounds (D_{50} = 600 nm). At lower BC concentrations, extensive aggregation between the oil droplets led to unstable emulsions due to bridging interactions. Higher BC concentrations resulted in stable emulsions, possibly due to the formation of a BC network between the oil droplets, which prohibited coalescence. These results confirm the greater efficiency of the US homogenization as compared to the HPH treatment in obtaining stable emulsions.

The fourth part of this thesis, aimed at encapsulating EGCG into various emulsion carriers. Firstly, emulsions containing WPI and BC were produced. Two different catechins: hydrophilic (H-EGCG) or lipophilized (L-EGCG) were incorporated in the aqueous or the oily phase of the emulsions. At the optimal EGCG concentration the highest encapsulation efficiency of 85 ± 2% yielded with reasonable droplet diameter of 680 ± 10 nm. The EGCG that incorporated in the oil phase was the lipophilized one, L-EGCG. Moreover, the produced emulsions did not present any phase separation.

As a second step, solution electrospraying was evaluated as a method of encapsulating EGCG. WPI-BC solutions at various concentrations were studied for their ability to be electrosprayed. Surface tension and electrical conductivity were found to increase as BC concentration increased, while they remained unaffected in terms of the protein concentration. A good correlation was found between the interfacial rheology values of the solution and the distribution of the produced particles. The produced particles varied in size from 120 to 380 nm and polydispersity from PDI 0.8 to 3. The encapsulation efficiency (EE) of catechin yielded relatively high values up to 51%. The EGCG degradation from the particles stored under various conditions was also studied. EGCG in the particles was more stable when stored at low relative humidity (RH). WPI-BC particles protected EGCG from moisture, heating, and dissolution conditions, leading to the potential use of them as a substitute in order to enhance EGCG shelf life when incorporated within various food products.

Finally, the potential of emulsion electrospraying that contained BC and WPI for the encapsulation of EGCG was tested. Again, two different catechins, H-EGCG or L-EGCG, were encapsulated either in the aqueous or the oily phase of the emulsions in order to compare the antioxidants' stability. Emulsion properties in terms of stability, droplet size, bulk and interfacial viscosity were studied combined with the evaluation of the properties of the produced particles, namely the morphology and size of the particles, the EE and the stability of the EGCG within the particles under different storage conditions: humidity, pH and temperature. Low emulsion viscosity combined with low oil droplet size and high stability yielded particles with the smallest diameters. Ultrasound homogenization combined with L-EGCG proved to be the most adequate combination, reaching EE up to 97%. The use of low RH (26-53%) and neutral or alkaline pH (6-9) are necessary for protecting EGCG in the particles. Emulsion electrospraying can be used as a promising technology for encapsulation in the food industry.

All in all, incorporation of EGCG in food systems, could potentially lead to the commercialization of products with enhanced properties.

Scientific field: Food Engineering

Keywords: Emulsion; Encapsulation; Catechin; Rheology; Bacterial Cellulose; Electrospraying

In loving memory of my parents

Nothing in life is to be feared,

it is only to be understood.
Now is the time to understand more,

so that we may fear less.

- Marie Sklodowska Curie,
Polish-French physicist & chemist, 1867 - 1934

Acknowledgements

The completion of my dissertation and subsequent Ph.D. has been a long journey. I couldn't have finished this journey without the invaluable support of several people.

Firstly, I would like to express my special appreciation and thanks to my supervisor Professor Dr. Ioanna Mandala, as she has been a tremendous mentor for me. I would like to thank her for encouraging my research and for allowing me to grow as a researcher. Her advice on both research as well as on my career have been priceless.

Besides my supervisor, I would like to thank the rest of my thesis committee: Prof. Vasiliki Evangeliou, for her academic support and personal cheering, and Prof. Nikolaos Stoforos, for his insightful comments and encouragement, but also for helping me to widen my research from various perspectives.

I would also like to thank the members of my examination committee, Prof. Constantinos Fasseas, Prof. Apostolos Koutinas, Prof. Golfo Moatsou and Prof. Elke Scholten for their brilliant comments and suggestions.

I would like to express my gratitude to both Prof. Elke Scholten for accepting me in the laboratory of Food Physics in Wageningen University (the Netherlands) and Dr. Jose Maria Lagaron for hosting me in the Novel Materials & Nanotechnology Group in IATA-CSIS (Spain). Their support throughout the experiments conducted there was of utmost importance for the completion of my experiments.

I am also grateful to the following university staff: Manolis Anagnostaras and Maria Georgiadou for their unfailing support and assistance throughout the years. I thank my fellow labmates: Olga Kaltsa, Elli Panagopoulou, Stella Protonotariou, and Kleopatra Tsatsaragkou for the stimulating discussions and for all the fun we have had in the last four years.

Of course no acknowledgments would be complete without giving thanks to my parents for teaching me about hard work and self-respect, about persistence and about how to be independent. Many thanks to my sister and family who helped me get through the toughest part of my life in the last six months of my PhD.

I am also grateful to my friends who have always been there: Fivi, Olga, and Maria, who are always by my side. Thanks for believing in me, when I couldn't! Last, but certainly not least, I must acknowledge with deep thanks my partner, Nikos. I know I gave you a hard time, especially during the writing of the thesis.

Table of Contents

List of figures

List of tables

List of abbreviations

BC	Bacterial Cellulose
BCN	Bacterial Cellulose Nanofibers
CD	Conjugated Dienes
C_{final}	Concentration of free EGCG content in the aqueous phase.
CMC	Carboxymethylcellulose
C_{total}	Concentration of EGCG added to the emulsions
d_{50}	Mean diameter
EGCG	Epigallocatechin gallate
EE	Encapsulation efficiency
E_v	Energy density transferred from the homogenization valve to the sample
G'	Storage modulus
G''	Loss modulus
H-EGCG	Hydrophilic epigallocatechin gallate
HP	High Pressure Homogenizer
HPMC	Hydroxy propyl methylcellulose
k_1, k_2	Kinetic constants
L-EGCG	Hydrophobic epigallocatechin gallate
LBG	Locust bean gum
m	Fickian diffusional exponent
M_o	Total mass of the loaded EGCG in the particles
M_t	Mass of EGCG released at time t,
Mw	molecular weight
P-AnV	p-anisidine value
PDI	Polydispersity index
SEM	Scanning electron microscope
US	Ultrasounds
UT	Ultra-turrax
WPI	Whey protein isolate

W_c	Dry content of cellulose
W_r	Mass of the removed water during drying
XG	Xanthan gum

t	elapsed time
γ	interfacial tension
$\dot{\gamma}$	shear rate
ΔP	the pressure difference operating at the nozzles

Samples coding in Chapter 4

Sample name	Acid	Hydrolysis temperature (^{o} C)	Hydrolysis time (h)
H400	HCl	40	0
H402	HCl	40	2
H4024	HCl	40	24
H4048	HCl	40	48
H4072	HCl	40	72
S400	H_2SO_4	40	0
S402	H_2SO_4	40	2
S4024	H_2SO_4	40	24
S4048	H_2SO_4	40	48
S4072	H_2SO_4	40	72
H600	HCl	60	0
H602	HCl	60	2
H6024	HCl	60	24
H6048	HCl	60	48
H6072	HCl	60	72
S600	H_2SO_4	60	0
S602	H_2SO_4	60	2

S6024	H_2SO_4	60	24
S6048	H_2SO_4	60	48
S6072	H_2SO_4	60	72

Samples coding in Chapter 5

Emulsions	gum	% wt. WPI
HPMCH	Hydroxy-propyl methylcellulose high viscosity	-
HPMCL	Hydroxy-propyl methylcellulose low viscosity	-
CMC	Carboxy-methylcellulose	-
BC	Bacterial cellulose	-
WPI-BC	Bacterial cellulose	2
WPI-XG	Xanthan gum	2
WPI-LBG	Locust bean gum	2

Samples coding in Chapter 6

% wt WPI	%wt BC	Oil phase (%)
2	0, 0.5, 0.7, 1	10
3	0, 0.5, 0.7, 1	10
4	0, 0.5, 0.7, 1	10
5	0, 0.5, 0.7, 1	10

Samples coding in Chapter 7

Emulsions	Type of EGCG	Addition phase
BLANK	-	-
HW	Hydrophilic	Aqueous
LW	Lipophilized	Aqueous
HO	Hydrophilic	Oil
LO	Lipophilized	Oil

Samples coding in Chapter 8

% wt WPI	10, 20, 30
%wt BC	0, 1, 2, 4, 8,16

Samples coding in Chapter 9

Emulsions	Homogenization method	Type of EGCG	Addition phase
BLUT	High shear homogenizer	-	-
BLUS	Ultrasounds	-	-
UTHW	High shear homogenizer	Hydrophilic	Aqueous
USHW	Ultrasounds	Hydrophilic	Aqueous
UTLW	High shear homogenizer	Lipophilized	Aqueous
USLW	Ultrasounds	Lipophilized	Aqueous
UTHO	High shear homogenizer	Hydrophilic	Oil
USHO	Ultrasounds	Hydrophilic	Oil
UTLO	High shear homogenizer	Lipophilized	Oil
USLO	Ultrasounds	Lipophilized	Oil

Chapter 1. Introduction

1.1. Background

Mayonnaise, margarines, dressings, sauces, creams, drinks…Food emulsions are a big part of our life, contributing to our body with calories, nutrients and other beneficial substances. Emulsions are mixture of two immiscible liquids (typically oil and water) with one of the liquid being dispersed as small droplets in the other. When placed in a food matrix, emulsions tend to interact with other ingredients. Hence, emulsion stabilization is a main challenge for food industry.

Emulsifiers, thickeners and surfactants are some of the ingredients that are currently used to stabilize a food emulsion. Approximately 500000 tons of emulsifiers are sold worldwide every year. Within the last decade there has been a significant shift of the scientific and industrial interest towards the development and use of more natural emulsifiers that are being produced using by-products from the industries.

To this regard, new polymers are particularly interesting to be used as thickeners. Bacterial cellulose (BC) is a polysaccharide produced from *Komagataeibacter sucrofermentans* in the form of pellicles. BC has brought increased attention and has been used in various areas such as biomedicine, cosmetics and paper industry. BC has good water binding capacity and ability to form a network through fiber-like structures. In the food industry, the use of BC is still limited, but it has been used to texturize a dessert from the Philippines (Nata de coco). To make this dessert, thick gel sheets are fermented with coconut water, cut into cubes and immersed in sugar syrup. Hence, BC has great potential as a food ingredient, changing the rheological profile of a food, as it serves as thickening, stabilizing or gelling agent. Recently, BC has been shown to act as a stabilizer in emulsions. However, BC as a thickener for the continuous phase has not been studied extensively and the effect on the rheological behavior of emulsions is not well known.

On the other hand, consumers nowadays are more and more concerned about well-being and healthy food options. To meet this, more and more products are produced, enriched with vitamins, antioxidants ect.

Tea and tea products are known to contain substantial amounts of bioactive flavonoids, particularly catechins. The main substance of tea catechin is epigallocatechin-3-gallate (EGCG). EGCG is considered a powerful antioxidant, and has been proved by *in vitro* assays to be effective in radical scavenging, reduction and metal chelation. Thus, adding EGCG to food products could potentially benefit the consumers, as their awareness concerning healthier lifestyles is certainly

growing. However, one of the major pitfalls of EGCG is its chemical instability and its low lipophilicity which makes it difficult to be incorporated in lipid-based foods, such as fats and oils. Considering these drawbacks, structural modification of EGCG can increase its lipophilicity and widen its application in lipophilic media.

A plausible approach to overcome the limitations of EGCG is its encapsulation. The protective means of coating by encapsulation processes such as spray drying, liposome entrapment and emulsification can make them into the stable deliverable form. The encapsulation of catechins in O/W emulsion can be the easiest method as compared to others. The encapsulation of bioactive compounds in emulsion delivery systems brings several advantages for the compound such as the stabilization in aqueous systems (such as foodstuffs) of lipophilic bioactive compounds with scarce solubility in water; the protection of bioactive compounds against degradation reactions with food constituents and minimization of the alteration of the food matrix; the control of the release and the enhancement of cell uptake and bioavailability.

A wide variety of processes have been proposed to prepare particles as carriers for bioactives, including spray drying, emulsion formation, supercritical fluid or complex formation(Liu et al., 2016; Wei et al., 2015)(Liu et al., 2016; Wei et al., 2015). However, these techniques require heating, organic agents or expensive equipment, damaging encapsulated compounds due to the heating.

To this regard, electrohydrodynamic (EHD) processing, and specifically electrospraying is beneficial for producing particles entrapping the active ingredients. During electrospraying, a high-voltage electro-static field is used to charge the surface of a polymer solution droplet formed at the end of a capillary tube. Electrospraying presents advantages over conventional spraying systems as it does not require heat and produces particles with small diameter.

Lipophilized EGCG (L-EGCG) is known to exhibit low water solubility, thus, electrospraying and subsequent encapsulation of this compound in water-based solutions is not possible. To this regard, emulsion electrospraying can be used to encapsulate immiscible compounds. During emulsion electrospraying, hydrophobic ingredients could be encapsulated in low cost biopolymers. Several studies have shown the potential use of emulsion electrospraying. However, the encapsulating materials used are, in most cases, not edible.

1.2. Thesis objectives

The overall aim of this thesis was to develop o/w emulsions for the encapsulation of EGCG for further use in processed foods which are nutritionally balanced. The aims and objectives set at the beginning of this investigation can be summarized as follows:

- Design a processing method as a pre-treatment in order to improve the physical properties of BC fibrils in order to improve BC applicability
- Evaluate the homogenizing method that results in the production of o/w emulsions with enhanced physical properties
- Study the role of BC as a stabilizer and as a thickener in o/w emulsions and the potential substitution of commercial thickeners with BC
- Encapsulation of catechins in i) emulsions, ii) nanoparticles derived from biopolymer solution, and iii) nanoparticles derived from emulsion

1.3. Thesis structure

This manuscript is composed of ten chapters: an introduction, a literature review, an experiment chapter, four chapters presenting the experimental findings of the present work followed by the main conclusions and the future perspectives.

- Chapter 1 is an introduction underlining the interest and objectives of this study
- Chapter 2 is a literature review defines the scientific knowledge related to the subjects mentioned in this thesis
- Chapter 3 includes the materials and the experimental design of the dissertation
- Chapter 4 is the first result chapter, regarding the properties of aqueous bacterial cellulose suspensions
- Chapter 5 is the second result chapter, in which the influence of various thickeners on the properties of emulsions, is investigated
- Chapter 6 is the third result chapter that emphasizes the effect of the homogenization method on the properties of emulsions containing WPI and BC
- Chapter 7 is the fourth result chapter, in which EGCG is encapsulated in the emulsions
- Chapter 8 is the fifth result chapter in which EGCG is encapsulated in particles through solution electrospraying
- Chapter 9 is the fifth result chapter in which EGCG is encapsulated in particles through emulsion electrospraying

- Chapter 10 summarizes the conclusions made throughout this study and suggests the future work

1.4. Publications and conferences

Articles in journals

1. Paximada P., Echegoyen Y., Koutinas A. A., Mandala I. and Lagaron J.M. (2017) Encapsulation of hydrophilic and lipophilized catechin into nanoparticles through emulsion electrospraying, *Food Hydrocolloids*, 64, 123-132.

2.Paximada P., Dimitrakopoulou E.A., Tsouko E., Koutinas A. A. and Mandala I. (2016) Structural modification of bacterial cellulose fibrils under ultrasonic irradiation, *Carbohydrate Polymers*, 150, 5-12.

3. Paximada P., Koutinas A. A, Scholten E. and Mandala I. (2016) Effect of Bacterial Cellulose addition on physical properties of WPI emulsions. Comparison with common thickeners, *Food Hydrocolloids*, 54, 245-254.

4. Paximada P., Tsouko E., Kopsahelis N., Koutinas A. A. and Mandala I. (2016). Bacterial Cellulose as stabilizer of o/w emulsions, *Food Hydrocolloids*, 53, 225-232.

5. Kaltsa O., Paximada P., Scholten E. and Mandala I (2014).Physical characteristics of submicron emulsions upon partial displacement of WPI by small molecular weight surfactant and pectin addition, *Food Research International*, 68, 401-408.

Chapters in books

1. Jafari S.M., Paximada P., Mandala I., Assadpour E., Mehrnia M.A. (2017). Encapsulation by nano-emulsions, in Nanoencapsulation Technologies for the Food and Nutraceutical Industries, Chapter 2. Jafari S.M. (Eds), Elsevier, Netherlands (In press).

2. Tsatsaragkou, K., Paximada, P., Protonotariou, S. Mandala, I. (2016). Functional Foods, in: Handbook of Food Processing: Food Safety, Quality, and Manufacturing Processes, Chapter 17. p 585-606 , T. Varzakas and C. Tzia, (Eds), CRC Press, Taylor & Francis Group, Boca Raton, FL, USA.

Articles in conferences proceedings

1. Paximada P., Sanz Y., Lagaron J. and Mandala I. Emulsion electrospraying for the encapsulation of catechins. Nanotech, Valencia, 26-27/9/2016 (talk).

2. Paximada P., Lagaron J. and Mandala I. Catechin-containing nanoparticles produced through emulsion electrospraying. Internatonal conference on bioencapsulation, Lisbon, 21-23/9/2016 (talk).

3. Paximada P., Papadopoulou E., Evageliou V., Koutinas A. A, and Mandala I. Antioxidant activity of natural or lipophilic epigallocatechin gallate (EGCG) in emulsions containing Bacterial Cellulose. 29th EFFoST International Conference, Athens-Greece, 10-12/11/2015(poster).

4. Paximada P., Koutinas A. A, Scholten E. and Mandala I. Bacterial Cellulose as an alternative thickener for o/w emulsions. Comparison with common thickeners. The 7th International Symposium on Food Rheology and Structure - ISFRS 2015, Zurich-Switzerland, 7-11/6/2015 (talk).

5. Paximada P., Dimitrakopoulou E.A., Protonotariou S., Fasseas C., Koutinas A. A, and Mandala I. Ultrasound homogenisation to alter the physical properties of bacterial cellulose aqueous suspensions.The 7th International Symposium on Food Rheology and Structure - ISFRS 2015, Zurich-Switzerland, 7-11/6/2015 (poster)

6. Paximada P., Papadopoulou E., Tsatsaragkou K., Panagopoulou E., Evageliou V., Fasseas C., Koutinas A. A, and Mandala I. Incorporation of Epigallocatechin-3-gallate (EGCG) in emulsions containing Bacterial Cellulose. The 7th International Symposium on Food Rheology and Structure - ISFRS 2015, Zurich-Switzerland, 7-11/6/2015 (poster).

7. Paximada P., Dimitrakopoulou E.A. and Mandala I. Acid hydrolysis to improve the production of Bacterial Cellulose nanocrystals , NanoTech Paris, Paris, 15-18/6/2015 (poster)

8. Paximada P., Kopsahelis N., Koutinas A. A. and Mandala I. Stabilising properties of bacterial cellulose, 3rd International ISEKI_Food Conference, Athens, 21-23/5/2014 (poster)

9. Paximada P., Kopsahelis N., Koutinas A. A, Scholten E. and Mandala I. Bacterial Cellulose as emulsifier for o/w emulsions prepared with different techniques, 1st Congress on Food Structure Design. Porto-Portugal. 15-17/10/2014 (poster)

10. Paximada P. and Mandala I. Stability and rheological properties of o/w emulsions containing bacterial cellulose ,12th International Hydrocolloids Conference, Taipei, 5-9/5/2014 (poster)

11. Paximada P. and Mandala I. Effect of HPMC on the encapsulation of curcumin in o/w emulsions prepared with ultrasounds. COST Meeting Action FA 1001, Bucurest, Romania, 2/2014 (poster)

Chapter 2. Literature Review

2.1. Bioactives in food products

In recent years, the food industry requires the addition of bioactive compounds in products. Bioactive compounds are used to control flavor, color, texture or preservation properties.

Food bioactive compounds are natural components that have biological activity and in some instances provide nutritional value (Saldaña et al., 2015). It is found that they play a major role in public health and safety due to potential roles in human ageing and in the reduction of several disease risks. These foods are frequently referred as functional, when they comprise nutritional components required for human's health, or nutraceuticals, when the aim is to treat or prevent a disease (Kalra, 2003), with various reported bioactive functions (e.g., antioxidants, antimicrobials, immunomodulators, hypocholesterolemic, etc.), many times due to the incorporation of functional enzymes, probiotics, prebiotics, fibers, phytosterols, proteins, etc. (Aryee and Boye, 2014). Table 2.1 summarizes the features of the most commonly used bioactives in foods.

Table 2. 1 Features of common bioactives

Bioactive	Source	Example	Limitations	Functionality	References
Phenolics	Tea, grape, berries &rosehip	Anthocyanins, flavonols, flavones	Color instability due to temperature, light, presence of oxygen and metal ions Limited stability	Antioxidant, anti-inflammatory, antiviral, antibacterial, decrease the risk of cancer and heart disease	(Arts and Hollman, 2005)
Carotenoids	Fruits, carrot, rosehip & tomato	β-carotene, lutein	Unstable	Reduces risk of cataract and prostate cancer	(Edge et al., 1997)
Tocols & vitamins	Almond, hazelnut, rice bran & wheat germ	Tocopherols (vitamin E)		Reduces risks of certain types of cancer	(Lu et al., 2015)
Sterols	Walnut, hazelnut	Sitosterol, campesterol	Low solubility	Reduces risk of coronary disease	(Genser et al., 2012)

However, the Panel on Dietetic Products, Nutrition and Allergies (NDA) alongr with the European Food Safety Authority (EFSA) have been published a guidance on the specific requirements for health claims related to antioxidants (Efsa Panel on Dietetic Products and Allergies, 2011). Specifically, they postulated that the tested foods do not have the capability to scavenge free radicals in the human body. What is more, the antioxidants of the tested foods could not be related to the human "healthy ageing" (Regulation EC No 1924/2006). Hence, it is of high importance for someone to be accurate when making a health claim about a bioactive.

The food industry has augmented bioactive compounds identification in foods due to increased interest by consumers for healthier products, for example, polyphenols in white wine (Teixeira et al., 2014), caffeine in coffee (Panusa et al., 2013), and glucoraphanin, which is present in broccoli (Dai and Mumper, 2010).

Bioactive compounds may be related to different properties and health benefits, such as antioxidant compounds (Zhang and Mutilangi, 2011) which can be used as foodstuffs and nutritional supplements, fermented foods which are able to retain the original nutritional ingredients and incorporate some active ingredients that contribute to consumers' health (Parvez et al., 2006), foods that incorporate plants powder (e.g., *Cruciferae*) for food supplements (Dai and Mumper, 2010), and the incorporation of glycolysis inhibitor for preventing and reduce obesity as food sweetener (Kim et al., 2012).

2.1.1 Catechins

In the last few decades, increasing interest has been given to natural bioactives, including flavonoids found in many fruits and vegetables, red wine and tea, for their protective effects against the destruction of organic oxidants (Frankel and German, 2006).

Tea (*Camelia sinensis L.*) serves an interesting source of polyphenol antioxidants, especially catechins. Green tea catechins' concertation is higher than black and oolong tea due to the lack of fermentation during the production of green tea (Toschi et al., 2000). It is known that the catechins are flavonols, which belongs to the class of polyphenols. The most significant tea catechins include: (-) epigallocatechin gallate (EGCG), (-) epicathechin gallate(ECG), (-)epigallocatechin (EGC), (-)epicatechin (EC). It can be seen that catechins consist of two aromatic rings and a number of hydroxyl groups. According to the hydroxyl groups, catechins can be classified into two groups: free (C, GC, EC, EGC) and esterified catechins (EGCG, ECG, GCG, CG). They are colorless, water soluble, and they have a major contribution on the flavor and taste of tea.

Surprisingly, 50-80% of catechins in green tea constitute of EGCG (Khan and Mukhtar, 2007). Table 2.2 depicts some of the physical properties of EGCG.

Table 2. 2 Physical properties of EGCG

Physical properties	*Value*	*Reference*
Appearance	White powder	(Karaosmanoglu and Kilmartin, 2015)
Taste	Bitter & sour	
Molecular weight	458	
Max absorbance	273 nm	
Melting point	224^{o} C	(Gadkari and Balaraman, 2015a)
Solubility	Time/temperature/solvent dependent	
Water/ethanol	soluble	
Chloroform	insoluble	

Biological potential of catechins

Scientific studies to encourage the potential health benefits of green tea consumption begin to appear. Those benefits include improving blood flow, preventing cardiovascular disease, eliminating various toxins and improving resistance to various diseases. These might be due to EGCG which has anti-oxidative, anti-carcinogenic, anti-microbial, anti-viral, anti-inflammatory and anti-diabetic properties (Khan and Mukhtar, 2007; Lakenbrink et al., 2000). Specifically, a recent study by Miura et al. (2000) indicated a prolongation of the lag time of the LDL oxidation in humans who had consumed 300 mg green tea polyphenol extract twice daily for 1 week compared to the ones having a regular diet. This study suggests that daily consumption of 7-8 cups (100 mL each cup) of green tea may have positive effects on the resistance of LDL to oxidation, leading to reduction of the risk of cardiovascular diseases. Kuriyama (2008) showed that habitual tea consumption had a significant risk reduction in CVD, including stroke.

What is more, Nagao et al. (2007) demonstrated that the consumption of green tea high in catechin content over 12 weeks produced significant body weight loss and a reduction in anthropometric parameters, systolic blood pressure and LDL cholesterol. However, another study showed that the daily consumption of 1200 mg of green tea extract over 12 weeks in otherwise healthy obese women produced a non-significant weight loss of just 0.15 kg (Hsu et al., 2008). A large study demonstrated a decreased risk for the development of gastric cancer among women, not men, drinking more than 5 cups daily (Sasazuki et al., 2004). Hoshiyama et al. (2004) showed that there was no risk reduction for the development of stomach cancer in a case-control study involving 157 cases. There was a trend

towards reduced risk of oral cancers in women, not men, in a cohort in Japan (Ide et al., 2007). Furthermore, in a cross-sectional study, Muraki et al., (2007) reported that at an osteoporosis outpatient clinic, patients with the habit of green tea drinking had significantly higher bone mineral density at the lumbar spine than those without the habit, after adjusting for age, body mass index, and other variables related to lifestyle. Also, results from the Mediterranean Osteoporosis Study showed that drinking up to 3 cups of tea per day was associated with a 30% reduction in the risk of hip fractures in both women (Johnell et al., 1995) and men (Kanis et al., 1999) older than 50 years.

Tea catechins are known to have an inflammatory effect on animal organs. Specifically, Pae et al. (2012) when fed rats with 1% EGCG, they produced more pro-inflammatory cytokines tumor necrosis factor-α and macrophages. Spleens from the mice fed 1% EGCG diet also had higher proportions of regulatory T cells and natural killer cells compared to those from mice fed the regular diets. These results suggest that high intake of EGCG may induce a pro-inflammatory response, and this change may be associated with a disturbed homeostasis of immune cells involving changes in both function and number of specific immune cell populations. In addition, EGCG has various pharmaceutical activities such as antihypertensive and hypolipidemic (Chan et al., 1999).

Interactions with proteins

Proteins constitute a fundamental food ingredient, found mostly in milk, meats, eggs, legumes and cereals. In foodstuffs, there are interactions between the phenolic compounds and proteins during production and storage of foods. Interactions between catechins and proteins could affect the color, odor and taste of food, resulting in desirable or undesirable results. Proteins are known to form complexes with polyphenols leading to changes in the structural, functional and nutritional properties of both ingredients (Kanakis et al., 2011; Zorilla et al., 2011). The phenolic group of EGCG is an admirable hydrogen donor leading to the formation of hydrogen bonds between itself and the carboxyl group of the proteins. This attraction could be maximized when the phenols are small enough to penetrate the inter-fibrillar zone of proteins, while they are large enough to crosslink peptide chains at various points (Mulaudzi et al., 2012).

Charlton et al. (2002) indicated that a sufficient coating of the surfaces of proteins with polyphenol molecules is needed in order for the protein molecules to fully aggregate, leading to the precipitation of polyphenol-protein complexes. When the proteins are present at low concentration, precipitation is caused due to the formation of a hydrophobic layer of polyphenols in the protein surface. On the other hand, at higher concentrations of proteins, precipitation is caused due to the combination of the complexation of phenols in the surface of the protein and the crosslinking between the various protein molecules with the polyphenols.

Interactions between proteins and polyphenols depend on the size, shape and charge of the protein molecules.

The mentioned interactions between proteins and catechins could alter the physicochemical and nutritional properties of proteins, such as thermal stability, solubility and digestibility (Kroll et al., 2003; Labuckas et al., 2008). The interactions between proteins and polyphenols could be both reversible and irreversible. In reversible interactions, usually non-covalent forces such as hydrogen bonding, hydrophobic bonding and van der Waals forces are involved Ozdal et al., (2013); Richard et al., (2006); Siebert, (2006),whereas in irreversible interactions, covalent bonds are formed between the polyphenols and proteins (Haslam, 1996). Recent studies dealing with the addition of EGCG in protein solutions have shown that EGCG was reacting with the proteins and that the protein-bound catechin had antioxidant properties (Almajano et al., 2007b).

There are many parameters that affect protein–phenolic interactions such as temperature, pH, types of proteins, protein concentration, types and structures of phenolic compounds, salt concentration, and addition of certain reagents (Stern et al., 1996). Hence, someone should be very careful when making a food product with proteins and polyphenols.

Catechins in food systems

Green tea catechins act as antioxidants in food delaying free radical accumulation and hence increasing oxidative stability (Ananingsih et al., 2013). Table 2.3 summarizes the main applications of catechins in foods.

Table 2. 3 Green tea catechins in food systems/products

Food systems	Comments	Limitations	References
O/w emulsion	The highest antioxidant activity found at high EGCG concentrations	Low pH promotes pro-oxidant activity	(Zhou and Elias, 2013)
O/w emulsion	Antioxidant activity when adding EGCG	Polarity determines the efficiency of antioxidants	(Di Mattia et al., 2009)
Bread	Higher EGCG stability in the crumb	Decrease of EGCG during baking	(Wang et al., 2008a)
Cake	Enhanced antioxidant activity	High substitution values of flour with tea affect sensory properties	(Lu et al., 2010)
Pork patty	Reduced lipid oxidation	Effect on the sensory properties	(Jo et al., 2003)
Cheese	Enhanced antioxidant activity	Effect on the formation of rennet-based casein curd	(Han et al., 2011)
Dry apple	Enhanced antioxidant activity	Slight effect on the color	(Lavelli et al., 2010)

The major role of tea catechins in lipids or emulsions is to hinder lipid oxidation, prolong the shelf life of the product or to stabilize the emulsions. Nonetheless, it is known that the antioxidant activity of tea catechins is related to the lipid/emulsion system, temperature, pH etc. Studies observed that tea catechins act as pro-oxidants in solutions at low catechin concentration, while they found to act as antioxidants at higher catechin concentration (Almajano et al., 2007a). Other studies dealing with the incorporation of EGCG in o/w emulsions indicated that EGCG was observed to exhibit pro-oxidant activity in low pH (2-4) and at low catechin concentration (Zhou and Elias, 2013). What is more, Di Mattia et al., (2009) found that catechin showed

an interfacial localization which was reflected in the enhancement of primary oxidation and in the inhibition of secondary oxidation.

Fortification of bakery products with catechins has been established to augment their potential health benefit. (Wang et al., 2008a) when adding catechins into bread, observed that, during the baking process, EGCG decreased while its epimer increased. They also indicated that the catechin stability in the crumb was higher than the crust.

Lipophilized EGCG

While EGCG is water soluble, it is slightly soluble in lipophilic media (Xu et al., 2004). The low lipophilicity of EGCG jeopardizes its application in lipophilic media, such as oils, fats, emulsions and lipid-based foods. Studies have shown that the low lipophilicity is the main factor affecting EGCG's low cellular adsorption *in-vivo* (Zhong and Shahidi, 2012). Considering these drawbacks, structural modification of EGCG can serve as a solution to increase its lipophilicity and to widen its application in lipophilic media.

EGCG can be esterified with the aid of long-chain saturated fatty acids (e.g. stearoyl chloride). At the end of this procedure, derivatives with enhanced lipophilicity could be collected. (Zhong and Shahidi, 2012) have shown that lipophilized EGCG derivatives displayed a promising antioxidant potential in food model systems, such as bulk oi, emulsion and muscle food systems. What is more, the lipophilized derivatives exhibited higher antioxidant activities compared to the natural EGCG when placed on biological model systems such as LDL-cholesterol, DNA and liposomes.

2.2. Encapsulation

In recent years, consumers have more and more attention for functional foods. The development of new functional foods requires technologies for incorporating the bioactive compounds, without affecting their functionality and bioavailability. A plausible strategy to defeat the susceptibility of these bioactive compounds during processing or storage is to encapsulate them.

Encapsulation is a process that encloses one compound within another compound with ultimate goal the production of structured matrices with diameters of a few nm to a few mm (Chellaram et al., 2014). The encapsulated compound may be named core material, active agent or internal phase, while the encapsulating compound may be named coating, shell, wall material, carrier material or external phase.

When the delivery system has spherical shape could be called particle. Depending on their diameter size, particles could be classified into nanoparticles (diameter <0.2 μm) and microparticles (diameter range from 0.2 to 5000 μm) (Ray et al., 2016). Depending on their shape, particles could be classified into capsules (reservoir type) and spheres (matrix type) Fig. 2.1. The reservoir type is composed of a bioactive compound surrounded by a wall material. This type may also be named capsule, single-core or core-shell type. When pressure is applied to the reservoir type of particles, it may lead to their breakage and, ultimately, to the release of bioactive compounds. On the other side, in the matrix type, the bioactive compound is significantly more dispersed over the wall material, leading to the formation of very small droplets and to a more homogenously distributed bioactive.

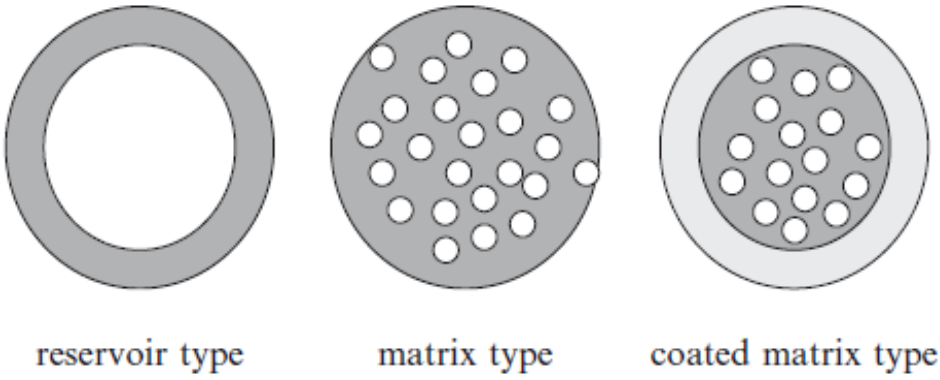

Fig. 2. 1 Reservoir type (left), matrix type (middle), and coated matrix type (right) encapsulates (Fang and Bhandari, 2010)

The encapsulation techniques offer various advantages in the food industry such as improved bioavailability and stability, controlled release, enhanced sensory properties, protection against oxidation, ease of handing, and retention of sensible compounds (Neethirajan and Jayas, 2011).

Encapsulation techniques

The selection of the most suitable encapsulation method depends not only on the physicochemical properties of the bioactive compound and the wall material but also on the final application. Depending on the encapsulation strategy, the current encapsulation methods in the food industry could be classified as top-down or bottom-up (Jia et al., 2016).

Specifically, in the top-down approach, the large structures (bulk oils or solids) break down into smaller particles by external mechanical disruptive forces, such as shear and compression. In this category, extrusion and emulsion production falls. In order to make these processes plausible, sophisticated equipment is required, which could increase the running and maintenance costs. The development of structured particles is a challenge with these techniques (Joye and McClements, 2014).

On the other hand, in the bottom-up approach, small particles are associated into larger ones by self-assembly of the small particles. Mixing the wall and core material in a solution may lead to the formation of particles. Normally, further treatments are required such as alteration of the pH, concentration, ionic strength, and temperature (Tavares et al., 2014). In this category spray drying, electrospinning, coacervation, and anti-solvent precipitation fall. This approach requires less energy and the characteristics of the final particles (size and morphology) can be more efficiently controlled than the top-down approach.

The encapsulation methods that are currently used in the food processing and industry are being shown in Table 2.4.

Table 2. 4 Overview of the commonly used encapsulation techniques

Method	Advantages	Disadvantages	Load (%)	Particle size (μm)	References
Emulsification	Suitable for both hydrophilic & lipophilic compounds	Sophisticated equipment required	1-100	0.2-5000	(Joye and McClements, 2014)
Spray drying	Simple, quick, low cost	Low encapsulation yield, not suitable for heat-sensitive compounds	5-50	10-400	(Ray et al., 2016)
Electrospinning/ electrospraying	Long shelf life, simple, low cost	Difficult scale-up	70-100	0.1-1000	(Gouin, 2004)
Extrusion	Mild process, suitable for both hydrophilic & lipophilic compounds	Suitable for limited number of wall material	70-90	150-8000	(Gouin, 2004)
Coacervation	High encapsulation efficiency	High cost, process sensitive to pH	40-90	10-800	(Augustin and Hemar, 2009)
Freeze-drying	High encapsulation efficiency	High cost	various	20-5000	(Fang and Bhandari, 2010)
Liposome entrapment	Targeted delivery	Difficult scale-up	5-50	10-10000	(Desai and Jin Park, 2005)
Fluidized-bed coating	High batch size, simple	Suitable for limited number of wall material	5-50	5-5000	(Ronsse et al., 2009)

The most widely used encapsulation techniques are summarized below.

1. Spray drying

Spray-drying is widely used in large-scale production of encapsulated compounds, such as antibiotics, medical ingredients, additives, vitamins and polyphenols. The process initiates with the homogenization of the bioactive compound to be encapsulated with the wall material at the selected ratio. The mixture is then fed into a spray-dryer and atomized with a nozzle or spinning wheel. Water is

evaporated by the hot air contacting the atomized material. The resulting particles are then transported to a cyclone separator for recovery (Ray et al., 2016).

The main factors in spray-drying that must be optimized are feed temperature, air inlet and air outlet temperatures. The best spray-drying conditions are a compromise between high air temperature, high solid concentration of the solution, and easy drying without expansion and cracks of final particles (Gharsallaoui et al., 2007).

One limitation of the spray-drying technology is the limited number of wall materials available. Since almost all spray-drying processes in the food industry are carried out from aqueous feed formulations, the wall material must be soluble in water at an acceptable level (Desai and Jin Park, 2005). Typical shell materials include gum acacia and maltodextrins.

Spray drying has been used in a variety of applications in the food industry. Recent studies dealing with the production of catechin-loaded particles showed that with spray drying, they achieved high phenol and flavonoids content, as well as high antioxidant activity (Vladić et al., 2016). Additionally, Anandharamakrishnan (2016) prepared vitamin E microparticles with spray drying technique and observed high encapsulation efficiencies of 89%.

2. Freeze drying

Freeze-drying, also known as lyophilization, is a process used for the dehydration of almost all heat-sensitive substances that are unstable in aqueous solutions. Freeze-drying works by freezing the material and then reducing the surrounding pressure and adding enough heat, to allow the frozen water in the material to sublimate directly from the solid phase to the gas phase (Fang and Bhandari, 2010). Recently, Laine et al. (2008) encapsulated phenolic-rich cloudberry extract by freeze-drying, using maltodextrins as wall materials. The microencapsulated cloudberry extract offered better protection of phenolics during storage, while the antioxidant activity remained the same or even improved slightly. Nevertheless, there is also some evidence of freeze-drying induced encapsulation being unable to improve stability or bioactivity. In addition, this drying technique is less attractive than others because its costs are up to 50 times higher than spray-drying.

3. Electrospinning/ electrospraying

This technique is one of the processes that have been used in this dissertation. Hence, a detailed presentation will be given in 2.4.

4. Extrusion

Extrusion is an entrapping method, which involves forcing a wall material in a melted carbohydrate mass through a series of casts into a bath of dehydrating liquid. The pressure and temperature employed are typically <100 psi and 115^{o} C (Joye and McClements, 2014). In this process, the wall material hardens when contacting the

liquids, forming an encapsulating matrix to entrap the core material. Extruded filaments are then separated from the liquid bath, dried to decrease the moisture content and sized.

High-dextrose equivalent corn syrup and a combination of sucrose and maltodextrin are often used as the encapsulation matrix (Fang and Bhandari, 2010). Extrusion has been used to encapsulate different types of flavors and vitamin C (Madene et al., 2006). Recent studies have shown that proteins can be mixed with sodium alginate acting as the matrix materials (Xu and Dumont, 2015).

The major advantage of this method is that the bioactive compound is completely surrounded by the wall material, providing a good stability against oxidation and therefore prolonging the shelf life. The limitations of extrusion include its relatively high cost, and high process temperature. The extruded product is not readily soluble in cold water and usually has large particle size.

5. Emulsion

This technique is one of the processes that have been used in this dissertation. Hence, a detailed presentation will be given in 2.4.

6. Fluidized bed

In fluidized bed coating, the coating polymer, usually in the form of an aqueous solution, is continuously sprayed downwards onto the top surface of the fluidized bed. Each particle receives a small amount of coating material each time it passes through the spraying region, which is the bed region in which sprayed droplets and fluidized particles coexist. Repeated movement from and towards the spraying region results in a gradual built-up of a relatively uniform coating layer surrounding each particle (Ronsse et al., 2009).

This technique is applicable for hot-melt coatings such as hydrogenated vegetable oil, stearines, fatty acids, emulsifiers, and waxes, or solvent-based coatings such as starches, gums, maltodextrins. This technique is used to encapsulate nutritional substances such as vitamin C, B vitamins, ferrous sulfate, ferrous fumarate, sodium ascorbate, potassium chloride, and a variety of vitamin/mineral premixes (Desai and Jin Park, 2005). The main constraints of fluidized-bed coating as an encapsulation process are the type of coating material (i.e. mainly water-soluble biopolymers) (Dewettinck et al., 1998).

7. Coacervation

Coacervation is defined as the separation of colloidal systems into two liquid phases. The basic mechanism involved in this method is the formation of an emulsion and subsequent precipitation of the continuous phase around the droplets of the discontinuous phase. It employs a three phase system, which includes a manufacturing vehicle (solvent), the material to be encapsulated and the coating

material. Coacervation process consists of three steps: First, the formation of the three immiscible phases while mixing under controlled conditions; secondly the deposition of the coating material around the core material; and finally, the shrinkage and solidification of the liquid coating to form the solid microparticles, by thermal or cross-linking techniques (Desai and Jin Park, 2005).

Natural extracts, such as Yerba mate extract, has been encapsulated by coacervation in a polysaccharide based system of alginate-chitosan, to promote its protection and controlled release, with a loading efficiency of 50% (Deladino et al., 2008). Coacervation technique is widely used in the industry; however, the coacervation method possesses some drawbacks. This process is not well suited for producing spheres in the low size range, is very expensive and rather complex.

8. Liposomes

Liposomes are colloidal particles consisting of a membranous system formed by lipid bilayers encapsulating an aqueous phase (Fang and Bhandari, 2010). When phospholipids, such as lecithin, are dispersed in an aqueous phase, the liposomes form spontaneously. One can have either aqueous or lipid-soluble material enclosed in the liposome. The underlying mechanism for the formation of liposomes is a hydrophilic-hydrophobic interaction between phospholipids and water molecules. Kirby et al. have developed a process to stabilize vitamin C in the aqueous inner core of liposomes. Encapsulation of vitamin C gave significant improvements in its shelf life. A major advantage of their use is the target delivery and the ability to control the release rate of the incorporated materials. The main disadvantage in liposome encapsulation is the difficulty in scaling up (Desai and Jin Park, 2005).

2.3. Emulsion

An emulsion is defined as a 'fluid system in which liquid droplets are dispersed in a liquid' (IUPAC, 1997). The two liquids in emulsions are immiscible to one another, and they are typically oil and water (McClements, 2005). The liquid which exists as droplets is referred as dispersed phase or internal phase, whereas the surrounding liquid forms the external or commonly called continuous phase. The process of dispersing one fluid in the form of droplets within another is known as emulsification. Emulsification requires four components, oil, water, an emulsifier and energy (Walstra and van Vliet, 2003). An emulsifier is a material which is often necessary to stabilize emulsion droplets, as oil or water droplets tend to merge together in a process known as coalescence (McClements, 2005; Walstra and van Vliet, 2003). Energy is required for emulsification so as to disrupt and breakup the dispersed phase into droplets within the continuous phase and this is opposed by the Laplace pressure, the pressure differential between the convex and concave side of a curved interface (Walstra and van Vliet, 2003).

Emulsions can be conveniently classified in two main categories according to the state of the dispersed and continuous phase or their droplet size (Ostwald, 1910). A system which consists of oil droplets dispersed in the aqueous phase is called oil-in-water emulsion (O/W), whereas the inverse system (water droplets dispersed in oil) is referred as water-in oil-emulsion (W/O). Typical examples of O/W emulsions include foodstuffs such as milk, mayonnaise, salad dressings, soups and sauces, while margarine, butter and spreads suggest the most common examples of W/O emulsions.

Regarding droplet diameter size as the criterion of classification, emulsions can be distinguished in macroemulsions-, nanoemulsions (submicrometer size droplets) and microemulsions. The main properties of these emulsions are summarized in Table 2.5.

Table 2. 5 Properties of emulsions

Physical properties	**Emulsion**	**Nanoemulsion**	**Microemulsion**
Droplet size	10- 100 µm	50- 200 nm	1- 100 nm
Stability	Thermodynamically unstable	Kinetically stable	Thermodynamically stable
Appearance	Cloudy/ milky	Cloudy/ milky/ translucent	translucent

Formation techniques

Emulsions can be fabricated utilizing a number of different techniques, which are generally categorized as either high-energy or low-energy approaches depending on the energy input requirements (Tadros et al., 2004).

As the name suggests, high-energy methods use a high mechanical energy. Their main advantage is that the size distribution and composition is controlled. Typically, the droplet size is controllable as it decreases with increasing energy input and duration (Walker et al., 2015), although there are some reports of the recoalescence of emulsion droplets during high energy emulsification (Jafari et al., 2008b).

High energy methods produce emulsions with enhanced properties such as the stability, rheology and color of the emulsion(Chime, 2014). Their main disadvantages include: chemical degradation due to the intense production process. Also, it might be challenging to scale up the process (Walker et al., 2015). However, according to other scholars they have industrial scalability but the equipment is more sophisticated and requires a careful approach (Chime, 2014). Energy consumption is still a treatable issue. The actual amount of energy per unit volume expended during homogenization is very high, ranging from around $2x10^7 J/m^3$ to $3x10^8$ J/m^3 depending on the volume fraction and the droplet size. The energy is so high because only a small fraction it is used for the droplet breakup. In HPH around 99.8% of the energy is converted to heat (Schubert et al., 2003) or according to Tadros et al. (2004) a high-pressure homogenizer has an efficiency of only 0.1%, where 99.9% is dissipated as heat during preparing emulsion of 600nm in diameter. Finally, applying high energy methods alone normally do not yield oil droplets of low size (<100nm) (Chime, 2014). In particular, the use of emulsifiers of large molecular weight surfactant facilitates the formation of very small droplets.

On the other hand, low-energy emulsification success depends on the physicochemical properties of the surfactants and the oil phase. Its main advantages are low energy consumption and that their scale-up is more straightforward (Date et al., 2010; Walker et al., 2015).

Low-energy emulsification drawbacks can be the requirement of large amounts of surfactants, typically needed in some cases. Natural surfactants have to be further investigated for food applications. Moreover, natural biopolymer-based emulsifiers; such as, proteins or polysaccharides, can only be used to form emulsions by high-energy methods (Qian and McClements, 2011). An overview of emulsion preparation techniques is given in Table 2.6, while the advantages and disadvantages according to preparation methods are summarized in Table 2.7

Table 2. 6 Overview of emulsion preparation techniques

Technology	Process steps	Ref.
Hot homogenization technique	1. Melting the lipid and dissolving/dispersing the bioactive compound in the lipid 2. Dispersing the bioactive-loaded lipid in hot aqueous surfactant mixture 3. Pre-mixing using a stirrer to form a coarse pre-emulsion 4. High pressure homogenization at temperatures above lipid melting point 5. Hot O/W nano-emulsion 6. Solidification of the nano-emulsion by cooling down to room temperature	(Selvamuthukumar and Velmurugan, 2012)
Cold homogenization technique	1. Melting the lipid and dissolving/dispersing the bioactive compound in the lipid 2. Solidification of the bioactive loaded lipid in liquid nitrogen or dry ice 3. Grinding in a powder mill (50-100µm) 4. Dispersing the powder in an aqueous surfactant dispersion medium (pre-mix) 5. High pressure homogenization at room temperature or below	(Mehnert and Mäder, 2001)
High pressure homogenization	1. The lipid is pushed with high pressure (100 – 2000 bars) through a very high shear stress 2. Disruption of particles down to the submicrometer or nanometer range	(Liedtke et al., 2000)
Solvent emulsification–evaporation method	1. Lipids and bioactive compounds are dissolved in a water immiscible organic solvent with low boiling point 2. The solution is then emulsified in the aqueous emulsifier solution 3. Solvent removal in rotary evaporation at 50-60°C	(Sjöström and Bergenståhl, 1992; Wissing et al., 2004)
Solvent emulsification-diffusion technique	1. Both the solvent and water are mutually saturated in order to ensure the initial thermodynamic equilibrium of both liquids 2. Lipid and bioactive compound are dissolved in water saturated solvent and this organic phase is stirred using mechanical stirrer 3. After formulation of O/W emulsion, water in typical ratios from 1:5 to 1:10, is added to the system in order to allow solvent diffusion into the continuous phase, thus leading to the aggregation of the lipid in the nanoparticles.	(Trotta et al., 2003)
Microemulsion technique	1. Lipids are melted and bioactive compound is incorporated into molten lipid 2. Mixture of water, co-surfactant and surfactant is heated to the same temperature as lipids and added under mild stirring to the lipid melt 3. A transparent, thermodynamically stable system is formed when the compounds are mixed in correct ratios for	(Pascual-Pineda et al., 2015)

	microemulsion formation 4. This microemulsion is then dispersed in a cold aqueous medium under mild mechanical mixing of hot microemulsion with water in a ratio in the range 1:25 – 1:50.	
Ultrasonication technique	1. The core material is melted 2. Addition of phospholipids along with an aqueous medium 3. Dispersing the melted material at increased temperatures by ultra-sonication	(Puglia et al., 2008)
Double emulsion technique	1. Bioactive compound (mainly hydrophilic ones) is dissolved in aqueous solution emulsified in melted lipid 2. The primary emulsion is stabilized by adding stabilizer that is dispersed in aqueous phase containing hydrophilic emulsifier 3. Emulsion is stirred and filtered.	(Esfanjani et al., 2015)

Table 2. 7 Advantages and disadvantages of high and low energy methods of emulsion fabrication

Technique/Points	High energy	Low energy
Techniques	• High speed homogenizer • High pressure valve homogenizer • Microfluidizer • Ultrasounds-based devices	• Phase Inversion by phase mixing • Phase Inversion by altering the conditions of the phase • Membrane emulsification
Advantages	• Control of composition • Control of stability • Production of emulsions with desired properties	• Low energy consumption • Low manufacturing costs • Simple production methods
Disadvantages	• Energy consumption • Chemicals degradation • Limits in droplet size • Recoalescence	• Surfactant choice-edible materials • No use of biopolymers • Stability is influenced by environmental parameter • a large concentration of surfactant may be necessary • droplet polydispersity
Under consideration	Scale-up: sophisticated careful approach Core degradation upon storage	Surfactants' use Core degradation upon storage

In this study, emulsions were prepared with high pressure homogenization or ultrasounds. Hence focus will be given in these techniques.

- High pressure homogenization

High pressure valve homogenization is the most common high pressure device used to produce emulsions (Lee et al., 2014). High-pressure (valve) homogenizers (HPH) have a piston pump to force under high pressure a premixed coarse emulsion through a specially designed valve containing a gap of 10–100 μm and velocities of hundreds of m/s (Håkansson et al., 2011; Innings and Trägårdh, 2007; Lee et al., 2014). In addition, some homogenizers are equipped with one or two nozzles instead of valves. The operated pressure is usually in the range of 100 to 500 MPa.

Briefly, the droplet disruption occurs due to laminar and turbulent flow at the entrance, therefore creating two flows fluid and cavitation bubbles by pressure decrease and the collapse of bubbles at the end by pressure increase.

High pressure processing always increases the temperature of the sample depending on its specific physicochemical properties and the refrigeration system used in the

homogenization valve case. At least a 15 to 20°C shear-induced increase in temperature is typically observed per 100 MPa increment in homogenization pressure. Moreover, when several cycles are performed to reduce the particle droplet size, coalescence occurs due to the high kinetic energy of the particles (Floury et al., 2002). To reduce the droplet size to the level required in nanoemulsions, it is usually necessary to operate at extremely high pressures and to use multiple passes through the homogenizer. Even then, it is only possible under certain circumstances to obtain droplets less than 100 nm in radius (e.g., high emulsifier levels, low interfacial tensions, and appropriate viscosity ratios).

- Ultrasonication

Apart from high pressure devices, an ultrasound generator has been patented since 1944, furthermore it is considered an effective way of producing emulsions. High intensity ultrasonication (US) with a frequency range between 16 and 100 kHz, and power density of 10 to1000 W/cm^2 results in the production of oil droplets in the nano-scale (up to 100 nm), with improved stability over time and the need for small amounts of emulsifying agents (Chemat et al., 2011).

Ultrasonic emulsification is believed to occur through two mechanisms, cavitation and high shear. The phenomenon of cavitation is known since 1895, it was observed in a submarine propeller that became pitted and eroded after a short period of operation, as a consequence of collapsing bubbles due to hydrodynamic cavitation that generated intense pressure and temperature gradients in the nearby vicinity (Leong et al., 2009).

According to Li and Fogler (2006) the mechanism of ultrasound emulsification comprises two separate stages. The first stage involves the generation of primary droplets, due to the eruption of the oil phase into water caused by the interfacial waves of the acoustic field. During the second stage the primary droplets deform and eventually implode during the high-pressure cycle of the sound wave. This phenomenon is termed cavitation. Cavitational collapse produces intense local heating (~5000 K), high pressures (~1000 Atm) (Suslick, 2003), turbulence and shear forces resulting in violently imploding bubbles and liquid microjet streams. Both bubble implosion and microjets lead to further breaking of the primary formed oil droplets into nano-sized ones.

Commercial-scale ultrasonic emulsification requires the use of a sonochemical reactor in an industrial size in order to control the operating parameters. The ultrasonic amplitude, which is related to the intensity of cavitation-generated shear forces, should be kept at high levels for the emulsification process to be efficient. The problem is that in an industrial scale, when the size of ultrasonic horn-based processor is increased, the amplitude should be significantly decreased in order to be adjusted to a significant cavitation zone volume. Amplitude should be about 75-100

μm to produce high quality nanoemulsions, whereas the ultrasonic transducers generate vibration amplitudes of about 25 μm, thus a high-gain acoustic horn that increases the vibration amplitude is required (Peshkovsky et al., 2013). When converging horns are used, the produced amplitudes are high, as long as their diameter remains very low at about 15-20 mm. Large volumes in process are then excluded.

Ultrasonication is then considered more practicable with respect to production costs as well as equipment contamination compared with microfluidization (Freitas et al., 2006; Jafari et al., 2008b; Karbstein and Schubert, 1995). A number of recent studies have used ultrasonic homogenization to produce nanoemulsions with the possibility of being used in the food and pharma industry. As a rule of thumb it is observed that as the irradiation power and time increase, the mean droplet diameter decreases (Kentish et al., 2008; Leong et al., 2009; Tang et al., 2013). This is because of the fact that as the irradiation power increases, the pressure amplitude of the applied sound pressure increases, which will increase the cavitation phenomena (number of events and the cavity collapse intensity) (Leong et al., 2009).

However, the over-processing effect may also occur under high shear conditions leading to coalescence of droplets and increase of the average diameters (Jafari et al., 2006). For instance, the decrease of droplet diameter and preparation of flaxseed o/w nanoemulsions (< 200 nm) was feasible when increasing the nominal power up to 200 W, whereas further power increase had detrimental effect on size. This was associated with secondary Bjerknes forces which increase in intensity and increase the proximity of the droplets when increasing the applied power (Kentish et al., 2008).

Increasing the frequency of ultrasound waves also contributes to droplet size reduction. Submicron oleic acid/water emulsions formation in the absence of emulsifier has been reported with decreasing droplet diameters to less than 400 nm with increasing the frequency from 40 kHz up to 1 MHz (Kamogawa et al., 2004).

Mechanisms of emulsion instability

Emulsion systems have the potential to undergo a number of types of droplet aggregation, including flocculation (bridging or completion) or coalescence (partial or complete), due to the thermodynamic instabilities between the dispersed and continuous phases. Emulsions are dynamic systems, whereby droplets are in a state of motion due to gravitational forces and Brownian motion. This droplet motion inevitably leads to droplet collisions, which may lead to either flocculation or coalescence depending on the nature if the interfacial layer of the droplet (McClements, 2005).

- Phase separation

As emulsions are dispersions of two immiscible fluids there is a thermodynamic tendency for the phases to separate due to the interfacial tension between the two phases and that the system aims from a thermodynamic perspective to achieve the lowest possible entropy. This may be achieved by reducing the interfacial area between the two phases. In emulsion systems with sufficient emulsifier to prevent phase separation due to coalescence of the two phases, emulsions can be destabilized by the difference in density of the two phases. The two phases in emulsions often have different densities, and this leads to gravitational separation, called creaming in O/W emulsions where oil droplets rise to the surface, or sedimentation in W/O emulsions where water droplets go to the bottom of an emulsion (Chanamai and McClements, 2000; Dickinson and Ritzoulis, 2000).

- Flocculation

Flocculation is the process whereby two or more emulsion droplets associate with one another, whilst maintaining their discrete integrity. These associations of droplets are referred to as flocs. The association of emulsion droplets as flocs increases the effective volume of the associates, increasing the rate of gravitational separation as described by Stokes' law. Additionally, the development of flocculated emulsions yields a pronounced increase in the viscosity, due to the increase in the effective hydrodynamic volume of the floc. There are two main mechanisms by which flocculation of emulsion systems occurs, bridging or depletion flocculation (Chanamai and McClements, 2000; McClements, 2005).

Bridging flocculation commonly occurs in emulsions stabilized with biopolymers (e.g. proteins), whereby the associative non-covalent interactions between the hydrophobic moieties adsorbed to one droplet interface interact with either the hydrophobic moieties of another or the hydrophobic dispersed phase, yielding the development of flocs. This type of flocculation tends to occur in systems containing insufficient emulsifier where regions of the emulsion droplet surface are not covered completely by emulsifier. Additionally, bridging flocculation may occur if an oppositely charged biopolymer is present within the continuous phase, linking emulsion droplets. These types of bridging flocculation can be mitigated against by sufficiency of emulsifier and ensuring that emulsifier and added biopolymer have similar charges(McClements, 2011; Tan and McGrath, 2012).

Depletion flocculation occurs due to the presence of unadsorbed or nonadsorbing colloidal entities within the continuous phase. These nonadsorbing entities may be an excess of emulsifier in the form of surfactant micelles or protein associates. These nonadsorbing colloidal entities cause an attractive interaction between emulsion droplets due to the osmotic effect arising from the exclusion of these colloids from the confined volume between two adjacent emulsion droplets. This attractive force,

due to osmotic pressure, increases as a function of concentration of free colloids in the continuous phase, eventually causing emulsion droplets to associate with one another in the form of flocs. The concentration of free biopolymer which initiates depletion flocculation is referred to as the critical flocculation concentration (CFC). Therefore reduction of emulsion droplet size reduces the CFC, and the potential for depletion flocculation (Chanamai and McClements, 2000; McClements, 2011; Tadros et al., 2004).

- Coalescence

Coalescence is an emulsion destabilization mechanism by which emulsion droplets merge together yielding a larger emulsion droplet. This is a thermodynamically driven process, whereby the system is minimizing the surface area, and thus the free surface energy. This growth in emulsion droplet size causes an increase in the rate of gravitational separation, often leading to an increased rate of coalescence due to greater contact of emulsion droplet surfaces. In water continuous emulsions the coalescence of emulsions results in the formation of an oil layer on the surface, known as oiling off, in oil continuous emulsions, coalescence leads to the collecting of free water at the base of the material (McClements, 2011).

There are two primary methods for controlling and minimizing coalescence within emulsions, the prevention of droplet contact and the development of a thicker interfacial layer. The prevention of droplet contact can be achieved the increase of viscosity of the continuous phase or the development of a gelled network reducing the mobility of emulsion droplets through the bulk. The development of a thicker interfacial layer is achieved through the use of sufficient emulsifier, or alternatively a layer-by-layer build up on the emulsion droplet surface, using oppositely charged biopolymers, such as positively charged chitosan and negatively charged proteins (e.g. sodium caseinate, gelatin, etc.) (Dickinson, 1992; Guzey and McClements, 2006).

- Ostwald ripening

Ostwald ripening is an emulsion destabilization mechanism whereby emulsion droplet size increases at the expense of smaller droplets, due to mass transfer of dispersed phase through the bulk from one droplet to another. However, for standard food emulsions the effect of Ostwald ripening is minimal due to the limited solubility of food lipids (e.g. triglycerides) in water (Wooster et al., 2008). Ostwald ripening plays a prominent role in emulsion stability where the lipids are more water soluble, such as the case for flavor oils (e.g. limonene, eugenol, etc.), or when the continuous phase contains alcohol, such as cream liqueurs (Williams and Phillips, 2003).

2.4. Electrospraying

Electrohydrodynamic processes namely electrospinning and electrospraying are effortless, inexpensive and flexible dry spinning processes that utilize electrically charged jet of polymer solution in order to produce fibers or particles at micron, submicron, and nanoscale (Rezaei et al., 2015).

History

In 1600 William Gilbert was the first to point out the electrostatic attraction of a liquid. After that, in 1887 Charles Vernon Boys described the electrospinning process in a paper on nano-fiber manufacture. In the early 1900's, several experiments were performed to study electrically formed droplet formation such as work from Cooley, (1902); Zeleny, (1914), while the first patent was awarded for electrostatically produced polymer fibers in 1934 to Anton Formhals (Anton, 1934). Not much attention was given to the scientific aspect of electrostatic phenomenon until a British scientist, Sir Geoffrey Taylor, began to investigate the phenomena that occur when an electric field is applied to a liquid. In one of the most famous papers Taylor modelled the shape of the (Taylor) cone formed by the fluid droplet under the effect of an electric field (Taylor, 1964). Every year, the number of publications about electrohydrodynamic process has been increasing exponentially every year.

Principles and mechanism

The set up for the electrospinning process is sufficiently simple and it is presented in Fig. 2.2.

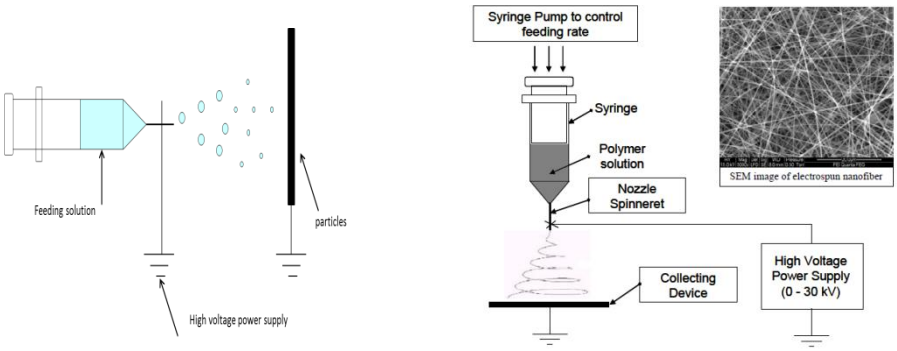

Fig. 2. 2 Schematic representation of the typical setup for electrospraying (left) and electrospininning (right).

This set up consists of four components:

- A feeding pump (e.g. a syringe pump)
- A spinneret system (e.g. a metallic needle mounted to the syringe)
- A high-voltage power supply generator (> 0.5 kV/cm) to supply the potential in order to charge the syringe
- A grounded collecting device to collect the produced structures

In the beginning of a typical electrohydrodynamic process, a droplet of the solution is formed at the end of the nozzle. The droplet has spherical structure due to various forces that exist. When a high voltage is applied from few to tens of kilovolts, an electrical field is simultaneously induced between the spinneret and collecting device. The spherical drop pendent on the nozzle exit is then deformed, as a consequence of the force interactions between the coulombic force (exerted by the external electric field) and the surface tension of the polymer solution, into a conical shape which was commonly termed as the Taylor Cone (Taylor, 1964). When the electric field strength overcomes a critical value, the electrostatic forces overcome the surface tension, resulting in an ejection of a polymer liquid jet. This jet is then subjected to an extremely high ratio of stretching and rapid evaporation of solvents, leading to its breakage and, ultimately, to the formation of nano-/micro- meter sized fibers (electrospinning) or particles (electrospraying) on the collecting device (Bhardwaj and Kundu, 2010; Ghorani and Tucker, 2015).

The stable jet is fundamental in the formation of nanostructures; however it is dependent on quite a few factors and is comprised of four distinct regions. The jet initiates at the bottom of the Taylor cone and then travels as a single jet decreasing in diameter toward the ground electrode. The jet experiences what is most commonly referred to as 'whipping' instability, where the jet is accelerated, stretched, and dried. The final region is the collection region (Reneker et al., 2007).

Many modes of spraying are appeared in literature depending on the form of the meniscus, the pattern of the jet, and a way it separates into droplets (Jaworek and Krupa, 1999). Various forms of the modes of electrospraying are presented in Fig. 2.3.

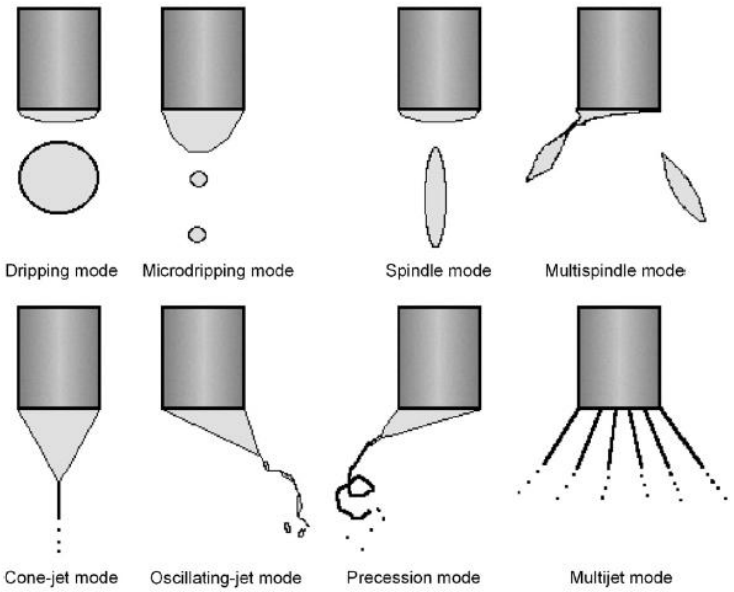

Fig. 2. 3 Various modes of electrospraying (Drosou et al., 2017)

These modes can be categorized into two groups:

Dripping modes: The characteristic of these modes is that only fragments of liquid are ejected directly from the nozzle. These fragments can be in the form of regular large drops (dripping mode), fine droplets (micro-dripping mode), elongated spindles (spindle or multi-spindle modes), or sometimes irregular fragments of liquid. However, at some distance from the nozzle exit, these fragments contract into spherical droplets.

Jet modes: In this case, the liquid is elongated into a long, fine jet, which can be smooth and stable (cone-jet mode) or can move in any regular way. For example, it may rotate around the capillary axis (precession mode) or oscillate in its plane (oscillating mode). In each case, the jet separates into droplets due to electrostatic forces.

The most important mode of spraying is the cone-jet mode. In this mode, the liquid meniscus assumes the form of regular, axisymmetric cone with a thin jet (<100 mm in diameter) at its peak (Jaworek and Sobczyk, 2008).

The minimum flow rate at which the cone-jet mode can operate at steady state was determined by Barrero and Loscertales, (2007):

$$Q_{min} = \frac{\sigma_1 \, \varepsilon_o \, \varepsilon_\tau}{\rho_1 \, \gamma_1} \quad Eq. 2.1$$

Where:

Q_{min} is the minimum flow rate for a steady cone-jet mode

σ_1 is the surface tension of the liquid

ε_o is the permittivity of the free space

ρ_1 is the mass density of the liquid

γ_1 is the liquid bulk conductivity

Differences between electrospinning and electrospraying

The difference between electrospinning and electrospraying, which may be considered as “sister” technologies, is based on the degree of molecular cohesion in the raw material - a property which is most readily controlled by variation in concentration of the polymer solution (Chakraborty et al., 2009).

When the solution concentration or the molecular chain entanglement in the liquid is high, the jet formed in electrospinning does not break into droplets but produces a micro- or nanofiber. If the solution concentration is low, the jet is destabilized due to varicose instability and hence fine spherical micro-particles are formed. These highly charged droplets self-disperse in space due to electrostatic repulsion, thereby preventing droplet agglomeration and coagulation. The evaporation of the solvent

leads to contraction and solidification of droplets resulting in solid polymeric particles deposited on the grounded collector (Ghorani and Tucker, 2015).

For food and nutraceutical applications, particles are generally preferred instead of fibers, since apart from facilitating handling and subsequent incorporation into different products, they usually present greater surface/ volume ratio and thus, are expected to have better release profiles than fibers (Hong et al., 2008). Hence, in this dissertation electrospraying process has been used with final goal the production of particles for food applications.

Types of electrospraying

Electrospraying can occur with some variations. The types of electrospraying are discussed below.

- Solution electrospraying

Solution electrospraying is one of the most well-known methods among the EHD processes used for the production of particles. In this technique, electrosprayed particles are formed from polymers using solutions. In the food sector, biopolymers in aqueous solutions are generally used (Gómez-Estaca et al., 2015; López-Rubio and Lagaron, 2012; Torres-Giner et al., 2010). In these cases, encapsulation of hydrophilic compounds is plausible and has been extensively examined in literature (Anu Bhushani and Anandharamakrishnan, 2014; López-Rubio and Lagaron, 2012; Neo et al., 2013; Torres-Giner et al., 2010).

- Emulsion electrospraying

Lipophilic compounds exhibit very low water solubility, hence electrospraying and subsequent encapsulation of this compound from water-based solutions is not possible. In this regard, emulsion electrospraying is the plausible technique that can be used for the encapsulation of immiscible compounds (Abu-Ali and Barringer, 2005; García-Moreno et al., 2016; Wang et al., 2014). During the emulsion electrospraying, an immiscible liquid phase is dispersed into a polymer solution with final goal a stable emulsion. When the emulsion is being processed with EHD process, the aqueous phase forms the shell material and the oil phase forms the core material (Khan et al., 2013). Several studies have been shown the potential use of emulsion electrospraying in food applications (Angeles et al., 2008; Camerlo et al., 2014; Gordon et al., 2015; Li et al., 2009).

- Coaxial electrospraying

Coaxial electrospraying also serves as a technique for the encapsulation of lipophilic compounds. In this case, the sensitive compound and the polymer are independently dissolved in their relevant solvents, and the core and the shell solutions are then ejected separately through two confocal nozzles (Cao et al., 2014). By this method, the components immiscibility problem is solved (Pérez-Masiá et al., 2014). Various

studies have been shown the potential use of coaxial electrospraying mostly in pharma applications (Cao et al., 2014; Kiatyongchai et al., 2014).

Processing parameters

Many variables may influence the electrospraying process of a polymer and the resultant morphology. These variables can be summarized in Table 2.8.

Table 2. 8 Variables affecting electrospraying

Solution properties	Operating parameter	Ambient conditions
Type of polymer	Applied voltage	Temperature
Molecular weight of polymer	Flow rate	Humidity
Viscosity	Tip-to-collector distance*	Atmospheric pressure
Electrical conductivity	Jet current	
Surface tension*		
Dielectric constant		

- Polymer concentration, molecular weight

It is well known that by increasing the molecular weight of a polymer, its solubility decreases. On the other side, by increasing the molecular weight of a polymer, its viscosity and its degree of molecular chain entanglement increase (Shenoy et al., 2005). Fig. 2.4 represents an electrospinning – electrospraying device.

Fig. 2. 4 Typical electrospinning – electrospraying device

Many studies have reported that higher molecular weights of the polymer (larger chains) accompanied with higher polymer concentrations could lead to the formation of fibers (Bhardwaj and Kundu, 2010; Huang et al., 2003). Other studies have observed that for the production of fibers with the electrospinning process, high molecular weight solutions are favored, while for the production of particles with the electrospraying process, low molecular weight solutions are preferred (Bhardwaj and Kundu, 2010; Gupta et al., 2005). Moreover, the number of particles in the fiber structure decreases with increasing molecular weight (Deitzel et al., 2001).

Optimum solution concentration is also a critical parameter in electrospraying. At high solution concentrations, fibers are formed instead of particles. Specifically, there is a certain maximum polymer concentration that is fundamental for the formation of particles. Above this critical value, application of voltage results in the formation of fibers (Sukigara et al., 2003). Failure to obtain electrosprayed particles from pure biopolymer dispersions has been previously reported and it is usually an indication of low viscosity and lack of sufficient entanglement (Buchko et al., 1999; Wongsasulak et al., 2007).

Shenoy et al., (2005) have evolved a semi-empirical analysis to explain the transition from electrospraying to electrospinning. According to them, an entanglement number- $(\eta_e)_{soln}$ - for the solution may be used to predict the formation of fibers in electrospinning where the entanglement number can be calculated by the following equation:

$$(\eta_e)_{soln} = \frac{\varphi\, M_w}{M_e} \qquad (Eq.\ 2.2)$$

M_w is the molecular weight of the polymer in the solution

M_e is the polymer entanglement molecular weight

φ is the polymer volume fraction

They showed that when the entanglement number is more than 3.5, smooth fibers were formed, while for numbers between 2 and 3.5 a mixture of beads and fibers can be seen. Below 2, electrospraying occurs wherein only particles are formed (Munir et al., 2009).

- Viscosity

Another important parameter that affects the electrohydrodynamic process is the solution viscosity. Viscosity is known to have a relation with the extent of the polymer molecule chain entanglement into the solution. Viscosity is directly related to concentration, molecular weight, and the structure of the polymeric chains (Bhardwaj and Kundu, 2010).

Generally, highly viscous solutions favor the production of fibers. However, above a viscosity value, the electrical charges may not exhibit sufficient strength to stretch the solution to form nanostructures. If a solution is so viscous or it ist gel-like, it may be necessary to reduce the concentration of the solution. Thus, extremely high viscosity makes it difficult for the polymer solution jets to eject and, thus, no fiber will form (Demir et al., 2002).

However, below a certain viscosity value, the electrospinning jet may breaks up into droplets and particles could be formed in this case. Electrospinning, therefore, requires an optimum solution viscosity. In most cases, an increase in viscosity increases the fiber or particle diameter and uniformity (Gomez-Estaca et al., 2012).

Interfacial viscosity is another property that significantly affects the electrospraying process. Interfacial rheology depicts the relationship between the deformation of an interface and the stresses exerted on it and the reorganization of the polymer molecules at the interface. The majority of published papers on electrosprayed or electrospun materials examined the viscosity of the polymer solutions (Aceituno-Medina et al., 2013; Charernsriwilaiwat et al., 2010; Sarhan and Azzazy, 2015). Interfacial viscosity may bear an effect on the sprayability of the polymers (Pelipenko et al., 2012) suggesting that, given the area of a Taylor cone, rheological characteristics play a significant role due to the larger diameter of the jet. Hence, measurement of the rheological parameters of the bulk may not be sufficient when dealing with electrospraying.

Palangetic et al., (2014); Regev et al., (2010); Rošic et al., (2012) dealt with the effect of elasticity of the polymer solution on the electrospinning process. The authors hypothesized that elastic forces resist the bending of the jet and hinder a jet from breaking up. Interfacial viscosity may bear an effect on the sprayability of the

polymers. Pelipenko et al., (2012) suggested that, given the area of a Taylor cone, rheological characteristics play a significant role due to the larger diameter of the jet. During jet thinning, interfacial characteristics prevail due to the significant increase in the surface-to-volume ratio (S/V = 4D–1). The jet diameter (D) is reduced from approximately 1 mm (inner diameter of the needle used) to a few hundred nanometers or less (diameter of the obtained nanofibers). Moreover, solvent evaporation creates a concentration gradient in polymer molecules, leading to a more pronounced effect of the interfacial characteristics. Hence, a detailed investigation of the rheological parameters of the bulk may not be sufficient when dealing with complex processes, such as electrospraying.

- Electrical conductivity

Electrical conductivity is a key factor determining the ability of a solution to be treated with EHD. The electrical conductivity of a solution reflects a charge density on a jet thus elongation level of a jet by an electrical force. Therefore, under the same applied voltage and tip-to-collector distance, a solution with a higher electrical conductivity may cause higher elongation of a jet along its axis and thus it could form structures with smaller diameter (Tan et al., 2005).

What is more, at low conductivity, insufficient charge builds up so that electrospraying doesn't occur, while at high conductivity, the liquid conducts the charge back along the feed line, causing a short to the nearest ground (Anu Bhushani and Anandharamakrishnan, 2014; Bhardwaj and Kundu, 2010). On the other hand, the intensity of the electrical field must overcome the surface tension of the solution, expelling an electrified jet from the Taylor's cone formed on the needle tip (Anu Bhushani and Anandharamakrishnan, 2014; Bhardwaj and Kundu, 2010; Taylor, 1964). According to Jaworek and Sobczyk, (2008), the optimum conductivity for a solution to be successfully processed varies from 10^{-4} to 10^{-8} s/m.

In order to improve the conductivity of the solution, salt can be added so that they can function as carriers of the charges in the spinning solution and may play an important role in increasing the production rate of the process. High solution conductivity can be also achieved by using organic acid as the solvent (Chaobo et al., 2006).

- Surface tension

Formation of droplets, particles, or fibers depends on the surface tension of the polymer solution. Hence, surface tension of the solution plays a major role in the electrospraying process (Palangetic et al., 2014), because the intensity of the electrical field must overcome the surface tension of the solution, expelling an electrified jet from the Taylor's cone formed on the needle tip (Anu Bhushani and Anandharamakrishnan, 2014; Bhardwaj and Kundu, 2010; Taylor, 1964).

In solutions with low surface tension, a lower electric field is required for electrospinning than is required in solutions with a higher surface tension (Haghi and Akbari, 2007). At very high surface tensions particles form because the jet may spray out to facilitate the electrospraying process (Shutov, 2008).

According to Jaworek and Sobczyk, (2008), the surface tension for a solution to be successfully processed should surpass 50 mN/m. Surfactants are usually used as material with final goal the increase of the surface tension and the improvement of the process (Wang et al., 2008c).

- Applied voltage

A critical element in any EHD process is the application of high voltage to the polymer solution. Variation of this voltage controls the electrical field strength between the spinneret and the collection point, and thus the strength of the drawing force.

It is known that solution concentration and viscosity have an influence on the morphology and diameter of the obtained structures. Specifically, increased polymer concentrations lead to increased viscosities. As the viscosity increases, more force is required to overcome both the surface tension and the viscoelastic force to attenuate the jet and form fibers. The critical voltage needed to eject a charged jet from the drop at the nozzle depends mainly on the solution concentration (Doshi and Reneker, 1995).

Generally, increasing applied voltages lead to decreasing diameters of nanofibers due to increasing electrostatic repulsive forces on the fluid jet e.g., for chitosan nanofibers produced by electrospinning it was noted that by increasing the voltage, the diameter of nanofibers decreased (Sencadas et al., 2012).

A critical voltage is necessary for initiating the electrospinning process and fiber formation. The role of this critical voltage is well established. Some researchers have suggested that increasing the voltage can increase the ejection power of the polymer that will then give rise to the formation of fibers with larger diameters (Demir et al., 2002).

According to other studies, the average fiber diameter reaches a minimum value after an initial increase in the applied voltage and then becomes larger as the applied voltage increases (Lin et al., 2008). This trend has been attributed to the shorter deformation time that is available to form fibers as the voltage increases.

- Flow rate

A minimum flow rate of the polymer solution is required for EHD processing. It has been observed that increasing the polymer flow rate results in increased diameters of both fibers and particles (Megelski et al., 2002). High flow rates may result in beaded fibers as this will not allow sufficient time for the fibers to dry before

reaching the collector (Zong et al., 2002). Several studies have systematically investigated the relationship between solution flow rate on the final morphology and size. For instance, Okutan et al., (2014) investigated the influence of feed rate during electrospinning on properties of electrospun gelatin and reported that with increasing feed rate there were larger fiber diameters and bead formation.

A power law dependence exists between flow rate and applied voltage, i.e., the flow rate is proportional to the cube of the voltage supplied (Demir et al., 2002). Consequently, any change in flow rate in a given electrical field may be expected to substantially affect fiber morphology.

- Tip-to-collector distance

It follows that the needle should be placed at an optimum distance from the collector to allow sufficient time for the fibers to dry and the solvent to evaporate before reaching the collector. As may be expected, the tip-to-collector distance has a direct influence on jet flight time and the electrostatic field strength. Inadequate drying of the fiber/particle is attributed to insufficient distance between the needle tip and the collector. In this instance, the drying time is not long enough to evaporate the solvent before the fibers/particles are deposited on the collector and consequently partially dried fibers with densely packed structures (Barhate et al., 2006). Shorter tip-to-collector distances favor the production of particles; while larger favor the formation of fibers (Ghorani and Tucker, 2015).

- Ambient conditions

Ambient parameters such as temperature and humidity have an effect on the electrospinning process. This is because a direct relationship exists between solvent evaporation and temperature as well as between the conductivity of the solvent and temperature. Both can influence the electrospinnability of a polymer solution. Furthermore, polymer viscosity and surface tension of the polymer solution are influenced by temperature ((Chen and Yu, 2010). Increasing temperature causes the fiber diameter to decrease; this may be attributed to the decrease in the polymer solution viscosity (Ghorani and Tucker, 2015). Increasing humidity leads to the increase of the diameter of the final products, in most cases (Casper et al., 2004).

Comparison with other encapsulation techniques

A variety of well-established processes have been proposed to prepare nano- or submicron-particles. The most commonly used techniques in the food industry were analyzed in paragraph 2.2 and include spray-drying, emulsification or coacervation.

However, these techniques require the use of high temperatures, organic agents or expensive equipment, damaging encapsulated compounds due to the heating or to non-edible particles (Lian et al., 2002). What is more, some of these techniques form big particles (>200 μm) that may affect food sensory qualities (Augustin and Hemar,

2009). Hence, electrohydrodynamic (EHD) processing, and specifically electrospraying has emerged as an alternative encapsulation technique, which can generate small-diameter particles. Electrospraying has some advantages over conventional mechanical spraying systems such as:

- It is a simple, easy technique
- It is a non-thermal process
- It consist of a slightly–priced equipment
- The droplet size is in most cases smaller than the other techniques, reaching the nano-scale
- The droplet size exhibit very narrow size distribution that allows production of particles of nearly uniform size
- The droplet size can be easily controlled
- Particle morphology can be tailored from spherical particles to sophisticated hollow particles
- The particles exhibit high surface-to-volume ratio
- The particle aggregation is prevented due to their own mutual electrical repulsion
- Both hydrophilic and hydrophobic bioactives could be encapsulated
- The bioactive compounds that are incorporated exhibit high encapsulation efficiencies
- Does not require a tedious separation process to remove the particles from the solvent
- The stability of the bioactives is enhanced compared to the other techniques
- It could produce food-grade particle

However, one of the major disadvantages of electrospraying is that the productivity yield is low in food-grade solutions.

Applications

Even though EHD process is an innovative technology, commercial products produced with this technique have been already formed. These products can be found in various areas such as air filtration (SETA from HRV, New Zealand; Micrograde NF filter from Mann& Hummel, Germany), water filtration (NanoFIber from AstraPool, Spain; Nanotrap from Coway, S. Korea), biomedical (Healsmart personalized antimicrobial dressings from Polyremedy, USA; drug loaded electrospun fibers from Biosurfaces, USA), medical (AVflo Vascular Access Graft from Nicast, Israel; Rebossis synthetic bone from Ortho Rebirth, Japan), fabrics (Filtering Cloth from Sorbent, Russia; Return focus pod from IQ commercial, New Zealand), paper industry (Nanofiber coated paper from Hirose paper, Japan), and lab tissue culture (Cell culture dish from Sigma-Aldrich, Germany; nanofiber dish from Nanofiber solutions, USA).

Moreover, a growing interest in the use of electrosprayed particles in the food industries has seen electrospraying of biopolymers and the encapsulation of food ingredients, enzymes and other active compounds related to the food industry (Ghorani and Tucker, 2015). The most interesting benefit of electrospraying food material is the introduction of different textures and mouth feel to the food (Nieuwland et al., 2013).

The potential of electrospraying for drug delivery systems (Bock et al., 2012), film coating on foods (Khan et al., 2013), chocolate processing (Luo et al., 2012), preparation of solid lipid nanoparticles containing active compound (Eltayeb et al., 2013), stabilization of nutraceuticals (Torres-Giner et al., 2010) and specifically encapsulation of bioactives and probiotics (López-Rubio et al., 2012) have recently been reported.

Preservation of active compounds through encapsulation in electrosprayed particles is probably the most widely investigated field in the application of food technology (Neethirajan and Jayas, 2011). The bioactive compounds encapsulated in electrosprayed particles are shown to possess enhanced stability and functionality and may be used as ingredients in functional foods (Pérez-Masiá et al., 2015). In Table 2.9, a review of recent studies dealing with electrosprayed particles in food applications is summarized.

The use of food-grade polymers and biopolymers as shell material in food systems is widely being investigated (Nieuwland et al., 2013). In this regard, the natural biopolymers, proteins and carbohydrates are commonly used for encapsulation, such as proteins, starch, cellulose, pectin, guar gum, chitosan, alginate and carrageenan, xanthan, dextran, and cyclodextrins.

Table 2. 9 Electrospraying technique for the encapsulation of bioactive compounds

Bioactive compound	Shell material	Size (nm)	Reference
ω-fatty acid	Zein prolamine	490 - 530	(Torres-Giner et al., 2010)
Peppermint oil	Alginate- pectin	1600-3200	(Koo et al., 2014)
EGCG	Gelatin	230-500	(Gómez-Mascaraque et al., 2015)
lycopene	Chitosan	200	(Pérez-Masiá et al., 2015)
ω-fatty acid	Gelatin- protein	1000-2800	(Gomez-Mascaraque and Lopez-Rubio, 2016)
Curcumin	Gelatin	< 1200	(Gómez-Estaca et al., 2015)
β-carotene	protein	300-1800	(López-Rubio and Lagaron, 2012)

However, there are a number of limitations in the encapsulation of bioactive compounds with electrospraying for food applications. Firstly, the solvent in which the materials will be dissolved should be food-grade in order to avoid toxicity issues. It is known that solvent type could influence the dryness and the structure of the final product. Most polymers used for electrospraying of food-based application are dissolved in water or ethanol (Kayaci and Uyar, 2012). However, water has higher density and boiling point than the other solvents such as. Dichloromethane and N,N,-dimethylformamide. This difference of the water, could lead to a drying of the Taylor cone after few hours of processing. This effect could be avoided by modifying the processing or solution parameters, so as to facilitate the elimination of the solvent.

Another issue to consider is the selection of the most suitable polymer. As a carrier for bioactive compounds, the selected polymer for electrospraying should be natural, edible and can be electrosprayed to give particles without the need to introduce manmade polymer as a spraying aid into the mixture (López-Rubio and Lagaron, 2012). Regarding the food encapsulation matrices, proteins and

polysaccharides have attracted a considerable interest. However, pure proteins, as well as most natural polymers, are difficult or even impossible to be electrosprayed due to their three-dimensional network (López-Rubio and Lagaron, 2012; López-Rubio et al., 2012). These limitations can be overcome by blending them with polysaccharides, such as starch (López-Rubio et al., 2012) or pullulan (Aceituno-Medina et al., 2013), which significantly improve the natural polymer's sprayability.

Hence, it is to be expected that with electrospraying, the mild process conditions will make it an attractive alternative route for processing temperature sensitive materials, if the combination of the used materials is successful.

2.5. Food polymeric ingredients used as surfactants and emulsifiers

The selection of an appropriate emulsifier (or combination of emulsifiers) is one of the most important factors for the proper design of an emulsion. An emulsifier is a surface-active molecule, which is capable of adsorbing onto droplet surfaces, facilitating droplet disruption and protecting droplets against aggregation (McClements et al., 2007). In the food and pharmaceutical industry, the most important types of emulsifiers are small molecule surfactants, phospholipids or proteins. Most emulsifiers function by decreasing the interfacial tension of the oil and water phases, leading to electrostatic or steric stabilization (Henry et al., 2009, 2010).

In the present study the main emulsifier used for the emulsion fabrication was whey protein isolate.

- Whey protein isolate

Whey protein is a mixture of globular proteins isolated from whey, the liquid material created as a by-product of cheese production resulting from the coagulation of milk. In cow milk, whey proteins represent the 20 % of total milk proteins, while the main fraction (80%) is caseins. Whey consists of a mixture of globular protein molecules comprising β-lactoglobulin (β-LG∼50% wt/wt), α-lactalbumin (α-LA∼20% wt/wt), immunoglobulins (IgG; ∼10% wt/wt), and bovine serum albumin (BSA∼6%, wt/wt) and other minor protein or peptide components (lactoferrin, lactoperoxidase, lysozyme) and growth factors (Walstra and van Vliet, 2003).

The functional properties of whey proteins in foods include solubility, dispersibility, heat stability, network formation (gels and edible films), and surface activity (emulsions and foams) (Foegeding et al., 2002). β-Lactoglobulin (β-LG) is the most abundant protein in whey, and the functionality of a commercial whey form is mainly reflecting the functionality of this protein. β-LG is a globular, amphiphilic protein with the ability to adsorb at the water/oil interface. β-LG contributes in this way to dressing formation by lowering the interfacial tension, and also by stabilizing the film formation at the interphase. β-LG unfolds at the interphase and forms intermolecular associations, either by hydrophobic interactions or S–S bridges. α-lactalbumin (α-LA), represents the second most abundant protein in whey, which is also reported to exhibit emulsifying and stabilizing properties. Together with β-LG it participates in the S–S bridging and film formation at the droplet interphase (Leman, 1999). Different whey products are categorized based on their protein concentration. The most typical commercial form of whey proteins are whey protein concentrates (WPCs) and whey protein isolates (WPIs). Protein concentration in WPCs may vary between 20 to 89 % and they also contain low levels of fat, and

carbohydrates in the form of lactose. WPIs are processed to remove the fat and lactose and contain at least 90 % protein (Dickinson, 1992; Williams and Phillips, 2003). For the production of WPC and WPI, whey may be subjected to several treatments to recover whey protein in a more concentrated form. The afore-mentioned membrane-based separation technologies include ultrafiltration (UF) to concentrate proteins, or diafiltration (DF) to remove most lactose, minerals and low molecular weight components (Foegeding et al., 2002).

- Bacterial cellulose

Cellulose is the most abundant natural polysaccharide, being the major structural component of plants. It is a linear homopolymer of β(1-4)-D-glucose residues linked together by glycosidic bridges. Chemically modified cellulose is a food additive, which is mainly used for its gelling and thickening properties (Dickinson, 1992). The most common cellulose derivatives used in food are: carbomethyl cellulose (CMC) and hydroxypropyl methylcellulose (HPMC). Many studies have proven the stabilizing properties both of CMC (Arancibia et al., 2013; Hayati et al., 2009) and HPMC (Camino and Pilosof, 2011; Camino et al., 2011; Futamura and Kawaguchi, 2012).

Nevertheless, it has been well known that bacteria (*Komagataeibacter sucrofermentans* DSM 15973) could synthesize cellulose (Martinez-Sanz, Lopez-Rubio &Lagaron,2011;Okiyarna et al., 1992; Ougiya et al., 1997). Specifically, when being fermented in a culture rich in polysaccharides, these bacteria produce pellicles of bacterial cellulose (BC). Bacterial cellulose (BC) is an environmentally-friendly polymeric material, which is now receiving increased attention in human society. It is an unbranched polymer with nanofibrils, made up of (1/4)b-glycosidic linked glucose units. These linear glucan chains form highly regular intra- and inter molecular hydrogen bonds. In the process of forming these fibers, polymerization and crystallization occur together to include both characteristics. Then, these nanofibrils have cross-sectional dimensions in the nm range, which can then aggregate to form microfibrils with a width of 50 - 80 nm, and a thickness of 3 - 8 nm (Tabuchi, 2007). These can then form a 3D network structure. This fine structure makes BC different from other microbial polysaccharides.

It is well established that dietary fiber offers a range of health benefits and can assist in reducing the risk of chronic diseases such as diabetes, obesity, cardiovascular disease, and diverticulitis (Cho and Almeida, 2012). Bacterial cellulose is a type of such dietary fiber, and regulatory is classified as “generally recognized as safe” (GRAS) and was accepted as such by the USA Food and Drug Administration in 1992.

When compare with other dietary fiber (DF), BC has several advantages:

Bacterial cellulose produced by microorganism, is a highly pure form of cellulose and does not require harsh chemical treatments for the isolation and purification as it is necessary for cellulose derived from plant sources.

Bacteria can utilize a culture medium resource such as fruit syrup to grow, reproduce and secrete in situ the flavor and color of the medium. The BC cultured in these medium can acquire the nature flavor and pigment of the fruit.

Producing a range of shapes and texture, such as films, multishaped pulps, filaments, spheres, particles, whiskers, etc. can endow BC with many different applications in food.

BC' fibers are within the nano-scale with a fine three dimensional network structure, which enables BC to be used in novel food manufacturing processes. Thanks to these properties, bacterial cellulose has been used in various areas such as biomedicine (Bodin et al., 2011; Fu et al., 2013; Meftahi et al., 2010), cosmetics, the paper industry (Iguchi et al., 2000) and many others. In the food industry, the use of BC is still limited, but it has been used to texturize a dessert from the Philippines (Nata de coco). To make this dessert, thick gel sheets are fermented with coconut water, cut into cubes and immersed in sugar syrup (Iguchi et al., 2000; Shi et al., 2014). Although not used extensively in food yet, BC has great potential as a food ingredient, where it could be used to alter the rheological behavior of food as a thickening, stabilizing or gelling agent. Recently, BC has been shown to act as a stabilizer in emulsions (Kalashnikova et al., 2011; Paximada et al., 2014). However, BC as a thickener for the continuous phase has not been studied extensively and the effect on the rheological behavior of emulsions is not well known.

2.6. Concerns about nanotechnology

Numerous points of view have been established regarding the utilization of nanotechnology in food products and its potential danger to human health. It is well known that nanoparticles have, by definition, different physicochemical properties compared to the macro-particles. This difference is more evident when the nanoparticles pass through the human gastrointestinal (GI) tract. Specifically, nanoparticles exhibit a higher cellulose uptake in the GI tracked compared to the conventional ones, due to their ability to penetrate the mucus layer across the gut wall (Bouwmeester et al., 2009). This could affect the absorption and bioavailability of compounds used in nanoparticles. Hence, the consumption of nano-foods could potentially lead either on beneficial health consequences or harmful. For example, bioactive components encapsulated in nanoemulsions can increase their bioavailability in foods, but some bioactive components may exhibit toxic effects when consumed at high levels due to greater absorption (Chaudhry et al., 2008).

This is attributed to the larger area they occupy in comparison to the same amount of material in a larger lump and also to the fact that their phenomena are interpreted by quantum physics. Therefore, there's an ongoing concern that some nanomaterials/particles could be toxic towards humans, animals or plants (Kong et al., 2011).

What is more, nanoparticles, due to their small size, have the ability to pass through cells walls and ultimately to be absorbed into bloodstream. The macro-particles do not show this ability, so they may affect the human health. The nanoparticles may also adsorb or bind to various components in the body and act as a carrier to transport them across different parts of the body (Bouwmeester et al., 2009).

Exposure to nanomaterials as a result of nanotechnologies being used in the food industry can take three main routes; dermal contact, inhalation and ingestion, with the most common one the ingestion (Cushen et al., 2012). When the nanoparticles insert in the GI tract, either they form compounds with other food material or interact with one another or remain stable. The effect of the intake of nanofoods on the absorption is still unknown. For instance, the use of nanoemulsification in ice cream or mayonnaise allows the use of significantly less fat than their traditional equivalents without the loss of mouthfeel (Chaudhry et al., 2008). Whoever, there is still limited knowledge on whether the smaller fat globules would be absorbed across the gut epithelial.

Recent studies have observed that various nanoparticles lead in inflammation, oxidative stress, DNA breakdown, stimulation or suppression of the immune system, and signs of early tumor formation (Carlson et al., 2008). Polysaccharide nanocrystals derived from chitin, chitosan, cellulose (nanocrystalline cellulose, NCC) or starch as

well as cellulose nanofibers are mainly concerned about toxicity. No evidence of inflammatory effects or cytotoxicity on mouse and human macrophages was observed due to exposure to nanofibrillated cellulose (NFC) (Vartiainen et al., 2011). On the contrary, clear genotoxic effects depending on the material source have been shown for cellulosic nanofibers in plant, human and animal cells (de Lima et al., 2012).

Potential toxicity of lipid nanoparticles could be associated with increased bioavailability of bioactive compounds that are toxic at high levels, direct absorption, interference with normal gastrointestinal function and compositional (high levels of specific surfactants or solvents used for their production) (McClements, 2013). Nanoemulsions formed with modified starch and WPI showed increased cytotoxicity on HepG2 cells, hence more *in vivo* investigation is required, since there has been no evidence that nanoemulsions can reach the liver tissues by permeating the epithelium layers lining the digestive tract (Yu and Huang, 2013). Adverse results have been reported for nanoemulsions prepared with food-grade proteins and surfactants intended as drug release systems (He et al., 2011). According to this research nanoemulsions prepared with whey, soy or β-lactoglobulin proteins demonstrated higher Caco-2 cell viability in comparison to traditional emulsifiers such as egg phosphatidylcholine, and Tween 80, indicating significant cytotoxicity.

To sum up, toxicological properties vary among particulate nanomaterials; hence it is of high importance to apply a risk assessment on a case by case basis (Munro et al., 2009).

Consumers & nano

The nano-foods should be accepted by consumers. Clear communication of the benefits of using nanotechnologies for preparing foods over existing technologies must be addressed to the public. Both benefits and risks should be acknowledged; however, for acceptance it must be clear to the public that not only do the benefits outweigh the risks, but that the risks are acceptable. It was found that public knowledge about nanotechnologies in general was limited in the United States (cobb and Macoubrie, 2004), but the results show that perceptions were generally optimistic. In Europe it was found that perceptions were less positive (Gaskell et al., 2005).

Recently, the trust and willingness of consumers to buy a functional juice containing nanoencapsulated vitamin D was assessed (Roosen et al., 2015). The authors concluded that nanotechnology raises concerns in consumers regarding the product itself or its packaging, although it was not established if this is generated from the lack of awareness of nanotechnology in the general public or lack of awareness of nanotechnology uses in the food industry. Another research revealed that

consumers are more hesitant in buying foods with nanotechnology packaging and even more hesitant towards nanotechnology foods (Siegrist et al., 2007).

Legislation

Recently, European Union had established a group to observe the implications of nanotechnology, named the Scientific Committee on Emerging and Newly Identified Health Risks. The deliberation of the Committee resulted in the publication of a list of risks related to nanoparticles, in the opinion of “Scientific basis for the definition of the term nanomaterial” (EU, 2011).

Currently, the nanomaterials and nanotechnologies in EU fall under the regulations of horizontal and vertical legislation. However, the initial scope of the existing horizontal legislation (General Product Safety Directive - GPSD, Evaluation, Regulation on Authorisation and Restriction of Chemicals-REACH) was broad and did not specifically aim to enclose the attributes of nanotechnologies (Cushen et al., 2012).

GPSD provides the definition of a safe product, covering all types of products on the market. Nanomaterials are regulated by REACH because they are covered by the definition of a chemical "substance" in both Regulations. The general obligations in REACH therefore apply as for any other substance, although there are no provisions referring explicitly to nanomaterials. REACH provides an over-arching legislation applicable to the manufacture, placing on the market and use of substances on their own, in preparations or in articles. Nanomaterials that fulfill the criteria for classification as hazardous under Regulation (EC) No 1272/2008 on classification, labeling and packaging (CLP) of substances and mixtures must be classified and labeled.

Vertical legislation, which was introduced within the last few years, specifically regulates nanotechnologies and industrial sectors that utilize them. Revisions made on the regulation for cosmetics (EC No 1223/2009) were able to provide a first vertical regulation with a legal definition for nanomaterials. Within the revised regulation it is declared that nanomaterials used for the production of cosmetics should be assessed with regards to toxicity safety before allowed to commercialization. Their presence should also be included in the list of ingredients indicated with the word “nano” in brackets (Cushen et al., 2012). The Regulation on Novel Foods (EC No 258/97) contains indirectly a legal definition of nanomaterials. According to the Regulation novel foods are defined as “foods and food ingredients that have not been used for human consumption to a significant degree within the Community”. As a consequence, food products containing nanomaterials are regarded as novel foods, rising safety assessment and authorization requirements before commercialization.

Another vertical regulation relates to food additives. The Food Additives Directive, (EC No 1333/2008), entered into force in 2010, represents the first piece of legislation referring exclusively on nanotechnologies. As mentioned in article 12, if an already approved starting material or additive undergoes any changes in particle size for example through nanotechnology, shall be considered a different additive requiring de novo safety evaluation and authorization.

The trend to be cautious towards nanotechnology legislation has been followed globally. It is of interest to mention that Taiwan is the first country where a Nano Mark System has been established. Specifically, this system certifies the consumers whether a food has been produced with nanotechnology (Chau et al., 2007). In the USA, various agencies has been established that regulate products with nanotechnology, however there is still no regulatory framework that provides protection for consumers (Corley et al., 2009). Finally, in Australia they follow the horizontal legislation procedure for nanotechnologies (Cushen et al., 2012).

Chapter 3. Materials & Methods

3.1. Materials

3.1.1. Materials

Whey protein isolate (WPI), Lacprodan DI-9224, was kindly provided by Arla (Arla Foods Ingredients, Amba-Denmark). HPMC Tylopur SE-15 (HMPCL) and SE-4000 (HPMCH) were obtained from SE Tylose GmbH & Co. KG (Wiesbaden, Germany). CMC (food grade) was kindly donated from F Gutkind& Co Ltd (Oxon, United Kingdom). The viscosity (20^{o}C) of 1%wt CMC solution was 5000mPa s according to the manufacturer. Tween 20 was purchased from Fisher Scientific (St. Louis, USA). Extra virgin olive oil was purchased from a local supermarket and used as such. (-)-Epigallocatechin gallate hydrate (EGCG) was purchased from TCI (TCI, USA). All the remaining chemicals used were of analytical grade.

3.1.2. BC production

Bacterial cellulose (BC) was produced as described previously (Tsouko et al., 2015). Briefly, bacterial cultivations (*Komagataeibacter sucrofermentans* DSM 15973) were grown using a synthetic medium as described by Hestrin and Schramm, (1954) containing a carbon source (20 g/L), yeast extract (5 g/L), peptone (5 g/L), Na2HP04 (2.7 g/L) and citric acid (1.15 g/L). The inoculum was prepared by growing the microorganism at 30 °C and 100-120 rpm during 2 days, in Hestrin and Schramm liquid medium. Fermentations were carried out in 250 mL Erlenmeyer flasks containing 50 mL of synthetic medium and were inoculated with 10% v/v inoculums volume. All shake flasks were incubated at 30 °C in static mode for 15 days.

After cultivation, bacterial cellulose was removed from the cultures and rinsed with tap water to remove any residual media. Next, it was treated with 2 M NaOH to eliminate bacterial cells and then washed repeatedly with tap water until the BC dispersions obtained a neutral pH.

The purified BC pellicles were cut into small pieces and mixed with deionized water to prepare a BC suspension. The BC pieces were further disintegrated with a high shear blender (13500 RPM, Ultra Turrax T25, IKA, Germany) which led to the formation of a white precipitate.

In Chapters 5, 6, and 7, the precipitate was treated with ultrasounds by an ultrasonic homogenizer model Sonopuls 3200 (Bandelin Electronic Gmbh& Co, Berlin) equipped with a 3 mm in diameter microtip (MS 73, 284 μmss peak-to peak amplitude). Ultrasonication carried out at a frequency of 20 kHz, while the processing time was 3 min and the final nominal power added to the sample was 82 W. The temperature was maintained at 25 (± 1)^{o}C by circulating cold water with a pump.

In Chapters 8 and 9, the precipitate was treated with sulfuric acid (60% w/w), in a cellulose/acid ratio of approximately 20 g/L, at 60°C for 4 days, until homogenous solution was obtained. The cellulose nanowhiskers were obtained as a white precipitate after several centrifugations and washing cycles at 12.500 rpm and 25^{o}C for 10 min. The pH of the samples was measured after the washing-centrifugation cycles, being around 3 for all the samples. Then, the material was re-suspended in deionized water to obtain the final product as a partially hydrated precipitate.

3.1.3. EGCG structural modification

The esterification of EGCG was carried out with stearoyl chloride, according to the procedure described by Panagopoulou, Evageliou and Mandala (unpublished data). Briefly, and in the presence of pyridine, the chloride was added to EGCG dissolved in ethyl acetate. The mixture was stirred and then cooled to ambient temperature and filtrated. The collected upper organic layer was converted by solvent evaporation to a light yellow dry powder. The powder was stored in desiccators at -20°C until further use.

3.2. Experimental procedure

3.2.1. Experimental procedure for the production of emulsions containing BC fibrils treated by ultrasounds or acid hydrolysis (Chapter 4)

The purified BC pieces (3.1.2) were further disintegrated with a high shear blender for 10 min (13500 RPM, Ultra Turrax T25, IKA, Germany) which led to the formation of a white precipitate.

In order to evaluate ultrasounds as a pre-treatment method for BC fibrils, a dilution of the suspensions with deionized water took place leading to a final concentration of 0.1, 0.5 and 1% wt. respectively. The suspensions were then submitted to ultrasonic treatment by an ultrasonic homogenizer model Sonopuls 3200 (Bandelin Electronic Gmbh& Co, Berlin) equipped with a 3 mm in diameter microtip (MS 73, 284 μm_{ss} peak-to peak amplitude). Ultrasonication carried out at a frequency of 20 kHz, while the processing time was 1 (BC1), 3 (BC3) and 5 min (BC5) and the final nominal power added to each sample was 82 W. The temperature was maintained at 25 (± 1)^{o} C by circulating cold water with a pump. All samples were prepared in triplicate.

In order to evaluate acid hydrolysis as a pre-treatment method for BC fibrils, various acids and processing conditions had been tested. Specifically, BC fibrils were treated with either sulfuric acid (60% w/w) or with hydrochloric acid (2 N). The fibrils were dissolved in the solvents and then they were put into water bath with standard temperature at 40°C or 60°C for 0 to 72 h. The cellulose nanowhiskers were obtained as a white precipitate after several centrifugations and washing cycles at 12.500 rpm and 25^{o}C for 10 min. The pH of the samples was measured after the washing-centrifugation cycles, being around 3 for all the samples. Then, the material was re-suspended in deionized water to obtain the final product as a partially hydrated precipitate.

The optimal processing conditions for both procedures were found and then the ability of the BC fibrils to stabilize o/w emulsions was investigated. For this purpose, emulsions with 20% wt. olive oil and various BCN concentrations (0.1-1% wt) were produced.

3.2.2. Experimental procedure for the production of emulsions containing various thickeners (Chapter 5)

A 50mM, pH 3.8 citrate stock buffer solution was prepared by dissolving the appropriate amounts of citric acid monohydrate and sodium citrate in deionized water. HPMC stock solutions (2% wt) were prepared by dissolving the appropriate amount of powder into buffer solutions under continuous stirring at 70^{o}C for 90min, left to cool down at room temperature and then stored in the refrigerator at 4^{o}C

overnight. CMC stock solutions (2%wt) were also prepared using the same procedure. A 1.5% wt xanthan gum (XG) stock solution and a 2% wt locust bean gum (LBG) stock solution were prepared by adding the thickeners to hot water at 60 ^{o}C and continuous stirring for 90 min. After the thickeners were completely dissolved, the solutions were left to cool down at room temperature and then stored overnight in the refrigerator at 4 ^{o}C.

Coarse oil-in-water emulsions of a total of 20g in a ratio of 10:90 w/w were prepared. Specifically, extra virgin oil (5%) was added to the aqueous solution (which total ratio was 95%) containing different celluloses (HPMCL, HPMCH, CMC, BC) at various concentrations (0.1, 0.3, 0.5, 0.7 and 1% wt). Samples were prepared at pH 3.8 and subsequently mixed in a high-shear blender (13500 RPM, 2min, Ultra Turrax T25, IKA, Germany). For the secondary emulsions, this procedure was followed by 2min of ultrasonication through an ultrasonic device (Sonopuls 3200, equipped 13mm diameter MS 73-492 probe, Bandelin Gmbh& Co, Berlin, Germany) operating at a frequency of 20 kHz and 20% amplitude).

In order to compare the ability of BC as a thickener, the secondary emulsions containing WPI were also prepared with XG and LBG. In this case, the concentration of WPI in the secondary emulsions was chosen as 2% wt. In this case, we assume that the interactions between WPI and polysaccharides could be neglected and the differences in emulsion properties are merely an effect of the thickeners themselves. The amount of BC, XG and LBG added to the emulsions was chosen in such a way that the apparent viscosity at shear rate 0.1 s^{-1} is similar. These emulsions were prepared by a lab-scale high-pressure homogenizer (LabhoScope Homogenizer, Delta Instruments, The Netherlands) for 8 min of recirculation at 200 bar.

3.2.3. Experimental procedure for the production of WPI-BC emulsions with various homogenization techniques (Chapter 6)

WPI stock solutions (11% wt) were prepared by dissolving the appropriate amount of powder into a 50mM citric acid solution under continuous stirring at room temperature for 90 min and stored in the refrigerator at 4^{o}C overnight to ensure complete hydration.

Primary oil-in-water emulsions of 50 g in total with an oil percentage of 10% wt were prepared. Specifically, extra virgin olive oil was added to WPI solutions (90% wt aqueous phase) at a pH of 3.8 containing WPI at various concentrations (4-10% wt) and subsequently mixed in a high-shear mixer (16800 rpm, 3 min, Ultra Turrax T25, IKA, Germany).

The emulsions were further treated by a lab-scale high-pressure homogenizer (LabhoScope Homogenizer, Delta Instruments, The Netherlands) for 8 min of recirculation at 200 bar or by an ultrasonic device (Sonopuls 3200, Bandelin

GmbhandCo, Berlin, Germany) operating at constant frequency of 20 kHz, while the processing time was 2 min and the final nominal power added to the sample was 82 W. The amplitude was constant at 60%. The resulting emulsions were further diluted with the appropriate amount of buffer (pH 3.8) and BC solutions under continuous stirring to achieve a final concentration of 5% wt oil, 2- 5% wt WPI and 0- 1% wt BC in the secondary emulsions. The samples were prepared in triplicate and the results were reported as the average values and the standard deviations.

3.2.4. Experimental procedure for the incorporation of EGCG in emulsions (Chapter 7)

The aqueous phase of the emulsions consisted of a BC-WPI solution. BC-WPI solutions were prepared by mixing the precise amounts of the WPI and BC solution through gentle stirring. The final concentrations were those reported at Chapter 6: i.e. 5% wt. WPI and 1% wt. BC. The pH of the solutions was adjusted at 3.8.

Primary oil-in-water emulsions with an oil percentage of 10% w/w were prepared. Specifically, extra virgin olive oil was added to BC-WPI solutions (90% w/w aqueous phase) and subsequently mixed in a high-shear mixer at 16800 rpm for 3 min (Ultra Turrax T25, IKA, Staufen, Germany). During the second homogenization process, the emulsions were further treated with an ultrasonic homogenizer model Sonopuls 2200 (Bandelin Electronic Gmbh & Co, Berlin, Germany). Ultrasonication was carried out at a frequency of 20 kHz, while the processing time was 3 min and the final nominal power added to each sample was 82 W.

In order to compare the ability of the emulsions to encapsulate EGCG, the emulsions were also prepared with H-EGCG or L-EGCG. In this case, the both EGCG was incorporated in the oil or the aqueous phase of the emulsions with a total concentration varying from 0.1 to 0.5% w/w of the total mass content. EGCG was added in the aqueous phase under continuous stirring of the BC-WPI solution. However, when EGCG was incorporated into the oil phase, it was first dissolved in ethanol and then the appropriate amount of oil was added and the solution was placed in a rotary evaporator until the ethanol was evaporated.

3.2.5. Experimental procedure for the production of particles through solution electrospraying (Chapter 8)

BC-WPI solutions were prepared by dissolving a precise amount of the WPI and Tween 20 in the BC solution through gentle stirring for 2 hours at room temperature. The pH of the solutions was adjusted at 3.6. The resulting solutions achieved a final concentration of 0- 16% wt BC, 10- 30% wt WPI and 2% wt Tween 20.

The electrospinning apparatus, equipped with a variable high voltage0–30 kV power supply, was a Fluidnatek LE-10 (BioInicia S.L.,Valencia, Spain). Solutions were

introduced in a 5 mL plastic syringe and were electrosprayed under a steady flow-rate using a stainless-steel needle (inner diameter 0.7 mm). The syringe was lying on a digitally controlled syringe pump while the needle was in horizontal towards a copper grid used as collector. The experiment was carried out at ambient conditions. The electrospraying conditions for obtaining the particles were optimized and fixed at 20-80 μL/ h of flow-rate, 10-20 kV of voltage and a tip-to-collector distance of 10 cm. The product yield was determined according to the following equation:

$$\text{Product yield } (\%) = \frac{Mass\ of\ electrosprayed\ product\ recovered\ from\ collector}{Mass\ of\ solids\ in\ the\ processed\ emulsion} * 100 \quad \text{(Eq. 3.1)}$$

All samples were prepared in duplicate.

In order to compare the ability of the solutions to encapsulate EGCG, the optimum solution (8% wt. BC, 20% wt. WPI, 2% wt. Tween) were also prepared by adding EGCG under continuous stirring of the BC-WPI solution. Two different amounts of EGCG were added reaching a final concentration of 0.1% and 0.2 w/w of the total mass content.

3.2.6. Experimental procedure for the production of particles through emulsion electrospraying (Chapter9)

The aqueous phase of the emulsions consisted of a BC-WPI solution. BC-WPI solutions were prepared by mixing the precise amounts of the WPI, Tween 20 and BC solution through gentle stirring. The pH of the solutions was adjusted at 3.8.

Primary oil-in-water emulsions with an oil percentage of 10% w/w were prepared. Specifically, extra virgin olive oil was added to BC-WPI solutions (90% w/w aqueous phase) and subsequently mixed in a high-shear mixer at 16800 rpm for 2min (Ultra Turrax T25, IKA, Staufen, Germany). During the second homogenization process, the emulsions were further treated with an ultrasonic homogenizer model Sonopuls 2200 (Bandelin Electronic Gmbh & Co, Berlin, Germany). Ultrasonication was carried out at a frequency of 20 kHz, while the processing time was 1 min and the final nominal power added to each sample was 82 W. The temperature was maintained at 25 (± 1) ^{o}C using an ice bath. The resulting emulsions had a final concentration of 90% w/w aqueous phase containing 8% w/w BC, 20% w/w WPI, and 5% w/w Tween 20 and 10% w/w olive oil.

In order to compare the ability of the emulsions to encapsulate EGCG, the primary and secondary emulsions were also prepared with H-EGCG or L-EGCG. In this case, the EGCG was incorporated in the oil or the aqueous phase of the emulsions with a total concentration of 0.1% w/w of the total mass content. Table 3.1 summarizes the different emulsions tested during the present study.

Table 3. 1 Preparation parameters of emulsions studied in this chapter

Emulsions	Homogenization method	Type of EGCG	Addition phase
BLUT	High shear homogenizer	-	-
BLUS	Ultrasounds	-	-
UTHW	High shear homogenizer	Hydrophilic	Aqueous
USHW	Ultrasounds	Hydrophilic	Aqueous
UTLW	High shear homogenizer	Lipophilized	Aqueous
USLW	Ultrasounds	Lipophilized	Aqueous
UTHO	High shear homogenizer	Hydrophilic	Oil
USHO	Ultrasounds	Hydrophilic	Oil
UTLO	High shear homogenizer	Lipophilized	Oil
USLO	Ultrasounds	Lipophilized	Oil

EGCG was added in the aqueous phase under continuous stirring of the BC-WPI solution. However, when EGCG was incorporated into the oil phase, it was first dissolved in ethanol and then the appropriate amount of oil was added and the solution was placed in a rotary evaporator until the ethanol was evaporated.

The emulsions were processed using a lab benchtop Fluidnatek LE10 system from Bioinicia, S.L., Spain equipped with a variable high voltage 0–30 kV power supply. Emulsions were introduced in a 5 mL plastic syringe and were electrosprayed under a fixed flow-rate and voltage using a stainless-steel needle (inner diameter 0.9 mm). The experiments were carried out at ambient conditions, the voltage was set to 15 (± 1) kV, the flow rate was set to 60 (± 5) µL/h, while the tip-to-collector distance was 10 cm. The product yield was determined according to equation 3.1. All samples were processed in duplicate.

3.3. Methods

3.3.1. Stability of emulsions (Chapters 5, 6, 7, 8, 9)

The simplest method to evaluate emulsion stability is visual observation for the calculation of the separation percentage caused by serum formation in the bottom. However, even optically homogenous samples that do not exhibit gravitational separation can still destabilize by aggregation phenomena. Nowadays, multiple light scattering (MLS) is the most widely used technique to monitor the dispersion state of a product, identifying and quantifying destabilization phenomena. It works on concentrated dispersions (up to 40 % total solids) without dilution.

The multiple light scattering device allows the optical characterization of any type of dispersion by using a mobile reading head composed of a transmitting NIR diode (λ=850 nm) and two synchronous detectors analyzing the transmitted (T) and backscattered (BS) light with acquisitions every 40 µm. Emulsion or dispersion samples are inserted in a borosilicate tube and scanned from bottom to 80 mm tube height in order to obtain back scattering and transmission intensity vs. tube height profiles. When light is sent through the sample, it is backscattered by the particles/ droplets. The backscattering or transmission intensity is directly proportional to the size and volume fraction of the dispersed phase. Therefore, local changes in concentration (creaming and sedimentation) and global changes in size (flocculation, coalescence) can be detected and monitored (McClements, 2005).

The gravitational stability of emulsions or suspensions upon storage was followed by measuring using a Turbiscan MA 2000 apparatus (FormulAction, Toulouse, France). Emulsion samples (approximately 6 mL) were put into test tubes and stored at 4 ^{o}C. Measurements were performed with intervals of 24 hours and a total time of 30 days. The stability is presented as the serum Index (SI), which is calculated as:

$$\mathrm{SI}\ \% = \frac{\mathrm{H_s}}{\mathrm{H_e}} * 100 \ (\mathrm{Eq.}\ 3.2)$$

where Hs is the height of the serum layer and He is the total height of the emulsion/ suspension. A lower SI therefore represents a more stable emulsion/ suspension.

3.3.2. Droplet size analysis (Chapters 5, 6, 7, 8, 9)

Currently, a variety of methods are available to evaluate the droplets size distribution of emulsions. Most commonly used techniques include laser scattering, ultrasonic attenuation spectroscopy, nuclear magnetic resonance and microscopy-image analysis. Light scattering technologies used in the field of particle characterization include two main techniques: static light scattering (SLS, the measurement of scattering intensities due to light–particle interaction at various spatial locations) and dynamic light scattering (DLS, the measurement of scattering due to light–particle interaction as a function of time) (Xu, 2015).

In SLS technique (also known as laser diffraction), a high intensity monochromatic light, usually a laser, passes through a dilute solution containing the particles. The laser beam is scattered by the particles in many directions and detectors are used to measure the scattering intensity at one or many angles. The scattering pattern (intensity of scattered light vs scattering angle) is related to the particle size profile of the dispersion, which can be analyzed using the Mie theory of light scattering to calculate the particle size distribution, assuming a volume equivalent sphere model. Mie theory applies when the particles are of similar or not significantly higher

diameter than the wavelength of the beam. On the contrary, the Fraunhofer theory is used for larger particles.

Dynamic light scattering (DLS) is the most popular and common technique that is used to determine the size and size distribution of macromolecules, polymers and submicron sized particles typically dissolved in suspensions. The ability of the method to estimate particle size is based on the Brownian motion – random thermal, translational, or rotational (diffusion) movement- of the particles in suspensions. Due to the constant movement of the particles, the intensity of the scattered light changes temporarily with time. These time-dependent variations are related to the size of the particles, which can be detected and recorded as Intensity vs time profiles. The auto-correlator of the device generates afterwards a correlation function, which is an exponentially decaying time equation. The decay constant can be used to calculate the diffusion coefficient of the particle, which provides an estimation of the hydrodynamic radius of the droplet. Devices of the latest technology can provide measurement of particles with size smaller than 1 nm up to several microns which is difficult to achieve with other techniques (McClements, 2005).

The droplet size distribution of the emulsions and the diameter size of the electrosprayed particles was determined using SLS (Malvern Mastersizer 2000, Malvern Instruments Ltd, UK) in Chapters 5,6 and 7; or DLS (Zetasizer Nano ZS, Malvern Instruments, Worcestershire, UK) in Chapters 8 and 9. The refractive indices of olive oil and water were taken as 1.467 and 1.330, respectively, and the Mie theory was used for the analysis (Chapters 8,9). The size distribution was expressed as the mean diameter (D_{50}) the surface-weighted mean diameter, ($D_{3,2}$) and as the volume-weighted mean diameter ($D_{4,3}$). The polydispersity index was also evaluated used the following equation:

$$\mathrm{PDI} = \frac{D_{90} - D_{10}}{D_{50}} \quad \text{(Eq. 3.3).}$$

Where D_{10}, D_{50} and D_{90} are diameters at 10%, 50%, and 90% cumulative volume respectively.

At least three measurements were performed on freshly prepared emulsions at ambient temperature, and the results are expressed as the average value.

3.3.3. Emulsions' and particles' structure (Chapters 5, 6, 7, 8, 9)

Optical microscopy is a technique often used to observe the structure and phenomena taking part in solutions or emulsions. A typical optical microscope consists of four basic elements: an illumination source, mechanical stage for samples, optical system and detector. The illumination source of visual light interacts with the sample and the optical system with lenses collects and focuses the light into

the eye and/or camera. Images obtained can be also used for droplet size estimations by using image analysis software.

Optical microscopy is a technique often used to observe the structure and phenomena taking part in emulsions. The four basic elements of a microscope are an illumination source, mechanical stage for samples, optical system and detector. The illumination source of visual light interacts with the sample and the optical system with lenses collects and focuses the light into the eye and/or camera. Images obtained can be also used for droplet size estimations by using image analysis software.

Samples of freshly prepared emulsions were placed on a microscope slide, covered with a cover slip and observed under 40x magnification using an optical microscope (Kruss Optronic, Germany) (Chapter 5,6,7,9). Several pictures were taken from random sample positions representing the overall appearance of the emulsions. The micrographs were recorded using a camera (SONY, Hyper HAD, CCD-Iris) connected to a computer.

The microstructure of cellulose aqueous suspensions (Chapter 4) was determined using a JEOL 100s equipped with an image acquisition system. Samples of freshly prepared suspensions were diluted 20 times with deionized water, stained with PTA and placed on the grid. After drying at room temperature, several pictures were taken from random sample positions representing the overall structure of the suspensions. These pictures were analyzed with an image analysis software (Image-Pro Plus 7.0, Media Cybernetics, Rockville USA) in order to measure the fibrils' width.

Scanning electron microscopy (SEM) is being used as a means of evaluation the microstructural characteristics of materials with scales ranging from millimetres to nanometres. Typically, a SEM consists of an electron source to generate a beam of primary electrons; a column with electromagnetic lenses for focusing and demagnifying the primary electron beam; coils for scanning the electron beam across the specimen surface; a chamber containing a stage to hold the specimen; vacuum pumps to maintain the system under high vacuum (usually of the order of 10^{-5} to 10^{-7} Pa); and one or more detectors for collecting signals generated by electron irradiation of the specimen. Finally, the magnified image is displayed on a monitor, as the beam is scanned pixel- by-pixel across the field of view. When the sample is electrically insulating, such as polymers, coating with conductivie materials, such as gold, could serve as a solution to characterize samples through SEM.

The microstructure of the electrosprayed particles was determined using a JEOL 100s (Chapter 8) or a Hitachi S-4100 (Chapter 9) microscope at an accelerating voltage of 5 kV equipped with an image acquisition system. The pressure in the specimen chamber was $7 \cdot 10^{-4}$ atm, while in the gun chamber 1·10-4 atm.

Samples were sputtered with a gold-palladium mixture (SC 7640, Polaron, Kent, UK) under vacuum before examining their structure. After 120 s the thickness of the coating was 8 nm. Several pictures were taken from various positions representing the overall structure of each sample. The magnification was set at x 10000.

3.3.4. Samples' rheology (Chapters 4, 5, 6, 7, 8, 9)

Rheology is the study of the deformation and flow of the materials, a term invented by Bingham and accepted by the American Society of Rheology in 1929. The materials under investigation can range from low-viscosity fluids to semisolids and gels to hard, solid-like food products.

The importance of the flow properties of emulsions lays on both technical and consumer acceptance issues. Considering technical matters, numerous industrial processes and handling (pumping, filling, mixing, and packing) of emulsified products require information regarding the flow properties to estimate pump transfer rates, energy consumption and mixing efficiency. Consumers' buying intention is also driven by several rheological properties, the most important of them being creaminess, consistency, body as well as pourability easiness (Barnes, 1994).

The bulk rheology of emulsified systems can be assessed using steady state (shear stress as a function of shear rate), constant stress or oscillatory methods (Tadros, 1994). Most commonly used rheology techniques in food emulsions or dispersion include flow and small amplitude oscillatory tests.

Flow measurements

Depending on the operation principle of the rheometer used (stress-controlled or strain-controlled), during a flow test the fluid sample is being subjected to different values of shear rates (γ), while the resulting values of shear stress (τ) are measured, or inversely. Stress-controlled rheometers provide an advantage, since they can operate in both controlled stress (torque) as well as controlled strain (rotational speed) mode (McClements, 2005). The resulting flow curves can be used to characterize the dispersion regarding Newtonian (no shear dependency of viscosity) or non-Newtonian behavior (pseudoplastic or dilatant). Usually, the flow curves begin with increasing shear rates (or stress), although it is also possible to conduct experiments starting at high shear rates which gradually decrease. Performing, both upward and downward measurements can provide information on the time dependent flow behavior of the sample derived from the surface area in between the two flows (Barnes, 1994).

Rheological measurements of the solutions/ emulsions at Chapters 4, 5, 6, 7, 8 and 9 were performed on a stress-controlled rheometer (Discovery HR-3, TA Instruments, New Castle, DE, USA or (Physica MCR 501, Anton Paar, Graz, Austria) equipped with a concentric cylinders, cone and plate geometry (30mm cup diameter, 28mm bob

diameter). Temperature was kept constant (25.0 ± 0.1 ^{o}C) using a water bath and the gap was set at 0.1 cm. The apparent viscosity was determined versus the imposed shear rate from 0.1 to 1000 s^{-1}. 10 points per decade were measured while the whole measuring time was 10 min. Solvent evaporation was neglected within this period. All the flow curves were analyzed using the Herschel-Buckley model:

$$\tau = \tau_o + k\dot{\gamma}^n \quad (Eq. 3.4)$$

where τ is the shear stress (Pa), τ_o is the yield stress (Pa), k is the consistency coefficient (Pa s^n), $\dot{\gamma}$ is the shear rate (s^{-1}) and n is the flow behavior index (dimensionless).

The viscosity measurements are reported as the average of at least three different samples in order to assure reproducibility. All rheological measurements were completed at freshly prepared emulsions.

Small amplitude oscillatory measurements

Oscillatory measurements were also performed on the BCN suspensions. Before the dynamic viscoelastic measurements, the linear viscoelastic region (LVR) was determined by strain sweep experiments with the strain varied from 0.01 to 10% at a fixed frequency of 10 rad/s. The region, where the G' and G'' values were parallel was characterized as LVR and in this case was 0.3% of strain. Subsequently, a dynamic frequency sweep was conducted by applying a constant strain, with a frequency range between 0.1-100 rad/s. All the rheological measurements are reported as the average of at least three different samples in order to assure reproducibility.

Thixotropy

Moreover, the same rheometer was used in controlled shear mode to test the shear rate/ time dependency of the suspensions. The used conditions were the same as the viscosity measurements. The shear rate increased from 0.01 to 1000 s^{-1}, followed by a pause at 1000 s^{-1} for 10 min and by a deceleration of shear rate from 1000 to 0.01 s^{-1}.

Interfacial flow measurements

Interfacial viscosity has been analyzed thoroughly in paragraph 2.4. In Chapters 8 and 9, the same rheometer (Discovery HR-3, TA Instruments, New Castle, DE, USA) was used to carry out interfacial rheological measurements. The geometry that was used was the Du Nouy ring (inside cup diameter 12.7 mm, outside cup diameter 25.6 mm, inside ring diameter 19 mm, outside ring diameter 25.4 mm, volume 4 ml). The shear rate was set between 0.1 and 100 s^{-1}. The system was positioned at the interface and the sample was kept in direct contact with the ambient atmosphere. The soaking time of the sample was 10 min.

3.3.5. Samples' water holding capacity (Chapters 4)

To determine the water holding capacity (WHC) of BCN suspensions, they were centrifuged at 5000 RPM for 15 min. After the removal of the supernatant, the sediment was weighed and dried at 60 ^{o}C in order in order to ensure complete drying. WHC was calculated by the following equation:

$$\mathrm{WHC} = \frac{\mathrm{W_r}}{W_c} \quad (\mathrm{Eq.\ 3.5})$$

Where W_r is the mass of the removed water during drying and W_c is the dry content of cellulose. The results are reported as the average of at least three samples.

3.3.6. Samples' ζ-potential (Chapters 4, 5, 6, 7, 8, 9)

In commercial instruments, the particle velocity is often determined automatically using sophisticated light scattering techniques (Hunter, 1986). Briefly, two coherent beams of light intersect with each other at a particular position within a measurement cell so that they form an interference pattern that consists of regions of low and high light intensity. The charged sample droplets are made to move through the interference pattern by applying an electrical field across the cell. As the droplets move across the interference pattern they scatter light in the bright regions, but not in the dark regions. By measuring and analyzing the frequency of these regions it is possible to determine the particle velocity, which can then be mathematically related to the ζ-potential.

ζ-potential measurements were carried with Dynamic Laser Light Scattering (Zetasizer Nano ZS, Malvern Instruments, Worcestershire, UK) at 25^{o}C. As the ζ-potential is related to the electrophoretic mobility of the particles, the ζ-potential is calculated from the measured velocity using the Smoluchowski equation. The samples were previously diluted (1:100) with deionized water to avoid multiple scattering effects. The measurements are reported as the mean of at least two differently prepared injections, with five readings per injection.

3.3.7. EGCG encapsulation efficiency (Chapters 7, 8, 9)

EGCG encapsulation efficiency was determined by dividing the EGCG concentration found in the particles by the initial EGCG concentration added to the formulations. The particles' concentration was evaluated from the UV-Vis absorbance of the particles at the maximum wavelength of 274 nm using a SP-2000UV spectrophotometer (Spectometer UV-1800, Shimadzu, North America).

In Chapter 7, the methodology used for the extraction of EGCG was adopted from Gadkari and Balaraman, (2015b) with minor adjustments.

Briefly, 3 mL of emulsion was diluted with 3ml of citrate buffer (pH= 3.6) and was subjected to centrifugation at 4000 RPM for 15 min.

The aqueous phase was then separated and subjected again to centrifugation at 4000 RPM for 15 min. The supernatant was further passed from filters (0.22 µm) in order to remove the remaining proteins. The EGCG content in the aqueous phase was analyzed using spectrophotometer at 280 nm. The incorporation efficiency (IE) of the emulsions was calculated using simple relation given in below equation (3.6),

$$IE\% = \frac{C_{total} - C_{final}}{C_{final}} \cdot 100\ \% \quad (Eq. 3.6)$$

Where, C_{total} is the concentration of EGCG added to the emulsions and C_{final} the concentration of free EGCG content in the aqueous phase.

In Chapter 8 and 9, the methodology which was used for the extraction of EGCG was adopted from de Freitas Zompero et al., (2015) with minor adjustments. Briefly, for the particles formed through solution electrospraying (Chapter 8), the particles were dissolved in water. When EGCG which was incorporated in the emulsions' aqueous phase (Chapter 9), was extracted from the particles by dissolving the particles in water. For the evaluation of the EE of the ECGC from the oil phase of the particles, ethanol was added to disrupt the particles (releasing the entrapped EGCG) before hexane was added to extract the EGCG, generating 2-phase system. The organic (upper) phase was separated, and the EGCG concentration was determined.

3.3.8. Lipid oxidation of emulsions containing EGCG (Chapters 7)

Conjugated dienes (CD) was used as a method to determine the primary oxidation products of the emulsions. CD were measured using the IUPAC 2.505 method adapted from (Mei et al., 1998). Briefly, emulsion samples (20 µL) were added to 10 ml of isooctane: 2-propanol (2:1, v/v) and mixed by vortex. Then they subjected to centrifugation at 2500 RPM for 10 min. The absorbance was then measured at 232 nm using a spectrophotometer. The amount of CD in the emulsions was calculated the following equation:

$$\text{CD in the sample } \left(\frac{g}{\text{kg}}\right) = \frac{1.0769 \cdot Abs_{234}}{C_{samle\ in\ solvent\ solution}} \quad (Eq. 3.7)$$

Para-Anisidine value (*p*-AnV) was used as a method to determine the secondary oxidation products of the emulsions.

P-AnV was determined according to the AOCS Official Method Cd 18-90 (AOCS, 2009) with minor modifications. Briefly, 1 mL of emulsion sample was added into a 11.5 ml volumetric flask and made up to volume with isooctane. After mixing thoroughly, the sample was transferred to a centrifuge tube and vortexed twice for 10 s each. After

centrifugation at 4000 rpm for 10 min, absorbance (A1) of the upper layer was measured at 350 nm against isooctane as a blank. Then, 5 mL of p-anisidine solution (prepared by mixing 0.25 g of p-anisidine in 100 mL of acetic acid) was added and vortexed for 10 s. After incubation at room temperature for 10 min, absorbance (*A*2) was measured at 350 nm against isooctane containing *p*-anisidine solution as a blank. *p*-AnV was determined using the following equation:

$$p - AnV = \frac{25 \cdot (1.2 \cdot A_2 - A_1)}{2} \quad (Eq. 3.8)$$

The oxidation products were measured every 7 days for a total period of 1 month.

3.3.9. Samples' surface tension (Chapters 8, 9)

Surface or interfacial tension measurements can be used as a mean for emulsifier screening regarding their ability to stabilize emulsions. The du Noüy ring method is a technique by which the surface tension of a liquid can be measured. In this method, a platinum wired ring is slowly lifted from the surface of a liquid. The force, F, required to raise the ring from the liquid's surface is measured and related to the liquid's surface tension, γ:

$$F = 4.\ \pi.\ R.\ \gamma.\ \beta \qquad \text{(Eq. 3.9)}$$

Where, R is the radius of the ring, and β is a correction factor that depends on the dimensions and the density of the ring (McClements, 2005).

The Du Nouy ring method with a KSV Sigma 701 tensiometer (KSV Instruments Ltd., Helsinki, Finland) was used to determine the surface tension of the formulations. All measurements were made in triplicate at 25 ^{o}C.

3.3.10. Samples' electrical conductivity (Chapters 8, 9)

Electrical conductivity depends on several factors, such as liquid concentration, physical state of ingredients, movement of the ions and temperature. The electrical conductivity of a solution/ emulsion can simply be determined using a conductivity cell (McClements, 2005). This cell consists of two electrodes that are connected to electrical circuit that is capable of measuring the electrical conductivity of the sample contained between the electrodes.

A conductivity meter was used for the determination of electrical conductivity (SensoDirect 110, Lovibond, Dortmund, Germany). All measurements were made in triplicate at 25 ^{o}C.

3.3.11. Stability assay of particles during storage (Chapters 8, 9)

The stability of encapsulated EGCG in Chapter 8 and 9 was carried out in three different conditions that are a usual practice in the food industry, namely:

dissolution in aqueous media with different pH, storage at different humidities and temperature exposure. To test the stability in different pH conditions 1 mg of the particles was suspended in 1.5 mL of the release medium and kept at 25^{o}C for 1 month. Three different release media were used: citrate buffer with pH 3, tap water with pH 6 and phosphate buffer with pH 9. At different time intervals, an appropriate amount of the suspensions was removed and analyzed with UV-Vis spectrophotometer in order to evaluate the release of catechin, and with ζ-sizer in order to evaluate the breakage of the particles. In addition, the EGCG particles were stored in desiccators with different humidity conditions (RH= 26, 53 and 75%), and, in a similar way, the content of the bioactive was analyzed at different time intervals up to 30 days. To evaluate the stability when exposed to high temperature, the samples were placed in a heating oven at 37 or 60 ^{o}C for 1 month. During the heating process, samples were taken out of the oven and suspended in the release medium (1 mg/mL w/v) before being transferred to the UV-Vis spectrophotometer to determine the amount of EGCG as it was mentioned in the previous section. In parallel, a solution of 0.1 mg/ml of pure H-EGCG and L-EGCG was assayed following exactly the same methodology described above, to evaluate the effect of encapsulation process in the stability of this bioactive.

The release kinetics of bioactive compounds by a encapsulation matrix have been illustrated in numerous semi-empirical mathematical models (Higuchi, 1961; Peppas and Sahlin, 1989; Ritger and Peppas, 1987). The Peppas- Sahlin model fit better the experimental data of this study (R2= 0.9801- 0.9997) (Peppas and Sahlin, 1989). Its general equation is depicted in Eq. 3.10:

$$\frac{M_t}{M_o} = k_1 * t^m + k_2 * t^{2m} \quad \text{(Eq. 3.10)}$$

Where M_t is the mass of EGCG released at time t, M_0 is the total mass of the loaded EGCG in the particles, m is the Fickian diffusional exponent and k_1, k_2 are kinetic constants. For a carrier with spherical geometry m was set at 0.43 (Peppas and Sahlin, 1989). The first term of the equation represents the Fickian diffusional contribution, whereas the second term the case-II relaxational contribution.

3.3.12. Statistical analysis(Chapters 4, 5, 6, 7,8, 9)

Statistical analysis of the results was performed with Statgraphics Centurion XV (Statgraphics, Rockville, MD, USA) and an ANOVA was applied in order to compare the mean values of selected properties at a 95% level of confidence. Data are represented as mean ± S.D. of at least 3 measurements form 2 experiments replicates if not otherwise specified. The same software was used in order to perform Pearsons' multiple variable analysis.

Chapter 4. Effect of bacterial cellulose processing conditions on the physical properties of emulsions

4.1. Introduction

Cellulose is a linear biopolymer of glucose that mainly exists in plants as a structural component of cell walls. Cellulose consists of an amorphous and a crystalline portion. While crystalline cellulose consists of long chains bound together by strong hydrogen bonds, amorphous cellulose is made up of shorter and weaker chains(Türünç and Meier, 2012).

BC and plant derived cellulose have the same chemical structure, but BC is obtained from bacterial species, such as *Komagataeibacter sucrofermentans*, which have the ability to synthesize pellicles of cellulose, when placed in a culture medium (Martinez-Sanz et al., 2011; Okiyama et al., 1992b). This pellicle consists of a bundle of fibrils of about 4 µm wide, which are composed of random nanofibrils less than 100 nm wide (Okiyama et al., 1993).

A number of technological approaches have been developed to enhance the physical properties of the colloidal suspensions of polymer fibrils. The most commonly used method is to submit polymer to controlled acid hydrolysis conditions (Hirai et al., 2009; Martinez-Sanz et al., 2011; Olsson et al., 2010). However, this is of high energy and cost process that causes intense degradation of the polymer and hence the industry would have had benefit from cheaper alternative methods.

Chemically less aggressive concepts could be the mechanical treatment of cellulose, such as a high pressure homogenization which is used to treat microfibrillated cellulose (MFC) resulting in changes in the microstructure of the cellulose (Agoda-Tandjawa et al., 2010; Saito et al., 2006).

What is more, high-intensity ultrasound (16–100 kHz, 10–1000 W cm^{-2}) has immense potential for structural and functional properties of cellulose modification. By this method, the energy of ultrasound is transferred to the polymer chains through a process called cavitation, which is the formation, growth and violent collapse of cavities in the water. Therefore, the effect of ultrasound is related to cavitation, heating, dynamic agitation, shear stresses, and turbulence (Vilkhu et al., 2008). Recently, structural and functional changes in ultrasound irradiated plant cellulose, have been reported by (Dehnad et al., 2014; Liu and Yang, 2008; Wang and Cheng, 2009). These authors reported that the controlled depolymerization of plant cellulose can be achieved by employing suitable ultrasonication settings.

Hence, the objective of the present study is to investigate various processing methods as treatments for the enhancement of the physical properties of BC fibrils. What is more, the incorporation of these fibrils onto emulsions was investigated together with the emulsion properties.

4.2. Morphology of BCN fibrils treated by ultrasounds

The morphology of a polysaccharide is a fundamental factor to its applications in the industry. As it is already known, the microstructure of BCN consists of a dense reticulated structure with widths varying from 1 to 9 µm, which is formed by ultrafine microfibrils with widths from 6 to 15 nm connected in between with hydrogen bonds (Iguchi et al., 2000).

This morphology can be altered when a treatment is applied to the system and hence it is an essential property to understand the underlined mechanisms that occur during US treatment. It is of interest to note that 1 min of ultrasonication treatment yield to energy up to 5 kJ in the BCN suspension, while 3 and 5 min yield to energies up to 15 and 25 kJ respectively. Therefore, the structure of the BCN fibrils after ultrasonication is presented in Fig 4.1 A-D.

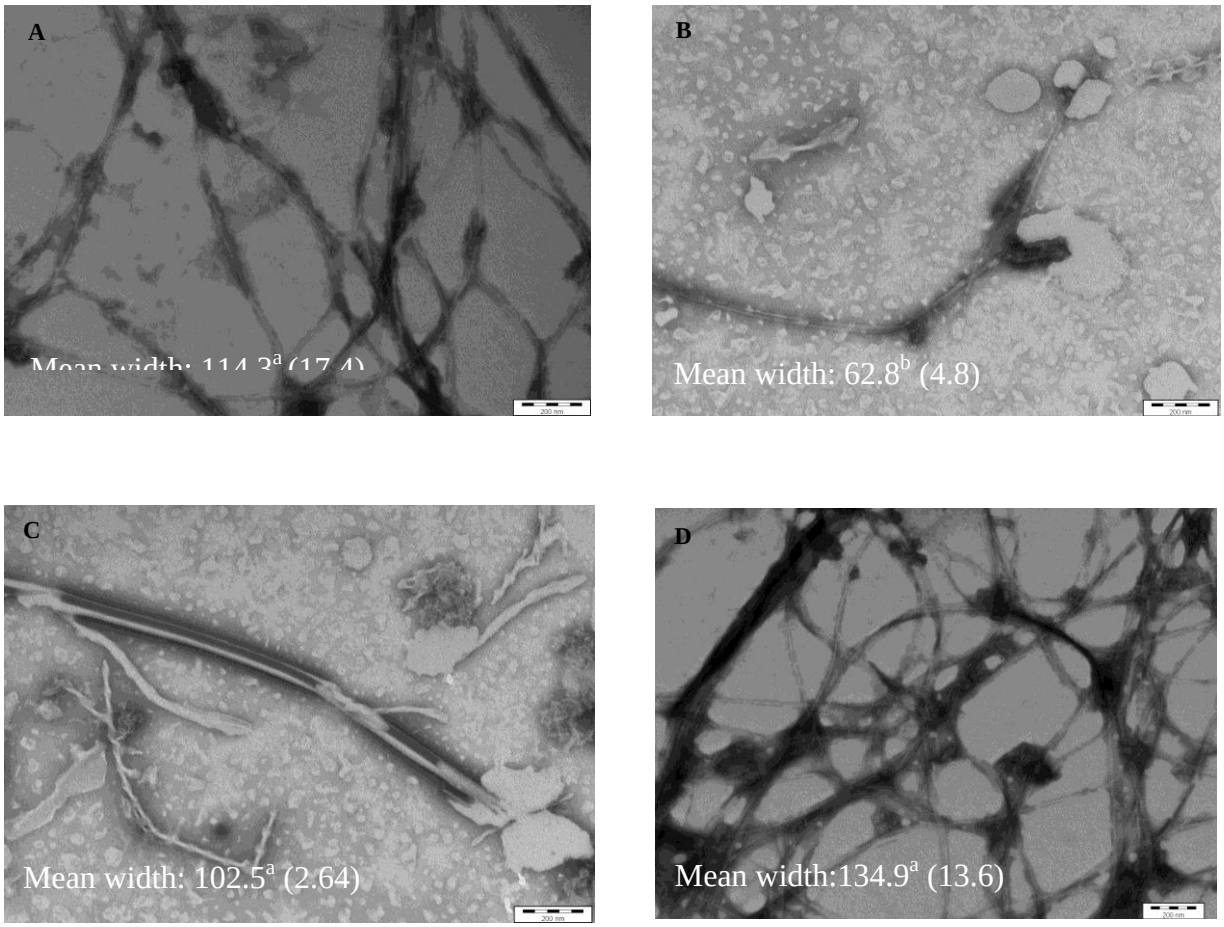

Fig. 4. 1 Typical TEM micrographs and the fibrils' mean width of the untreated BCN suspensions (A) and the ultrasonicated BCN suspensions at different time intervals: 1 min (B), 3 min (C) and 5 min (D).

In parenthesis standard deviation values. Mean values followed by the same letters are not significantly different (P > 0.05).

While, ultrasounds do not have a significant effect on the fibrils' length, as it varies between 2.9 and 3.1 μm (data not shown), there is a predominant effect on the fibrils' width. The TEM micrographs of untreated BCN suspensions (BC0) show an extensively entangled fibril network with irregular fibril and void arrangement (Fig 4.1A). The width of the BC0 is found to be 114 nm. The highly bundled network of BCN after high energy processing was previously reported by Lin et al., (2015b), who found a range of 95 nm for their BCN fibrils' width.

In BC1, a significant decrease in fibrils' width occurs; lowering the width to roughly 60 nm. Moreover, the morphology of the fibrils also changed (Fig. 4.1B). The entangled network becomes less bundled and smaller fibrils are present. However, longer sonication time (BC3) causes an increase in the width to roughly 100 nm and changes in the structure as well (Fig. 4.1C). The main structure is individual ribbons as shown the micrograph. The BCN fibrils consist of smaller fibrils, which associate together by hydrogen bonds. Previous studies have already evidenced a structure composed of nanofibrils, attached together through interconnecting amorphous cellulose chains, in order to produce fibrils (around 100 nm width) that are the basic units of network of BCN (Klemm et al., 2005; Nishiyama, 2009).

Even higher sonication time (BC5) lead to a more pronounced increase of the width to 135 nm and to a reformation of the entangled network (Fig. 4.1D) of the untreated samples. This unexpected trend of fibrils' width to increase could be attributed to the ultrasonic treatment effect on the structure of the fibrils; it is tried to be explained below (Fig. 4.2).

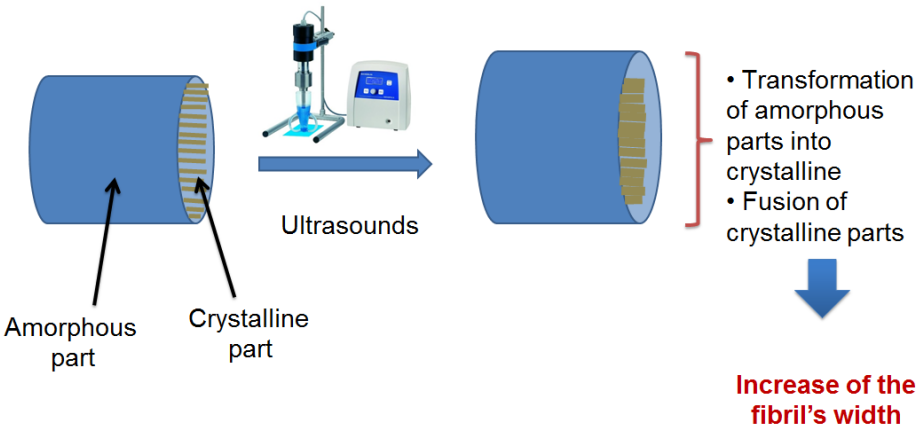

Fig. 4. 2 Alterations of fibrils' width during ultrasonication.

It is well known that due to the linearity of the cellulose backbone, adjacent chains of cellulose form a framework of water-insoluble aggregates of varying length and width. These microfibrils consist of both highly ordered (crystalline- cellulose I) and

less ordered (amorphous) regions (Moon et al., 2011). Studies revealed that ultrasounds could increase the crystallinity of BC membranes(Tischer et al., 2010). They attributed this increase in crystallinity index on the conversion of the amorphous cellulose into cellulose I (crystalline). The activation energy required for this process is provided by the cavitation from the ultrasonic treatment. This process primarily occurs in the amorphous regions. Therefore, when ultrasounds are applied in the suspensions, the amorphous parts of the bundled fibril transform into crystalline and fuse the neighboring nanofibrils which lead to higher width values. From our results, it can be seen that this phenomenon happens only when longer sonication time are applied (3-5 min).

The role of electrostatic interactions in stabilizing suspensions is examined by measuring the electrical charge of the BCN suspensions. The effect of sonication time on the charge of the fibrils is presented in Table 4.1.

Table 4. 1 Physical properties (ζ-potential and water holding capacity -WHC) of 0.1-1% wt BCN suspensions treated by 0-5 min at ultrasounds.

BC treatment	% wt	ζ-potential (mV)	WHC (%)
BC	0.1	-12.9^{g} (1.3)	62.5^{a} (2.2)
	0.5	-17.7^{cd}(2.5)	83.4^{b} (5.1)
	1	-23.2^{ab}(2.1)	109.0^{cd} (7.6)
BC1	0.1	-16.1^{def} (0.8)	77.1^{b} (3.0)
	0.5	-20.3^{bc}(1.3)	104.9^{c} (6.6)
	1	-25.8^{a} (1.6)	140.0^{e}(8.8)
BC3	0.1	-14.7^{efg}(1.0)	64.7^{a}(2.1)
	0.5	-19.3^{bc} (0.8)	86.8^{b} (5.7)
	1	-24.8^{a} (1.4)	116.6^{d} (7.6)
BC5	0.1	-13.4^{fg}(1.4)	61.4^{a} (2.3)
	0.5	-18.23^{bcd}(1.9)	81.4^{b} (5.7)
	1	-23.6^{ab}(2.5)	102.5^{c} (7.7)

In parenthesis standard deviation values.

Mean values followed by the same letters are not significantly different ($P > 0.05$).

It can be clearly seen that BC bears a negative charge in all systems. This is in accordance with studies showing that BC fibrils are negatively charged independently of their pH, as most of the celluloses (Paximada et al., 2016b).

When increasing the concentration of BCN in the suspensions, the ζ-potential values remain negative and increased in value and can be attributed to the amount of BCN that is added. Similar findings of the effect of concentration of polysaccharides on the charge have been previously reported (Winuprasith and Suphantharika, 2013).

As far as the effect of sonication time in concerned, it has a predominant effect on the overall charge of the suspensions. The short treatment (1 min) increases the overall charge of the suspensions. For example, at 0.1% BCN suspensions, the overall charge increased (in absolute values) from -13 mV (BC0) to -16 mV (BC1). However, prolonged treatments (BC3, BC5) cause a decrease in ζ-potential values regardless of the BCN concentration. For instance, at 0.1% BCN suspensions, the overall charge dropped from -16 mV (BC0) to roughly -15 mV (BC3) and to -13 mV (BC5). This variation in the overall charge of the BCN suspensions is consistent with the idea that prolonged sonication yields aggregated fibrils with larger width, an outcome which tends to have a relatively lower charge than fibrils that are not aggregated. This is in agreement with works showing that larger droplets have lower charges in comparison with smaller droplets which tend to have higher charge (Salvia-Trujillo et al., 2015). The results obtained in the present study showed that WHC follow the same trend as the fibrils' width (Fig.4.1).

4.3. Physical properties of BCN fibrils treated by ultrasounds

A modification in the physical structure of a polysaccharide normally affects its physical properties. Hence, it is necessary to determine the effect of the ultrasonic treatment on the WHC of the BCN suspensions. In Table 4.1 the WHC of BCN suspensions treated at different sonication time intervals (0-5 min) with varying BC concentrations (0.1-1% wt) is depicted.

Increasing BCN concentration resulted in higher WHC values from 63-77 % for suspensions containing 0.1% BCN up to 102-140 % for suspensions containing 1% BCN. This can be attributed to the fact that by increasing the concentration on an anionic biopolymer in a suspension, such as BCN, a bigger matrix of fibrils is created which has the ability to retain more water into it and thus increase the WHC. This phenomenon is previously reported (Everett and McLeod, 2005). Specifically, they showed that an increase in the added concentration of anionic polysaccharides (λ-carrageenan or LM pectin) on yogurt causes an increase in the WHC.

Tested materials that have been subjected to a short period of treatment (BC1) show an increase in WHC regardless of BCN concentration. For instance, the WHC

increases up to 140% (BC1) when ultrasonic irradiation is applied in suspensions containing 1% wt BCN. On the other hand, a significant reduction in WHC is observed when longer treatments occur. WHC of suspensions containing 1% wt BCN decrease accordingly to 116% (BC3) and to 102% (BC5). The variation in the WHC of these BC samples can be attributed to their respective porosity and surface areas. The water molecules are trapped physically on the surface and inside the BCN matrix consisting of reticulated fibrils(Watanabe et al., 1998). If there are plenty of empty spaces among the BCN fibrils then more water can penetrate and adsorb onto the material. Thus, the greater the surface area and the larger the pore size, the greater will be the WHC of the BC sample (Guo and Catchmark, 2012; Meftahi et al., 2010). BC has a wide range (100–200 times its dry weight) of WHC values (Lin et al.; Schrecker and Gostomski, 2005). This variation may be due to differences in the fibril arrangement, surface area, and porosity of different BCN samples. The results obtained in the present study showed that WHC follow the same trend as the fibrils' width (Fig.4.1).

Moreover, the term stability for a biopolymer refers to the ability to resist changes in its properties through time, while the time during which the biopolymer is stable depends mainly on its nature (McClements, 2005). Hence, phase separation (PS) for all suspensions was recorded for a 20-day period and presented in Fig. 4.3.

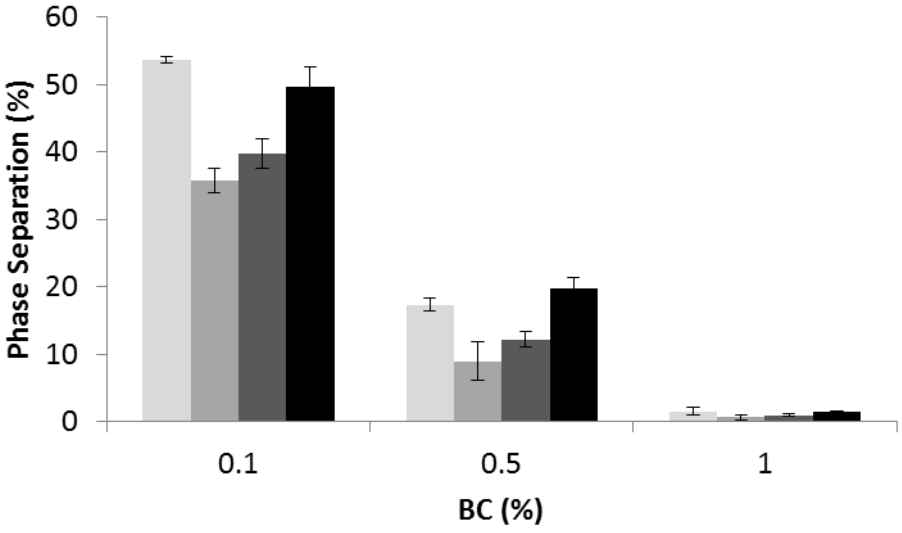

Fig. 4. 3 Phase separation (PS) as a function of BCN concentration and ultrasonic treatment for the aqueous suspensions. PS was determined after 20 days of storage at 25^{o}C. Bars indicating standard deviations. From lighter to darker grey, sonication times: untreated, 1 min, 3 min and 5 min

As it can be seen, the higher the BCN concentration, the lower the phase separation and hence the higher the stability is. The increase in stability by increasing the

polymer concentration is a well-known behavior, extensively studied. By the addition of higher amounts of BC a network is formed decreasing phase separation(Paximada et al., 2016c).

What is more, ultrasonic treatment bears an effect on the stability profile of BCN suspensions. Reduction of phase separation has been observed (Fig. 4.3) in a short period of time (1 min) in the current study, meaning higher stability for the suspensions. By way of explanation, the PS of the BC1 samples containing 0.5% wt BC decreases up to 9% after 1 min, while for the untreated suspension the PS is 35%. In spite of that, further sonication treatment leads to an increased PS, meaning a decrease in suspensions' stability. The PS of the samples containing 0.5% wt BC decreases up to 12% (BC3) and to 18% (BC5). Clearly, this trend is in accordance with the previous mentioned results (size, WHC, ζ-potential) and could be attributed to the structural changes that ultrasounds have on the fibril. A reduction in the PS of BCN suspensions from 20% to 7% has previously reported using high pressure (Lin et al., 2015b). Also, ultrasounds are known to be an efficient method to increase the stability of suspensions when the processing parameters are being optimized (Price et al., 1994; Trzciński and Staszewska, 2004).

4.4. Rheological properties of BCN fibrils treated by ultrasounds

The viscosity of the suspensions as a function of different sonication time intervals and BCN concentrations is presented in Fig.4.4.

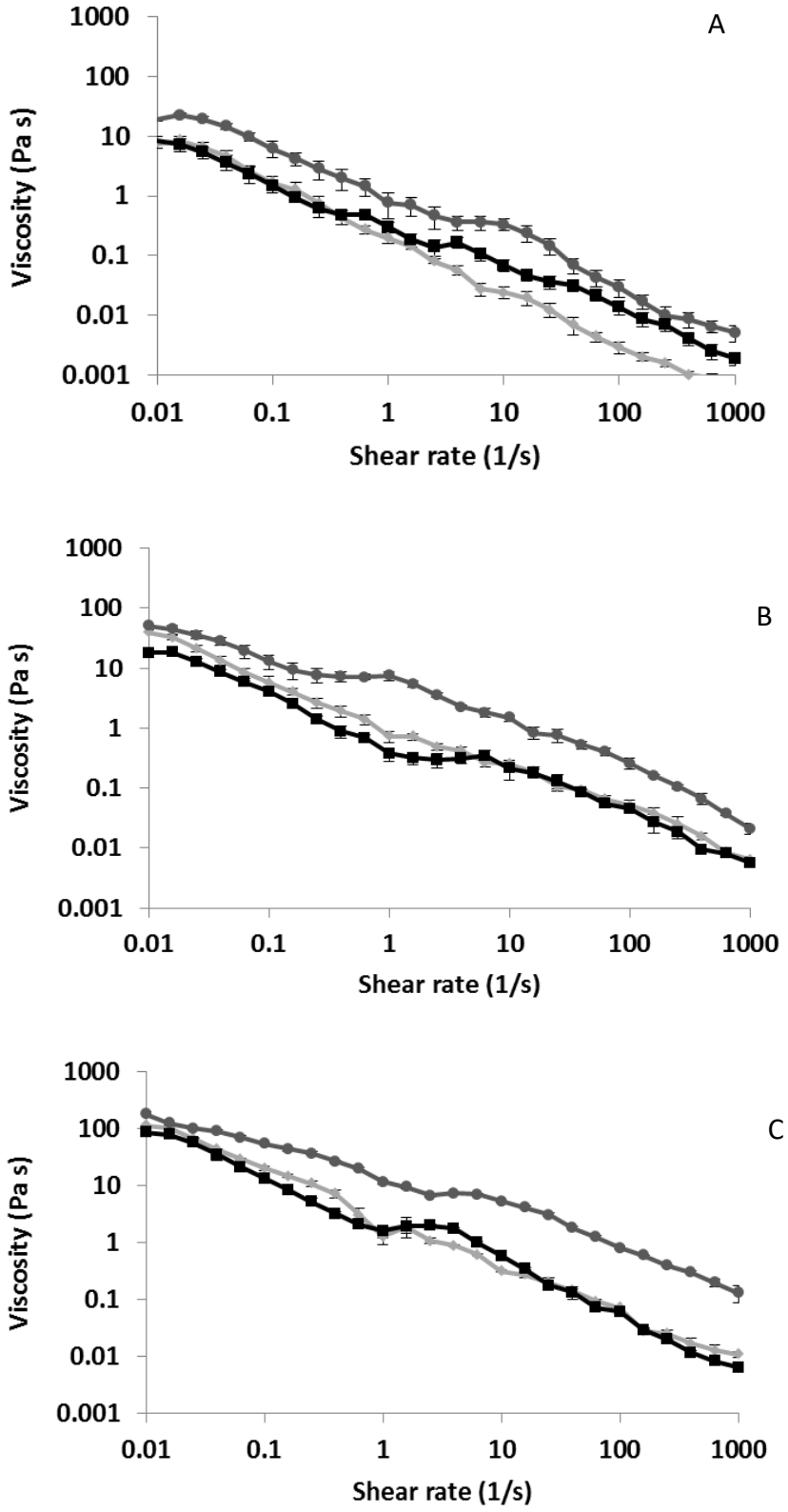

Fig. 4. 4 Viscosity curves of suspensions treated at different time intervals: 0 min (A), 1 min (B), 3 min (C) and containing 0.1% (◆), 0.5% (●), 1% (■) wt BC. Bars indicating standard deviations.

It is obvious that viscosity depends on the concentration of the polymer, as an increase in the fibril concentration results in a significant increase in the viscosity from roughly 10 Pas for 0.1% BCN (Fig. 4.3A) to 150 Pas for 1% BCN (Fig. 4.3C). This viscosity increase could be attributed to the fact that by adding more fibrils into the system, they create bonds between each other, leading to the formation of a stronger network(Iotti et al., 2011). The apparent viscosity of our sample is similar to literature findings (Lin et al., 2015b). Besides the large increase in viscosity, the suspensions also exhibit a pronounced shear thinning behavior, like most suspensions containing MFC (Iotti et al., 2011; Kuijk et al., 2013).

Worth noting is the fact that all the suspensions show a three-region behavior with viscosity showing shear-thinning behavior at low rates, a Newtonian-plateau region and then a precipitous drop in viscosity. Researchers have previously reported similar shear thinning regions in MFC (Jia et al., 2015; Karppinen et al., 2012; Naderi et al., 2014). It is obvious that the shear rate at which the plateau is present, is concentration dependent (Fig. 4.4). The explanation for such behavior is that at a critical shear rate, the fibrils align due to their rod-like nature, greatly easing their flow. Under enough shear the chirality of the suspensions breaks down in favor of a simple structure (Iotti et al., 2011).

At rest, the BCN fibrils are flocculated in the aqueous phase. The first shear thinning region observed at low shear rates (γ= 0.01 – 1 s^{-1}), where the applied force is low but sufficient enough to disrupt the flocculated fibril network. At intermediate shear rates (γ= 1 – 10 s^{-1}), a viscosity plateau is observed. An explanation for this plateau in the flow curve was previously proposed for MFC (Karppinen et al., 2012). They suggest that the Newtonian network is related to a significant increase in BCN floc size and homogeneity. In the second shear thinning region (γ= 10 – 100 s^{-1}), the higher shear rate disrupts the network structure of the BCN flocs again and hence the structure becomes rather uniform once more. This indicates that the contacts between the fibrils are reversible. Due to less connection between the BCN they orientate themselves in the direction of flow thereby causing highly shear thinning behavior at the high shear rates(Barnes, 1997).

What is more, the duration of the sonication treatment significantly changes the viscosity of the BCN suspensions. As it can be observed in Fig. 4.4, the viscosity of the BC0 is the lowest. While in BC1 the suspensions' viscosity increased, in BCN, the viscosity of all samples decreased significantly. This tendency is the same as in the width results and can be attributed to the structural changes that ultrasounds exert in the BCN fibrils. This unusual tendency of viscosity with sonication time was also reported for suspensions containing chitosan (Baxter et al., 2005). Specifically, the untreated chitosan dispersions had lower viscosity than dispersions submitted to US for few minutes, while in prolonged treatments, the viscosity fell again.

Thixotropy is a term used in rheology which means that the viscosity of a material decreases significantly with the time of shearing and then, increases significantly when the force inducing the flow is removed (Whelan, 1994). Time dependency of polysaccharides is fundamental to understand possible utilizations in food industries (e.g. the flow in mixers or pipes, coating applications, as thickening agent, in extrusion processes).

Hence, the effect of the sonication time on the thixotropic behavior of BCN suspensions has been evaluated and selected aqueous suspensions containing 0.5% BCN and treated for0 (◆), 1 (●) or 3 min (■) at ultrasounds are depicted in Fig. 4.5.

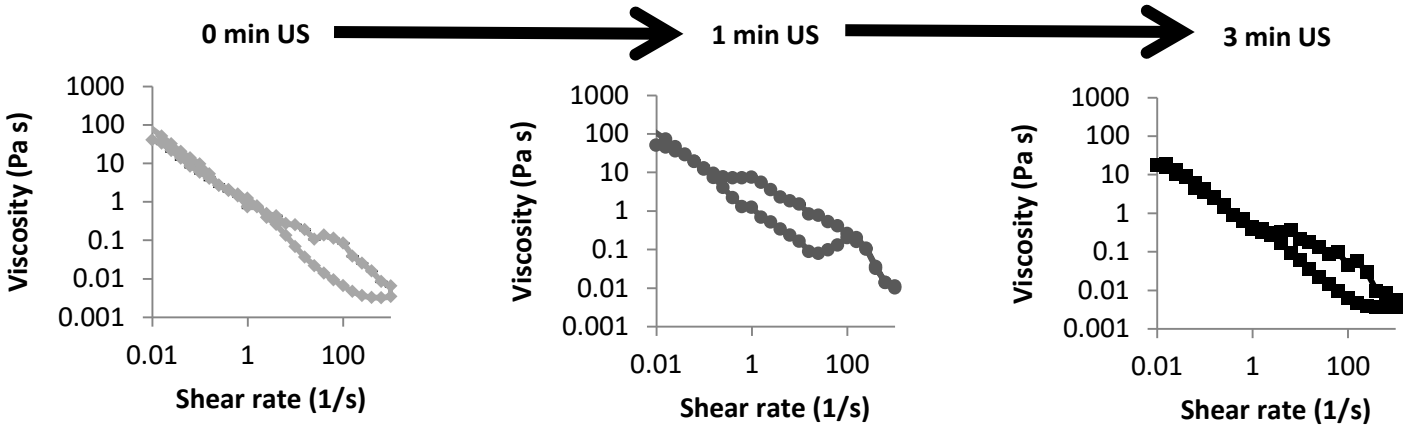

Fig. 4. 5 A typical hysteresis loop test of BC aqueous suspensions: 0.1% (■) and 1% (■) treated by ultrasounds for 3 min. Bars indicating standard deviations.

As it can be seen, all samples exhibited typical thixotropic behavior, which is usually associated with systems containing flocculated particles or aligned fibrils (Barnes, 1997). Similar thixotropic behavior was found for MCC as well as for MFC (Jia et al., 2014). Researchers revealed a thixotropic behavior for amorphous cellulose suspensions at concentrations of 0.77% and 2.33% w/v, while Araki et al., (1998) found the same behavior for MCC prepared by HCl hydrolysis at concentrations >0.5% w/v.

It is also interesting to focus on the size and the shear rate that the hysteresis loop appears in relation to the sonication time. As it can be seen, there is a shift of the shear rate values that the loop is depicted by imposing sonication for 1 min (Fig. 4.5B), while for longer US treatment of 3 min, it returns to similar shear rates of the untreated samples (Fig. 4.5C). The reason for that phenomenon probably stems from the structural changes that take place in the BCN fibrils during the US treatment.

An explanation for the thixotropic behavior of MFC was previously reported (Iotti et al., 2011). We assume that this is the case for our samples as well. BCN suspensions

exhibit a structural breakdown. As the shear rate increases, shear thinning is the dominating effect. In the area that the loop takes place the shear rate velocity does not allow the preservation of the high shear structure that has been formed. Thus, the high shear structure breaks down and a formation of a new low shear structure is present. In this case (Fig. 4B), the high shear structure seems present until the drop in viscosity measured around 0.2 s^{-1}, where the curve suggests the end of the high shear structure and the reorganization in a different low shear organization.

The elastic modulus *G'* (solid symbols) and loss modulus *G''* (open symbols) as a function of frequency for the BCN suspensions at various total BCN concentrations and US treatments are shown in Fig. 4.6. These measurements were obtained by applying a constant strain of 0.3%, which is within the linear viscoelastic region.

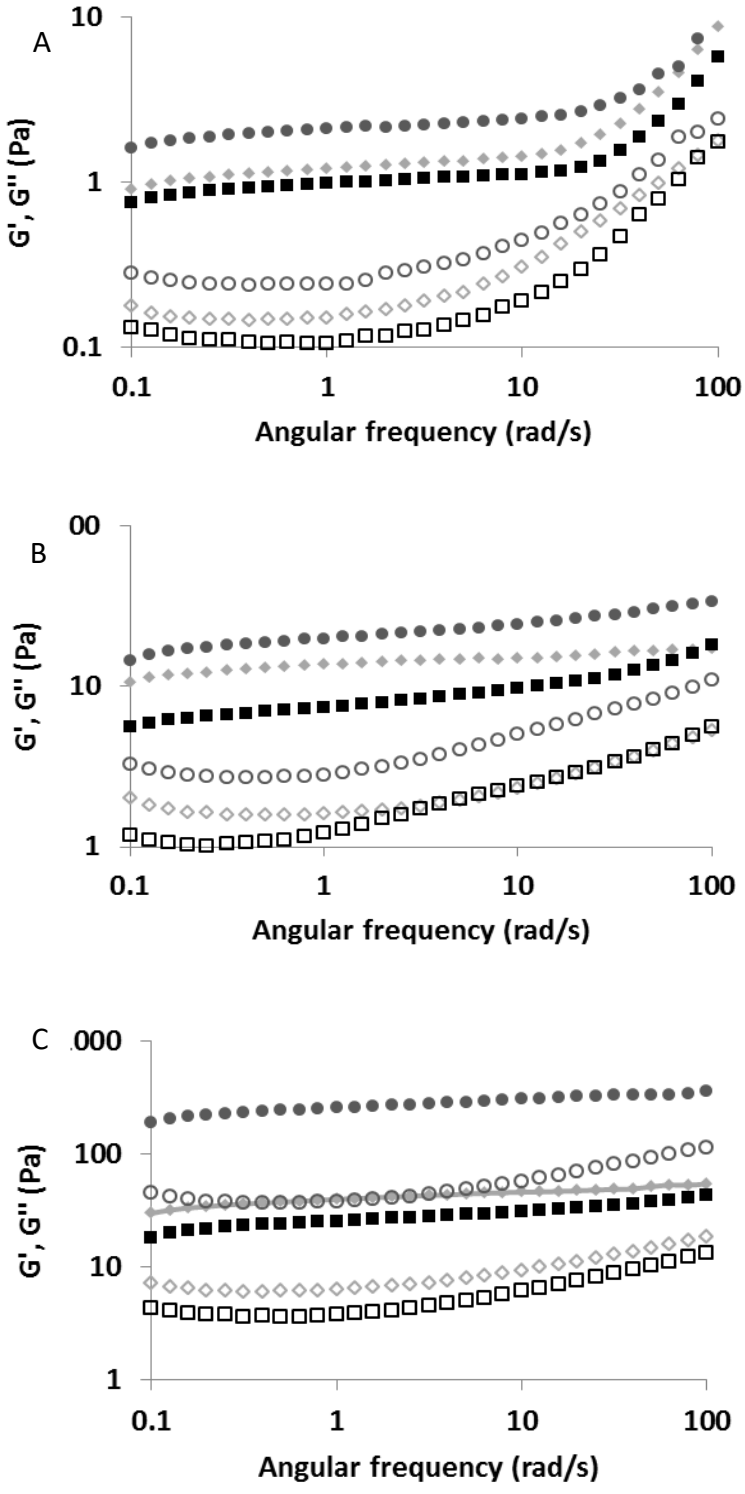

Fig. 4. 6 Storage modulus and loss modulus as a function of frequency for suspensions treated at different time intervals: 0 min (A), 1 min (B), 3 min (C) and containing 0.1% (◆), 0.5% (●), 1% (■)wt BC. G' filled symbols, G'' empty symbols. Bars indicating standard deviations.

As it can be seen, all suspensions exhibit G' values higher than G'' (G' > G'') at all frequencies, meaning that the suspensions could return in their initial situation when the oscillation stops (Iotti et al., 2011). Hence, all the suspensions exhibit a gel-like behavior. This viscoelastic behavior of the BC suspensions and their effective increase with the concentration is a result of the rigid elongated nature and the entanglement of the fibrils. The previous mentioned rheological measurements confirm the viscoelastic character of the suspensions already reported in the literature (Iotti et al., 2011; Rezayati Charani et al., 2013). Moreover, increasing the BCN concentration leads to an augmentation in both moduli. For example, the storage modulus at 1Hz frequency increases from roughly 1 Pa for 0.1% BCN (Fig. 4.6A) to 13 Pa for 0.5% BCN (Fig. 4.6B) and to 40 Pa for 1% BCN (Fig. 4.6C).

Moduli as a function of ultrasounds treatment has the same trend as the viscosity: the moduli of the untreated suspensions are the lowest. In BC1, the moduli increased, while in BC3 the moduli decreased significantly, regardless of the concentration of BCN. The augmentation of hydrogen bonds and non-freezable bound water together with the crystallinity in suspensions by increasing the treatment has been brought forward earlier as explanation for this behavior (Kunzek et al., 1997). Specifically, studies found good correlation between the water retention capacities and the rheological properties for swollen cell wall material originating from apples. In summary, the viscoelastic properties of the fibril suspensions altered significantly with progressive modification. This is in relation with the viscosity and the morphology results.

Ultrasonication treatment for 1 min was found to have positive effect on the physical properties of the suspensions. Taking all the measurements into consideration, it is obvious that ultrasonication treatment for 1 min resulted in the lowest phase separation values, yielding values between 0 and 36%,. Also, BC1 increases the viscosity, the viscoelasticity and the water holding capacity of the suspensions. It is well known that viscosity and viscoelasticity are key factors when choosing a thickener as the higher the viscosity is the higher the network the thickener can make. To this regard, ultrasonication treatment for 1 min is the optimal processing condition of the BC aqueous suspensions and is proposed to be used as a thickener in emulsions.

4.5. Physical properties of BCN fibrils treated by acid hydrolysis

In the present chapter, acid hydrolysis is evaluated as a potential method for preparing colloidal suspensions of BCN fibrils by HCl or H_2SO_4. Several parameters of the acid hydrolysis procedure were tested in order to obtain the suspension with the optimal properties. Specifically, the tested parameters are summarized in Table 4.2.

Table 4. 2 Acid hydrolysis parameters

Sample name	Acid	Temperature (^{o} C)	Time (h)	Mean length (μm)	Mean width (nm)
H400	HCl	40	0	37.5^{a} (6.8)	120^{d} (8)
H402	HCl	40	2	2.3^{c} (0.5)	21^{e} (7)
H4024	HCl	40	24	-	-
H4048	HCl	40	48	-	-
H4072	HCl	40	72	2.1^{c} (0.7)	23^{e} (12)
S400	H_2SO_4	40	0	37.5^{a} (6.8)	120^{d} (8)
S402	H_2SO_4	40	2	1.8^{c} (0.3)	4^{e} (2)
S4024	H_2SO_4	40	24	-	-
S4048	H_2SO_4	40	48	-	-
S4072	H_2SO_4	40	72	0.9^{c} (0.0)	21^{e} (10)
H600	HCl	60	0	37.5^{a} (6.8)	120^{d} (8)
H602	HCl	60	2	6.7^{b} (0.6)	57^{c} (26)
H6024	HCl	60	24	-	-
H6048	HCl	60	48	-	-
H6072	HCl	60	72	0.9^{e} (0.1)	21^{e} (9)
S600	H_2SO_4	60	0	37.5^{a} (6.8)	120^{d} (8)
S602	H_2SO_4	60	2	6.9^{b} (1.9)	31^{c} (7)
S6024	H_2SO_4	60	24	-	-
S6048	H_2SO_4	60	48	-	-
S6072	H_2SO_4	60	72	0.9^{e} (0.1)	33^{e} (15)

The different processing conditions yield fibrils with different morphologies and sizes as can be seen in Fig. 4.7 and Table 4.2 respectively. The first that someone should mention here is the entangled network that native BCN fibrils form (Fig. 4.7A). In this case, the size of the fibrils is high, as the length reaches sizes up to 38 μm, while the width reaches sizes up to 120 nm.

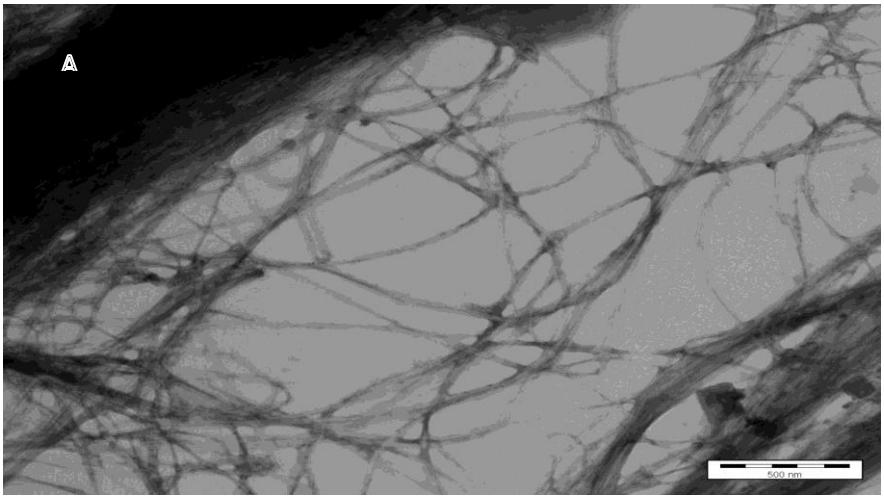
A
500 nm

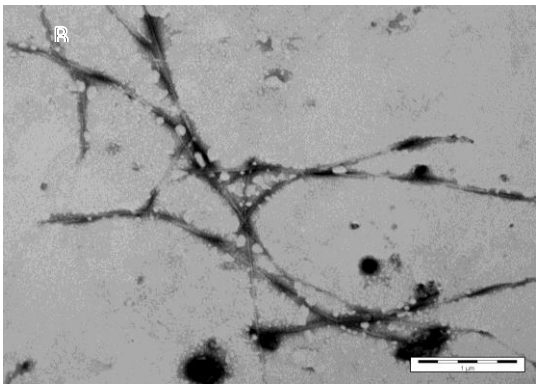
B

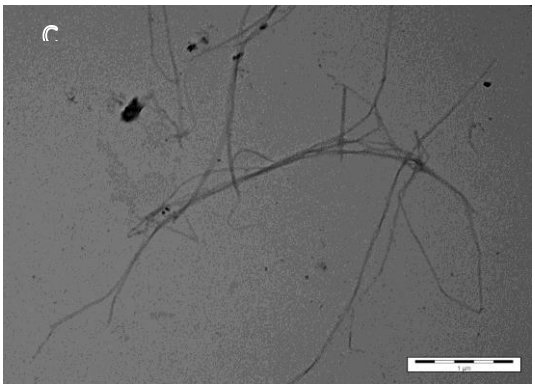
C

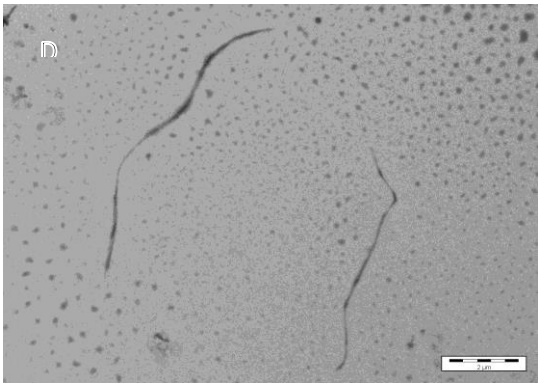
D

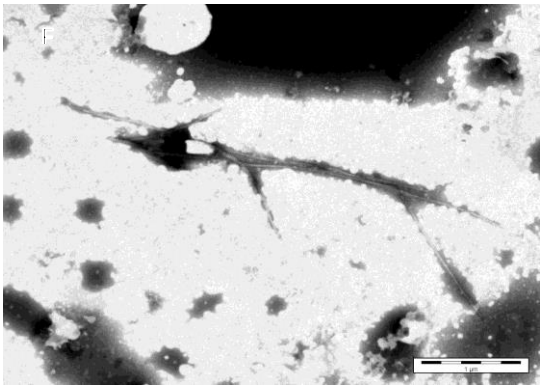
E

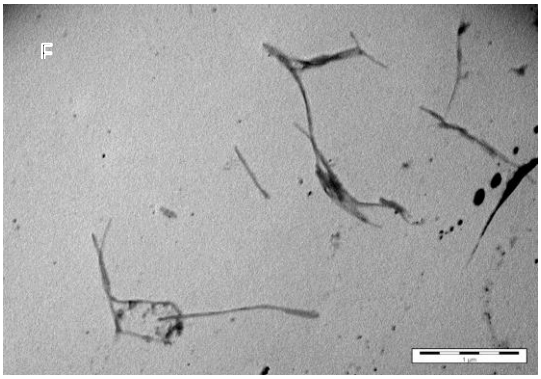
F

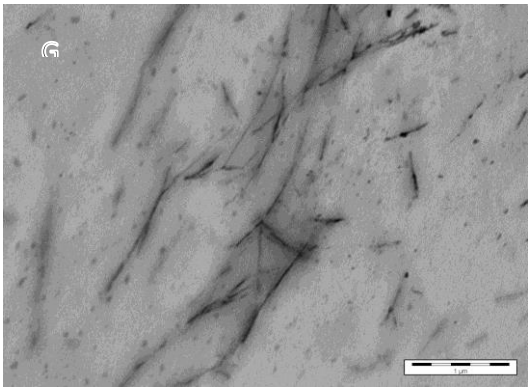
G

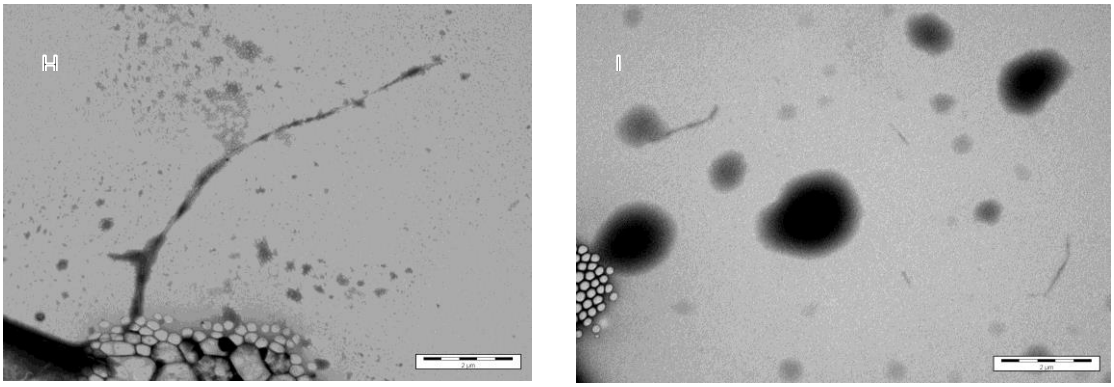

Fig. 4. 7 Typical microstructures of the untreated BCN suspensions (A), H402 (B), H4072 (C), H602 (D), H6072 (E), S402 (F), S4072 (G), S602 (H), and S6072 (I).

After short hydrolysis time (2 h) with HCl at 40^{o} C, there is a significant decrease both in the width and in the length of the fibrils. After this treatment, the entangled network becomes less bundled. By increasing the hydrolysis time (up to 72 h), further reduction of the fibrils size is not depicted. This could lead to the assumption that the optimal hydrolysis time with HCl at 40^{o} C is 2 h. By increasing the temperature of hydrolysis at 60^{o} C, there is a significant decrease both in the width and in the length of the fibrils. For instance, the length of fibrils after 72 h of treatment with HCl at 40^{o} C is 2.1 μm, while the length of fibrils after 72 h of treatment with HCl at 60^{o} C is 0.8 μm. Also, by increasing the processing temperature, the network of the fibrils becomes less bundled.

What is more, the type of acid strongly affects the morphology of the produced fibrils. Specifically, sulfuric acid yields the lowest sizes in all the tested conditions. Hence, hydrolysis with sulfuric acid leads to the reduction of the fibrils size even after 2 h of treatment at 40^{o} C, and more pronounced reduction after 72 h. Worth noting the fact that hydrolysis with H_2SO_4 at 60^{o} C, a delay can be observed, as after 2 h of treatment the differences on the sizes are not significant.

The reduction of the fibrils' size under hydrolysis could be attributed to the fact that the acids disintegrate the amorphous regions of the BCN fibrils, leading to a size reduction. Hence, longer hydrolysis treatments lead to more crystalline cellulose regions, as the amorphous regions have been disintegrated by the acids.

Comparable results have been found by other researchers. Specifically, Martinez-Sanz et al., (2011) indicated a reduction of the BCN fibrils size by increasing the hydrolysis time from 2 to 48 h with H_2SO_4 at 50^{o} C. Also, the same declining trend on the fibrils size has been reported by Bondeson et al., (2006), when dealing with the hydrolysis of cellulose fibrils by sulfuric acid. They also indicated that the augmentation of temperature had significant effect on the size of the fibrils. Finally,

according to Roman and Winter, (2004), when the cellulose is being hydrolyzed in more severe conditions, less bundled networks tend to occur.

In order to gain deeper understanding on the effect of the processing parameters on the final properties of the BCN fibrils, the ζ-potential of the fibrils after the hydrolysis was evaluated and presented in Fig. 4.8.

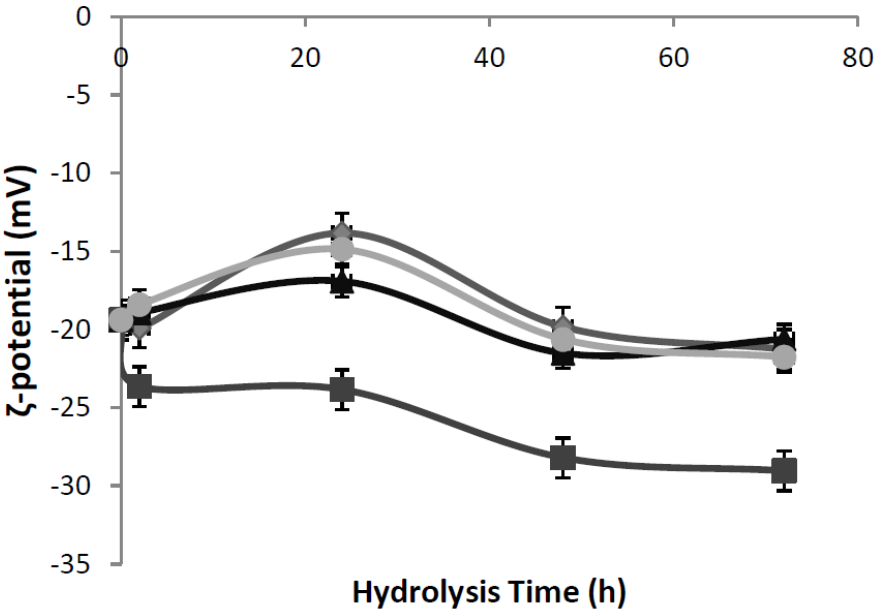

Fig. 4. 8 ζ-potential of the hydrolyzed fibrils with HCl at 40°C (▲),HCl at 60°C (●), H_2SO_4 at 40°C (◆), and H_2SO_4 at 60°C (■).

As it was previously reported, BC is negatively charged (Paximada et al., 2016a). After the hydrolysis with strong acids, the BC exhibits negative values of ζ-potential in all tested conditions. This could be attributed to the presence of large amount of negatively charged sulfuric groups on to the surface of the cellulose nanocrystals, resulting in the augmentation of the surface charge of the crystals (Bondeson et al., 2006; Habibi et al., 2010; Roman and Winter, 2004). However, this is not the case for hydrochloric acid, and hence it explains the lower differences of ζ-potential values that can be seen when using HCl. Increase of the ζ-potential by increasing the hydrolysis time was previously reported by Azizi Samir et al., (2005), when dealing with sulfuric acid.

As far as the hydrolysis time is concerned, an increase of the ζ-potential values can be seen after 24 h of treatment, while a decrease in the charge can be seen after 72 h of processing, regardless the used acid and processing temperature. As far as the processing temperature is concerned, lower ζ-potential values can be found for the treatment with sulfuric acid at 60° C. On the other hand, higher ζ-potential values

can be found for the treatment with sulfuric acid at 40^{o} C. The hydrolysis with HCl does not significantly affect the ζ-potential values at the tested temperatures. Finally, worth noting is the fact that higher temperatures lead to more negative ζ-potential values. The same incident was reported from Guo and Catchmark, (2012).

The stability of cellulose fibrils is known to be affected by numerous factors, such as the processing time, temperature and the type of the acid that is being used. Hence, in this study, the stability of the BCN suspensions (phase separation-PS) was evaluated after 20 days of storage and presented in Fig. 4.9.

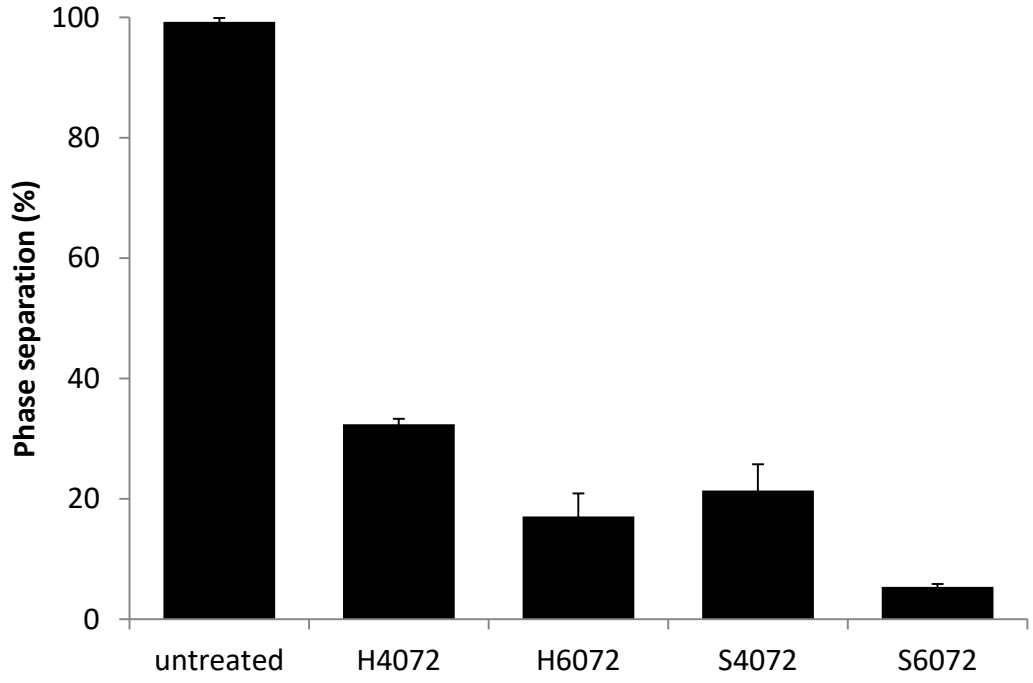

Fig. 4. 9 Phase separation of BCN suspension after 20 days of storage. Bars indicating standard deviations.

As it can be seen, stable suspensions were obtained by treating the cellulose fibrils with either H_2SO_4 or HCl.

Moreover, by increasing the hydrolysis time, the PS (%) is decreasing, regardless the temperature and the type of the acid (data not shown). For instance, PS for the S40 sample at 2 h is 76%, while for the same sample after 72 h of hydrolysis the PS is roughly 25%. It appears that by increasing the hydrolysis time up to 72 h in the samples treated with HCl, the PS decreases (with a 95% confidence level), which may indicate that only for long hydrolysis times, such as 72 h, the acid is able to start breaking down the fibrils' bundles thus decreasing the phase separation. These results are in accordance with the evaluation of fibrils' dimensions' (Table 4.2). This observation was reported by other studies (Martinez-Sanz et al., 2011; Olsson et al., 2010). From observation of Fig. 4.9 it can be deduced that no major changes in the

BCNs' phase separation were induced by varying the type of the acid used for the hydrolysis.

To sum up, it has been seen that BC fibrils exhibit higher stability, lower size and enhanced rheological properties when hydrolyzed at 60^{o} C, regardless the type of the acid, which is also the case in the work of (Guo and Catchmark, 2012). This phenomenon could be attributed to the fact that when BC is hydrolyzed in more severe conditions, tends to create less bundled networks and fewer flocs, due to the larger negative changes that their fibrils have. These charges enhance the repulsive forces between the fibrils, leading ultimately to the prevention of the development of flocs. What is more, in higher temperatures, the amorphous parts of BCN degrade with a quicker rate than on lower temperatures.

What is more, the hydrolysis with sulfuric acid lead to BCN suspensions with higher stability compared to the ones hydrolyzed with hydrochloric acid. This is in accordance with other studies (Angellier et al., 2005; Bondeson et al., 2006; Roman and Winter, 2004)and can be attributed to the presence of an amount of sulfuric ions into the surface of the nanocrystals. These ions are known to offer better stability in suspensions containing nanocrystals (Araki et al., 1998).

4.6. Rheological properties of BCN fibrils treated by acid hydrolysis

The viscosity of the suspensions as a function of different processing conditions is presented in Fig.4.10.

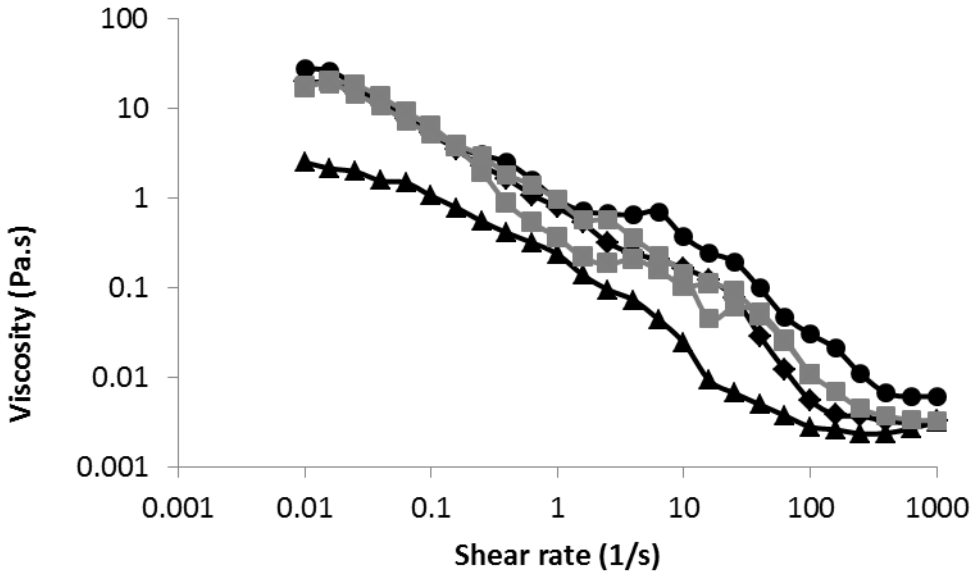

Fig. 4. 10 Apparent viscosity curves of BCN suspensions: untreated (●), H4072 (■), H6072 (◆) S4072 (×), and S6072 (▲).

In the present study, the effect of the hydrolysis parameters on the viscosity of the BCN suspensions was evaluated for all the tested samples (Table 4.2) but here the most caracteristic samples are being displayed.

First of all, all the tested suspensios exhibited shear thinning behavior as their viscosity is being reduced by increasing the shear rate. This shear thinning behavior is typical for BCN suspensions and is independent from the processing time and temperature (Paakko et al., 2007).

Moreover, the viscosity of the suspensions is found to decrease by increasing the hydrolysis time or temperature. Worth noting that for the suspension treated with hydrochloric acid at 40^{o} C, a signifacant decrease in the viscosity is observed even after 2 h of treatment, while the viscosity values do not alter after 72 h of treatment. These results are complimentary to the results for the fibrils size and the stability of the suspensions.

In the case of the hydrochloric acid, the BC nanocrystals display drastic decrease of the viscosity as a function of shear rate. This trend has been previously reported by Araki et al., (1998); Moon et al., (2011) and is associated with the quick disintegration of the BCN flocs that are created when the BCN is treated by HCl. On the other hand, the suspensions treated by sulfuric acid exhibit less dependence from the shear rate, probably due to the orientation that the nanocrystals have due to the flow rate (Paakko et al., 2007).

Previous studies have shown that the nanocrystals derived from hydrolysis with HCl, create loose flocs in the water due to the Van der Waals forces that take place due to the lack of surface charges. Hence, the viscosity of these suspensions is higher than those that are hydrolyzed with sulfuric acid. In the suspensions hydrolyzed with sulfuric acid the nanocrystals are being stabilized by the surface charges that are being created during the acid hydrolysis and they don't flocculate (Araki et al., 1998). These results are in accordance with our results, especially for the samples hydrolyzed for 72 h.

What is more, the 3-region viscosity profile can be observed in the untreated supsensions and in the suspensions that are treated at low temperature (40^{o} C). This could be attributed to the fact that the higher temperatures reduce the size of the fibrils leading to the elimination of the Newtonian plateau. The highest the processing temperature, the highest the dissintegration of the amorpous regions of the crystals and thus the highest the crystallinity of the BCN, leading to a reduction in the viscosity values (Baxter et al., 2005; Martinez-Sanz et al., 2011).

The shear rate-viscosity hysteresis of the BCN suspensions gives better insights on the solid-like behavior and gel structure of MFC suspensions. Hence, Fig. 4.11 shows typical viscosity curves for suspesnsions treated under various hydrolysis conditions.

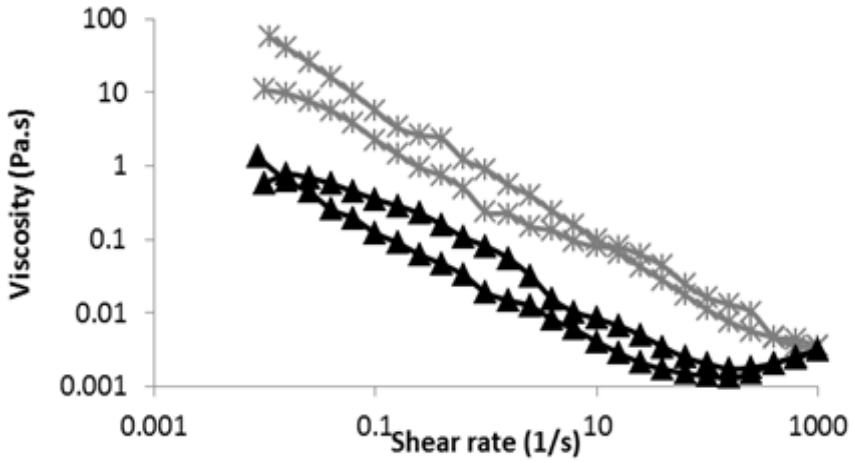

Fig. 4. 11 A typical hysteresis loop test: BCN suspensions H4072 (■), H6072 (◆) S4072 (×), and S6072 (▲).

From this Fig. it is possible to identify certain characteristics common for all the suspensions, specifically a yield stress, a shear thinning behaviour and a hysteresis loop located in different shear rate values for the tested samples.

Specifically, the S6072 (where BC is hydrolyzed by sulfuric acid at 60^{o} C for 72 h) sample exhibits a typical viscosity curve. The curve starts with a yield stress and a no-shear structure is present. The shear causes a slow breakdown of the no-shear structure and, as the shear rate increases, shear thinning is the dominating effect. Under shear, the BCN fibrils orient along flow lines like high polymers, causing a decrease of viscosity (Araki et al., 1998). At higher shear rates (1-1000 s^{-1}), an oriented structure is formed; the consequent decrease in viscosity is due to the stability of the structure and the orientation that allow less disturbance of the flow. In the first part of the decreasing shear rate curve, the behavior is again shear thinning. In lower shear rates (1-0.1 s^{-1}), the predominant phenomenon Is the disruption of the high shear structure and reorganization is present. Finally, a transition of the suspension from the low shear structure to the yield stress can be pointed out, typical for cellulose suspensions (Iguchi et al., 2000; Iotti et al., 2011).

Moreover, temperature dependency is condidered here. It is possible to see that the two different types of acid used for the hydrolysis (HCl and H_2SO_4) do not show significant differences in their rheological profile, except when treated at 40^{o} C. There is a clear reduction of viscosity with increasing temperature. Another point to add is that the hysteris loop of the suspensions treated at 40^{o} C can be observed in higher shear rates than the respective suspensiosn treated at 60^{o} C. The occurrence of the loop is being associated with the changes in BC's morphology (Iotti et al., 2011).

Taking all the above into condideration, the more intense the hydrolysis conditions (sulfuric acid at 60 ° C for 72 hours) the lower the viscosity of the suspensions is while the highest the thixotropic behavior is.

Another important rheological value, G' and G'', was evaluated and presented in Fig. 4.12.

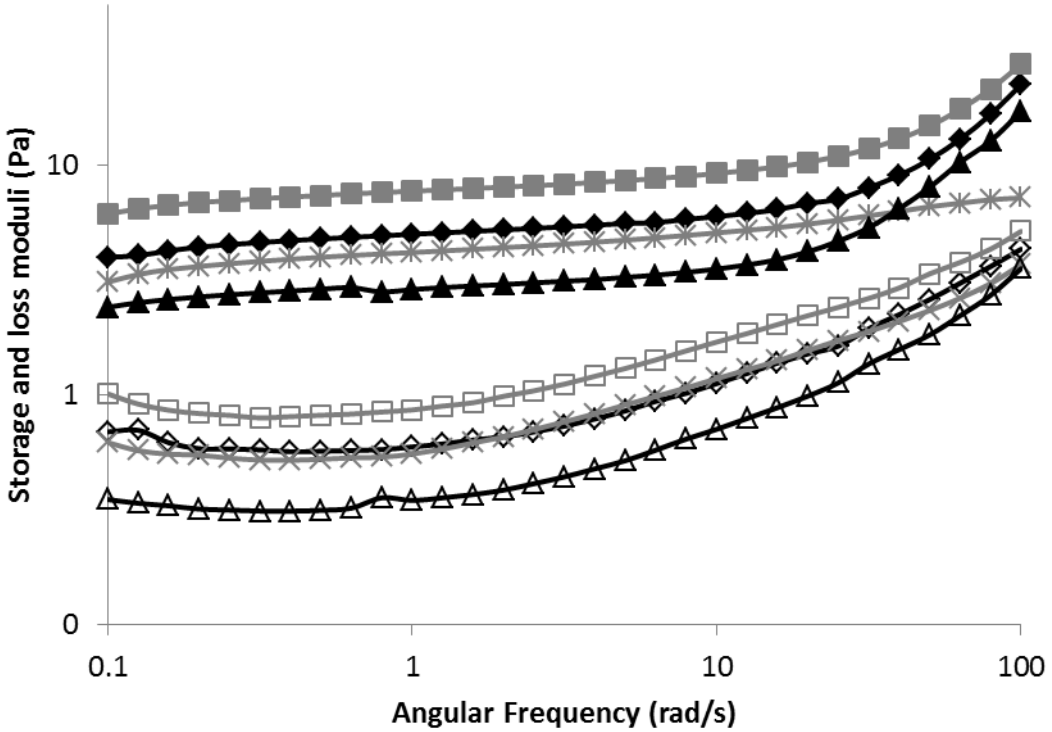

Fig. 4. 12 Storage modulus and loss modulus as a function of frequency for BCN suspensions: H4072 (■), H6072 (◆) S4072 (×), and S6072 (▲). G' filled symbols, G'' empty symbols.

As expected, the G' values are higher thatn the G'', indicating a gel-like behavior of the all the tested suspensions. Also, in all cases the moduli are not highly dependent on the angular frequency for angular frequency values less than 10 rad / s, while at higher values this dependence becomes more pronounced. This behavior is most pronounced in the untreated samples, the samples treated for 72 hours but also in the sample hydrolysed with sulfuric acid for 2 hours at 60 ° C. Moreover, increasing the hydrolysis temperature leads to a reduction of G 'and G" values, independently of the acid used or the processing time. These results are in accordance to the viscosity curves mentioned earlier.

To sum up, hydrolysis with sulfuric acid for 72 h at 60° C was found to have positive effect on the physical properties of the suspensions and is proposed to be used as a thickener in emulsions.

4.7. Influence of the processing method of BC on emulsions' physical properties

In the present chapter, BCN suspensions, after being treated by the optimal processing conditions, were incorporated into emulsions. Specifically, the optimal processing conditions for the ultrasounds was found to be 3 min, while for the hydrolysis was set to be with sulfuric acid for 72 h at 60° C. The physical properties of the emulsions containing various amounts of BC (0.1- 1% wt.) and treated by ultrasounds or hydrolysis are summarized in Table 4.3.

Table 4. 3 Physical properties (droplet size and serum index) of emulsions containing 0.1- 1% wt BC

BC treatment	Ultrasounds		Acid hydrolysis	
%wt BC	D_{50} (μm)	SI(%)	D_{50} (μm)	SI(%)
0.1	6^{a} (3)	35^{b} (2)	12^{a} (7)	52^{c} (7)
0.3	5^{b} (2)	29^{b} (7)	10^{b} (3)	41^{c} (3)
0.5	4^{b} (2)	22^{a} (6)	10^{b} (4)	38^{c} (1)
0.7	4^{c} (1)	24^{a} (2)	9^{b} (4)	31^{b} (1)
1	3^{c} (1)	20^{a} (5)	7^{c} (2)	27^{a} (1)

In parenthesis standard deviation values.

Mean values followed by the same letters in the same column are not significantly different ($P > 0.05$).

It is obvious that by increasing the concentration of BC in the emulsions, their droplet size is reduced, while their stability is increased. This phenomenon was previously described in literature and can be attributed to the predominant effect that the BC concentration has on the system (Huang et al., 2001; Jafari et al., 2006). Specifically, introducing higher amounts of polymers into the emulsions, leads to the fully coverage of the droplets and, ultimately, to the avoid flocculation.

In the case of ultrasonic bacterial cellulose, the droplet size of the emulsions is much smaller than in the case of acid hydrolysis. As it can be seen, the emulsions prepared with ultrasonicated BC yield lower stability (SI= 20-35%) in comparison to emulsions prepared with hydrolyzed BC (SI= 27-52%).

These results confirm the greater efficiency of the ultrasounds as compared to the hydrolysis pre-treatment in obtaining stable BCN suspensions. Hence, ultrasonication is recommended as a pre-treatment of the BCN suspensions in order to yield the enhanced physical properties.

4.7. Conclusions

An extensive study of the effect of ultrasonic and acid hydrolysis treatment on the physical properties of bacterial cellulose (BC) aqueous suspensions has been conducted, focused on their rheological behavior. Sonication was proved to be an appropriate method for the pre-treatment of BC. The time of the treatment is critical. Longer times (5 min) are not recommended, because the crystallinity of cellulose is increased and entangled fibrils are created. On the contrary, a short treatment (1 min) is beneficial for BC suspensions pretreatment. Acid hydrolysis could change the microfibrillar arrangement, leading to suspensions with different nanostructure and rheological properties. The major parameters that affect the final properties of the suspensions are the processing time, temperature and acid. Hydrolysis with sulfuric acid at 60^{o} C for 72 h, is found to be beneficial of the BCN suspensions.

Table 4.4. summarizes the physical properties of the optimal suspensions for the 2 tested procedures (ultrasonication and acid hydrolysis). As it can be seen, hydrolysis yields fibrils with the lowest width and ζ-potential. On the other hand, ultrasounds yield BCN suspensions with the highest stability and viscosity. Taking this into consideration, in the next chapters (Chapter 5, 6, and 7) the emulsions are being made with BCN that were previously treated by ultrasounds. For the production of emulsions, the high viscosity is a key parameter as it thickens the system more. On the other hand, in the chapters 8 and 9, the key parameter for the electrospraying in the low fibrils width and hence in these chapters BCN suspensions that were previously treated by acid hydrolysis, are being used.

Table 4. 4 Summary of the properties of the optimal suspensions

Sample	Ultrasounds 3 min, 1% BC	Hydrolysis with H_2SO_4 60°C (72h)
Fibrils' width (nm)	102 (3)	33 (0)
ζ-potential (mV)	-24 (1)	-29 (2)
Phase separation (%)	0.7 (0.1)	3.4 (0.4)
Viscosity (Pa.s)	86 (9)	3 (0)
Thixotropy	Small hysteresis	Great hysteresis
Viscoelastic behavior	Elastic behavior (G'>G'')	Move to viscous behavior
Incorporation into o/w emulsions (1% BC)		
D_{50} (µm)	3.6 (1.9)	7.5 (2.3)
Phase separation (%)	20 (7)	27% (1)

Chapter 5. Influence of different thickeners on the properties of o/w emulsions

5.1. Introduction

Thickeners are often used to increase the viscosity of the products they are incorporated in. Commonly used hydrocolloids as thickeners in o/w emulsions such as dressings, are carbomethyl cellulose (CMC) and hydroxypropyl methylcellulose (HPMC), xanthan gum (XG) and locust bean gum (LBG). Their ability to act as thickeners or stabilizers is well studied (Arancibia et al., 2013; Camino and Pilosof, 2011; Camino et al., 2011; Khouryieh et al., 2015; Renou et al., 2013). Most of the thickeners are highly priced, and the food industry would benefit from cheaper alternatives.

Cellulose fibrils have recently being used as particles to produce Pickering emulsions (Kalashnikova et al., 2011). However, little research has been done on the stabilizing properties of bacterial cellulose (Ougiya et al., 1997). Nevertheless, there is no report on the effect of preparation conditions of the emulsions stabilized by bacterial cellulose. Most studies investigated the mechanism of the stabilizing effect of microfibrillated cellulose (Andresen and Stenius, 2007; Winuprasith and Suphantharika, 2015; Xhanari et al., 2011) or microcrystalline cellulose (Adeyeye et al., 2002; Ougiya et al., 1998).

Hence, the objective of the present study is to investigate the preparation and characterization of olive oil-in-water (o/w) emulsions stabilized by various thickeners (HPMC, CMC, BC) taking into account the factors that influence the properties of these emulsions, such as thickeners' concentration and emulsification method (high shear or ultrasonication), pH, temperature and ionic strength. Also, to compare the rheological behaviour of emulsions thickened with bacterial cellulose (BC) or xanthan gum (XG) or locust bean gum (LBG).

5.2. Emulsions stability

BC has distinctive advantages over traditional sources of cellulose such as plants even though they have the same chemical structure. In particular, BC has lower density, higher crystallinity, higher water holding capacity, higher mechanical strength due to its web-like network structure and higher purity as it is pure cellulose and does not associate with lignin or hemicelluloses (Iguchi et al., 2000). Thanks to these properties, bacterial cellulose fibrils are increasingly being used in various areas, such as biomedicine (Fu et al., 2013; Meftahi et al., 2010), paper industry (R. et al., 2009) and many others. Its applications in the food industry are recently investigated. BC could be used to improve rheology of food as a thickening,

stabilizing or gelling agent. Also BC could produce low-calorie and low-cholesterol foods (Shi et al., 2014).

Solid colloidal particles have been shown to accumulate at the interface between two immiscible liquids and stabilize the emulsion drops against coalescence by forming a mechanically robust monolayer at the liquid-liquid interface. These emulsions are typically referred to as Pickering emulsions (Pickering, 1907). Good mechanical properties and high resistance to coalescence are only a few of Pickering emulsion properties (Chevalier and Bolzinger, 2013).

In this chapter, the thickening properties of BC are compared with the properties of CMC, HPMCH and HPMCL. Hence, to evaluate the stability of the different emulsions upon storage, phase separation for emulsions of various cellulose concentrations and types was recorded for a 7 days period, and is presented in Fig. 5.1 a to d.

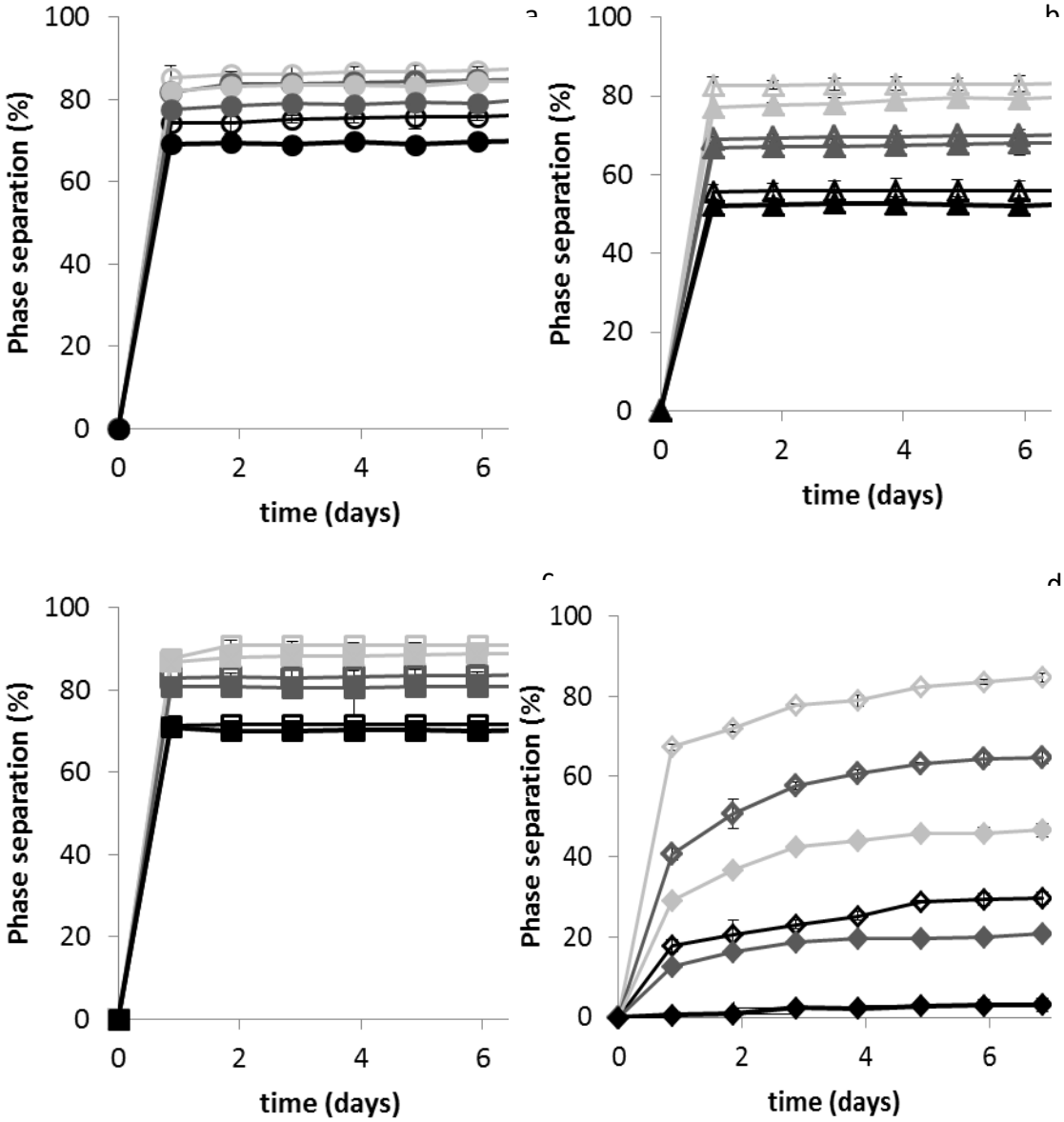

Fig. 5. 1 Effect emulsification method: high shear mixer (open symbols) or ultrasound (closed symbols) and cellulose concentration which varied from 0.1 (●), 0.5 (●) and 1% wt (●) on phase separation as a function of time for o/w emulsions stabilized by different cellulose types: HPMC L (a), HPMC H (b), CMC (c) and BC (d).

From this figure it can be conducted that the higher the concentration of cellulose used to stabilize the emulsions is, the lower the phase separation is. Specifically, by increasing cellulose concentration from 0.1 to 1% wt, all the emulsions become more stable against coalescence. As expected, the 0.1% wt emulsions show the higher creaming rate that is arrived due to its largest droplets (data not shown). As the concentration of cellulose is increased reaching 1%wt, emulsions become more

stable. This could be attributed to depletion-flocculation phenomena, which take place due to the presence of non-adsorbing cellulose molecules on the aqueous phase (Hayati et al., 2009; Moschakis et al., 2005; Zinoviadou et al., 2012). The increase of stability by increasing the cellulose concentration is independent from the cellulose type used.

However, the extent of phase separation is dependent to the cellulose, with BC emulsions having the highest difference between the SI of the various concentrations varying from 46 to 3% (Fig. 5.1). At the same time, HPMC L difference was varying from 84 to 70%. HPMC L emulsions have the weakest structure as evidenced by its lowest G' values (5.3). This leads to very high droplet mobility and therefore a high degree of creaming.

In all cases except BC, the emulsions phase separate rapidly after initial emulsification and reach their final creaming after one day from preparation, regardless of the concentration of cellulose used. On the other hand, BC shows better emulsifying capability as its emulsions separate with a slower rate and reach their final creaming after 4-6 days of storage regardless of the concentration of BC used. Ougiya et al., (1997) when studied BC emulsions with polarized light microscope, observed flocs composed of BC fibrils in their emulsion. However, they did not observe fibrils in emulsions stabilized by microfibrillated cellulose. That's probably the case in our systems as well. Specifically, flocs of BC fibrils are adsorbed to the surface of the oil droplet in accordance to Pickering stabilization method. This network acts as a mechanical barrier which prevents droplets' coalescence.

This network becomes even stronger when the emulsification method prolonged, that is from high shear mixer to ultrasound (Fig. 5.2 a& b).

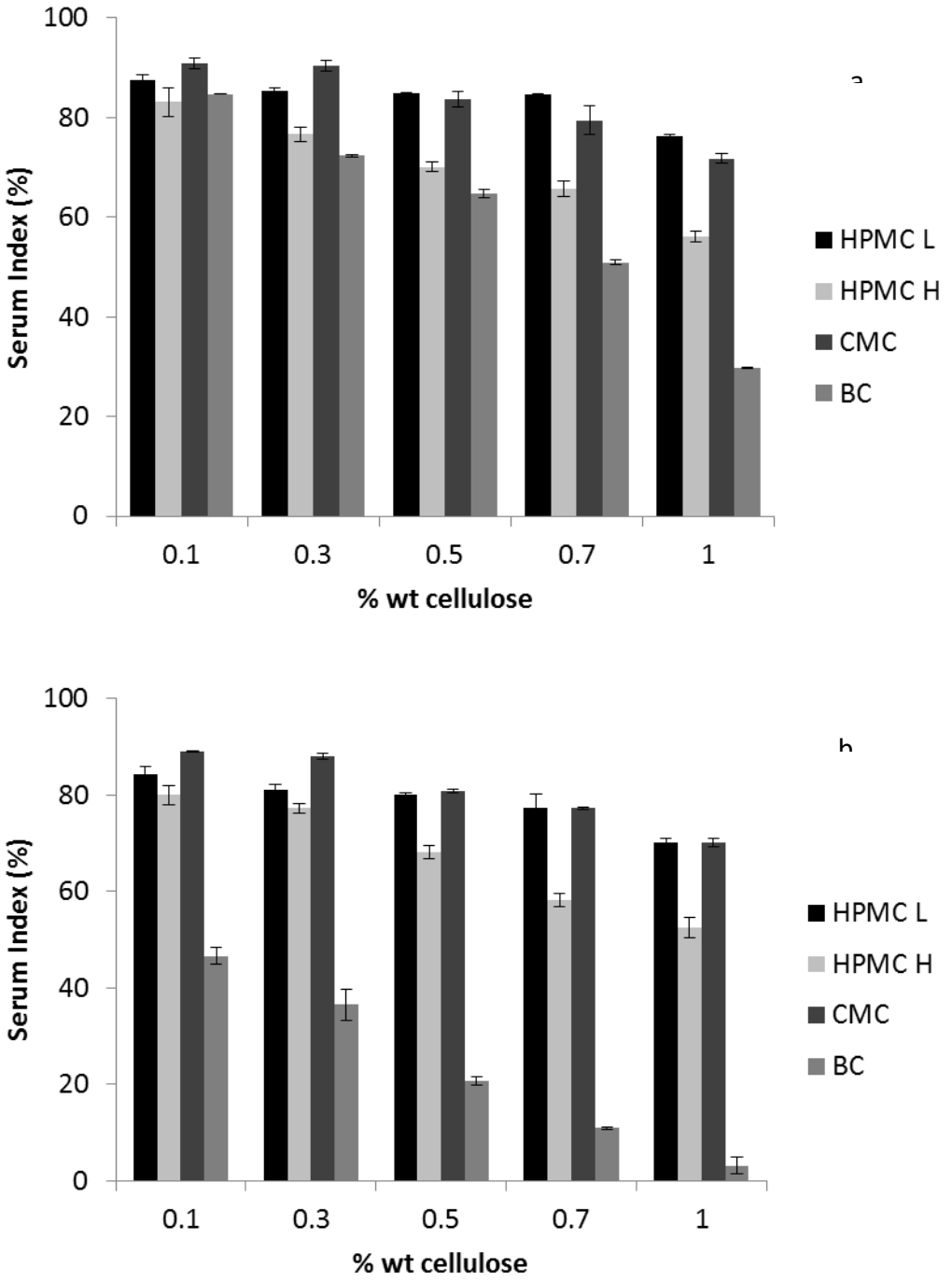

Fig. 5. 2 Serum index as a function of cellulose concentration for o/w emulsions (10% wt extra virgin olive oil) prepared by high shear mixer (a) and ultrasound (b) after 7 days of storage at 4^{o}C.

Specifically, by increasing the emulsification process, the SI of the emulsions decreases significantly. This is the result of a stronger network formation, which makes the emulsions more stable. It could be said that by the ultrasonication treatment, the previous mentioned BC flocs become smaller. Therefore, a stronger

network seems to be related by smaller flocs. This strong network could be evidenced by the high yield stress and G' values (5.3) that BC emulsions exhibit.

In all the other types used, the prolongation of emulsification method also resulted in more stable emulsions against coalescence, which was previously reported for HPMC emulsions (Camino and Pilosof, 2011). HPMCH showed better emulsions stabilization because of its high viscosity, inhibiting extensive coalescence.

5.3. Emulsions droplet characteristics

In order to understand the differences in the stability of the emulsions, the microstructure of the emulsions was investigated. In Fig. 5.3, typical optical micrographs of secondary emulsions containing 1%wt of various types of cellulose and stabilized either by high shear mixer or ultrasound are demonstrated.

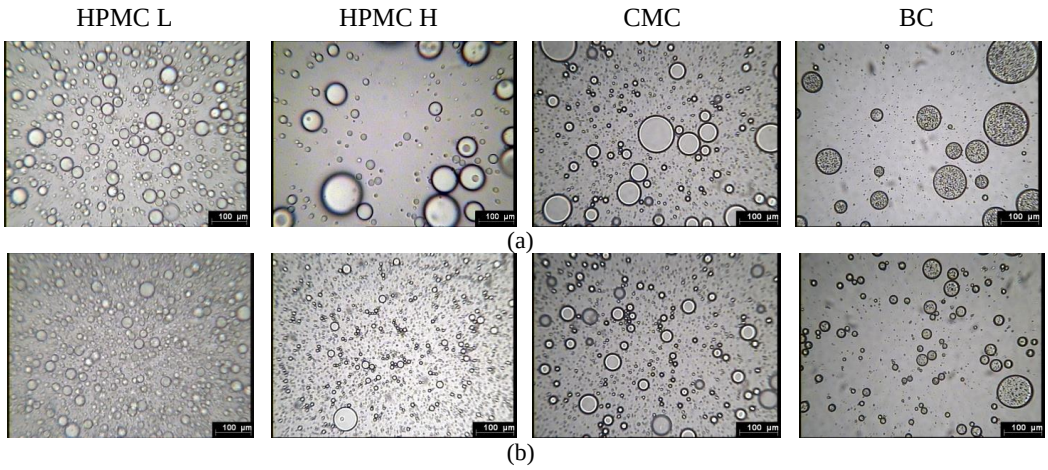

Fig. 5. 3 Micrographs of o/w emulsions stabilized with 1%wt different celluloses (from left to right HPMC L, HPMC H, CMC and BC) prepared by high shear mixer (a) and ultrasound (b).

It is clearly seen that emulsification method has a distinct influence on the size of emulsified droplets. The emulsions prepared with high shear mixer seem to have larger droplet sizes compared to those prepared by ultrasound. Hence, ultrasound produces emulsions with smaller oil droplets regardless of the type of cellulose used. These observations are in agreement with the stability results that were mentioned earlier.

On the other hand, cellulose type has a pronounced effect on the flocculation phenomena which took place. Specifically, in HPMC L emulsions it is obvious that extensive coalescence phenomena take place, while in CMC and even more in HPMC

H and BC emulsions the phenomena are less intense. These results are in agreement with the results from the storage stability and the study of Hayati et al., (2009). According to them, the more extensive the aggregation, the faster the creaming occurs. Also, in the micrographs of BC emulsions, it can be seen the formation of double emulsions probably because of the entrapped water in the droplets.

The following droplet size parameters are evaluated for emulsions prepared with ultrasound and stabilized by 1% wt of different types of cellulose and presented in Table 5.1.

Table 5. 1 Droplet size parameters of emulsions containing 1%wt of various celluloses prepared by ultrasound.

	$d_{3.2}$ (μm)	$D_{4.3}$ (μm)	Span (-)
HPMC L	1.8^{b} (0.64)	14.1^{b} (1.31)	2.8^{b} (0.31)
HPMC H	1.3^{a} (0.70)	10.6^{a} (1.28)	1.3^{a} (0.54)
CMC	2.6^{c} (0.38)	16.2^{c} (1.74)	7.2^{c} (1.79)
BC	26.8^{d} (1.09)	108.5^{d} (6.32)	1.5^{a} (0.38)

In parenthesis standard deviation values.

Mean values followed by the same letters are not significantly different ($P > 0.05$).

For all the emulsions, $d_{4,3}$ values are significantly higher than $d_{3,2}$. It is well known that $d_{4,3}$ is related with changes in particle size involving destabilization processes and therefore it is more sensitive to larger droplets and droplet aggregation (Camino and Pilosof, 2011; Relkin et al., 2008). Hence, the higher value of $d_{4,3}$ is a first indication of the polydispersity of the emulsion. Indeed, according to Span value, all the emulsions are bimodal or multimodal. An emulsion could be characterized as bimodal when its Span value is larger than 1 and this is in accordance with all the emulsions with cellulose (McClements, 2005). CMC emulsion showed a Span value at 7.25 which means that the droplet size distribution is multimodal and coalescence of droplets takes place.

HPMC L and H emulsions experience similar $d_{3,2}$ values: 1.87 and 1.34 μm respectively. However their $d_{4,3}$ and Span are significantly different, with HPMC L experiencing the higher values and therefore a broader distribution, resulting in a lower stability as shown earlier by serum values. Camino and Pilosof, (2011) produced HPMC emulsions with ultrasound and showed that polydispersity followed the order of decreasing HPMC molecular weight; while Schulz & Daniels (2000)

produced HPMC emulsions with high pressure homogenizer obtained smaller droplet sizes with the lower molecular weight HPMC. On the other hand, CMC emulsion $d_{3,2}$ value is higher than the emulsions containing HPMC. This finding corresponds to the formation of strongly bound aggregates that do not break up and can be attributed to the inability of CMC to fully cover the emulsion droplets. Depletion flocculation is quite common in polysaccharide stabilized emulsions as reported by Wollenweber et al. (2000) and Du et al. (2009).

BC emulsions show a $d_{3,2}$ value of 26.8 µm, which is similar to the findings of Ougiya et al. (1997), who used BC particles to stabilize their emulsions. Chevalier &Bolzinger(2013) indicated that in case of low amount of particles, only a small interfacial area can be stabilized, so that very large droplets should result. This may be the case for our system as well because the emulsification process used was fairly mild (total 2min). Nevertheless, BC emulsions show an extremely low serum index value, which implies that limited droplet coalescence occurred through the entire storage period. Such a combination of large droplet sizes ($d_{3,2}$= 26µm) and high stability (SI= 3%) is not usually noticed in surfactant-stabilized emulsions and it is a feature of particle-stabilized emulsions (Binks&Whitby, 2004; Chevalier &Bolzinger,2013).This can be attributed to the fact that the particles adsorbed at the oil-water interface can sterically hinder the close approach of the droplets, thus reducing the extent of coalescence (Chevalier &Bolzinger, 2013).

5.4. Emulsions rheology

Structural changes due to aggregation of emulsion droplets have a large influence on the viscosity of the emulsions. The steady flow curves and dynamic mechanical spectra of the emulsions stabilized with 1% wt of different cellulose types is presented in Fig. 5.4a and b respectively.

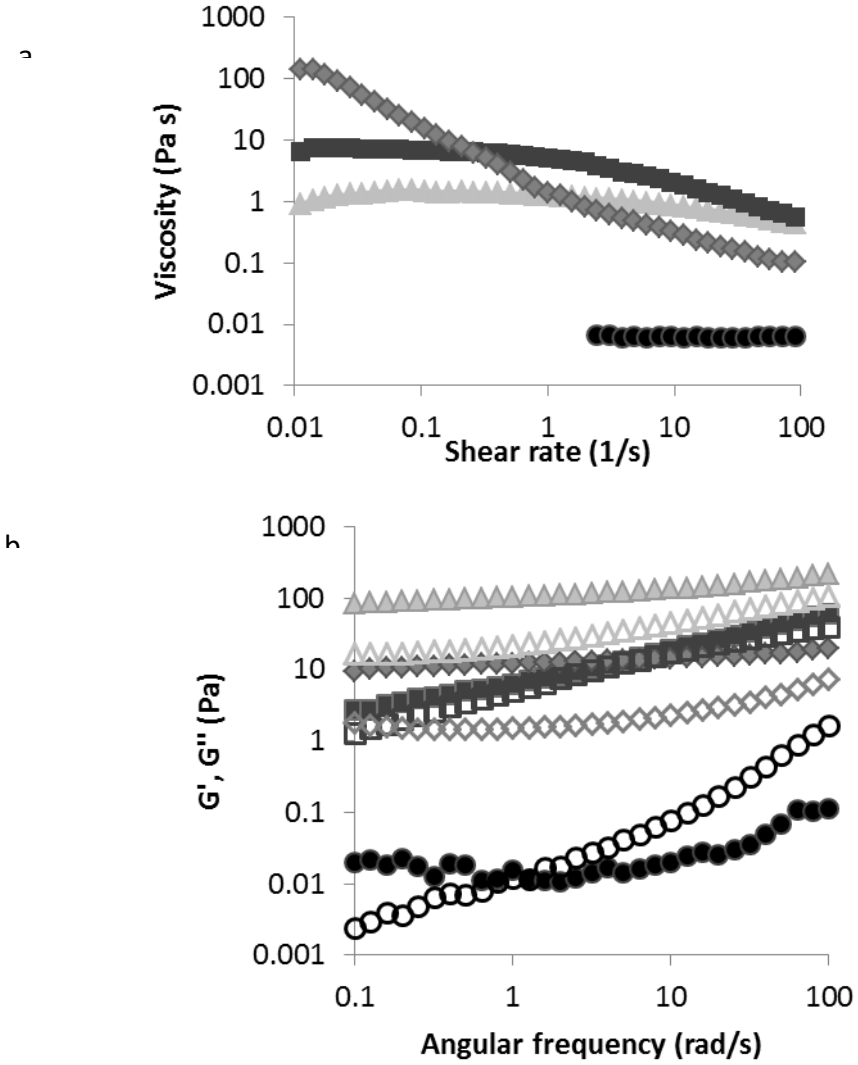

Fig. 5. 4 Apparent viscosity as a function of shear rate (a) and storage modulus, G' (closed symbols) and loss modulus, G'' (open symbols) as a function of angular frequency measured at 0.3% strain (b): (●) HPMC L, (▲) HPMC H, (■) CMC and (◆) BC. Error margins where within the limit of 2%.

The HPMC L emulsions exhibit Newtonian-like behavior as their viscosity is practically independent from the shear rate; however the emulsions prepared with all the other types of cellulose exhibit shear-thinning with yield stress behavior. The HPMC H emulsion shows less shear-thinning behavior, than CMC and BC as indicated by a relatively slow drop in viscosity with increasing shear rate. BC emulsions show the highest viscosities values at lower shear rates, followed by CMC, HPMC H and HPMC L. This is in accordance with the viscosity of the suspension of each cellulose.

The rheograms (Fig. 5.4a) of viscosity as a function of shear rate show an apparent yield stress. Hence, the rheograms are best fitted (R^2 = 0.97- 1.00) with the Herschel-Bulkley model as shown in Table 5.2.

Table 5. 2 Modelling of the flow curve between 0.01 to 100 s^{-1} of shear rate of the freshly prepared emulsions containing 1%wt of various celluloses using Herschel – Bulkley model

Sample	Herschel-Buckley factors		
	τ_o(Pa)	k (Pa s^n)	n (-)
HPMC L	-	0.006 (0.001)	1.005 (0.130)
HPMC H	0.035 (0.007)	1.078 (0.146)	0.792 (0.141)
CMC	0.236 (0.016)	3.491 (0.682)	0.411 (0.068)
BC	1.536 (0.280)	2.138 (0.284)	0.747 (0.093)

In parenthesis standard deviation values.

R^2 varied between 0.9776 and 0.9997.

The same model was also applied in emulsions containing celluloses (Hayati et al., 2009). As shown in Table 5.2, the highest yield stress (τ_o) was found in BC emulsions (1.536 Pa). The flow behavior index (n) indicates the degree of pseudoplasticity of the emulsions: it decreases, when pseudoplasticity increases. CMC emulsion is the most pseudoplastic, as it exhibits the lowest flow behavior index (n= 0.624). The flow index values of HPMC L emulsions near one (n=1.005) indicated that it exhibits Newtonian behavior. All the other emulsions shows a flow behavior index less than one, indicative of a non-Newtonian and shear-thinning flow behavior. As far as the consistency coefficient (k) is concerned, the emulsion with HPMC H shows the highest values. Consistency is an indicator of emulsion's viscous nature. These results are in accordance with other studies of CMC (Arancibia, Bayarri, &Costell, 2013) and HPMC emulsions (Camino&Pilosof, 2011b).

Mechanical spectra are quite different according to the cellulose type used (Fig. 5.4b) and can be shown that for HPMC H and BC emulsions, storage modulus (G') values are higher than loss modulus (G'') values and there is a weak frequency dependence, which is typical for weak gel-like behavior (Clark& Ross- Murphy, 1987). In particular, BC emulsions present an even lower frequency dependence of G' and G'', indicative of a solid-like behavior. However, the observed G' values are lower than those in HPMCH emulsion. High G' values indicate a cohesive/compact structure that can be found at high concentration of a hydrocolloid solution. HPMC L and CMC emulsion show a strong frequency dependent on dynamic moduli with the loss modulus exceeding the storage, indicating a fluid-like behavior. In particular, the cross-over between the two moduli found in CMC spectra is a behavior of a typical

concentrated emulsion. CMC emulsion presents similar dynamic moduli values to the ones previously reported (Arancibia, Bayarri, &Costell, 2013). This behavior is typical of weak associative interactions and indicates the formation of a weak droplet network formation.

Based on the previous mentioned rheological measurements, it could be conducted that an additional stabilizing mechanism in the BC emulsions is the formation of a gel-like viscoelastic network of BC particles in the aqueous phase, which remains between the droplets and prevents them from coalescence. These results is also reported by Winuprasith&Suphantharika(2013) and Tzoumaki et al., (2011) who stabilized emulsions by microfibrillated cellulose and chitin nanocrystals respectively. HPMC H emulsions have a high consistency and high G' values, both indicating a thickening effect of HPMC rather a stabilizing one through a network.

5.5. Application of environmental stresses on emulsions

Furthermore, in order to compare the stabilizing ability of BC with commonly used celluloses, the emulsions were subjected to different environmental stresses (pH, ionic strength, temperature) and their stability was evaluated.

For the pH stability test, the emulsions were prepared in deionized water as described above. The pH was adjusted to 3, 5, 7 by the addition of 0.1M HCl. For the ionic strength stability test, the emulsions were also prepared with deionized water. The ionic strength was adjusted to 0, 50, 100 and 200mM by the addition of the proper amount of NaCl. Finally, for the temperature stability test, the freshly prepared emulsions were placed in a water bath for 30min at 30, 50 and 70^{o}C. Serum Index (SI) as described above (Eq. 3.2) was evaluated for the different samples and presented in Fig. 5.5.

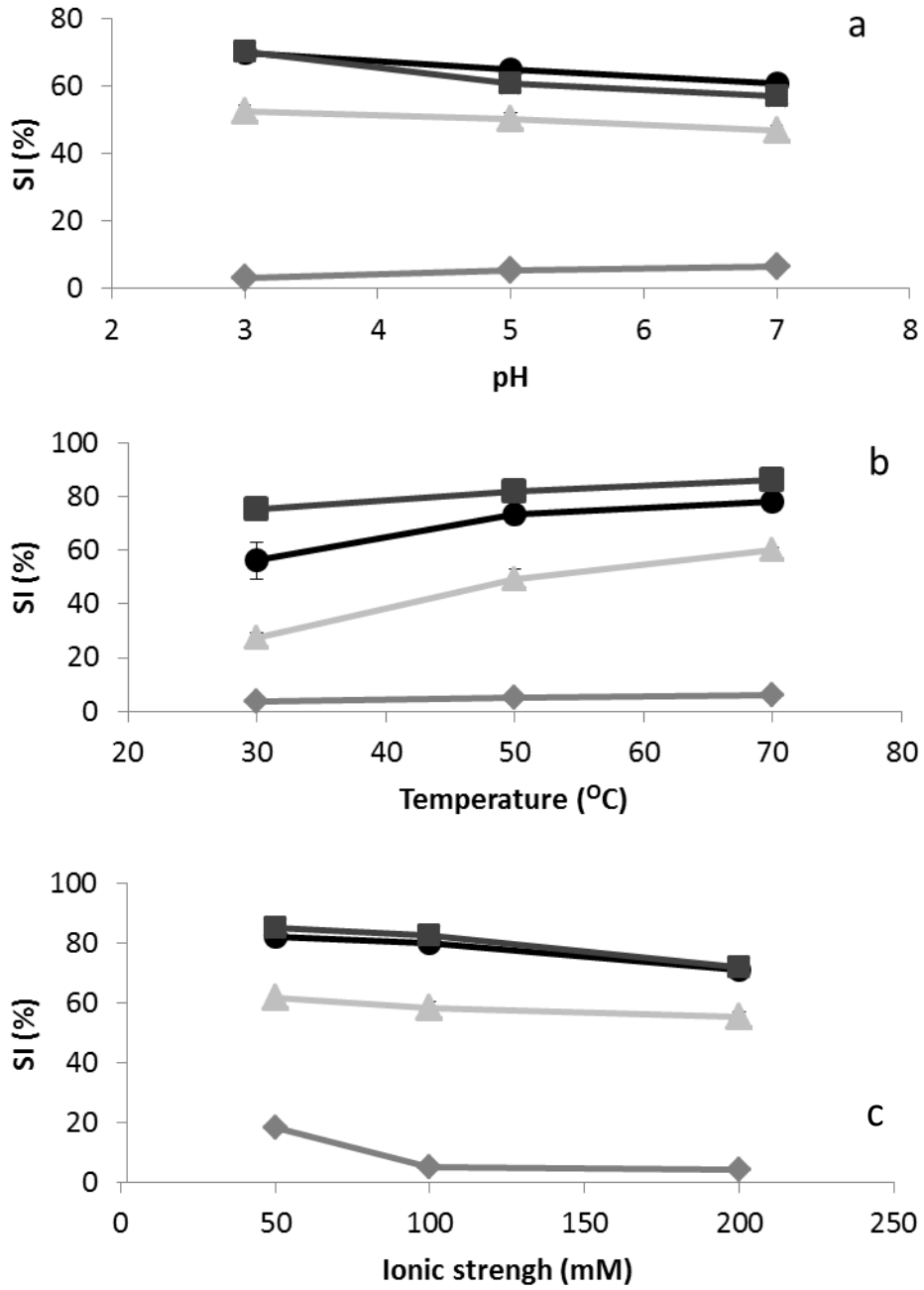

Fig. 5. 5 Influence of environmental stresses: pH (a), temperature (b) and ionic strength (c) on serum index of emulsions containing 1%wt of various cellulose types: (●) HPMC L, (▲) HPMC H, (■) CMC and (◆) BC and emulsified by ultrasound after 20 days of storage.

It is obvious that the stability of the emulsions depends not only on the environmental stresses but also on the type of cellulose used to stabilize the emulsions.

BC emulsions show a very low increase in serum index from 3 to 5% under changes from acidic (pH = 3) to neutral environment (pH = 7). Also, changes of temperature do not affect the SI of these emulsions. On the other hand, by increasing the ionic

strength up to 50mM, the SI yields higher values (SI= 18%). When the ionic strength increases from 100-200mM emulsions become much more stable, reaching a SI value close to 4%. Hence, BC emulsions tend to remain stable when treatments occurr. This is in accordance with the results of Ougiya et al. (1997) and Kalashnikova et al. (2011) who concluded that BC emulsions are not affected by the addition of NaCl, change in pH or change in temperature. This good stability against creaming could be attributed to the development of a gel-like network of BC flocs in the aqueous medium between the droplets, as it was obvious from our rheological measurements and Tzoumaki et al. (2011). Also, the good stability against creaming is characteristic for Pickering emulsions.

As far as the HPMCL emulsions are concerned, they are affected by the changes of pH, temperature and ionic strength. Specifically, changing the pH from 3 to 7 decreases the SI from 70 to 60%, indicating that HPMC L emulsions are more stable in neutral conditions. By increasing the temperature, they become unstable as SI varied from 56 to 78%. The cause of the instability of HPMC emulsions at high temperatures may be the partial desorption of cellulose molecules from the droplet surface that leads to flocculation and consequently creaming (Surh, Decker, &McClements, 2006). Emulsions with higher concentrations of NaCl are more stable as SI decreased from 82 to 71%. The same tendency in creaming is experienced at HPMC H and CMC emulsions as well (Fig.5 a, b and c). However, for these emulsions serum index values are lower for all the occurring treatments. This variation between the two types of HPMC is probably observed due to their viscosities. Specifically, HPMC H has much more high viscosity values leading to the formation of a more viscous network between the oil droplets which move closer with slower velocities and hence produce a more stable emulsion. Camino &Pilosof (2011b) measured the stability of HPMC emulsions and resulted that are more stable in neutral conditions. Schulz and Daniels (2000) indicated that HPMC emulsions prepared at 40^{O}C showed smaller droplet size than the ones prepared at higher temperatures, while Kumthekar&Nagarkar (2012) showed that a rise in temperature in emulsions prepared with CMC-Na linearly destabilized them during storage.

5.6. Comparison of BC with common thickeners

In order to evaluate the potential of BC to be used as an effective thickening agent, the BC-stabilized emulsions, that contained whey protein isolate (WPI) as well, were compared with emulsions stabilized with the more common thickeners xanthan gum (XG) and locust bean gum (LBG).

For this purpose, secondary emulsions were prepared with XG and LBG. In this case, the concentration of WPI in the secondary emulsions was chosen as 2% wt, the lowest concentration needed for emulsion stability as this was shown to provide

enough surface coverage from Chapter 6. In this case, we assume that the interactions between WPI and polysaccharides could be neglected and the differences in emulsion properties are merely an effect of the thickeners themselves. The amount of BC, XG and LBG added to the emulsions was chosen in such a way that the apparent viscosity at shear rate 0.1 s^{-1} is similar (Table 5.3). These emulsions were prepared as reported in Chapter 6.

Table 5. 3 The final tested emulsions

Emulsions	% WPI	% gum	Apparent viscosity (Pa s)*
WPI-BC1	2	0.01	0.3[a]
WPI-XG1	2	0.1	0.3[a]
WPI-LBG1	2	0.7	0.3[a]
WPI-BC2	2	0.1	1.6[b]
WPI-XG2	2	0.7	1.5[b]
WPI-LBG2	2	1	1.5[b]

* Measured at shear rate 0.1 s^{-1}.

Mean values followed by the same letters are not significantly different ($P > 0.05$).

It should be noted that the amount of BC needed to reach the same initial viscosity is much lower than the amount of XG and LGB required. For example, only 0.1% wt of the BC solution is required to reach an initial viscosity of roughly 1.5 Pas, while for XG and LBG an amount of 0.7% wt and 1% wt, respectively, is required. The viscosity profiles can be seen in Fig. 5.6, where all emulsions have a low-shear viscosity of either roughly 0.3 or 1.5 Pa s. Even though the low shear viscosity is the same, they present clear differences in the rheological profile.

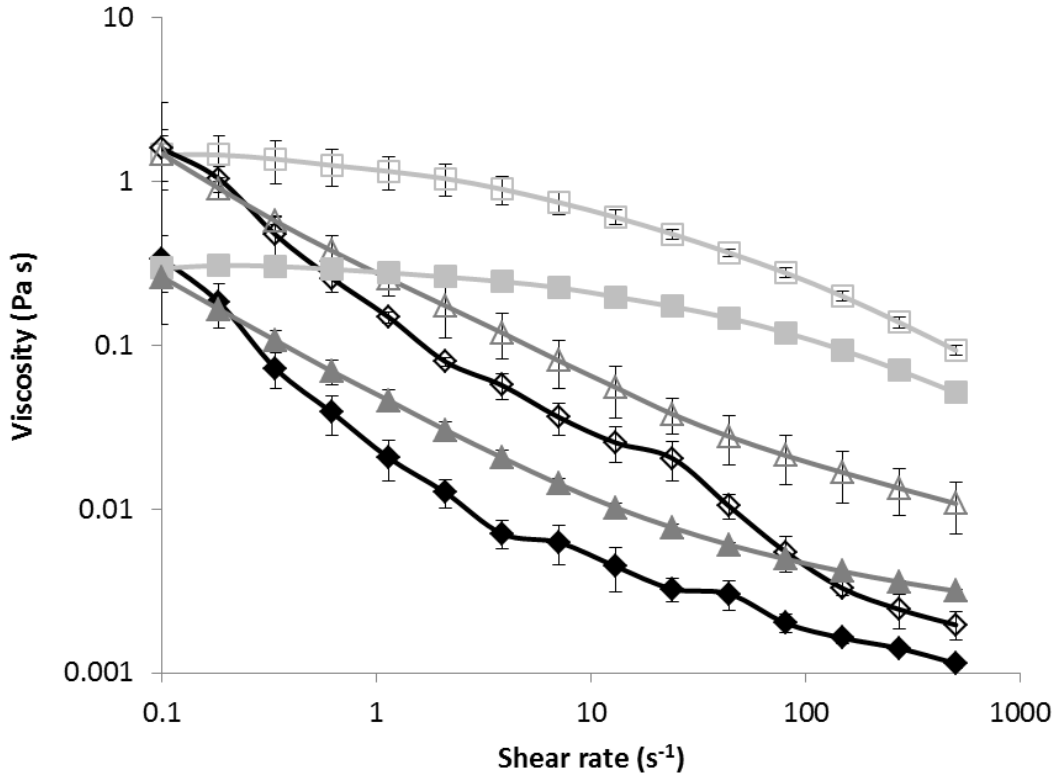

Fig. 5. 6 Viscosity curves of emulsions containing 2% wt WPI and various concentrations of BC or XG or LBG as mentioned in Table 1: BC1 (◆),XG1 (▲), LBG1 (■), BC2 (◇), XG2 (△) and LBG2 (□). Bars indicating standard deviations.

Emulsions stabilized by LBG exhibit the least shear thinning behavior, while emulsions stabilized with BC and XG show the most shear thinning effect. The rheological profiles of the emulsions are similar to those of the respective polysaccharides' solutions (data not shown). Xanthan gum is commonly used as a thickener due to this very shear thinning profile which gives structure to an emulsion at rest and good flow behavior in motion. Comparing XG and BC, we can observe that emulsions with BC show a similar high shear thinning behavior, even more than emulsions containing XG. BC might therefore has advantages over XG as it is more effective in increasing the low shear viscosity (yield stress) and it has a larger shear thinning behavior.

To investigate the emulsion properties, also droplet sizes, ζ-potential and serum index have been measured. The results are reported in Table 5.4.

Table 5. 4 Physical properties (droplet size, ζ -potential and serum index) of 2% wt WPI emulsions, stabilized by BC or XG or LBG.

Emulsions	% WPI	% gum	ζ-potential (mV)	D_{50} (μm)	D_{32} (μm)	D_{43} (μm)	SI (%)
WPI-BC1	2	0.01	$+44.7^{c}$ (0.8)	1.84^{b} (0.03)	1.26^{c} (0.08)	10.14^{d} (1.71)	34^{e} (2)
WPI-XG1	2	0.1	-14.3^{b} (0.9)	1.76^{b} (0.06)	1.41^{c} (0.03)	5.02^{b} (0.37)	41^{f} (2)
WPI-LBG1	2	0.7	$+20.0^{a}$ (0.1)	1.30^{a} (0.11)	0.95^{b} (0.22)	1.66^{a} (0.85)	12^{b} (1)
WPI-BC2	2	0.1	$+41.6^{c}$ (1.4)	1.75^{b} (0.11)	2.82^{d} (0.56)	12.28^{e} (1.20)	30^{d} (2)
WPI-XG2	2	0.7	-16.8^{b} (0.6)	1.82^{b} (0.08)	1.30^{bc} (0.04)	6.53^{c} (0.60)	18^{c} (1)
WPI-LBG2	2	1	$+16.7^{a}$ (0.2)	1.11^{a} (0.25)	0.64^{a} (0.08)	1.55^{a} (0.91)	3^{a} (1)

In parenthesis standard deviation values.

Mean values followed by the same letters are not significantly different ($P > 0.05$).

As far as the droplet size is concerned, the droplet size of emulsions containing LBG is significantly lower than the other emulsions. The formation of small droplet size was previously reported in emulsions containing LBG (Hayati, et al., 2009; Makri & Doxastakis, 2006). Mean droplet size (D_{50}) of BC emulsions does not show significant difference from emulsions containing XG. However, D_{32} and D_{43} values are much higher for the BC emulsions. These higher values can be attributed to bridging flocculation phenomena, as the oil droplets' surface is not saturated and hence increases the D_{32} and D_{43} values.

ζ-potential results are also useful in order to evaluate the mechanisms of destabilization of the emulsions. Emulsions with LBG show positive droplet charge (+16 to +20 mV). As LBG does not have a charge, it cannot be adsorbed at the droplets' surface and remains at the aqueous phase. Hence, the ζ-potential values are only from the WPI that is adsorbed onto the surface. Emulsions with XG show a negative droplet charge (-14.36 to -16.80mV), indicating that XG molecules are strongly absorbed onto the WPI-coated droplets, forming a second layer. Emulsions containing BC show positive droplet charges (+41.64 to +44.74mV), in accordance with the ζ-potential reported previously. These results show that the large difference

between XG and BC is related to their ability to adsorb onto the droplets and change the droplet charge. In the case of BC, a larger excess of BC remains in the aqueous phase.

As far as the stability is concerned, emulsions with LBG are the most stable ones as the serum index is the lowest varying from 3 to 13%. This high stability is ascribed to clustered galactose branch points that exist in LBG structure. Galactose units are known to form hydrogen bonds with the water molecules leading to retardation of creaming (Huang, Kakuda, & Cui, 2001). XG produce unstable emulsions with SI varying from 18 to 41%. This instability could be related to depletion flocculation induced by XG. XG is an effective depletion flocculation inducer (Dickinson, 1992). Finally, BC also produce unstable emulsions with SI varying from 30 to 34%. This instability could be an effect of the low amount of the added polysaccharide that could cause bridging flocculation and thus destabilize the emulsion.

5.7. Conclusions

In the present chapter, the stabilizing properties of bacterial cellulose in o/w emulsions and its differences between emulsions stabilized by commercial celluloses (HPMC, CMC) were studied. BC showed better emulsifying capability compared to HPMC and CMC as its emulsions separated with a slower rate. This higher stability is due to the flocs of BC fibrils which adsorbed to the surface of the oil droplet and formed a strong network. This strong network could be evidenced by the high yield stress and gel-like behavior that BC emulsions exhibited. HPMC H and L formed emulsions with similar droplet sizes, but HPMC L showed the highest instability as it had the weakest structures. Even the BC emulsions showed the largest droplets, showed an extremely stability against coalescence, phenomenon typical for particle-stabilized emulsions. BC emulsions were not affected by changes in pH, temperature or ionic strength unlike the emulsions prepared with all the other types of cellulose whose stability was significantly influenced by environmental stresses. Hence, it can be concluded that BC could be a useful stabilizer for o/w emulsions with further potential applications. Finally, to test the potential of BC to act as alternative thickener, emulsions stabilized with either BC, locust bean gum (LBG) and xanthan gum (XG) were compared. Their rheological profile showed that BC showed similar shear thinning behavior as XG, but smaller amounts of BC were needed to obtain the same low shear viscosity (yield stress). These results show that BC is a good alternative for commonly used thickeners that can be used in future applications in the food industry.

Chapter 6. Influence of the homogenization method on physical characteristics of emulsions containing bacterial cellulose

6.1. Introduction

Processing techniques such as high power ultrasound (US) and high pressure homogenization (HPH) are currently being used in the food industry in many applications as they have the ability to change the physicochemical properties of the ingredients (Canselier et al., 2002; Gulseren et al., 2007; Jambrak et al., 2009; Kaltsa et al., 2013; Price et al., 1994).

There are many studies showing the formulation of emulsions with droplets in the nano-range (10–100 nm radius), by using US and HPH, the so called high-energy emulsification methods (Lee et al., 2014; Tubesha et al., 2013). These methods reduce the droplet size by providing a high energy input in the system. The efficiency of HPH to generate nanoemulsions depends mainly on the geometry of the homogenization valve, while in the US systems cavitation is the main effect. Specifically, in HPH, pressures between 50 and 150 MPa are generally applied to emulsions (Dumay et al., 2013). The number of process passes usually varies between 1-10, while the increase of the passes leads to the reduction not only the mean particle diameter but also the width of the particle size distribution. Moreover, the emulsion stability against coalescence is being improved (Lee and Norton, 2013; Qian and McClements, 2011).

On the other hand, in the US, the energy is transferred to the fluid by the propagation of ultrasound waves in the frequency range of 20–100 kHz for a few seconds to several minutes (Floury et al., 2002). US emulsification is mainly believed to occur mainly in the vicinity of the collapsing bubbles, where the high fluid velocity causes the mixing of emulsion and droplet size reduction. The longer the treatment time the greater the droplet break-up, up to a threshold above which a further increase in residence time would not lead to a concomitant reduction of droplet diameter (Jafari et al., 2006).

What is more, thickeners are often used to increase the viscosity of the products they are incorporated in. Although not used extensively in food, BC has great potential as a food ingredient, where it could be used to alter the rheological behavior of food as a thickening, stabilizing or gelling agent. Recently, BC has been shown to act as a stabilizer in emulsions (Kalashnikova et al., 2011; Paximada et al., 2014). However, BC as a thickener has not been studied extensively and its effect on the rheological behavior of emulsions is not well known.

Hence, the objective of the present study is to investigate the effect of BC addition in whey protein isolate (WPI) emulsions. Two different homogenization processes were used: ultrasonication or high pressure homogenization.

6.2. Preliminary experiments

Emulsions with different functional properties can be obtained through the homogenization of polymer solutions depending on the process parameters and the solution properties. In this chapter, regarding the polymers' solutions, different combinations of WPI and BC were investigated in order to obtain an optimal range of WPI and BC concentrations, where phase separation is not observed. Figure 6.1 shows the tested solutions containing combinations of WPI and BC and their phase separation.

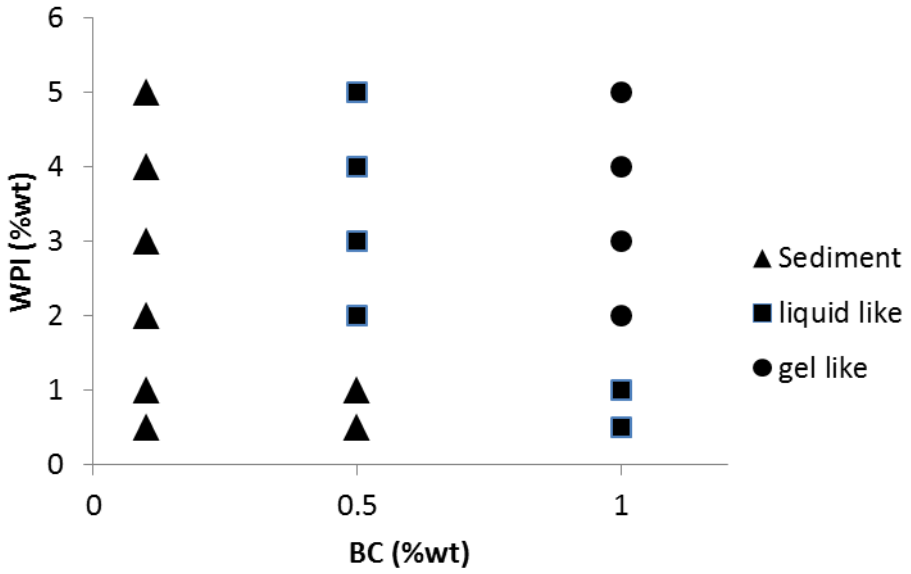

Fig. 6. 1 Phase diagram of the emulsions with 3 main behaviors: sediment formation (▲), liquid-like (■), and gel-like behavior (●).

As it can be seen, the solutions containing low concentration of BC (0.1% wt.) and with low concentration of WPI (0.5-1% wt.) are separated and WPI forms a sediment after the mixing. This could be attributed to interactions that take place between the protein and polysaccharide (Panaras et al., 2011). Moreover, by increasing the concentration of BC up to 0.5% wt., the solutions exhibit a liquid-like behavior, typical for solutions with inadequate amount of thickener (McClements, 2011). Finally, the solutions containing 1% wt. BC are found to possess a gel-like structure. The optimal concentrations of the two ingredients are those exhibiting a gel-like behavior, as the increased viscosity values are favoring the stability of the final emulsions. Preliminary trials also showed that the emulsion formulation used in this study was performed well in terms of mean particle diameter.

Hence, our different WPI concentrations (2, 3, 4, and 5% wt.) and three different BC concentrations (0.5, 0.7, 1% wt.) were finally selected in order to make 12 final

emulsions with all the possible combinations. The concentrations of the optimal final emulsions found in this study are summarized in Table 6.1. This emulsions were further homogenized by ultrasounds or high pressure homogenizer and their final physicochemical properties are discussed in this chapter.

Table 6. 1 The final tested emulsions

% wt WPI	%wt BC	Oil phase (%)
2	0, 0.5, 0.7, 1	10
3	0, 0.5, 0.7, 1	10
4	0, 0.5, 0.7, 1	10
5	0, 0.5, 0.7, 1	10

6.3. Droplet size of emulsions prepared with high pressure

When a protein and a polysaccharide are mixed, their mutual interactions greatly depend on the concentrations of the polymers in the mixture and their charge density as a result of environmental conditions, such as ionic strength, the charge, and pH of the solution (Dickinson, 2011). The interactions could be segregative when the polymers repel each other, due to similar charges, or associative when they attract each other as a result of opposite charges (McClements, 2006). This may lead to depletion interactions (segregative) or complex formation (associative), which can lead to either phase separation or network formation.

In this research, WPI was used as an emulsifier and BC was used as a thickener in the aqueous phase. The pH of the emulsions was 3.8, which is lower than the isoelectric point of WPI (pH <pI ~ 5.2), thereby providing a positive charge to the proteins (McClements, 2005). As previously reported, BC fibrils are negatively charged in a large pH range, as most of the celluloses (Martinez-Sanz et al., 2011). The pKa value of cellulose is 4; at this pH the charge density diminishes, whereas at higher pH values the charge density increases (McClements, 2005). When negatively charged BC is added to the protein-stabilized emulsion, the attractive interactions will lead to association between the proteins and the BC. At low BC concentrations, this leads to the formation of a secondary layer of BC at the droplet interface. Once the droplet surface is saturated, an excess of BC, at high concentrations, will remain in the aqueous phase and will potentially form a network. Different concentrations of BC will therefore lead to different stabilizing mechanisms. Droplet size measurements and droplet polydispersity for emulsions with different BC and WPI concentrations

were measured to gain insight in these mechanisms. Fig. 6.2 (A-C). shows the size distribution (as volume averaged) of emulsions containing different BC concentrations (0% (A), 0.5% (B), 0.7% (C) and 1% (D)), in which the concentrations of WPI as emulsifier, is changed from 2% to 5% wt.

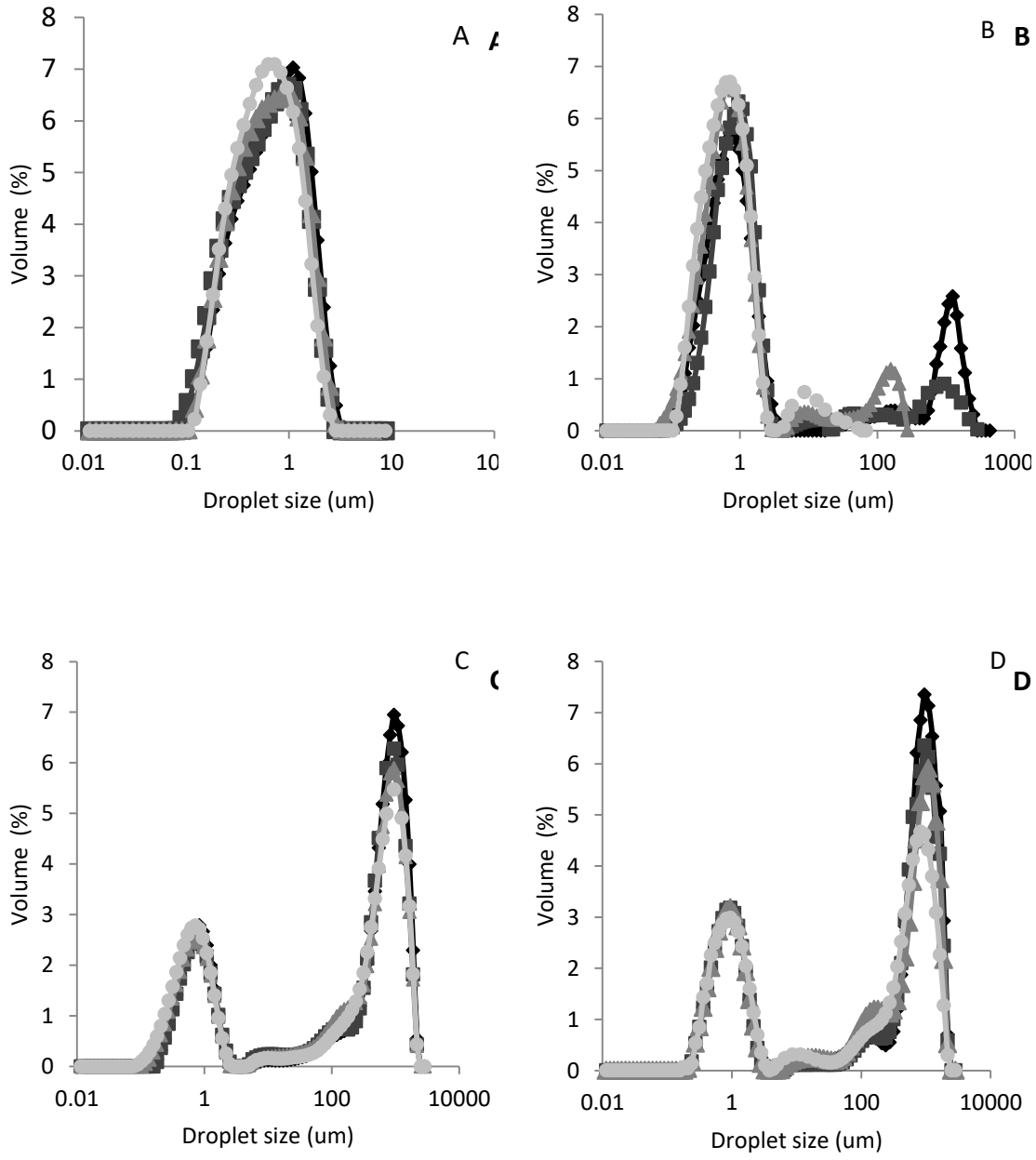

Fig. 6. 2 Droplet size distribution of emulsions prepared with 2% wt (◆), 3% wt (■), 4% wt(▲) and 5% (●) wt. WPI and stabilized by 0% (A), 0.5% wt (B), 0.7% wt (C) and 1% (D) wt BC.

In emulsions without BC present (Fig. 6.2A), the droplet size distribution shows one peak for all WPI concentrations used. For all concentrations, the average droplet size is found to be roughly 600 nm. Hence, it can be said that WPI concentration does not

affect the emulsions droplet size. The monomodal size distribution is confirmed by a polydisperisty Index (PDI), (Eq. 3.3) lower than 1 (McClements, 2005). This indicates that even the lowest WPI concentration (2%) can efficiently cover the droplets' surface while at higher concentrations, the excess WPI remains in the aqueous phase.

When BC is added to the emulsions, two distinct peaks can be observed (Fig. 6.2B-D). The first peak represents the emulsion droplets, with values of 600 nm, similar as the droplet size found when no BC is present (Fig. 6.2A). For all the BC concentrations, a second peak emerges around 500 μm. This peak most likely represents BC fibrils' flocs, which remain in the aqueous phase, as. 500 μm is a common size for BC flocs (Okiyama et al., 1993). These flocs are formed due to the forces that underlie between BC nanofibrils which forms the fibril network. As the concentration of BC in emulsions increases, the second peak in the droplet size distribution becomes more prominent, indicating that indeed the BC is responsible for the prevalence of the peak (Fig. 6.2B -D).

In the case of the lowest WPI concentration (represented by ◆ at Fig. 6.2B- D), this second peak is the largest. By increasing WPI concentration, the size of the peak decreases. This can be observed in both Fig. 2C and D, where the BC concentration is relatively high (0.7 and 1% wt). In the case of a low amount of BC (Fig. 6.2B), the second peak even moves to smaller sizes, indicating that the BC flocs decreased in size. This phenomenon was previously reported (Oshima et al., 2011). Specifically, it was shown that proteins can prevent the formation of BC flocs by adsorbing onto the surface of the BC fibrils (Oshima et al., 2011). The fine network structure of BC is able to hold a large amount of proteins, due to its large surface area (Oshima et al., 2011; Ougiya et al., 1998). More proteins therefore lead to less BC floc formation. Moreover, at low concentrations of BC, it adsorbs onto the WPI-coated oil droplets (as they are oppositely charged) and therefore BC is not present in the aqueous phase where floc formation can occur.

When the WPI content is increased from 2 to 5% wt, the size of the second peak decreases, indicating that indeed less large BC flocs are present. The excess of WPI in the continuous aqueous phase prevents the floc formation due to complexation between WPI and BC, and thereby leads to a reduction of the second peak.

Taking all the above into account, it can be said that the droplet surface is saturated at low amounts of WPI (2%). For low concentrations of BC, a second layer of BC is formed around the oil droplets, while for an excess of BC and WPI complexes are formed in the continuous phase. To gain more insight in the interactions between BC and WPI and the location of the BC, the ζ-potential of the emulsions was measured. The ζ-potential represents the charge density of the emulsions droplets. In Fig. 6.3, the ζ-potential of the emulsions with different BC concentrations is depicted.

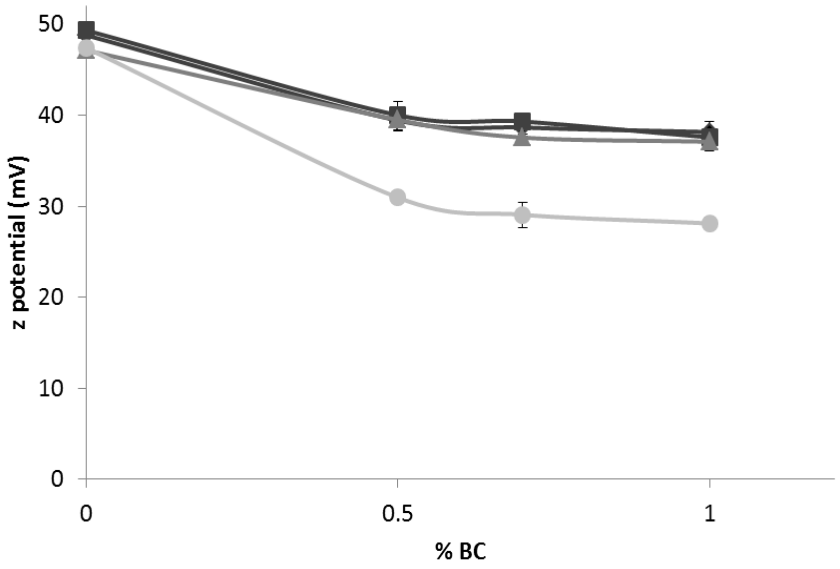

Fig. 6. 3 ζ-potential as a function of BC concentration for emulsions stabilized by 2% wt (◆), 3% wt (■), 4% wt(▲) and 5% (●) wt WPI. Bars indicating standard deviations.

When no BC is present, the emulsion droplets are stabilized by WPI and the overall charge of the oil droplets is positive (47.4 – 48.8 mV) charge at a pH of 3.8. The ζ-potential values are not significantly affected by the concentration of WPI in the final emulsions, confirming that even the lowest concentration of WPI (2% wt) is sufficient to completely saturate the droplet surface and the excess of WPI remains in the aqueous phase. This has been confirmed by many researchers (Camino et al., 2012; Liu et al., 2012; Long et al., 2013).

When negatively-charged BC is added, the ζ-potential values remain positive but decreased in value. Taking into account that the measuring range of the used equipment is 0.3 nm- 10μm, we assume that the larger BC flocs (500μm) are not included in the measurements. Hence, we assume that we only measure oil droplets. When low amount (2-4%) of WPI is present, the addition of BC leads to a drop in the ζ-potential to values of roughly 40 mV independently of the added BC concentration. The reduction of the droplet charge density indicates the adsorption of the BC fibrils onto the surface of the positively charged WPI-coated oil droplets, mainly through electrostatic attractions. As the charge density does not decrease further when the BC concentration increases, we can conclude that saturation of the WPI-coated droplets with BC already occurs at 0.5% wt BC. For higher BC concentrations (0.7 - 1%), the unadsorbed BC fibrils remain in the aqueous phase.

Worth noting is the fact that lower ζ-potential values can be seen in emulsions containing BC but only when a higher concentration of WPI (5% wt) was added to the

system. Instead of values of 38 – 40 mV (for 2-4% WPI), values of roughly 30 mV are seen for 5% WPI.

One explanation is the formation of a double layer around the droplets that contain low amounts of WPI. Formation of multi-layers by addition adsorption has been shown to contribute to lower charges around droplet surfaces (Sun and Gunasekaran, 2009; Tcholakova et al., 2003). Similar findings on the capability of negatively charged polysaccharides to be absorbed onto positively charged droplets with proteins have been previously reported by many others (Camino and Pilosof, 2011; Kaltsa et al., 2014b; Sun et al., 2007; Winuprasith and Suphantharika, 2013, 2015; Zinoviadou et al., 2012). However, the formation of multiple layers does not seem to occur for the emulsions containing WPI and BC. If more BC was adsorbed on the droplet surface, no further increase in the second peak in the droplet size distribution would be noticed (Fig. 6.2C - D).

Thus, the lower ζ-potential values could be probably attributed to the fact that less WPI is adsorbed to the oil droplets as it remains in the aqueous phase as a complex with BC.

Taking all the above into consideration, it is obvious that the emulsions have a positive charge of +40 mV which is still large enough to prohibit aggregation. This indicates that the second peak in Fig. 2 is most likely not due to droplet aggregates but larger BC flocs.

6.4. Stability of emulsions prepared with high pressure

The term stability for an emulsion refers to the ability to resist changes in its properties through time (McClements, 2005). The stability of emulsions is an important aspect since it determines the shelf-life of the products. The time during which the emulsion is stable depends mainly on the nature of the food product (Dickinson, 1992).

Emulsions are prone to large destabilization phenomena, such as creaming, flocculation, and coalescence, which can limit the stability of emulsions to large extent. These phenomena are mainly a result of interactions within the emulsion and the presence of thickeners can strongly influence stability. They may increase the shelf-life by either providing a steric stabilization or increased viscosity, or decrease the shelf-life due to bridging flocculation of the oil droplets or depletion effects. Specifically, fast creaming usually occurs in emulsions containing a non-adsorbing polymer like xanthan gum, due to the mechanism of depletion flocculation. Researchers reported that creaming would be completely retarded at a specific critical viscosity concentration, at which the droplets lose their mobility and remain separated from each other (McClements, 2005). Hence, the evaluation of the stability upon storage in our systems is a very helpful tool in order to understand the

behavior of the emulsions. For this reason the serum index, SI (Eq. 3.2), for the different emulsions was determined after 14-days of storage at 4^{o}C and the results are given in Fig. 6.4.

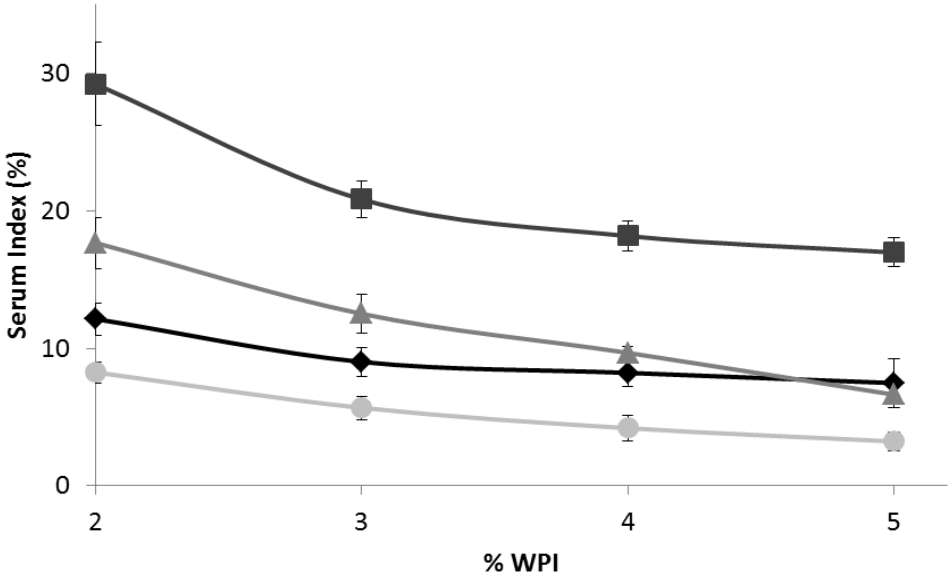

Fig. 6. 4 Serum index as a function of WPI concentration for emulsions stabilized by 0% (◆), 0.5% wt (■), 0.7% wt (▲) and 1% (●) wt BC. The serum index was determined after 14 days of storage at 4^{o}C. Bars indicating standard deviations.

Without the addition of BC (represented by the ◆ in Fig. 6.4), the WPI emulsions show a relatively low serum index, which does not significantly vary (8.2- 12.1 %) with the WPI concentration used. Thus, it can be said that WPI concentration does not affect the stability of the emulsions. These results are in agreement with the zeta-potential and droplet size measurements, which show that any addition of WPI above 2% does not have a large effect on the emulsion. Similar values for the SI have been previously found for emulsions stabilized with WPI, were SI values between 12 and 18% were reported (Kaltsa et al., 2014b).

The addition of BC leads to changes in the stability of the emulsions. For small amounts (0.5% wt) of BC (represented by ■ at Fig. 6.4), the SI increases to values of 17- 30% after 14 days of storage. This indicates that the stability of the emulsion decreased by the presence of a small amount of BC fibrils. This could be an effect of aggregation of the emulsion droplets, leading to faster creaming. This aggregation is due to bridging flocculation as a result of the attractive interactions of the BC with the WPI on the emulsion droplets. This phenomenon occurs when polysaccharides are adsorbed to the protein layer around the droplet and interconnects with two or more droplets (McClements, 2005), mostly in the case of low concentrations of polysaccharides.

The addition of higher BC amounts (0.7 % wt) lead to a significant decrease of the SI, indicating an increase in the stability of the emulsion. This could be attributed to the increase of adsorbed BC fibrils at the droplets surface leading to full coverage of the emulsion droplets with BC. In this case, sufficient BC is present to prevent bridging flocculation, and the additional layer of BC causes steric stabilization. Additionally, an increase in stability is due to the increase in the viscosity of the continuous phase as the added BC concentrations were increased. Specifically, BC fibrils could form a gel-like network in the aqueous phase which acts as a mechanical barrier and prevents droplets' coalescence (Paximada et al., 2014). When the concentration of WPI increases to 5%, the stability also increases (as SI decreased). This is probably due to the fact that more unadsorbed WPI is present in the aqueous phase. Here, it can form complexes with the unadsorbed BC, as mentioned above. These complexes may lead to the formation of a network between the droplets that partially prevent coalescence. The WPI can also prevent strong aggregation of BC into larger flocs, and the separate fibrils may provide better stabilization to the emulsion.

The addition of higher BC amounts (1 % wt) leads to a significant decrease in the SI, which ranged between 3-8%, indicating an increase in the stability of the emulsion. This high stability can be attributed to the steric stabilization and to additional network of BC that was formed. Additional WPI does not affect the stability of the emulsions in a large extent. These results indicate that the strength of the produced BC network plays a dominant role in the stability of the emulsions.

The results for the stability index are in agreement with images of the emulsion taken with the microscope. In Fig. 6.5 micrographs of emulsions containing 5% WPI and different BC concentrations are demonstrated.

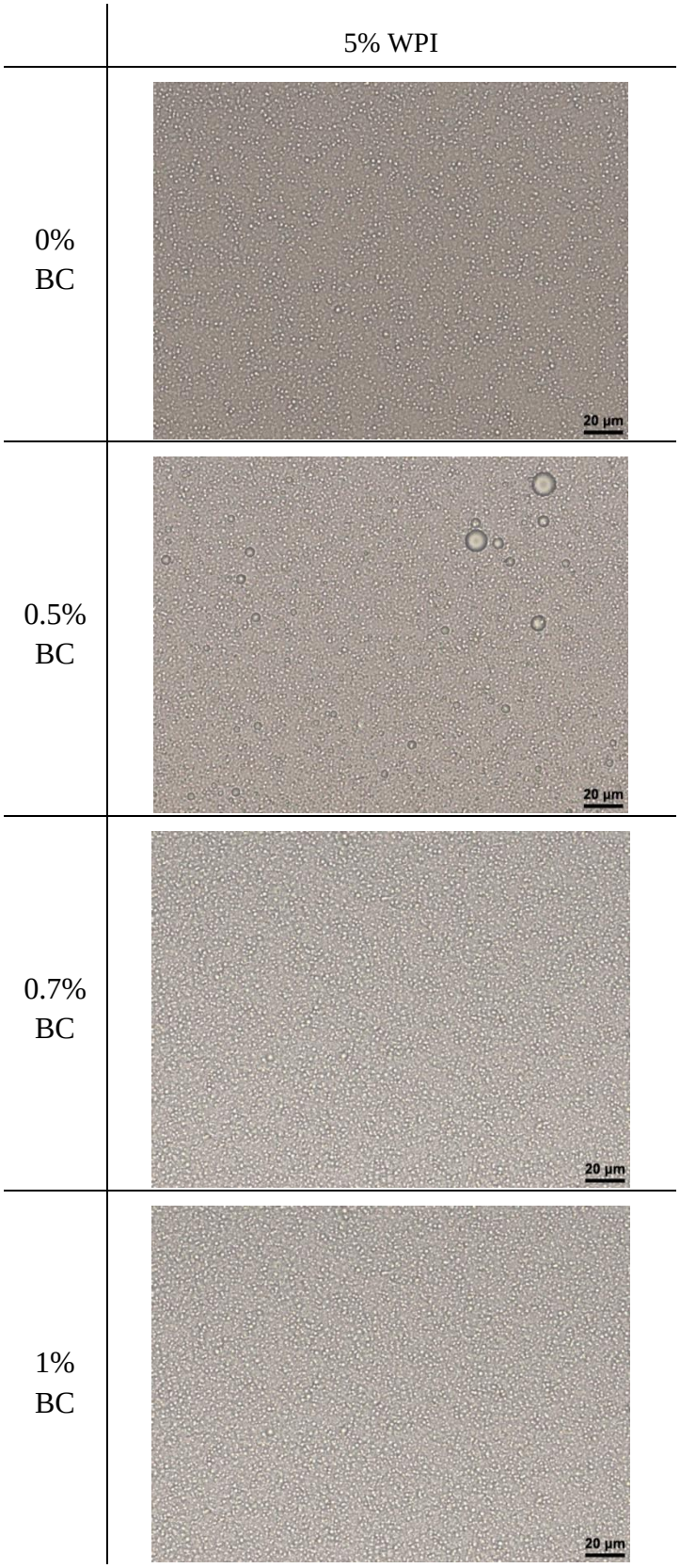

Fig. 6. 5 Typical light micrographs of o/w emulsions prepared with 5% wt WPI and 0-1% wt BC.

It is seen that in the absence of BC no flocculation can be observed, and phase separation is an effect of droplet creaming due to lower viscosity of the continuous phase. Upon the addition of BC in small amounts (0.5%) larger droplets are prominent, typical for droplets exhibiting coalescence. As it has been previously reported (stability results) the unstable emulsions were due to bridging flocculation phenomena as a result of the attractive interaction of the BC with the WPI on the emulsion droplets surface. Due to bridging flocculation, the droplets become closely packed and can then merge to form larger droplets. For the emulsions with a higher concentration of BC (0.7 and 1% wt), no aggregation was observed, indicating that bridging was prohibited.

To conclude, without addition of BC, the stability of the emulsion was independent on the WPI concentration, and showed similar values in all cases. The addition of BC can increase the stability of the emulsions, even at concentrations as low as 0.7%.

6.5. Rheology of emulsions prepared with high pressure

The primary function of thickeners in emulsions is to increase the viscosity of the aqueous phase of o/w emulsions to modify the texture and reduce the rate of creaming (Williams and Phillips, 2003). The rheological behavior is often determined by the structure; thickeners with rod-like structures, such as BC, are in general more effective volume than random-coil structures. Hence, the viscosity of the emulsions as a function of different WPI concentrations is presented in Fig. 6.6.

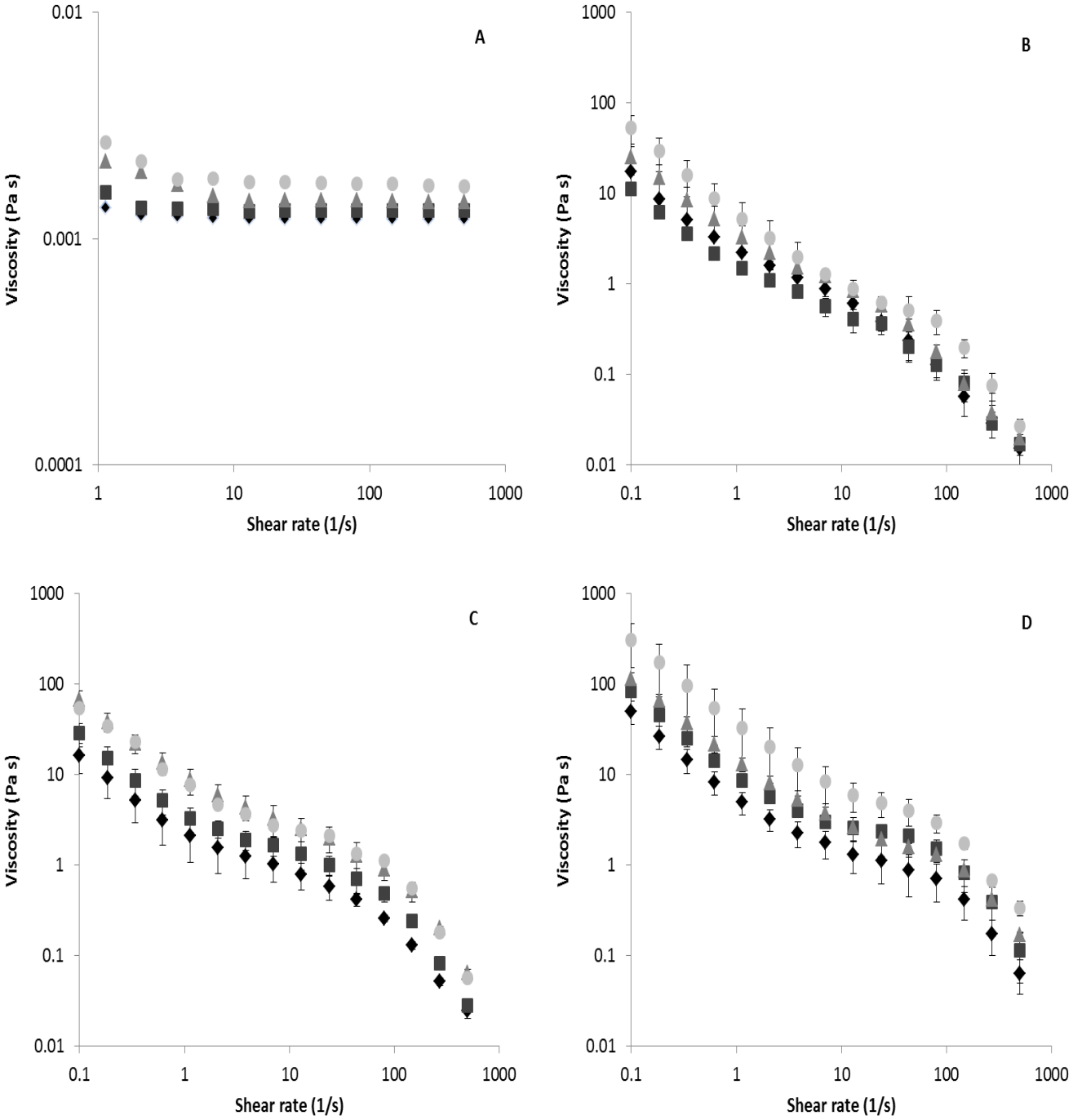

Fig. 6. 6 Apparent viscosity curves of emulsions prepared with 2% (◆), 3% wt (■), 4% wt (▲) and 5% (●) wt WPI and stabilized by 0% (A), 0.5% (B), 0.7% (C) and 1% (D) wt BC. Bars indicating standard deviations.

In the absence of BC, all the emulsions, independent on the WPI concentration, exhibit a nearly Newtonian-like behavior as their viscosity is practically independent from the shear rate (Fig. 6A). This Newtonian-like behavior is typical for emulsions with a low oil content and non-aggregated emulsion droplets as has been previously reported (Panaras et al., 2011; Zinoviadou et al., 2012).

For all emulsions containing BC, their viscosity increases significantly from roughly 1 mPas (no BC) to 10 -100 Pas, an increase of 4 to 5 orders of magnitude. Beside the large increase in viscosity, the emulsions also exhibit a pronounced shear thinning behavior, like most emulsions containing high molecular weight polymers (Hayati et al., 2009; Mandala et al., 2004; Perrechil and Cunha, 2012).

Worth noting is the fact that all the emulsions show two shear thinning regions separated by a region where the viscosity does not change, referred to as a viscosity plateau. The shear rate where the plateau is located increases as the concentration of BC increases. Researchers have previously reported similar shear thinning regions in microfibrillated and amorphous cellulose suspensions (Jia et al., 2015; Karppinen et al., 2012; Naderi et al., 2014). Specifically, they suggested that this characteristic was due to structural changes in cellulose suspension microstructure (Iotti et al., 2011). Moreover, these shear thinning regions occur because the fibrillar structures can order themselves in the flow direction, and therefore the viscosity decreased as they lose their network structure. However, these two shear thinning regions have not been reported for bacterial cellulose suspensions or emulsions.

At rest, the BC fibrils flocculate in the aqueous phase and form a strong gel-like network. The network is mainly a result of physical entanglements by partially disintegrated fibrils (Paakko et al., 2007). Under low shear rates (γ= 0.1 – 10 s^{-1}), the applied force is low but sufficient enough to disrupt the flocculated fibril network. At intermediate shear rates (γ= 10 – 100 s^{-1}), a viscosity plateau is observed. An explanation for the Newtonian plateau in the flow curve was previously proposed(Karppinen et al., 2012). They suggest that this Newtonian network is related to a significant increase in BC floc size and homogeneity. In this region, fibril free voids are present in the three-dimensional floc network. The voids appear in the direction of greatest compression, which is first between the flocs, where there are less contact points between the fibrils. Shear also induces collisions and thus new contact points between the fibrils in the fibril rich areas are formed. Such a large change in the macroscopic structure may explain viscosity plateau in the flow curve. In the second shear thinning region, the higher shear rate disrupts the network structure of the BC flocs again is and hence the structure becomes rather uniform once more. This indicates that the contacts between the fibrils are reversible. Due to less connection between the BC they orientate themselves in the direction of flow thereby causing highly shear thinning behavior at the high shear rates (Barnes, 1997).

The rheograms (Fig. 6.6) of apparent viscosity as a function of shear rate show an apparent yield stress at low shear rates. The rheograms were best fitted (R^2 = 0.95 - 1.00) with the Herschel- Buckley model (Eq. 3.4), and the best fit parameters are shown in Table 6.2. The same model was also applied in emulsions containing cellulose as a thickener (Hayati et al., 2009).

Table 6. 2 Rheological parameters The best fit parameters of emulsions containing 2-5% WPI and 0-1% BC. τ_o refers to the yield stress, k refers to the consistency coefficient, and n refers to the flow index.

	Rheological parameters								
	0.5% wt BC			0.7% wt BC			1% wt BC		
% WPI	τ_o (Pa)	k (Pa s^n)	n (-)	τ_o (Pa)	k (Pa s^n)	n (-)	τ_o (Pa)	k (Pa s^n)	n (-)
2	17.26^{a} (1.08)	3.617^{bc} (0.480)	0.12^{abc} (0.022)	16.33^{bcd} (1.29)	3.483^{bc} (1.068)	0.189^{cd} (0.005)	50.41^{def} (2.12)	7.134^{d} (1.622)	0.478^{e} (0.041)
3	11.20^{ab} (0.93)	1.750^{ab} (0.098)	0.045^{a} (0.001)	28.63^{cde} (2.91)	4.496^{c} (0.875)	0.166^{bcd} (0.003)	84.26^{ef} (2.37)	15.831^{f} (1.324)	0.418^{e} (0.101)
4	25.36^{ab} (1.64)	4.669^{c} (0.845)	0.079^{ab} (0.006)	67.12^{ef} (1.38)	10.247^{e} (1.480)	0.438^{e} (0.059)	114.09^{fg} (3.51)	36.881^{g} (2.810)	0.109^{abc} (0.012)
5	52.71^{bc} (1.16)	7.924^{d} (1.160)	0.406^{e} (0.008)	54.27^{ef} (1.21)	7.951^{d} (1.525)	0.246^{d} (0.012)	306.51^{g} (3.67)	43.780^{h} (2.537)	0.077^{ab} (0.002)

In parenthesis standard deviation values.

Mean values followed by the same letters are not significantly different ($P > 0.05$).

R^2 varied between 0.9753 and 0.9999.

Upon the addition of BC, all the samples show a yield stress (τ_o). In detail, the yield stress increases with increasing the concentration of WPI and BC, reaching to a maximum of roughly 307 Pa in the 5% WPI – 1% BC emulsion. Hence, yield stress increases when the viscosity increases, indicating that the applied stress we must exceed in order to make the emulsion to flow increases as well. It should also be noted that the addition of BC has a more pronounced influence on the yield stress than the presence of WPI in the emulsions. The flow behavior index (n) indicates the degree of pseudoplasticity of the emulsions and is an indicator of the viscous nature of the emulsion: a lower n indicates an increase is pseudoplasticity. All emulsions containing both BC and WPI show flow behavior index values lower than 1 (n= 0.077 – 0.478), indicative of a non-Newtonian and shear-thinning flow behavior. The emulsion containing 5% WPI and 1% BC shows the most pseudoplastic behavior as it has the lowest flow behavior index (n= 0.077). In the case of emulsion containing BC, the consistency coefficient varies from 1.75 to 7.92 Pas for emulsions containing 0.5% BC to values from 7.13 to 43.78 Pas for emulsions containing 1% BC. Hence,

these emulsions have particular characteristics; they are more solid like at rest but they flow easily at higher shear rates. These special characteristics may be important for consumers; they provide body to emulsion-based products but they are very pourable as well. Yield stress, flow behavior index and consistency coefficient results are in accordance with other studies of polysaccharide (Arancibia et al., 2013; Paximada et al., 2014) and protein - polysaccharide emulsions (Panaras et al., 2011).

6.6. Influence of the homogenization method on emulsions' physical properties

High pressure homogenization (HPH) and ultrasound (US) are known to induce changes of some physical and chemical properties of the produced emulsions and are under study for that effect (Arzeni et al., 2012). Hence, in order to evaluate the influence of the homogenization method on the final emulsions' physical properties, the WPI-BC-stabilized emulsions were homogenized either by HPH or US.

It is noteworthy that the energy density is an indicator of the treatment intensity, because it incorporates the transferred power, the duration of the treatment and the treated sample volume. In the case of HPH, the energy density (E_v, MJ/m^3) transferred from the homogenization valve to the sample was determined as described by Stang et al., (2001), according to Eq. 6.1:

$$E_v = \Delta P \qquad \text{(Eq. 6.1)}$$

where ΔP is the pressure difference operating at the nozzles.

As the pressure of the homogenizer was set for all samples at 200 bar, the energy density transferred from the HPH valve into the emulsions is found to be 50 MJ/ m^3 (Eq. 6.1).

On the other side, for the emulsions treated by ultrasounds, the energy density transferred from the ultrasound probe to the sample was determined calorimetrically by recording the temperature (T) increase during the homogenization process (Raso et al., 1999).The following Eq. 6.2 was used:

$$E_v = \frac{m\, c_p \frac{dT}{dt}}{V} \cdot t \qquad \text{(Eq 6.2)}$$

where m is the sample mass (kg), c_p is the sample heat capacity (4.186 kJ/kg K), V is the sample volume (m^3), and t (s) is the duration of the emulsification procedure.

As the volume of the sample and the duration of the process was set at 50 mL and 2 min respectively, the energy density transferred from the US probe into the emulsions is calculated to be 58 MJ/ m^3 (Eq. 6.2). Hence, the emulsions received the same amount of energy in their system regardless the emulsification procedure.

In all cases, droplet sizes, zeta-potential, serum index, and viscosity have been measured. The most characteristic results are reported in Table 6.3.

Table 6. 3 Physical properties (serum index and ζ-potential) of emulsions containing 0-1% wt BC and 3-5% wt WPI treated by high pressure homogenizer or ultrasounds

Physical properties	Homogeni-zation method	%wt BC / % wt WPI	0.5	1
SI (%)	HPH	3	21^{c} (1)	9^{d} (1)
	HPH	5	17^{b} (1)	3^{b} (0)
	US	3	18^{b} (1)	5^{c} (1)
	US	5	12^{a} (2)	1^{a}(0)
ζ-potential (mV)	HPH	3	40.1^{d}(1.5)	37.6^{d} (0.4)
	HPH	5	31.1^{c}(0.8)	28.1^{c} (0.7)
	US	3	15.6^{b} (0.3)	14.6^{b} (0.3)
	US	5	6.2^{a} (0.4)	5.3^{a} (0.2)

In parenthesis standard deviation values.

Mean values followed by the same letters in the same column are not significantly different ($P > 0.05$).

As it can be seen, the emulsions prepared with ultrasounds yield lower stability (SI= 1-18%) in comparison to emulsions prepared with high pressure homogenizer (SI= 3-21%), regardless the concentration of WPI and BC. These improvements in emulsion stability for US treated emulsions are associated with increases in hydrophobicity, which occurs as hydrophobic protein of the WPI residues within the interior of the untreated aggregate became revealed upon treatment with ultrasound, and improved interfacial packing at the emulsion droplet interface.

O'Sullivan et al., (2016) observed a significant reduction in the hydrodynamic volume of potato protein isolate which is associated to an increase in the hydrophobicity of proteins (Floury et al., 2002), accounting for the observed enhancements in emulsion stability in this instance. Proteins which have been treated with power ultrasound have shown improvements in both emulsion formation and stability, for milk protein

isolates studies reported a significant increase of the stability for emulsions prepared with ultrasounds (O'Sullivan et al., 2016).

What is more, emulsions prepared with US yield lower ζ-potential values in comparison to their HPH-treated counterparts. Specifically, the overall charge of the 5-1 emulsions treated by US is roughly 6 mV, while its HPH-treated counterpart is found to be 28 mV. This variation in the overall charge of the emulsions is consistent with the idea that prolonged sonication leaves ions in the sample, an outcome which tends to have a relatively lower charge than emulsions that are produced by HPH. This is in agreement with other works dealing with ultrasonication as a homogenizing method for emulsions (Salvia-Trujillo et al., 2015).

Moreover, the droplet size and distribution is found to be statistically independent from the homogenization process (data not shown). This could be attributed to the fact that both US and HPH transferred the same amount of energy density into the system. This phenomenon was previously described in literature (Calligaris et al., 2016).

Viscosity can be affected by the homogenization method. Hence, Fig. 6.7 shows the outcome of emulsion viscosity determinations.

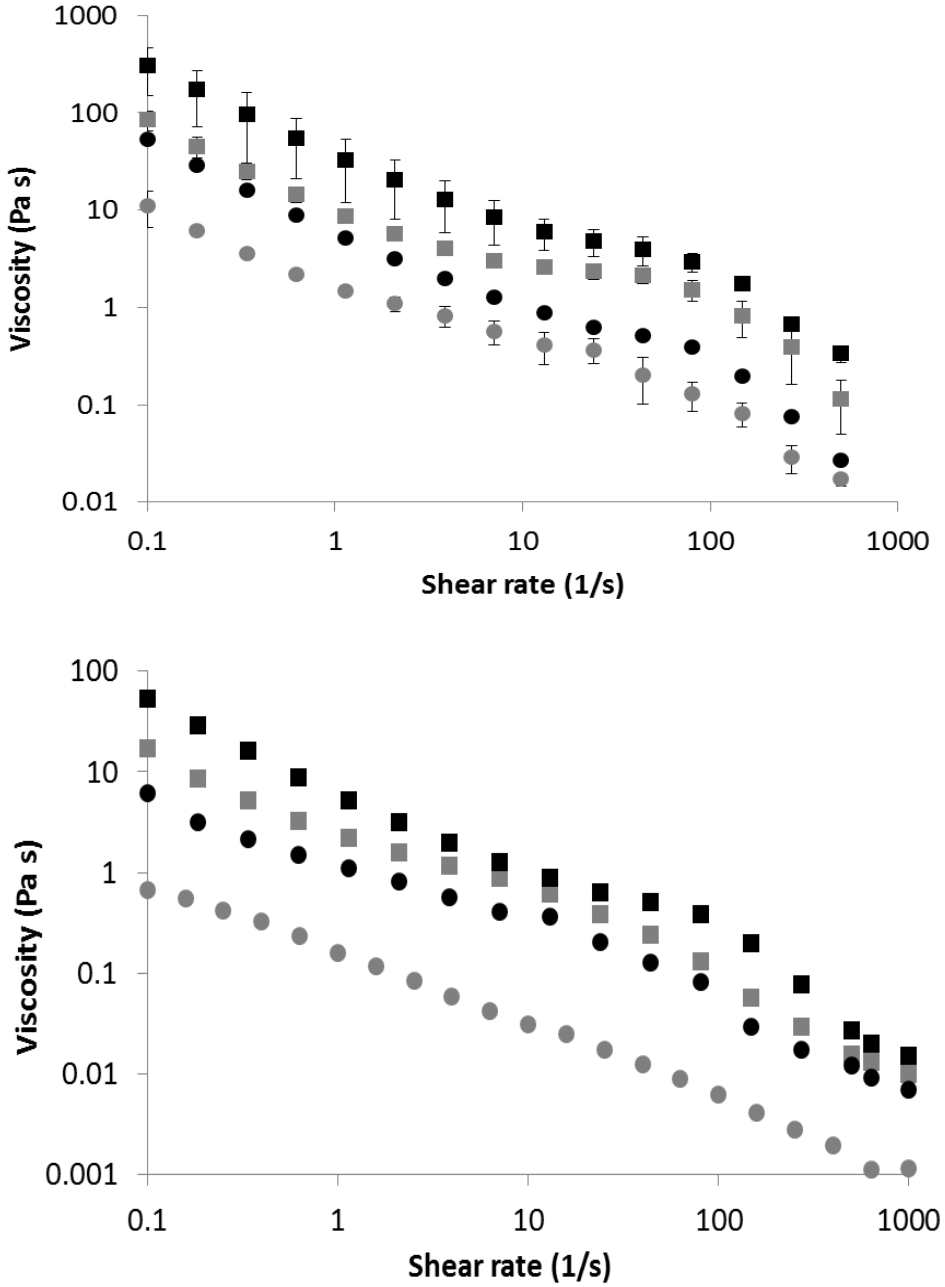

Fig. 6. 7 Viscosity curves of emulsions containing 3% WPI-0.5% BC(●), 5% WPI-0.5% BC(●),3% wt WPI-1% BC(■) and 5% wt WPI-1% BC(■) treated by HPH (A) or US (B). Bars indicating standard deviations.

Differences are found among emulsions obtained by means of the different homogenization processes. Sonication of WPI-BC emulsions has been shown to reduce the bulk viscosity compared to the HPH-treated counterparts. This is in agreement with previous studies focusing on ultrasonication as a potential homogenization method (Yanjun et al., 2014). The reduction in bulk viscosity is

attributed to the reduction in WPI and BC aggregate size as a consequence of ultrasonic cavitations. The spatial distance between adjacent protein and cellulose aggregates is increased upon size reduction via ultrasound treatment, increasing the critical overlap concentration, c*, for a given protein solution, and thus, decreasing the bulk viscosity with respect to increasing protein concentration (Lefebvre, 1982).

What is more, the sonication treatment significantly changes the 3-region plateau that is depicted in viscosity of the HPH-treated emulsions. This is attributable probably to the excessive cavitation phenomena that take place during the ultrasonication leading to the disruption of the BC structure. Several studies have pointed out that US energy employed in the system, provided sufficient energy to disrupt hydrogen bonding, altering the structure of polysaccharides (Jambrak et al., 2008).

These results confirm the greater efficiency of the US homogenization as compared to the HPH treatment in obtaining stable emulsions. Hence, US will be used in the following chapters as the emulsification method. Finally, the WPI and BC concentration that give the optimal emulsions' physical properties is found to be: 5% wt. WPI and 1% wt. BC and these conditions will be used in the experimental procedure of Chapter 7.

6.7. Conclusions

Emulsions containing extra virgin olive oil were prepared using whey protein isolate (WPI) as an emulsifier and bacterial cellulose (BC) as a thickener in various concentrations (0-1% wt). At lower BC concentrations (0.5-0.7% wt), extensive aggregation led to unstable emulsions due to bridging flocculation. However, at higher concentrations (1% BC), stable emulsions were obtained due to either steric stabilization or network formation of BC fibrils. The viscosity profile of the BC emulsions showed three regions, including two shear thinning regions separated by a constant viscosity plateau (Newtonian). This phenomenon was ascribed due to changes in BC floc size and homogeneity. Finally, to test the homogenization method effect on the emulsions' physical properties, emulsions were further processed either by ultrasounds or high pressure homogenizer. The results confirmed the greater efficiency of the US homogenization as compared to the HPH treatment in obtaining stable emulsions.

Chapter 7. Encapsulation of hydrophilic and lipophilized catechin using o/w emulsion

7.1. Introduction

EGCG is one of the many other phenolic antioxidants in nature, is soluble in water, while shows a very low solubility in lipophilic media, such as fats, oils, lipid-based foods and emulsions. Moreover, the poor lipophilicity of EGCG, accounts for its low cellular absorption in vivo (Xu et al., 2004). Considering these drawbacks, structural modification of EGCG can serve as a solution to increase its lipophilicity and to widen its application in lipophilic media (Zhong and Shahidi, 2012). The lipophilicity of EGCG could be enhanced by esterification of hydrophilic EGCG with fatty acids, followed by purification. By this method, the EGCG incorporation rate in food-based media could be enhanced (Zhong and Shahidi, 2012).

The protective means of coating by encapsulation processes such as spray drying, liposome entrapment and emulsification can make them into stable deliverable form (Gadkari and Balaraman, 2015a; Ru et al., 2010). The encapsulation of catechins in O/W emulsion can be the easiest method as compared to others. The encapsulation of bioactive compounds in emulsion delivery systems brings several advantages for the compound, such as the stabilization in aqueous systems (such as foodstuffs) of lipophilic bioactive compounds with scarce solubility in water; the protection of bioactive compounds against degradation reactions with food constituents and minimization of the alteration of the food matrix; the control of the release and the enhancement of cell uptake and bioavailability (Pool et al., 2013).

Hence, the objective of the present study is to investigate the effect of catechin addition on the physical properties of WPI-BC emulsions under storage. Two different catechins: one lipophilic and one hydrophilic were added either on the aqueous or the oil phase of the emulsions, in order to get deeper understanding on how they affect emulsion oxidative stability.

7.2. Optimization of EGCG concentration

In this study, the final thickeners' concentration was set taking into account the optimal conditions from Chapter 6: 5% wt. WPI, 1% wt. BC and 5% wt. olive oil. In order to compare the ability of the emulsion to encapsulate different structures of EGCG, H-EGCG or L-EGCG was added in the emulsion. In this case, the EGCG was incorporated in the oil or the aqueous phase of the emulsions with a total concentration varying from 0.1 – 0.5% w/w of the total mass content. Table 7.1 summarizes the different emulsions tested during the present study.

Table 7. 1 The final tested emulsions

Emulsions	Type of EGCG	Addition phase
BLANK	-	-
HW	Hydrophilic	Aqueous
LW	Lipophilized	Aqueous
HO	Hydrophilic	Oil
LO	Lipophilized	Oil

At a preliminary stage, various concentrations of catechin were tested that aimed to find the one that has the highest incorporation efficiency (IE). Figure 7.1 shows the tested emulsions containing EGCG varying between 0.1-0.5 mg/mL of emulsion.

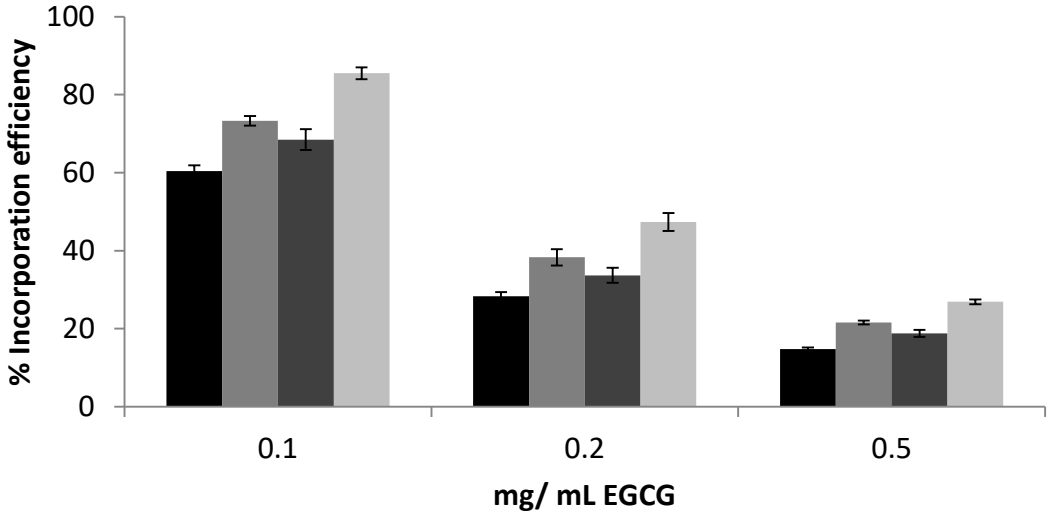

Fig.7. 1 Incorporation efficiency of different catechins: HW (■), LW (■), HO (■), and LO (■) in the emulsions.

As can be seen, high IE values are observed when low amounts of EGCG are added (0.1 mg / mL), regardless of the type of EGCG and the addition phase. For instance, the IE value for the emulsion containing 0.1 same value for the LO emulsion containing 0.5% EGCG is 27% ± 1%.

Moreover, high IE values are observed for the lipophilized EGCG (LO and LW) in all the tested concentrations. The IE value for the emulsion containing 0.1 mg / mL LO is 85.5% ± 1%, while the same value for the HO emulsion is 68% ± 2%.

EGCG type and addition phase significantly affect the IE. When H-EGCG is added to the aqueous phase of the emulsions (HW), a decrease in the IE can be observed. After the emulsification, the remaining catechin in the aqueous phase can interact with protein as stated below. In fact, it is known that large polyphenols, such as EGCG, are likely to bind with milk proteins and especially β-lactoglobulin due to the oxidation or polymerization of catechin monomers (Dubeau et al., 2010; Ozdal et al., 2013). This phenomenon leads to changes in physicochemical properties of proteins such as solubility, thermal stability and digestibility and mostly occurs when the pH of the emulsion (pH=3.8) is close to the isoelectric point of the proteins (pI=5.2), which is the case in this study (Naczk et al., 1996; Rawel et al., 2005). Specifically, it can be speculated that since EGCG is in the aqueous phase and directly meets with WPI, hydrogen bonds are formed between the protein and the catechin in the emulsion. This leads to poor incorporation efficiencies for the catechins that are added in the aqueous phase.

In contrast to the results of the preceding paragraph, when H-EGCG is added to the oil phase (HO), high IE is yielded, indicating that the addition of the EGCG is not efficient. This could be attributed to the fact that there is an excess of EGCG that could not be dissolved in the oil.

Another issue to consider is the incorporation of L-EGCG to the aqueous phase (LW). In these emulsions, the IE is higher than the other emulsions', revealing that interactions between the catechin and the protein took place. High IE values suggest that even though L-EGCG is mostly hydrophobic, some parts of it could potentially form complexes with the WPI. These complexes have the ability to adsorb at the oil-water interface more easily than the bulk WPI, a fact that can be attributed to the enhanced amphipathy and lower interfacial tension (Dickinson, 2009; Wei et al., 2015).

On the other side, when L-EGCG is incorporated to the oil phase (LO), the highest IE values can be observed. One explanation is that although L-EGCG is water insoluble, it has a polar head in its structure which provides enhanced compatibility through reorganization of the lipid molecules to expose their carboxyl groups to the water interface, a fact which can contribute to increased stability of the emulsions and, subsequently, an increase in the incorporation efficiency (McClements et al., 2007; Ozdal et al., 2013).

Taking all the above into account, the concentration that yields the highest incorporation values is 0.1 mg/mL emulsion. Hence, the following experiments of this chapter were done using the mentioned concentration.

7.3. Physical properties of emulsions containing EGCG

The type of EGCG and its addition phase are two factors that strongly affect the physical properties of the produced emulsions. Numerous studies showed that smaller oil droplets in the emulsion increased the bioactives' encapsulation efficiency (Wei et al., 2015; Yuan et al., 2008).

In the same direction, the stability of the emulsions proportionally affects the encapsulation efficiency of various compounds (Jo and Kwon, 2014; Salvia-Trujillo et al., 2013). Hence, the physical properties of the prepared emulsions stabilized with BC and WPI and containing different EGCG type were measured to gain insight in these mechanisms and are presented in Fig. 7.2 and Fig. 7.3. In the present study, two homogenization methods were used in order to prepare emulsions: a high shear homogenizer (UT) or an ultrasonic device (US).). Additionally, two types of EGCG; hydrophilic (H) or lipophilized (L) were added either on the aqueous (W) or oil (O) phase of the emulsions.

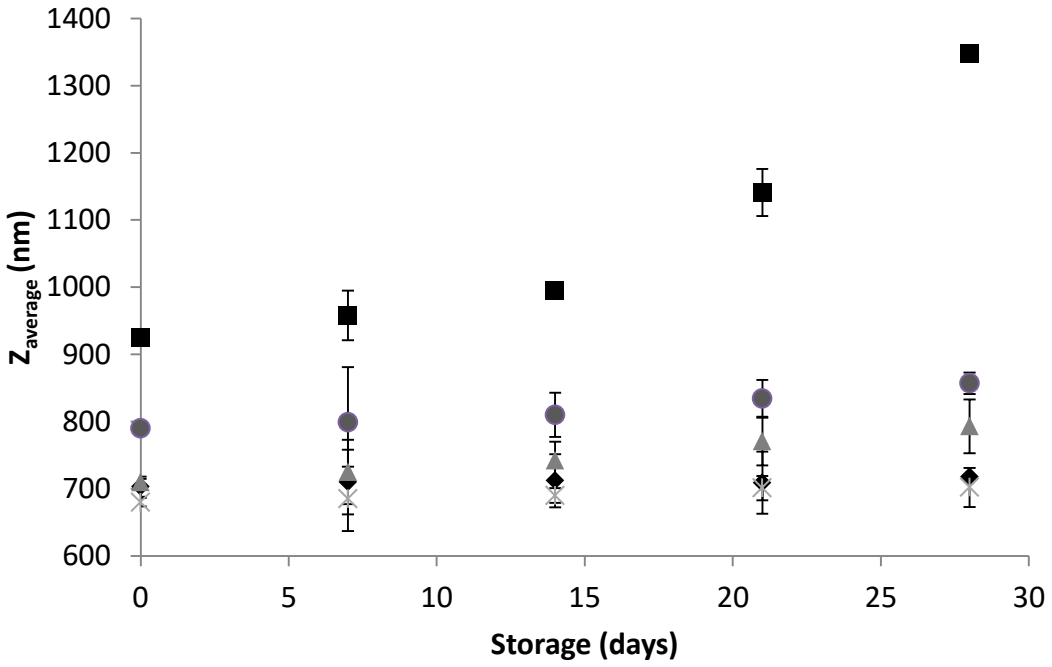

Fig.7. 2 Average droplet size of emulsions containing no EGCG (◆), HW (■), LW(▲), HO (●) and LO (✳) under storage. Bars indicating standard deviations.

As it can be seen from Fig. 7.2, the EGCG type and addition phase significantly affect the Z_{aver}. When H-EGCG is added to the aqueous phase of the emulsions (HW), a great increase of the droplet size compared to the blank emulsions by a factor of 2 times can be observed. EGCG loaded in the droplet could justify its size increase. Moreover, catechin remaining in the aqueous phase can interact with protein as stated below. In fact, it is known that large polyphenols, such as EGCG, are likely to

bind with milk proteins and especially β-lactoglobulin due to the oxidation or polymerization of catechin monomers (Dubeau et al., 2010; Ozdal et al., 2013). This phenomenon leads to changes in physicochemical properties of proteins such as solubility, thermal stability and digestibility and mostly occurs when the pH of the emulsion is close to the isoelectric point of the proteins, which is the case in this study (Naczk et al., 1996; Rawel et al., 2005). Specifically, it can be speculated that since EGCG is in the aqueous phase and directly meets with WPI, hydrogen bonds are formed between the protein and the catechin in the solution. When the emulsification process begins, WPI could not be adsorbed onto the interface of the oil droplets, leading to higher Z_{aver} and prolonged instability (McClements, 2005; Paximada et al., 2016b; Paximada et al., 2016c).

Another issue to consider is the incorporation of H-EGCG to the oil phase (HO) or L-EGCG to the aqueous phase (LW) or L-EGCG to the oil phase (LO). In these emulsions, the Z_{aver} are not significantly different than the blank emulsions', revealing that interactions between the catechin and the protein are not taking place. This phenomenon further enhances the assumption that in the LO and LW emulsions, WPI and EGCG do not interact. Small droplet size and low PDI suggest that even though L-EGCG is mostly hydrophobic, some parts of it could potentially form complexes with the WPI. These complexes have the ability to adsorb at the oil-water interface more easily than the bulk WPI, a fact that can be attributed to the enhanced amphipathy and lower interfacial tension. (Dickinson, 2009; Wei et al., 2015). The decrease in emulsions' droplet size by the addition of EGCG was previously reported by (Wei et al., 2015).

As far as the droplet size during storage is concerned, the Z_{aver} is not significantly affected by storage only for the HO, LW and LO emulsions. On the other side, the average droplet size of the HW emulsions dramatically increases after 1 month of storage. Specifically, the Z_{aver} of the LW fresh emulsion (0 day) is 925 nm, while it increases to values up to 1400 nm after 1 month of storage.

The term stability for an emulsion refers to the ability to resist changes in its properties through time (McClements, 2005). The stability of emulsions is an important property since it determines the shelf-life of the products. The time during which the emulsion is stable depends mainly on the nature of the food product (Dickinson, 1992).

Emulsions are prone to large destabilization phenomena, such as creaming, flocculation, and coalescence, which can limit the stability of emulsions to large extent. These phenomena are mainly a result of interactions within the emulsion, and the presence of thickeners can strongly influence stability. They may increase the shelf-life by either providing a steric stabilization or increased viscosity, or decrease the shelf-life due to bridging flocculation of the oil droplets or depletion effects. Hence, the evaluation of the stability upon storage in our systems is a very

helpful tool to understand the behavior of the emulsions. For this reason the serum index, SI (Eq. 3.2), for the different emulsions was determined after 30-days of storage at 4°C and the results are given in Fig. 7.3.

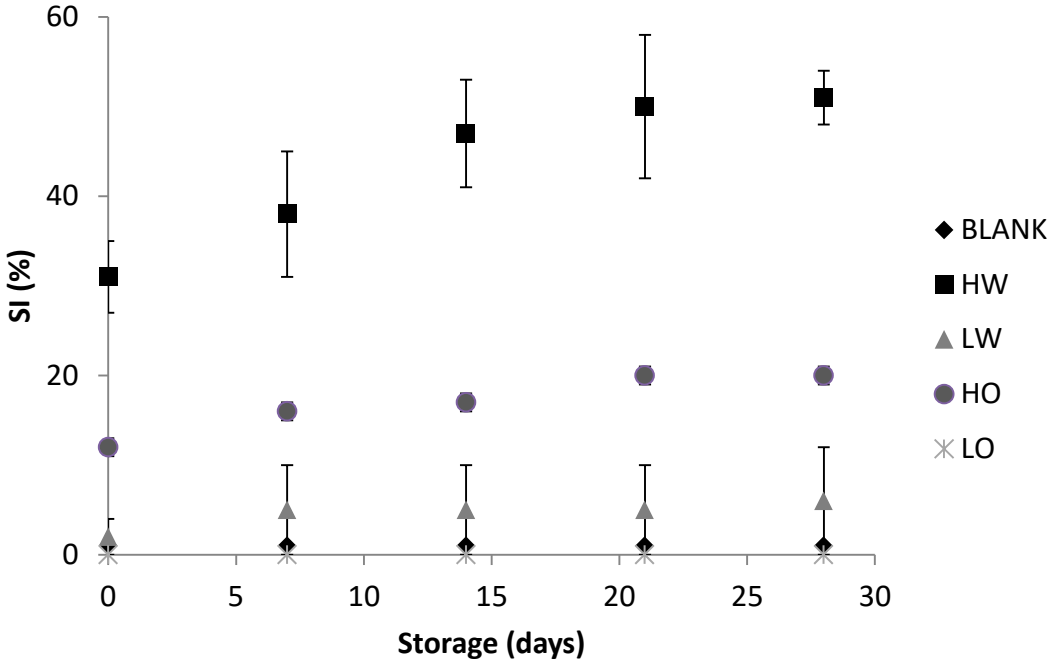

Fig.7. 3 Serum index as a function of the storage time for emulsions containing no EGCG (◆), HW (■), LW(▲), HO (●) and LO (✳). The serum index was determined after 28 days of storage at 25°C. Bars indicating standard deviations.

Emulsions' stability was found to be affected by EGCG type and addition phase. In the case that H-EGCG is added to the aqueous phase (HW), the complexes that are formed between EGCG and WPI destabilize the fresh emulsion, as its serum index is already 12%. The formulations with LW, HO, and LO exhibit stability values that do not significantly vary from the blank, confirming the previous measurements, which postulated the absence of interactions between WPI and EGCG. Instability evolution under storage is found to have the same trend as the droplet size evolution under the same storage conditions.

7.4. Rheology of emulsions containing catechin

The primary function of storage in emulsions is to increase their viscosity and to modify the structure (Williams and Phillips, 2003). O/w emulsions are, normally, pseudoplastic materials with yield stress, since their shearing stress, and hence viscosity, depend on the applied shear rate and they begin to flow provided their yield stress value is exceeded. Typically, this behavior is explained in terms of the

continuous break down of emulsion structure during the course of shear application and flow (McClements, 2005).

To identify the flow characteristics of the emulsions, data from flow measurements were fitted to the Herschel- Buckley model(R^2 = 0.95 - 1.00) (Eq. 3.4), which is commonly used for the rheological analysis of such systems (Hayati et al., 2009). The associated parameters, yield stress (τ_o), consistency (k), and flow behavior index (n) values are summarized in Table 7.2.

Table 7. 2. Rheological parameters: The best fit parameters of emulsions containing EGCG. τ_o refers to the yield stress, k refers to the consistency coefficient, and n refers to the flow index.

	BLANK			HW		
Storage (days)	τ_o (Pa)	k (Pa s^n)	n (-)	τ_o (Pa)	k (Pa s^n)	n (-)
0	16.3^a (0.9)	3.6^a (0.8)	0.19^c (0.01)	51.2^d (4.1)	21.4^f (1.0)	0.19^c (0.01)
15	16.6^a (1.2)	3.1^a (0.2)	0.15^b (0.02)	52.7^d (3.7)	20.3^f (1.2)	0.21^c (0.03)
30	16.4^a (1.0)	2.9^a (0.1)	0.16^b (0.08)	54.27^d (1.21)	19.5^f (1.7)	0.24^d (0.02)
	LW			HO		
Storage (days)	τ_o (Pa)	k (Pa s^n)	n (-)	τ_o (Pa)	k (Pa s^n)	n (-)
0	20.2^b (2.1)	5.4^c (0.6)	0.12^a (0.02)	36.3^c (3.2)	15.7^e (1.3)	0.15^b (0.05)
15	21.7^b (1.4)	4.90^c (0.3)	0.14^b (0.001)	38.7^c (2.9)	14.6^e (0.8)	0.18^c (0.03)
30	21.9^b (1.6)	4.1^b (0.6)	0.19^c (0.008)	37.2^c (1.2)	$12.\ 1^d$ (1.5)	0.19^c (0.03)
	LO					
Storage (days)	τ_o (Pa)		k (Pa s^n)		n (-)	
0	17.6^a (1.8)		$3.\ 7^a$ (0.4)		0.10^a (0.02)	
15	17.2^a (0.9)		3.3^a (0.3)		0.12^a (0.03)	
30	17.1^a (1.1)		3.1^a(0.2)		0.11^a (0.01)	

In parenthesis standard deviation values.

Mean values followed by the same letters are not significantly different (P > 0.05).

R^2 varied between 0.9892 and 0.9998.

The flow behavior index (n) indicates the degree of pseudoplasticity of the emulsions and is an indicator of the viscous nature of the emulsion: a lower n indicates an increase is pseudoplasticity. All emulsions show flow behavior index values lower than 1 (n= 0.10 – 0.24), indicating a non-Newtonian and shear-thinning flow behavior. The emulsion containing LO shows the most pseudoplastic behavior as it has the lowest flow behavior index (n= 0.10).

In the case of emulsion containing LO, the consistency coefficient varies from 3.1 to 3.3 Pas for emulsions containing HW to values from 19.9 to 21.4 Pas. Hence, these emulsions have particular characteristics; they are more solid like at rest but they flow easily at higher shear rates. Yield stress, flow behavior index and consistency coefficient results are in accordance with other studies of emulsions containing antioxidants (Arancibia et al., 2013; Paximada et al., 2014).

Overall, the blank and the emulsion containing lipophilized EGCG in the oil phase (LO) demonstrate similar rheological behavior. On the contrary, addition of hydrophilic EGCG in the aqueous phase (HW) results in thicker samples, as evidenced by the consistency values. K values for the blank and the LO samples are 3.6 and 3.7 Pas^{-1}, but significantly higher values (21.4 Pas^{-1}) are observed for HW ($p<0.05$). The interaction between WPI and EGCG that was described earlier (7.1) could be related to the increase in viscosity. Studies showed similar tendency in emulsions containing lipophilic compounds (Pérez-Masiá et al., 2014). All emulsions are highly pseudoplastic with flow behavior (n) values around 0.15 without significant differences among them.

Storage has a major influence on emulsions consistency index, which is a measure of viscosity. All the samples show a yield stress (τ_o). In detail, the yield stress increases with increasing the storage time, reaching to a maximum of roughly 54 Pa in the HW emulsion after 1 month of storage. Hence, yield stress increases when the viscosity increases, indicating that the applied stress we must exceed in order to make the emulsion to flow increases as well. It should also be noted that the type of EGCG and the addition phase has a pronounced influence on the yield stress.

It is worth noticing that within tested days of storage, a significant reduction the consistency is observed for all the tested emulsions. The decrease of emulsion viscosity is related to the existence of droplet coalescence in the system (Tadros, 1994) (as discussed at 7.2). Regarding the flow behavior, values are practically unaffected by long term storage.

7.5. Influence of the EGCG addition on emulsions' oxidative stability

The polyphenols of green tea are highly susceptible to oxidation and degradation due to change in pH and temperature during storage. So it is very essential to determine the favorable EGCG type and addition phase for the developed

formulation. In the present study, the emulsions were allowed to oxidize for 28 days at 25^{o} C. The progress of oxidation according to the primary lipid oxidation marker (CD) is summarized in Fig. 7.4.

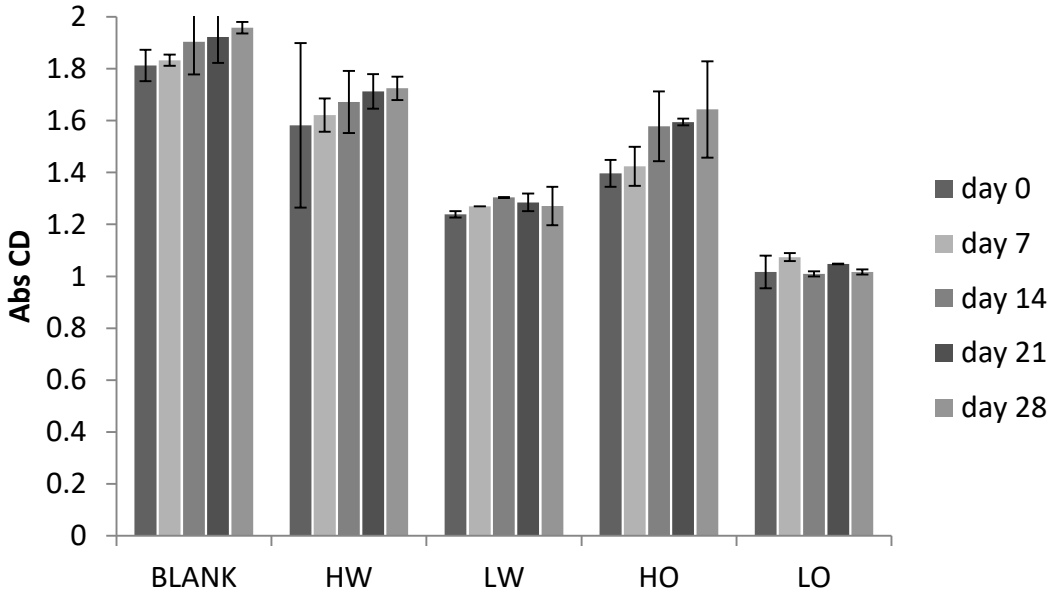

Fig.7. 4 Evolution of CD concentration in absorbance in emulsions containing various catechins. Bars indicating standard deviations.

The type of EGCG affects the oxidation of emulsions. The lowest CD levels are observed in the presence of LO and LW in the emulsions. Those containing hydrophilic EGCG (HO and HW) presented considerably higher absorbance values compared to their L counterparts, indicating that hydrophilic catechin promotes oxidation. The influence of EGCG on emulsion oxidation is considered relatively contradictive. For instance, several studies report that hydrophilic catechin may result in increased oxidation of emulsions (Zhong and Shahidi, 2012). This phenomenon is due to the reduced droplet size of the emulsions containing H-EGCG which increases the total surface area available for oxidation.

Emulsions containing H-EGCG are also characterized by lower viscosities compared to the LW and LO (as seen in 7.4) due to the complex formation between WPI and EGCG which can lead to increased diffusive mobility of reactants and reaction products, hence increased oxidation rates. On the contrary the CD of emulsions containing hydrophilic catechin was unaffected during storage (Zhou and Elias, 2013).

Also, the storage time has significant impact on CD values of the H-EGCG emulsions. Specifically, the CD values of the HO emulsion vary from 1.4 at the first day to 1.8 after 1 month of storage. However, the CD values remain unaffected by the storage

time for the emulsions containing lipophilized EGCG. This phenomenon increases the ability of L-EGCG to act as an antioxidant compound.

As it can be seen, emulsion oxidative stability followed the same trend as incorporation efficiency. Even though a more detailed research is required to fully elucidate the underlying mechanisms involved in lipid oxidation after the incorporation of EGCG, at concentration investigated LO seems to be more efficient against primary oxidation.

The p-Av is a reliable measurement for the evaluation and monitoring of the secondary oxidation products. During lipid oxidation the primary reaction products decompose to secondary products (aliphatic aldehydes, ketones, alcohols, acids and hydrocarbons), responsible for off-flavors and off-odors of edible oils (Poiana, 2012). Hence, the p-Anv of the evaluated emulsions can be seen in Fig. 7.5.

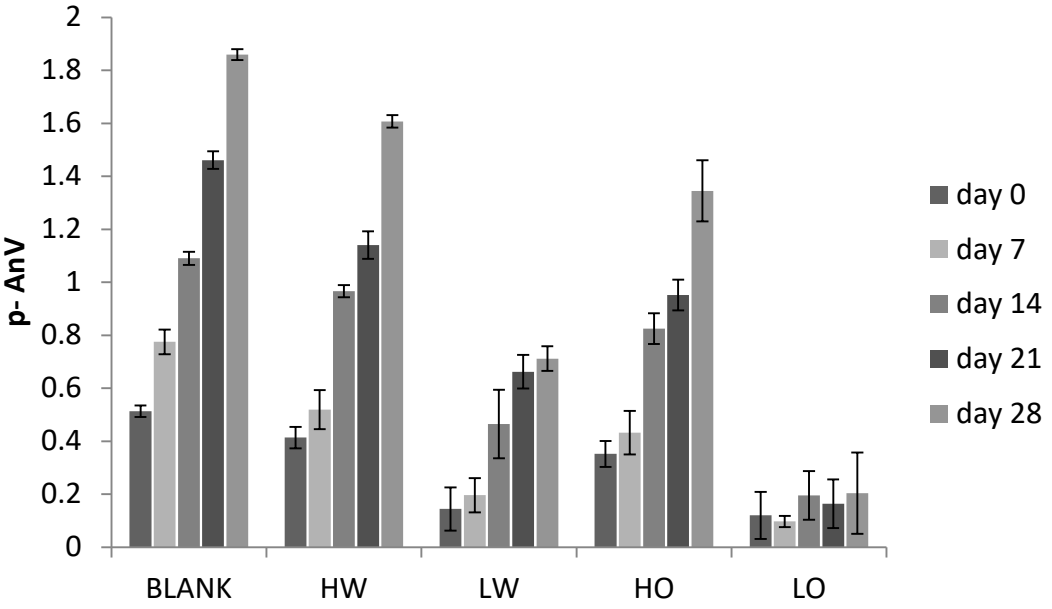

Fig.7. 5 Evolution of p-Anisidine value in emulsions containing various catechins as a function of storage. Bars indicating standard deviations.

As shown in Fig. 7.5 the samples containing lipophilized EGCG in the oil phase (LO) exhibit the lowest p-Av, while no significant differences are obtained between the reference and that containing hydrophilic EGCG in the aqueous phase (HW). Considering the addition phase, it is obvious that when EGCG is added in the oil phase it exhibits lower values of p-AnV compares to the ones that EGCG is incorporated to the aqueous phase.

Storage had a detrimental effect over the chemical stability of the emulsions, resulting in increased p-AV values ranging between 0.2-0.7 and 1.4-1.7 for L-EGCG emulsions and for the H-EGCG emulsions respectively.

These results confirm the greater efficiency of the L-EGCG as compared to the H-EGCG in obtaining emulsions with enhanced oxidative stability. Hence, L-EGCG is recommended as an antioxidant bioactive compound with potential health effects.

7.6. Conclusions

Emulsions containing whey protein isolate (WPI), bacterial cellulose (BC) and extra virgin olive oil were produced. Two different catechins: hydrophilic (H-EGCG) or lipophilized (L-EGCG) were incorporated in the aqueous or the oil phase of the emulsions. At optimized EGCG concentrations i.e. 0.1 mg EGCG/ mL emulsion, the highest EE of 85 ± 2% with reasonable droplet diameter of 680 ± 10 nm and 0% SI could be achieved for the LO emulsions. The HW addition not only increased the droplet diameter (920 ± 17 nm) but also lead to a drop in encapsulation efficiency (60 ± 4%) due to the formation of complexes between WPI and EGCG in the emulsion. On the other hand, LW, HO, and LO emulsions were more stable after 1 month of storage with slight change in droplet diameter, compared to the blank emulsion. Due to antioxidant effect of catechins, the oxidation rate of emulsion was decreased in all the evaluated emulsions. These results confirm the greater efficiency of the L-EGCG as compared to the H-EGCG in obtaining emulsions with enhanced oxidative stability. The encapsulation of lipophilized EGCG to the oil phase gave promising results to prepare catechin-enriched nanoemulsions and thus allowed the encapsulated catechins to sustained release. The present study gives the scope to conduct the scale up for commercialization of bulk production of catechins emulsion for food applications.

Chapter 8. Solution electrosprayed particles for the encapsulation of catechin

8.1. Introduction

The food industry is facing enormous challenges in the direction of developing and implementing systems that can produce functional foods (Manufuture, 2006). Much research is currently conducted for the protection of unstable bioactives in polymeric matrices in order to increase their stability and controlled release (Matos et al., 2015; Pérez-Masiá et al., 2015; Ray et al., 2016; Samtlebe et al., 2016; Santiago and Castro, 2016). Amongst the wide range of bioactive compounds, tea polyphenols and especially epigallocatechin-3-gallate (EGCG) have gathered attention due to their various potential therapeutic activities (Tsatsaragkou et al., 2016; Zhong and Shahidi, 2012).

Biopolymer particles may be used to protect and deliver bioactive compounds in food systems. Therefore, there is a considerable interest in the formulation of biopolymer particles from proteins and/or polysaccharides. One of the most promising approaches to preserve vulnerable bioactive ingredients in food systems is their encapsulation within matrices that act as barriers from the environment. Among the various techniques used for encapsulation, electrohydrodynamic processing (electrospraying) is an innovative technology for the production of particles containing bioactive compounds and successful examples of fish oil, and catechins encapsulated by food-grade material are given in many studies (Abu-Ali and Barringer, 2005; García-Moreno et al., 2016; Wang et al., 2014).

Recently, proteins and polysaccharides have attracted significant attention in the search of suitable encapsulants to be electrosprayed. However, pure proteins are difficult or even impossible to be electrosprayed due to their three-dimensional network (López-Rubio and Lagaron, 2012; López-Rubio et al., 2012). These limitations can be overcome by blending them with polysaccharides, such as starch (López-Rubio et al., 2012) or pullulan (Aceituno-Medina et al., 2013), which significantly improve the natural polymer's sprayability. Additionally, new polymers are particularly interesting molecules for electrospraying.

This study focuses on the properties of bacterial cellulose and whey protein isolate mixtures in terms of their ability to be electrosprayed and the properties of the solutions and the final particles that affect the process. The EGCG stability in the particles with optimal characteristics under various storage conditions (pH, RH, and temperature) is an aim of this study as well.

8.2. Solutions' physical properties

As it has been noted by several authors, the physical properties of polymer solutions such as viscosity, surface tension and conductivity play a key role in the successful formation of particles (Kriegel et al., 2009; Wongsasulak et al., 2007). What is more, the surface tension of the solution plays a major role in the electrospraying process (Palangetic et al., 2014), because the intensity of the electrical field must overcome the surface tension of the solution, expelling an electrified jet from the Taylor's cone formed on the needle tip (Anu Bhushani and Anandharamakrishnan, 2014; Bhardwaj and Kundu, 2010; Taylor, 1964). Hence, the solution properties for the various BC-WPI compositions are summarized in Table 8.1.

Table 8. 1 Physical properties (surface tension, conductivity and ζ-potential) of solutions containing 1-16% wt BC and 10-30% wt WPI and the polydispersity index (PDI) of the produced particles

Physical properties	%wt BC % wt WPI	1	2	4	8	16
Surface tension (mN/m)	0	20.1^{a} (2.9)	27.3^{b} (2.4)	30.0^{c} (2.3)	32.1^{d} (4.7)	36.8^{e} (1.7)
	10	20.6^{a} (0.7)	26.7^{b} (0.6)	30.1^{c} (0.5)	32.7^{d} (0.7)	38.6^{f} (1.2)
	20	20.2^{a} (1.7)	27.4^{b} (1.5)	30.1^{c} (1.5)	32.8^{d} (0.5)	40.5^{f} (1.2)
	30	20.2^{a} (1.1)	27.9^{b} (1.5)	31.1^{c}(1.7)	32.9^{d} (4.3)	40.7^{f} (0.8)
Conductivity (mS/m)	0	1.0^{a} (0.1)	2.2^{c} (0.1)	2.5^{d} (0.0)	3.1^{e} (0.0)	3.3^{f} (0.1)
	10	1.3^{b} (0.0)	2.4^{d} (0.0)	2.5^{d} (0.0)	3.1^{e} (0.2)	3.3^{f} (0.1)
	20	1.4^{b} (0.1)	2.5^{d} (0.2)	2.9^{e} (0.1)	3.1^{e} (0.1)	3.3^{f} (0.0)
	30	1.4^{b} (0.0)	2.6^{d} (0.0)	2.9^{e}(0.2)	3.1^{e} (0.0)	4.0^{g} (0.2)
ζ-potential (mV)	0	-20.6^{e} (0.7)	-21.5^{f}(1.4)	-21.6^{f} (1.5)	-25.9^{h} (0.4)	-28.3^{i} (0.8)
	10	-18.3^{c} (0.9)	-19.7^{d}(0.3)	-20.5^{e} (0.6)	-21^{e} (0.4)	-23.1^{j} (1.0)
	20	-15.3^{b} (1.2)	-17.1^{c}(0.9)	-17.3^{c} (1.8)	-17.8^{c} (2.1)	-18.8^{c} (0.8)
	30	-11.9^{a} (0.7)	-12.6^{a}(1.4)	-14.1^{b} (1.3)	-14.6^{b} (0.4)	-15.9^{b} (0.7)
PDI (-)	0	-	-	-	-	-
	10	0.8^{a} (0.0)	1.0^{b} (0.0)	0.9^{ab} (0.0)	0.9^{ab} (0.0)	1.0^{b} (0.0)
	20	0.9^{ab} (0.0)	0.9^{ab} (0.0)	1.1^{c} (0.0)	1.7^{d} (0.1)	2.1^{e} (0.1)
	30	1.0^{b} (0.0)	1.0^{c} (0.0)	1.6^{d}(0.1)	2.6^{f} (0.2)	3.1^{g} (0.3)

In parenthesis standard deviation values.

Mean values followed by the same letters in the same column are not significantly different ($P > 0.05$).

From Table 8.1, it can be observed that a drastic increase in the surface tension occurs by increasing the BC concentration of the solution. Specifically, for small amounts of BC (1% wt) the surface tension bears values of 20 mN/m, while for higher ones (16% wt BC) the values go up to 40 mN/m, regardless of the WPI concentration. This indicates that the BC plays a major role in the surface tension, although the contribution of a dissolved polymer to the overall surface tension is typically low, unless the polymer has amphiphilic properties. In our case, BC is not pure as it was found to contain a small amount of proteins (Paximada et al., 2016b).

Surface tension values are of high importance as they play a major role in the final size of the particles. Furthermore, differences in the size of the processed system could be mainly attributed to changes in the surface tension of the solutions. Specifically, a decrease in surface tension from 40 to 20 mN/m in solutions containing 16 to 1% wt BC and constant amount of WPI (20% wt) leads to a decrease of the particles size from 390 to roughly 300 nm (see section 8.4). This is observed due to the lower surface tension gradient around the droplet that causes the formed Taylor's cone to be expelled from the needle. It is found that the diameter of the particles could only be reduced with the stable cone-jet mode, which also improves the size of the particles (Jayasinghe and Edirisinghe, 2004). Also, (Pancholi et al., 2009a) postulated a decrease of the mean particle size of chitosan particles, by decreasing the surface tension from 80 to 50 mN/m.

However, the surface tension of BC-WPI solutions does not significantly vary with the WPI concentration (Table 1). This result could be attributed to the fact that BC with their containing proteins move faster and cover the interface and then only a small amount of WPI is sufficient in saturating the surface. This result could be attributed to the fact that BC with their containing proteins move faster and cover the interface and then only a small amount of WPI is sufficient in saturating the surface. When higher amounts of WPI are added to the system (20-30% wt) the excess protein remains in the solution and does not affect the surface tension. This is consistent with other studies that worked with proteins and found no effect of the proteins on the surface tension (Aceituno-Medina et al., 2013; Wongsasulak et al., 2007).

Conductivity is another important parameter for the successful production of particles with electrospraying technique. The conductivity values of the solutions followed a steady increasing trend when the BC concentration increased throughout the whole experiment (Table 8.1). Specifically, by increasing the BC concentration from 1 to 16% wt., the electrical conductivity increased from 1.3 to 3.3 mS/m,

regardless of the WPI content. This phenomenon could be attributed to the predominant effect that the addition of higher BC concentrations has to the system. In accordance to these results, Rošic et al., (2012) found an increase in conductivity by increasing polysaccharide concentration. Conductivity is influenced by the polymer concentration because both natural polymers display polyelectrolyte properties in aqueous media.

The formation of a Taylor cone for electrospraying generally depends on a high surface charge density that is influenced by the conductivity of the biopolymer solution (Yu et al., 2011). Differences in the conductivity of BC are relatively small and do not explain the observed large changes in particles diameter (see section 8.4). Nevertheless, if electrical conductivity is too high, there is too much charge carried by the electrospraying jet that can destabilize it (Bock et al., 2012). This is consistent with the 30% wt WPI solutions that exhibit high conductivity values and complicated the process.

The ζ-potential that represents the charge density of the BC-WPI solutions is summarized in Table 8.1. By the absence of BC, the WPI solution bears a positive charge (12 – 16 mV in terms of WPI concentration) at a pH of 3.8. This positive charge of proteins in pH lower than its isoelectric point has been confirmed by many researchers (Camino et al., 2012; Liu et al., 2012; Long et al., 2013).

It has been previously reported that BC bears a negative charge in all the pH range (Paximada et al., 2016b). Therefore, when negatively-charged BC is added, the ζ-potential values decreased in value. Specifically, by increasing the BC concentration from 1 to 16% wt, the overall charge of the solutions decreased from -18 to -23 mV for solutions containing 10% wt WPI. The same trend is also obvious in solutions containing 20 or 30% WPI. The reduction of the droplet charge density indicates the adsorption of the BC fibrils onto the positively charged WPI molecules, mainly through electrostatic attractions. Similar findings on the capability of negatively charged polysaccharides to be absorbed onto positively charged proteins have been previously reported by many others (Camino and Pilosof, 2011; Kaltsa et al., 2014b; Sun et al., 2007; Winuprasith and Suphantharika, 2013, 2015; Zinoviadou et al., 2012).

Worth noting is the fact that higher ζ-potential values can be seen in solutions by increasing the WPI concentration, regardless of the concentration of BC. Instead of values of -23 mV (for 10% WPI), values of roughly -16 mV are seen for 30% WPI. The predominant effect of the increase of WPI concentration is the cause of the drastic increase of overall charge and has been previously reported (Paximada et al., 2016b). To conclude, the increase of BC has an effect on the surface tension, conductivity and ζ-potential of the solutions, leading to differences in the electrospraying process and the produced particles.

8.3. Solutions' viscosity

The viscosity of the solutions as a function of different BC and WPI concentrations is presented in Fig. 8.1 (A-C).

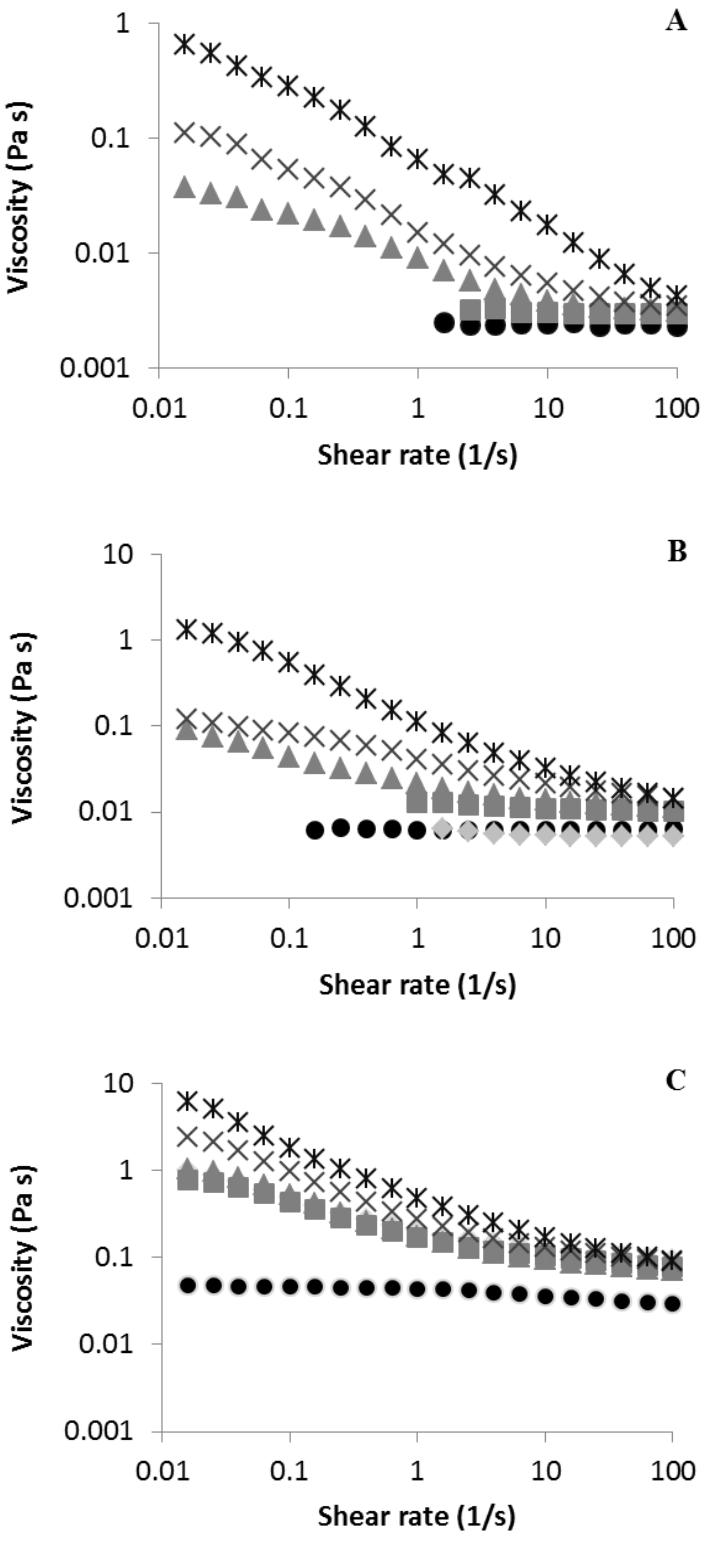

Fig. 8. 1 Apparent viscosity curves of solutions containing 0% wt (●), 1% wt(◆), 2% wt (■), 4% wt (▲), 8% wt (×), 16% wt (✳) BC and 10% (A), 20% (B), 30% (C) wt WPI.

In the absence of BC, all the solutions exhibit a Newtonian-like behavior as their viscosity is constant in all shear rate, regardless of the WPI concentration. This Newtonian-like behavior is typical for solutions with a low or medium WPI content (Kaltsa et al., 2014b; Panaras et al., 2011; Paximada et al., 2016b). The viscosity of solutions containing 10 or 20% wt and low amount of BC (1-4% wt) still exhibits Newtonian-like behavior, which is consistent with the idea that in solutions containing low amounts of biopolymers, WPI is the polymer that has the major effect on the viscosity of the mixture. This has already been postulated from others studied the properties of protein and polysaccharide mixtures (Kaltsa et al., 2014a; Kaltsa et al., 2014b).

As far as the rest of the solutions are concerned, their viscosity increases significantly from roughly 7 mPa s (no BC) to 0.7 -7 Pas, an increase of 2 to 3 orders of magnitude when BC is from 1-16%. The solutions also exhibit shear thinning behavior, like most solutions containing a high concentration of polymers (Hayati et al., 2009; Mandala et al., 2004; Perrechil and Cunha, 2012). A synergistic interaction between the anionic BC and the cationic WPI mixtures due to the intermolecular binding that occurs between side chains of the polymers or due to interactions between disordered segments of WPI molecules and BC enhances the viscosity (Renou et al., 2013).

The pseudoplasticity of the solutions increases with an increasing proportion of BC in the mixtures. The pronounced shear-thinning effect can be related to the structure of the polymer chains in the solutions. Without an external load, each single macromolecule can be found in the shape of a three-dimensional coil because this is lowest energy state. During the shear process, however, the molecules are more or less oriented parallel to the direction of shear, resulting in elongation, which lowers their flow resistance and results in a decrease in the bulk viscosity (Freeman, 1996). Viscosity is one of the crucial parameters in predicting the ability of one solution to be electrospun or electrosprayed. High viscosities give rise to dripping of solutions, which is the case in the solutions containing 30% WPI (see section 8.4). Studies that have examined different polymers in terms of their ability to form particles showed viscosities at the range of 50-250 mPa s for chitosan (Pancholi et al., 2009b), and 165 mPa s for zein (Neo et al., 2013).

Additionally, the interfacial viscosity of the solutions as a function of different BC-WPI concentrations is evaluated and summarized in Fig. 8.2 (A-C).

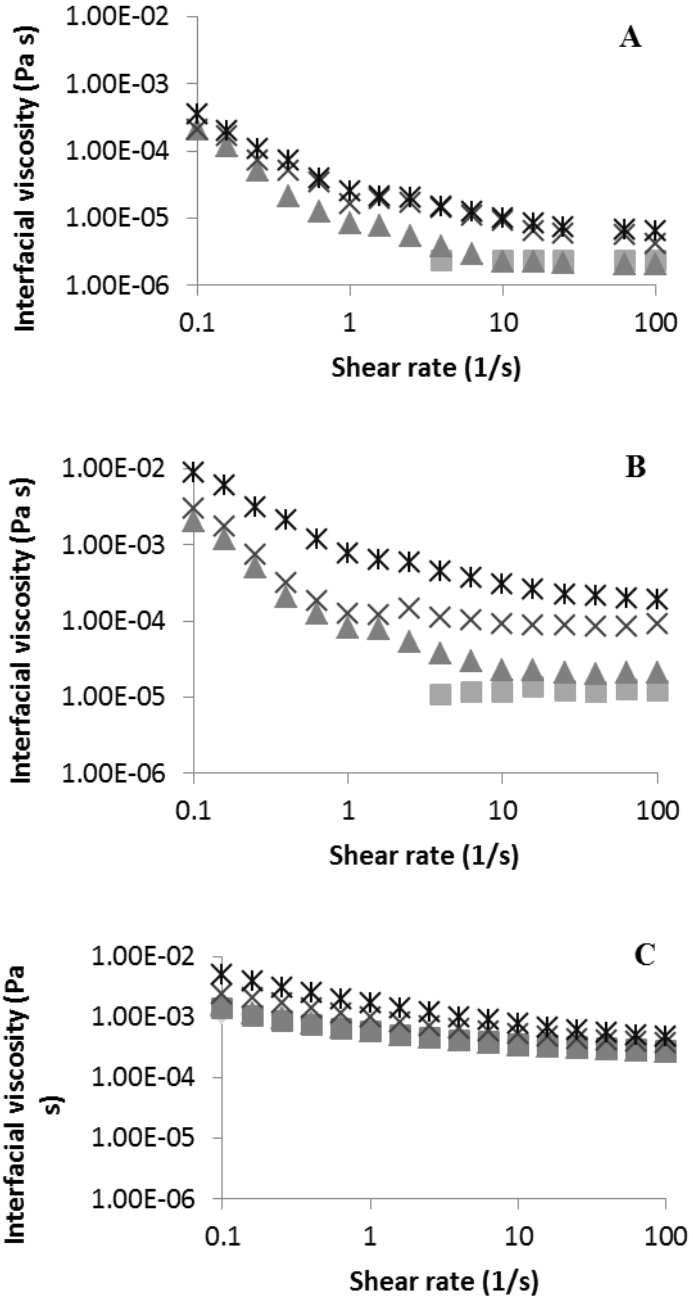

Fig. 8. 2 Interfacial viscosity curves of solutions containing 0% wt (●), 1% wt(◆), 2% wt (■), 4% wt (▲), 8% wt (×), 16% wt (✳) BC and 10% (A), 20% (B), 30% (C) wt WPI.

The results of the interfacial viscosity measurements show the same parameter trends as those observed in the bulk (Fig.8.1 A-C). However, the values of the interfacial viscosity are three to five orders of magnitude lower than those observed in the bulk, with the latter being comparable to data obtained by (Rošic et al., 2012).

From this figure it is obvious that the solutions with low concentrations of WPI (10-20% wt) and BC (2% wt) exhibit a Newtonian behavior, with a linear relationship

between the shear stress and the shear rate in the whole range of studied shear rate (0.1-100 s^{-1}). However, an increase in the polymers concentration (WPI from 10-30% wt and BC from 4-16% wt) alters the behavior of the solutions and a shear thinning profile is depicted. Another issue to consider is the viscosity values. Specifically, for all solutions containing BC, their viscosity increases significantly from roughly 0.001 mPa s (1% BC) to 5 mPa s (16% BC) regardless of the amount of WPI that they contain. This increase in interfacial viscosity is attributable to the amount of BC that is added to the system. Hence, BC acts as a thickener in the solutions, increasing both their bulk and interfacial viscosity, which is in agreement with other studies that evaluated the thickening effect of BC (Panagopoulou et al., 2015; Paximada et al., 2016b; Paximada et al., 2016c).

8.4. Electrosprayed particles properties

The morphology of the particles obtained through electrohydrodynamic processing of polymer solutions depends on either the process parameters or the solution properties. Fig. 8.3 shows SEM images of the structures obtained together with the mean particles' diameter, while Table 8.1 shows the polydispersity index (PDI) of the produced materials.

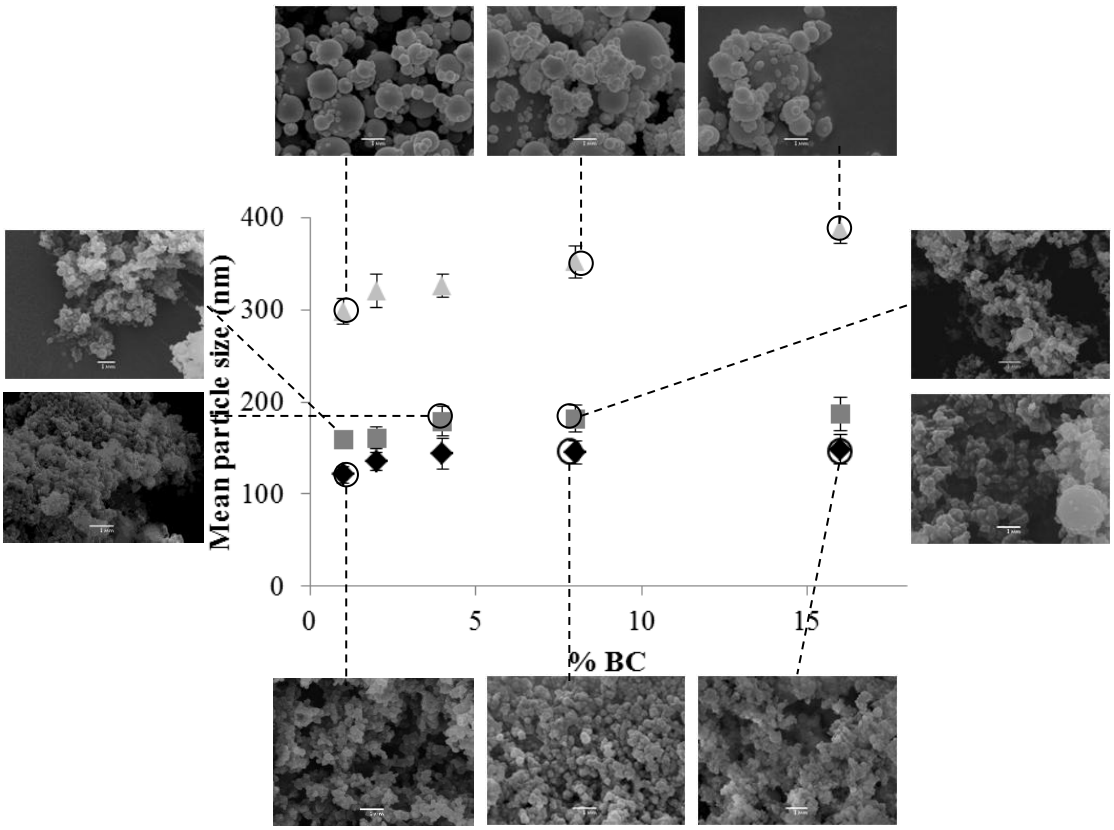

Fig. 8. 3 Average particle size and typical micrographs of the different BC-WPI particles obtained through electrospraying of 1-16% wt BC and 10-30 wt.% WPI solutions.

The mean diameter (z_{av}) of the produced particles is in the range of 120–390 nm for the different compositions of BC-WPI. In general, the diameter of the electrosprayed particles depends on the polymers concentration, an increase in both biopolymers causes an increase in the particles' diameter and PDI, in accordance with previously published data (Aceituno-Medina et al., 2013; Wongsasulak et al., 2007). For example, the z_{av} of electrosprayed BC-WPI particles increases from 121 to 148 nm by increasing the amount of BC from 1-16% wt while keeping constant the WPI (10% wt). Concerning the structure of the produced particles, the first observation is that particles with low WPI (10 -20% wt) exhibit a more homogeneous structure. This could be explained by the binding of BC monomers to the WPI backbone either through hydrophobic interactions or hydrogen bonding, forming a complex which affects intramolecular interactions and conformation of the protein. As previously hypothesized, interaction between BC and protein may result in a more open molecular structure which may help to establish interactions with the WPI, thus, decreasing the critical entanglement concentration and, thereby, facilitating electrospraying (Kriegel et al., 2009).

The addition of higher WPI amount (30% wt) leads to the particles with multimodal size distributions, with larger PDI values up to 3 (Table 1). Amorphous parts that are obvious in the micrographs of these materials are caused by dripping of the BC-WPI solutions during the process. WPI is mainly composed by albumins and globulins which have a globular structure and their polyelectrolytic character give rise to a multitude of inter- and intra-molecular interactions (McClements, 2005). The mentioned α-helical and β-sheet polymer chain configurations, which may be adopted in higher WPI concentrations keep the rigidity of the chains, preventing the formation of monodispersed particles through electrospraying.

The morphology and the diameter of the electrosprayed structures is affected by many parameters. Fig 8.4 illustrates the bulk and interfacial viscosity values as a function of the concentration of BC in the solutions. The values are referring at shear rate of $10s^{-1}$.

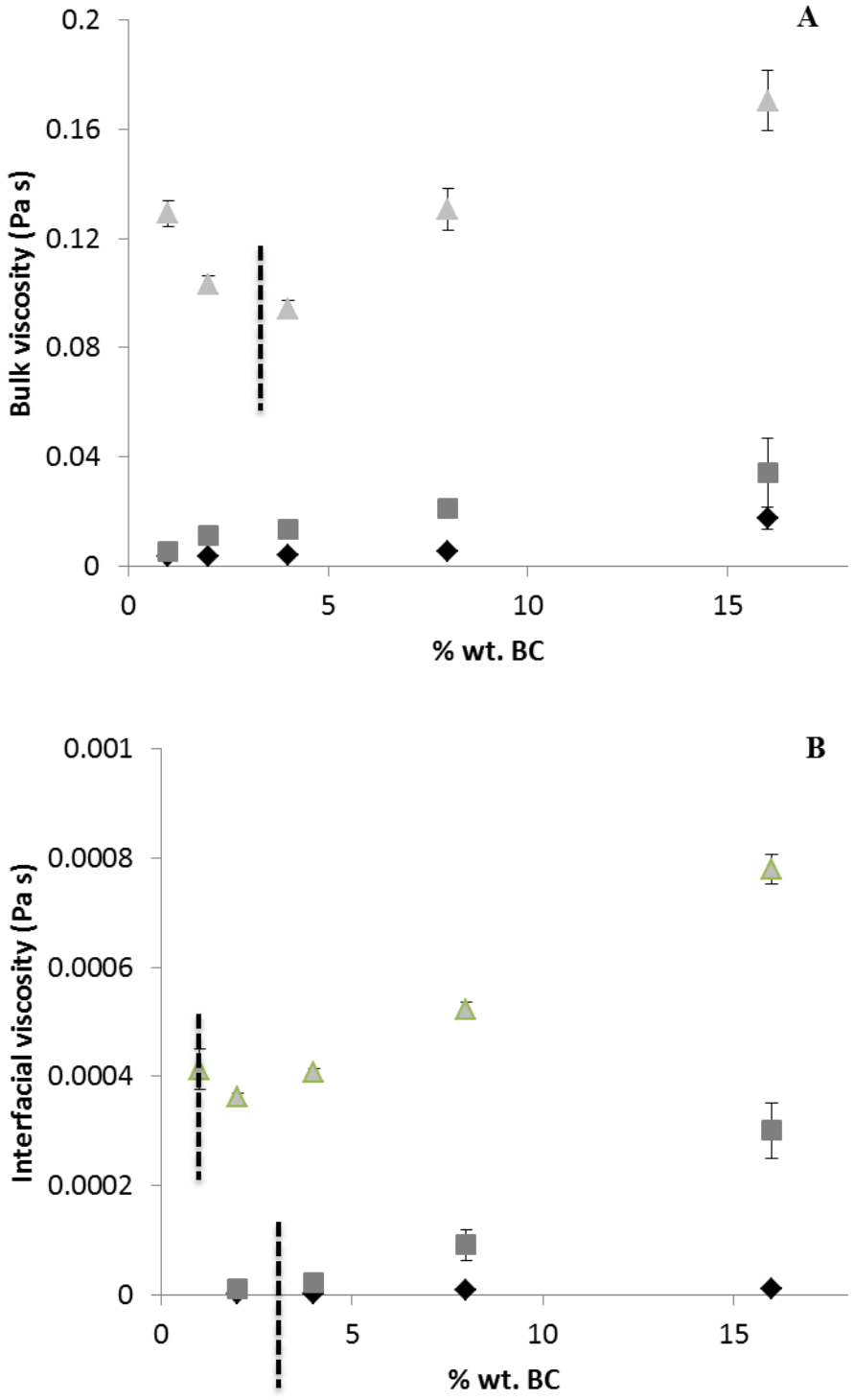

Fig. 8. 4 Bulk (A) and interfacial viscosity curves (B) as a function of blended solutions containing 1-16% wt BC and 10% wt (◆), 20% (■) or 30% (▲) wt WPI. Bars indicating standard deviations.

From this figure, it can be seen that, while for the solutions containing 10% wt WPI, the bulk and interfacial viscosity do not have significant differences due to the

Newtonian behavior of WPI at concentrations varying from 10 to 20% wt., when the concentration of WPI is increased (20-30% wt.) significant differences are found. Specifically, the interfacial viscosity for the 20% wt WPI solutions can be divided in 2 regions: one from 1-4% wt BC and the other from 4-16% wt BC. As far as the solution containing 30 % wt WPI is concerned, the bulk viscosity shows a 2 region profile as well, with the first region being from 1-4% wt BC and the second between 4-16% wt BC, while the interfacial viscosity values of the first region were between 1-2% wt BC and the second between 2-16% wt of BC.

What is more, a good correlation can be found between the viscosity values and the polydispersity index (PDI) of the particles diameter (Table 8.1). In the case of 10% wt WPI, only one region is depicted for both the bulk and interfacial viscosity values, while the PDI of all the produced samples was below 1, confirming the monomodal size distribution of the particles (McClements, 2005). Another issue to consider is the viscosity of the solutions with 20% WPI. Only one region is observed for the bulk viscosity. However, for the interfacial viscosity, 2 regions are observed and are in agreement with the polydispersity of the solutions which showed that from 1-4% wt BC the distribution is monomodal. However, when increasing the BC amount, the distribution becomes bimodal. Concerning the 2 observed regions at 30% wt WPI, the slope in the first region includes solutions having 4% wt or less BC in the solution, while the second region includes BC content of up to 16% wt. In contrast to the results of the bulk viscosity, interfacial viscosity also exhibits 2 regions, the first being for BC concentrations up to 2% wt and the second up to 16% wt.

The interfacial viscosity values are in better agreement with the polydispersity of the produced particles. Solutions falling in the first region gave particles of monomodal size distribution (PDI< 1), while those falling in the second region resulted in particles that exhibit a multimodal distribution. The correlations between the bulk or interfacial viscosity with PDI can be seen in Table 8.2. Specifically, the absolute value of the correlation for bulk viscosity and PDI is lower (0.68) than those for interfacial viscosity and PDI (0.81), indicating a stronger linear relationship between interfacial viscosity and PDI ($P<0.05$).

Table 8. 2 Correlation factors from multiple variant analysis

	surface tension	conductivity	ζ-pot	viscosity	inter viscosity	size	PDI
surface tension		**0.9564**	-0.3960	0.2135	0.3606	0.2342	**0.6963**
conductivity			-0.2899	0.2850	0.4035	0.3348	**0.6691**
ζ pot				**0.6931**	**0.6148**	**0.7323**	0.2315
viscosity					**0.9372**	**0.8750**	**0.6834**
inter viscosity						**0.9522**	**0.8130**
size							**0.7284**

The pairs of variables with bold have $P < 0.05$.

In a recent study a correlation between the rheological properties of the chitosan-PEO blends and their electrospinability can be seen (Rošic et al., 2012). They correlated the viscosity regions with the ability of the blends to form nanofibers via electrospinning. An interesting observation they made was that interfacial viscosity gave better response in predicting the electrospinability of the solutions. All in all, the correlation between the rheological characteristics of the interface and nanofiber morphology is far more distinctive than any correlations with rheological properties in the bulk.

A principle components analysis (PCA) is conducted to evaluate the properties that mostly affect the size and structure of the particles (Fig. 8.5).

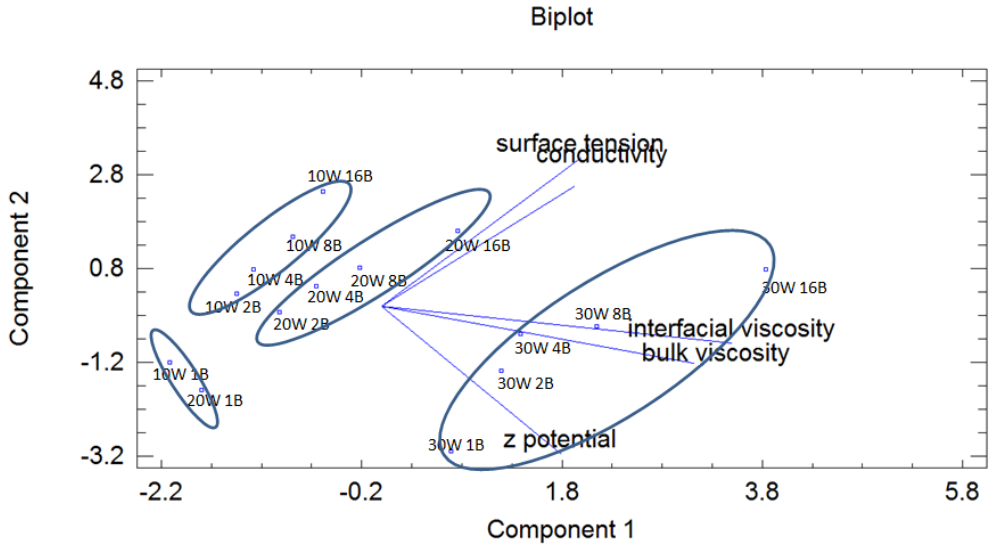

Fig. 8. 5 Principle components analysis of the electrosprayed particles.

In our case, 2 components have been extracted, since they have eigenvalues greater than or equal to 1.0. Together they account for 96.1% of the variability in our samples. As it can be seen, surface tension and conductivity are mostly affected by BC, as their eigenvalue is parallel to the increase of the BC. This is in good agreement with our previous measurements (8.1). On the other hand, bulk and interfacial viscosity are weighted more heavily in a positive direction by WPI concentration, as their eigenvalue is parallel to the augmentation of WPI. Another issue to mention is that the variables furthest from 0, make the largest contribution to the system, which in our case are interfacial viscosity and surface tension. Only with these properties, the structure of the electrosprayed particles could be successfully predicted.

Furthermore, a cluster analysis is performed to categorize the samples (Fig. 8.5). This procedure has created 4 clusters from the 15 observations supplied. Samples with 30% WPI consist of the first cluster, while the samples 10%WPI-1%BC and 20%WPI-1%BC the second. The samples with 10% WPI and 2-16% BC consist of the third cluster, and the samples with 20% WPI and 2-16% BC consist the fourth cluster. This categorization indicates that WPI plays a key role on grouping the samples, especially in the first cluster, which leads to dripping solutions. It is obvious that BC in low concentrations also plays an important role in grouping (cluster 2). These samples have low surface tension values leading to uneven particles. Cluster 3 also exhibit low viscosity and surface tension values, while cluster four (20% WPI, 2-16% BC) yields particles with the best properties.

In all cases, it was possible to produce particles with size distribution in the submicron range, which is very promising as a first step of the encapsulation of bioactive compounds in the BC-WPI particles. Taking all the measurements into consideration, it is obvious that solutions containing 20% wt. WPI and 8% wt. BC resulted in particles with the lowest size (180 nm), and the narrowest distribution (PDI= 0.9). It is well known that particle size distribution is a key factor when choosing a solution to encapsulate bioactive compounds, as the lower the particle size, the higher the encapsulation efficiency. To this regard, the formulation that yielded the optimum solution properties and produced particles with the lowest size is: 20% wt. WPI and 8% wt. BC. Hence, this formulation has been used for the encapsulation of EGCG.

8.5. Encapsulation of catechin

EGCG was added in the solutions according to method described in 3.2.5. All the solutions produce particles in the form of white powder when electrosprayed. The morphology of the produced particles is highly affected by the properties of the WPI-BC solutions. Fig. 8.6 shows SEM images and the mean particles diameter (D_{50}) of the

structures obtained after electrospraying of different solutions, while Table 8.1 summarizes the polydispersity index (PDI) of the produced materials.

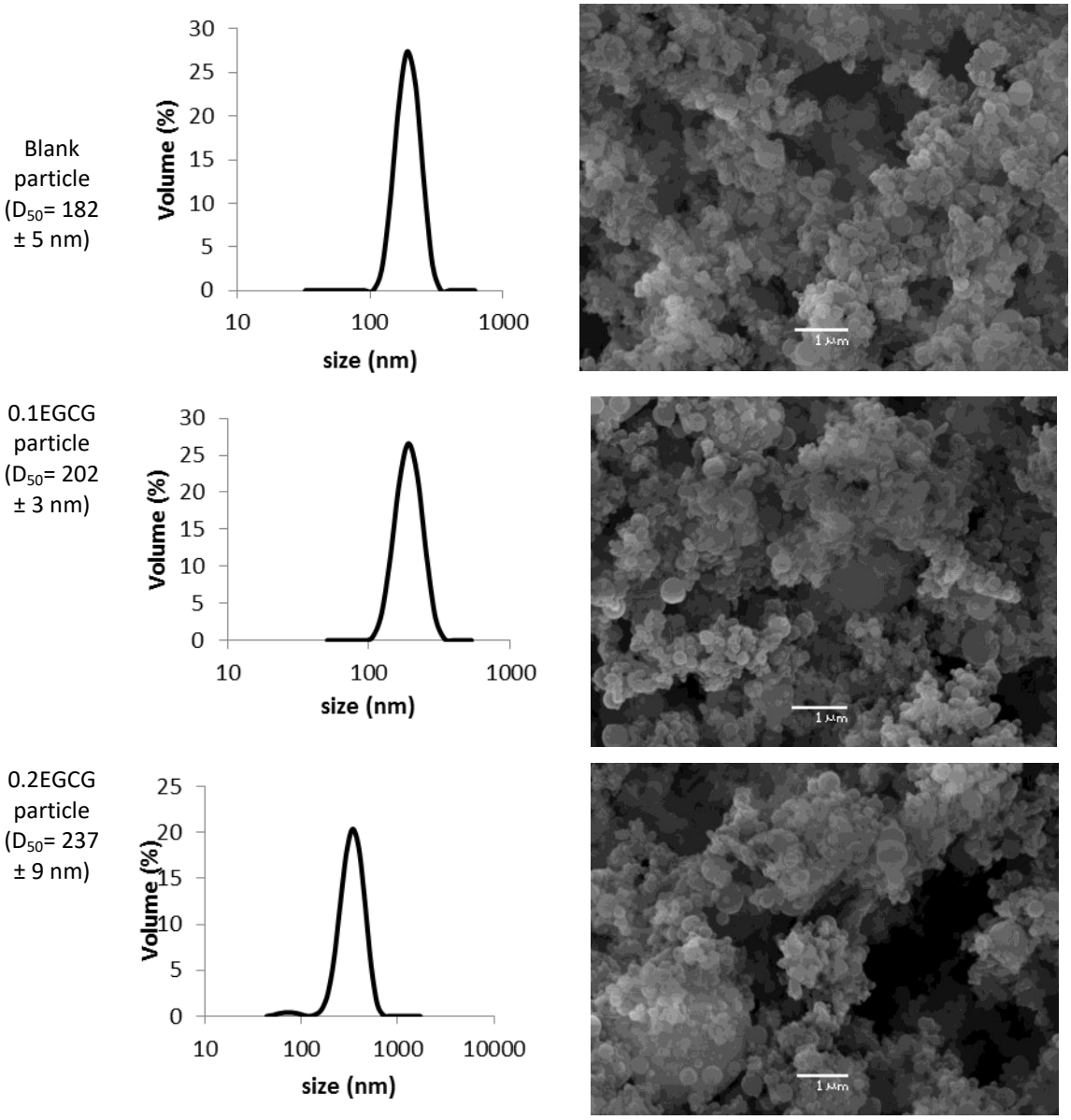

Fig. 8. 6 Diameter size distributions and microstructure of the blank, 0.1 and 0.2EGCG-loaded particles

It can be observed that spherical submicron and micron particles are obtained from the solutions (Fig. 8.6). However, there is an increase in the mean particle size and PDI by increasing the EGCG concentration. Electrospraying of EGCG-loaded solutions yields mixed heterogeneous structures combined with bigger average diameters and broader size distribution. For 0.2EGCG solutions, their particles had the highest D_{50} (237 nm), while the same solution without EGCG, gives rise to particles with smaller

size (182 nm). The particle size increases significantly with increasing EGCG concentration, due to addition of molecules into the system. Therefore, it is expected that blank solution leads to particles with the minimum size. EGCG loaded in the droplet could justify its size increase. Gómez-Mascaraque et al. (2015) postulated similar results by electrospraying solutions with EGCG. Furthermore, the PDI and size distribution follow the same trend. The 0.2EGCG size distribution of the final particles is broader compared to the blank's , indicating that catechin interacts with the ingredients of the solution.

What is more, there is a difference between the solids of the solutions and the amount of the collected final product, which is expressed by productivity yield (Table 8.3).

Table 8. 3 Productivity yield and EE of the EGCG-loaded particles

Electrosprayed particles	Productivity yield (%)	EE (%)
0.1EGCG	46^{b} (2)	51^{b} (8)
0.2EGCG	38^{g} (5)	30^{a} (5)

In parenthesis standard deviation values.

Mean values followed by the same letters in the same column are not significantly different ($P > 0.05$).

The lowest productivities are observed at the 0.2EGCG formulations (38%), which could be attributed to the extensive dripping of the solution. The productivity results are comparable or higher to other studies producing electrosprayed particles for encapsulation prospects (5-65%) (Gomez-Mascaraque et al., 2016).

As it can be seen from Table 8.3, EGCG concentration significantly affect the EE. Specifically, lower EE values can be seen in 0.2EGCG particles (30%) compared to 0.1EGCG particles (51%). The encapsulation values are both relatively low compared to Chapter 9. Some interactions between EGCG and WPI could be attributed for the low encapsulation of EGCG in the particles. In fact, it is known that large polyphenols, such as EGCG, are likely to bind with milk proteins and especially β-lactoglobulin due to the oxidation or polymerization of catechin monomers (Dubeau et al., 2010; Ozdal et al., 2013). This phenomenon leads to changes in physicochemical properties of proteins such as solubility, thermal stability and digestibility and mostly occurs when the pH of the solution is close to the isoelectric point of the proteins, which is the case in this study (Naczk et al., 1996; Rawel et al., 2005). Specifically, it can be speculated that since EGCG directly meets with WPI,

hydrogen bonds are formed between the protein and the catechin in the solution, leading to lower encapsulation efficiencies in the final particles.

8.6. Catechin stability during various storage conditions

To further investigate the stability of the particles, EGCG loss from the particles was evaluated as function of different storage conditions (relative humidity, pH, temperature). After electrospraying, the particles were stored at different conditions (RH, pH, T) as explained in 3.3.11. In Fig 8.7 the stability of EGCG in the particles that showed the best EE (0.1EGCG) together with the pure EGCG are depicted. The stability is expressed as the percentage of the initial amount of EGCG found in the particles (remaining EGCG), during a storage time of 45 days.

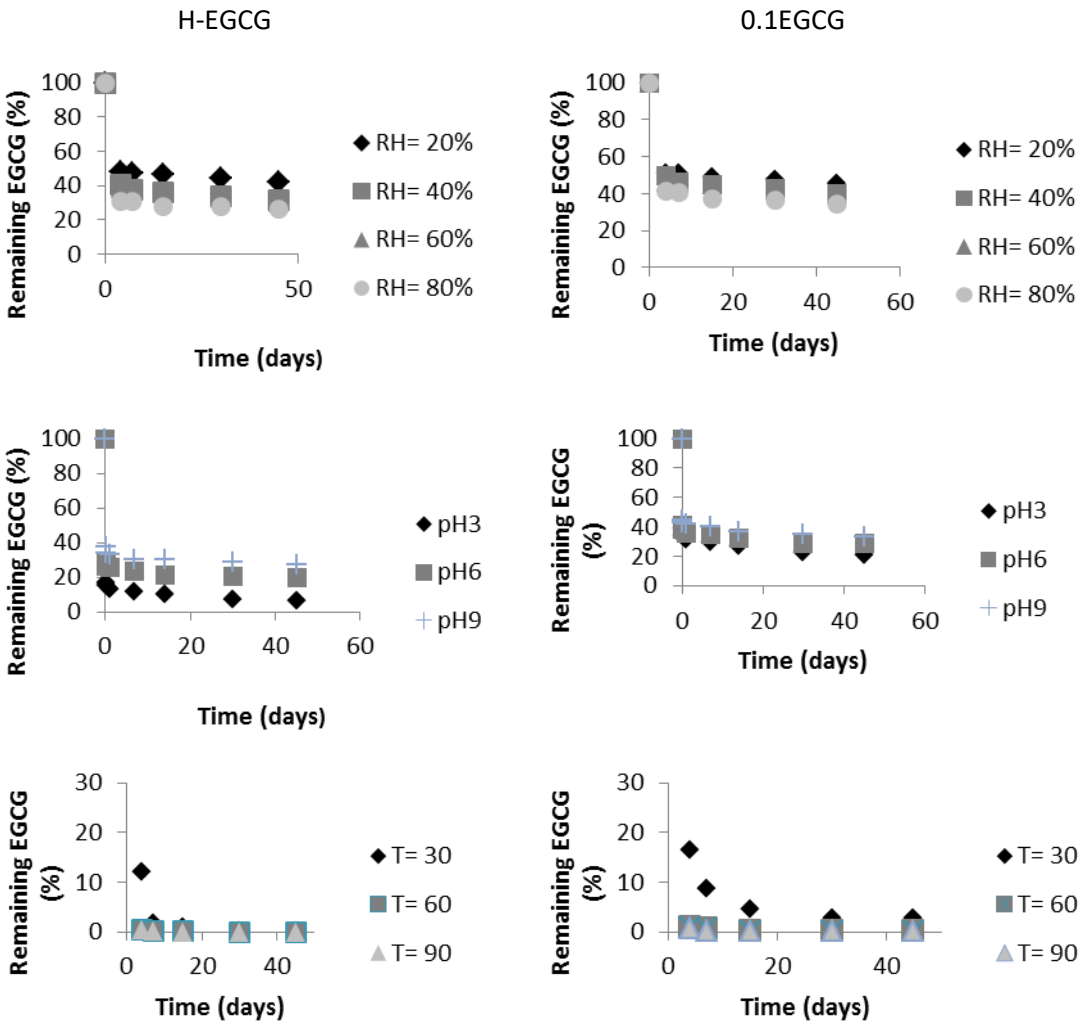

Fig. 8. 7 Stability of raw H-EGCG or loaded at the particles stored at various conditions.

From Fig. 8.7 it can be summarized that the stability of EGCG within the particles shows a different behavior depending on the storage conditions.

It is worth noting that non-encapsulated EGCG drastically decreases regardless of the storage conditions, and hence, even the 0.2EGCG particles provide enhanced EGCG stability. As far as the storage in different relative humidities is concerned, a decrease in the stability of EGCG occurred, as RH increased. Specifically, an increase in RH from 20 to 60 up to 80%, results in a decrease in the remaining EGCG in the 0.1EGCG particles from 45 to 40 to roughly 25%. Therefore, in all cases, EGCG deteriorates faster under high RH and is more stable under low humidity content (RH=20%). For other bioactives (orange oil), it has also been indicated that the optimum storage conditions are at low RH ie 20% (Anker and Reineccius, 1988). When the particles are exposed to higher RH, they tend to collapse probably due to the high solubility of BC in water (Aceituno-Medina et al., 2013). This rate of diffusion of water into the particles enhances the hydrolysis or other degradation reactions, thereby decreasing the stability of the encapsulated compounds. In addition, EGCG is known to exhibit higher stability in lower RH (Li et al., 2011). Recent study have shown that the catechin release is higher at RH=75% rather than 0%, when encapsulating EGCG into zein fibers (Li et al., 2009)

It was seen that for particles dissolved in solutions, the pH played a significant role on the stability of the catechin during storage. The remaining EGCG on the 0.1EGCG particles is 21%, close to pH 3, and it increased when the pH was changed. Under neutral pH conditions, the remaining EGCG augments up to 28% for the 0.1EGCG particles. In the alkaline pH range (pH=9) the remaining EGCG is significantly higher (33%) in comparison to the remaining EGCG measured at neutral or in the acidic pH range. At acidic pH, the WPI-BC particles are highly charged, thereby expected to swell significantly, which may increase EGCG diffusion from the particles (Zhou and Elias, 2013). These data could lead to the assumption that the produced particles could be effectively incorporated into food products with neutral pH, such as dairy products.

As far as the EGCG stability upon high temperature exposure is concerned, it is seen that non-encapsulated EGCG is completely degraded after 7 days at 30^{o}C or 1 hour at 90^{o}C. In contrast, the electrosprayed particles can significantly reduce the EGCG degradation. In this case the bioactive is completely degraded after 15 days at 30^{o}C or 4 hours at 90^{o}C. It is known that thermal treatment amounts to decrease the raw EGCG (Li et al., 2013). What is more, increasing the storage temperature from 30 to 90^{o}C, lead to faster degradation kinetics for the EGCG, as expected. It is well documented that EGCG is epimerized when exposed at high temperature, leading to the conversion to its corresponding isomers (GCG) and, ultimately, to the particle degradation (Ananingsih et al., 2013; Wang et al., 2008b). These results are in

agreement with studies evaluating the stability of omega-3 fatty acid on electrosprayed zein particles (Torres-Giner et al., 2010).

The particle size of the formulations is expected to be influenced by the storage conditions. Therefore, in Fig. 8.8 the particle size of 0.1EGCG particles is shown during 45 days of storage.

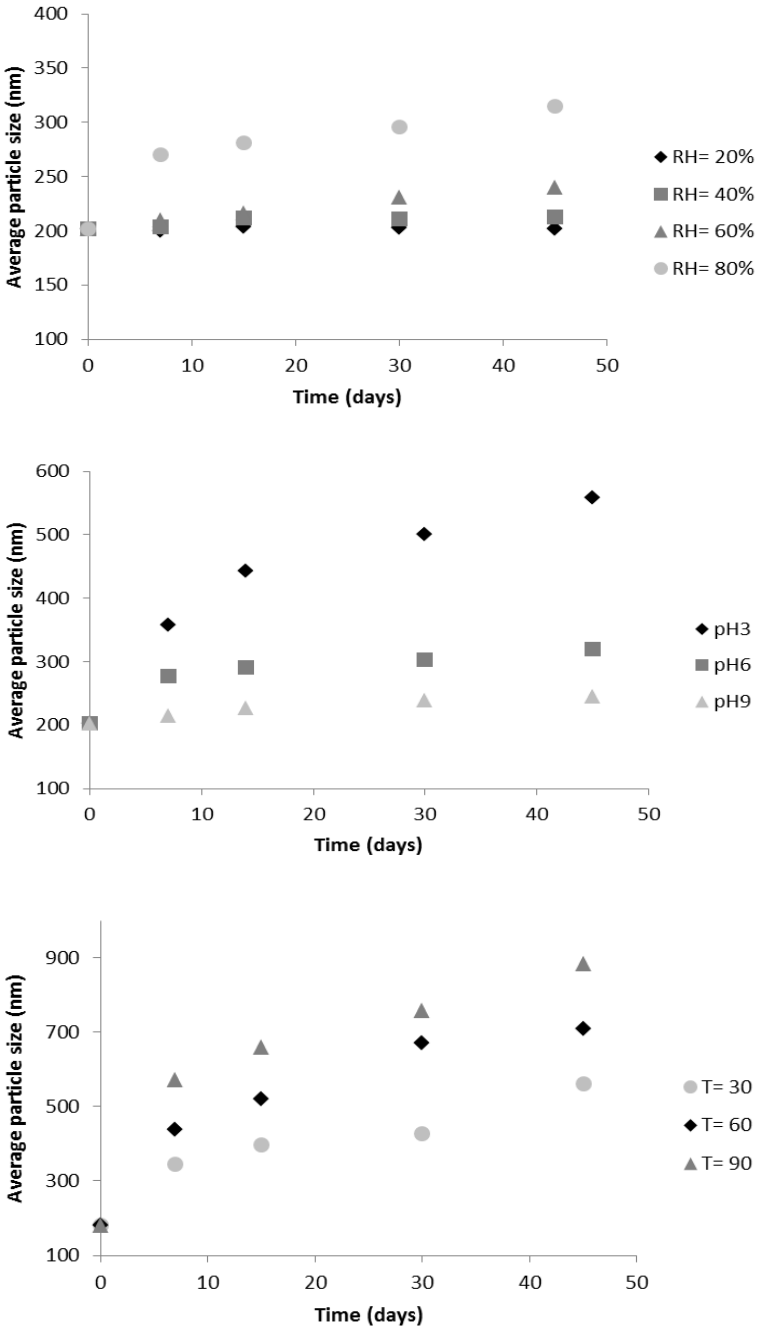

Fig. 8. 8 Average diameter of 0.1EGCG-loaded particles stored at various conditions.

In all cases, an increasing EGCG concentrations up to 0.2 increases the diameter of the particles (data not shown). From Fig. 8.8 can be seen that the RH significantly affects the average particle size. Specifically, by increasing the RH the size of the particles also increases. For instance, the particle size of 0.1EGCG sample is 200 nm after 45 days of storage at 20% RH, while the particle size of 0.1EGCG sample RH? is 320 nm after the same storage time at 80%. Another interesting point is that the particle size remains the same (202-209 nm) after 45 days of storage at RH varying from 20 to 40%. On the other side, the particle size significantly increases from 240 to 320 nm (150%) after 45 days of storage at higher RH (60-80%). This is attributable to the instability that WPI and BC exhibit in higher RH, leading to their dissolution in the environment. Recent studies encapsulating model drug in electrosprayed particles have found that the optimum conditions with steady particle diameters are at low RH (Cao et al., 2014).

For all particles, we observe similar changes in the average size: in the acidic pH range, the size distribution shifted towards larger sizes. This increase in the size is due to particle swelling, as no particle aggregation was observed at this pH range (SEM, data not shown). At pH 3, the average diameter of the 0.1EGCG particles is larger (D_{av}= 560 nm), than the particles prepared at pH 6 (D_{av}= 320 nm). In the alkaline pH range, a decrease in the size was observed at pH 9, reaching values up to 250 nm. In addition, the slope of the EGCG release is higher when the particles are stored at pH=3, meaning that in this condition the EGCG release takes place quicker than in the other pH. This could be attributed to the higher solubility that polysaccharides and proteins exhibit at acidic conditions (Torres-Giner et al., 2008).

As far as the particle size upon high temperature exposure is concerned, it is seen that 0.1EGCG particle size significantly increases from 200 nm to 670 nm and up to 1250 nm after 7 days of storage at 30 and 90^{o}C respectively. The increasing rate is quite high in all the tested temperatures. It is well known that whey proteins are thermally sensitive molecules and they tend to produce sediments during thermal treatment (McClements, 2005). Hence, when the particles are exposed in high temperatures, WPI and BC collapse leading to the increase of the particle size.

Table 8.4 depicts the EGCG kinetic constants for the Peppas- Sahlin equations at the different storage conditions for all the produced particles. The first observation is that k_1 constant show higher values than k_2 in all the electrosprayed particles, which is attributable to the diffusion which is the dominant mechanism on the particles. Similar behavior has been reported for other spherical carriers (Siepmann and Peppas, 2001).

Table 8. 4 Release kinetic parameters (k_1, k_2) of the different electrosprayed particles.

Storage conditions	Kinetic parameters	H-EGCG	0.1EGCG	0.2EGCG
RH= 20%	k_1	321 (8)	305 (6)	440 (18)
	k_2	-43 (2)	-40 (1)	-60 (12)
RH= 40%.	k_1	381 (17)	323 (19)	451 (15)
	k_2	-50 (12)	-42 (3)	-60 (7)
RH= 60%.	k_1	383 (21)	335 (14)	476 (14)
	k_2	-50 (5)	-44 (9)	-65 (8)
RH= 80%.	k_1	438 (13)	371 (14)	507 (18)
	k_2	-60 (5)	-49 (7)	-70 (10)
pH= 3	k_1	609 (37)	479 (16)	598 (8)
	k_2	-88 (4)	-67(10)	-87 (5)
pH= 6	k_1	530 (23)	449 (8)	574 (17)
	k_2	-77 (7)	-63 (7)	-83 (14)
pH= 9	k_1	444 (24)	379 (17)	516 (12)
	k_2	-61 (9)	-51 (6)	-71 (12)
T= 30^o C	k_1	664 (12)	590 (19)	646 (30)
	k_2	-103 (4)	-90 (6)	-105 (9)
T= 60^o C	k_1	696 (35)	642 (31)	686 (28)
	k_2	-118 (11)	-103 (10)	-115 (9)
T= 90^o C	k_1	717 (36)	698 (30)	725 (38)
	k_2	-124 (11)	-119 (9)	-126 (12)

In parenthesis standard deviation values.

Higher values of the kinetic constants indicate a much faster release of the antioxidant. Specifically, kinetic constants for the different particles seem to have the same trend as the EE results. For instance, 0.1EGCG particles stored at 20% RH show EE= 51%, k_1= 305 and k_2= -40, while the 0.1EGCG particles stored at the same conditions show EE=30%, k_1= 440 and k_2= -60. This phenomenon is in accordance with studies modelling the kinetics of antioxidants (Gómez-Mascaraque et al., 2016; Spizzirri et al., 2013). If comparing the k_1, k_2 values of the same particles in different

storage conditions, the higher the values of the constants, the faster the release in the different conditions. For instance, 0.1EGCG particles stored at 20% RH show k_1= 305 and k_2= -40, while when the same particles are stored at 80% RH show k_1= 371 and k_2= -50. The Peppas- Sahlin model also confirms the faster EGCG release kinetics from the 0.2EGCG particles rather than 0.1EGCG particles, which could partially be attributed to the interactions between protein and catechin that mentioned earlier.

One more point to add is that k_1 values decrease with the increase of pH, indicating that the Fickian contribution also decreases. Especially, 0.1EGCC particles stored at pH =3 show k_1= 480, while when the same particles stored at pH=9 show k_1= 380. Consequently, the contribution of Fickian diffusion to EGCG release is small, while both Fickian diffusion and relaxation controlled transport contribute to EGCG release from BC-WPI particles. This trend is consistent with other studies dealing with particles as encapsulants (Soares et al. 2002).

8.7. Conclusions

Whey protein and bacterial cellulose particles with flexible physical properties, such as morphology and size, are interesting for targeted delivery purposes, particularly for the food applications due to their biodegradability. In this chapter, we have investigated the WPI-BC particles efficiency to encapsulate EGCG. Specifically, we have found that surface tension and electrical conductivity increased as the BC concentration increased, while they remained the same in terms of the protein concentration. Viscosity and interfacial viscosity increased as the proportion of BC increased. The produced particles varied in size (120 to 380 nm) and polydispersity (PDI= 0.8 - 3). A good correlation (0.83) was found between the interfacial rheology values of the solution and the distribution of the produced particles. According to a PCA, it can be said that interfacial viscosity and surface tension could be used as structure predictors of the electrosprayed particles. The EE of catechin yielded relative high values up to 51%. The EGCG degradation from the particles stored under various conditions was also studied. The catechin in the particles was more stable when stored at low RH. Ultimately, WPI-BC particles protected EGCG from moisture, heating, and dissolution conditions, leading to the potential use of them as a substitute in order to enhance EGCG shelf life when incorporated within various food products.

Chapter 9. Emulsion electrosprayed particles for the encapsulation of hydrophilic and lipophilized catechins

9.1. Introduction

The main substance of tea catechin, epigallocatechin-3-gallate (EGCG), is considered as a powerful antioxidant, and has been demonstrated by in vitro assays to be effective in radical scavenging, reduction and metal chelation (Tsatsaragkou et al., 2016; Zhong and Shahidi, 2012). Thus, adding EGCG to food products could potentially benefit the consumers, as their awareness concerning healthier lifestyles is certainly growing. However, one of the major pitfalls of EGCG is its chemical instability and its low lipophilicity which makes it difficult to be incorporated in lipid-based foods, such as fats and oils (Xu et al., 2004). Considering these drawbacks, structural modification of EGCG can serve as a solution to increase its lipophilicity and to widen its application in lipophilic media (Zhong and Shahidi, 2012).

A plausible approach to overcome the limitations of EGCG is its encapsulation, through spray drying (Fu et al., 2011; Rocha et al., 2011), emulsion formation (Ru et al., 2010; Zhou and Elias, 2013), supercritical fluid (Gadkari and Balaraman, 2015a) or complex formation (Liu et al., 2016; Wei et al., 2015). However, these techniques require heating, organic agents or expensive equipment. The heating during the process could damage the encapsulated compounds (Lian et al., 2002).

To this regard, electrohydrodynamic (EHD) processing, and specifically electrospraying is beneficial for producing particles entrapping the active ingredients. Lipophilized EGCG (L-EGCG) is known to exhibit low water solubility, thus, electrospraying and subsequent encapsulation of this compound from water-based solutions is not possible. To this regard, emulsion electrospray can be used to encapsulate immiscible compounds (Abu-Ali and Barringer, 2005; García-Moreno et al., 2016; Wang et al., 2014). During emulsion electrospraying, hydrophobic ingredients could be encapsulated in low cost biopolymers. Several studies have shown the potential use of emulsion electrospray (Angeles et al., 2008; Camerlo et al., 2014; Gordon et al., 2015; Li et al., 2009). However, the encapsulating materials used are, in most of the cases, not edible.

The aim of this study is to better understand the use of emulsion electrospraying as a one-step preparation technique to obtain EGCG loaded micro and sub-micron structured bacterial cellulose-whey protein isolate (BC-WPI) particles. Various physicochemical characterizations of the prepared particles were carried out, including the morphology and size of the electrosprayed particles, and the encapsulation efficiency of EGCG. The EGCG stability under different storage conditions (pH, RH, and temperature) was also explored to gain a more fundamental understanding on the system. Two emulsification processes were tested prior to encapsulation. The influence of the emulsion properties, type of EGCG (hydrophilic

or lipophilized) and the addition phase of EGCG (aqueous or oil) on the particles' properties were studied as well.

9.2. Preliminary experiments

The preliminary step in this section is to optimize the concentration of the ingredients that they will be used in this study. Specifically, the minimum concentration of WPI and BC that is needed in order to form stable emulsions will be determined. For this purpose, emulsions with increasing concentration of WPI (2-20 % wt.) and BC (1-16%) were prepared with the aid of a high shear homogenizer for 1 min at 10000 RPM. Olive oil concentration remained constant at 10% wt., while Tween 20 concentration remained also constant at 5% wt. It is worth mentioning that higher amounts of WPI and BC could not be incorporated into the emulsions due to technical problems. The stability of these emulsions after 2 days of storage was evaluated and summarized by means of SI (%) in Fig. 9.1.

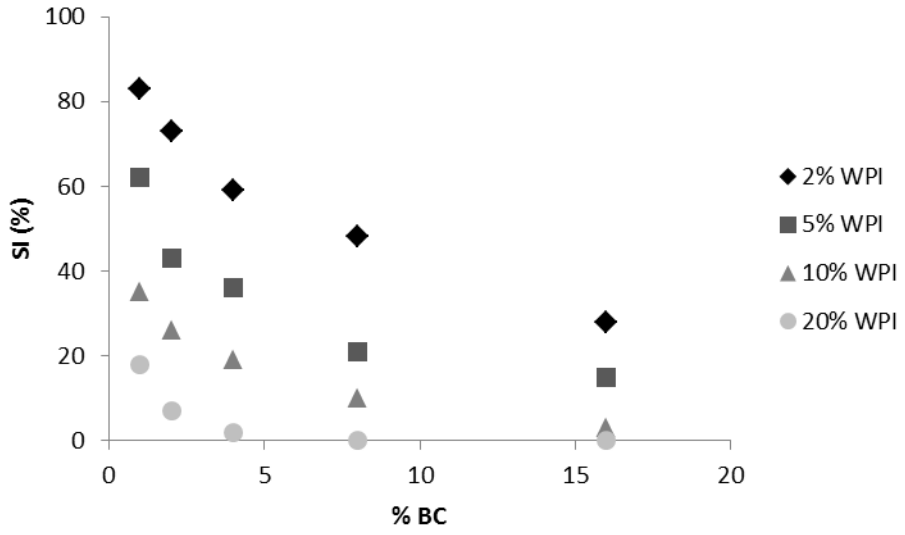

Fig. 9. 1 Stability of preliminary emulsions

It is obvious that by increasing the concentrations of WPI and BC, the stability meliorates, as it is expected. These results show that the highest emulsion stability is achieved for the formulations containing 20% wt. WPI, 8% wt. BC, 5% wt. Tween 20 and 10% wt. oil. Thus, this formulation was chosen as the starting point of the emulsion electrospraying process.

9.3. Emulsions' physical properties

Electrosprayability of an emulsion together with the properties of the produced particles are two factors strongly affected by the physical properties of the produced

emulsions. Numerous studies showed that smaller oil droplets in the emulsion increased the oil encapsulation efficiency of the produced particles (Jafari et al., 2008a; Wang et al., 2016b). In the same direction, the stability of the emulsions proportionally affects the produced particles. Due to the presence of the needle tip in the electrospraying apparatus as an emulsion position, stable emulsions are important for the success of the process (Wang et al., 2014). Hence, the physical properties of the prepared emulsions stabilized with BC and WPI and containing different EGCG type were measured to gain insight in these mechanisms and are presented in Fig. 9.2 and Table 9.1. In the present study, two homogenization methods are used in order to prepare emulsions: a high shear homogenizer (UT) or an ultrasonic device (US). What is more, two types of EGCG; hydrophilic (H) or lipophilized (L) were added either on the aqueous (W) or oil (O) phase of the emulsions.

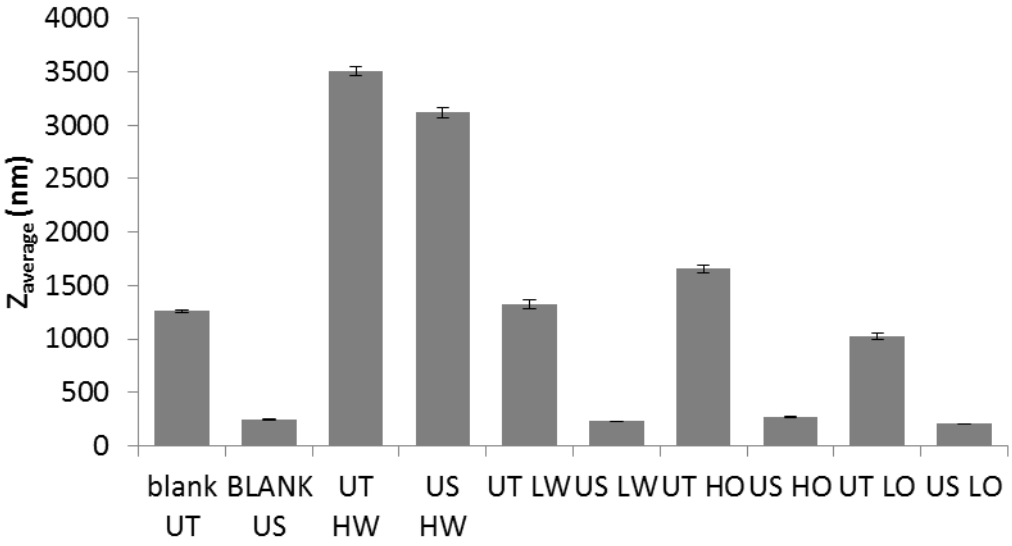

Fig. 9. 2 Emulsions' average oil droplet size

It is of interest to observe that ultrasonication as a homogenization method lead to emulsions with reduced droplet size than the emulsions homogenized by UT by a factor ~4.2 in average. For instance, in emulsions without EGCG present (BLUT, BLUS), the Z_{aver} falls from 1200 nm when it is homogenized with UT to roughly 250 nm for emulsions treated with US. This steady declining trend of the droplet size between the two homogenization methods is well known (Jafari et al., 2007; Kaltsa et al., 2016; Leong et al., 2009).

The same trend follows the polydispersity of the emulsions, which is expressed by means of a polydispersity Index (PDI) (Eq. 3.3, Table 9.1). A monomodal size distribution is confirmed by PDI values lower than 1, while a bimodal or multimodal by PDI values higher than 1. (McClements, 2005). Indeed, bimodal distributions are

observed in UT emulsions, with PDI varying between 1.2 to 2.7, while monomodal distributions are observed in US emulsion as their PDI varies from 0.4 to 1 (Table 2).

Table 9. 1 Physical properties (PDI, serum index, conductivity, surface tension, and ζ-potential) of BC-WPI emulsions.

Emulsions	PDI (-)	SI (%)	Conductivity (mS/m)	Surface tension (mN/m)	ζ-potential (mV)
BLUT	2.1^{e} (0.1)	2.1^{c} (0.2)	3.0^{f} (0.1)	28.5^{b} (0.6)	-2.7^{g} (0.1)
BLUS	0.6^{a} (0.0)	0.0^{a} (0.0)	3.1^{f} (0.0)	31.7^{c} (0.9)	-3.9^{i} (0.0)
UTHW	2.7^{f} (0.2)	10.4^{f} (0.7)	1.3^{a} (0.1)	40.1^{f} (0.4)	-8.5^{b} (0.2)
USHW	2.2^{e} (0.0)	7.3^{d} (0.5)	1.7^{b} (0.2)	43.2^{g} (0.3)	-9.6^{a} (0.2)
UTLW	1.7^{d} (0.4)	1.4^{b} (0.2)	2.4^{d} (0.1)	24.5^{a} (0.7)	-6.9^{d} (0.1)
USLW	0.5^{a} (0.1)	0.0^{a} (0.0)	2.7^{e} (0.0)	27.4^{b} (0.6)	-7.8^{c} (0.1)
UTHO	1.8^{d} (0.2)	1.9^{c} (0.2)	2.1^{c} (0.3)	28.4^{b} (0.7)	-6.1^{f} (0.1)
USHO	1.0^{b} (0.0)	0.0^{a} (0.0)	2.2^{cd} (0.1)	31.3^{c} (0.5)	-6.5^{e} (0.0)
UTLO	1.2^{c} (0.1)	2.3^{c} (0.1)	2.9^{f} (0.1)	28.1^{b} (0.5)	-4.8^{h} (0.1)
USLO	0.4^{a} (0.0)	0.0^{a} (0.0)	2.9^{f} (0.0)	31.8^{c} (0.8)	-5.8^{g} (0.0)

In parenthesis standard deviation values.

Mean values followed by the same letters in the same column are not significantly different ($P > 0.05$).

EGCG type and addition phase significantly affect the Z_{aver}, as well as the distribution. When H-EGCG is added to the aqueous phase of the emulsions (UTHW, USHW), a great increase of the droplet size compared to the blank emulsions by a factor of 3 times can be observed. EGCG loaded in the droplet could justify its size increase. Moreover, catechin remaining in the aqueous phase can interact with protein as stated below. In fact, it is known that large polyphenols, such as EGCG, are likely to bind with milk proteins and especially β-lactoglobulin due to the oxidation or polymerization of catechin monomers (Dubeau et al., 2010; Ozdal et al., 2013). This phenomenon leads to changes in physicochemical properties of proteins such as solubility, thermal stability and digestibility and mostly occurs when the pH of the emulsion is close to the isoelectric point of the proteins, which is the case in this study (Naczk et al., 1996; Rawel et al., 2005). Specifically, it can be speculated that since EGCG is in the aqueous phase and directly meets with WPI, hydrogen bonds are formed between the protein and the catechin in the solution (Fig. 9.3). When the

emulsification process begins, WPI could not be adsorbed onto the interface of the oil droplets, leading to higher Z_{aver} and prolonged instability (McClements, 2005; Paximada et al., 2016b; Paximada et al., 2016c).

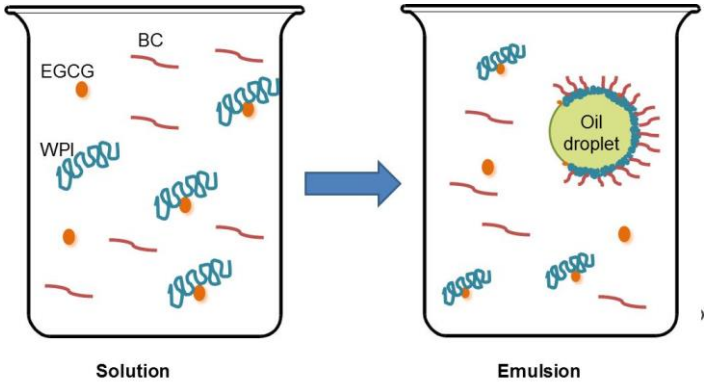

Fig. 9. 3 Proposed mechanism of the emulsification in the case that catechin is added in aqueous phase

In contrast to the results of the preceding paragraph, when H-EGCG is added to the oil phase (UTHO, USHO), the Z_{aver} and the PDI become larger, indicating that the addition of the EGCG is not efficient. This could be attributed to the fact that there is an excess of EGCG that could not be dissolved in the oil. This excess amount could possibly move onto the aqueous phase, forming small complexes and thus leading to higher Z_{aver}.

Another issue to consider is the incorporation of L-EGCG to the aqueous phase (UTLW, USLW). In these emulsions, the Z_{aver} and PDI are lower than the blank emulsions', revealing that interactions between the catechin and the protein took place. Small droplet size and low PDI suggest that even though L-EGCG is mostly hydrophobic, some parts of it could potentially form complexes with the WPI. These complexes have the ability to adsorb at the oil-water interface more easily than the bulk WPI, fact that can be attributed to the enhanced amphipathy and lower interfacial tension. (Dickinson, 2009; Wei et al., 2015). The decrease in emulsions' droplet size by the addition of EGCG was previously reported by (Wei et al., 2015)

On the other side, when L-EGCG is incorporated to the oil phase (UTLO, USLO), a decrease in the Z_{aver} and PDI, compared to the blank, could be observed. Specifically, the z_{aver} decreases from 246 nm for BLUS to roughly 200 nm for USLO. One explanation is that although L-EGCG is water insoluble, it has a polar head in its structure which provides enhanced compatibility through reorganization of the lipid molecules to expose their carboxyl groups to the water interface, fact which can contribute to increased stability of the emulsions and, subsequently, a decrease in droplet size (McClements et al., 2007; Ozdal et al., 2013). Moreover, it has been

reported that whey proteins could be unfolded at the interface at higher magnitudes for the non-polar oils (McClements, 2004).

The stability of the emulsions is expressed as the serum index (SI) (Table 9.1), which is an indicative of its stability to gravitational separation. High SI values express high emulsion instability; hence emulsions with low SI are desired. SI of UT emulsions is found to be higher than US emulsions, which are in agreement with the droplet size and PDI measurements. These higher SI values could be ascribed to bridging flocculation as a result of the attractive interactions of the BC with the WPI on the emulsion droplets. It is important to note that all the US emulsions except USHW, do not show any instability which is a promising result for the electrosprayability. Similar trend for the SI of UT and US emulsions have been found previously for emulsions stabilized with BC (Paximada et al., 2016c).

Emulsions' stability was found to be affected by EGCG type and addition phase. In the case that H-EGCG is added to the oil phase, an excess of EGCG that cannot be dissolved in the oil moves onto the aqueous phase forming small complexes and thus leading to higher stabilities. The formulations with LW and LO exhibited stability values that do not significantly vary from the blank, confirming the previous measurements, which postulated the absence of interactions between WPI and EGCG.

It is well known that electrical conductivity is a significant factor determining the ability of a solution to be electrosprayed (Palangetic et al., 2014). It is of interest to observe that the conductivity values of the US emulsions follow an increasing trend compared to the UT emulsions throughout the whole experiment. Specifically, the electrical conductivity of the UT emulsions varies from 1.3 to 3.0, while for the US emulsions varies from 1.7 to 3.1 mS/m regardless of the type of EGCG or the addition type. These values are similar with other studies dealing with WPI solutions, in which the conductivity of WPI varied from 1.7 to 2 mS/m (Arzeni et al., 2012). The phenomenon of the increased conductivity of US emulsions could be attributed to the predominant effect that ultrasounds have to the system. Specifically, the high local temperatures in combination with the high pressures that take place during ultrasonication, lead to the formation of hydroxyl radicals, which causes an increase in the conductivity (Hart and Henglein, 1985; Petrier et al., 1992). Makino et al. (1983) postulated that free radicals and other compounds are generated during cavitation, so ultrasounds induce oxidant species. In accordance to these results, other studies found an increase in conductivity when WPI or soy protein isolate suspensions were sonicated (Jambrak et al., 2009; Jambrak et al., 2008).

The EGCG type and the addition phase are found to possess a significant effect on the conductivity of the emulsions. Addition of HW in the emulsions leads to a decrease on the conductivity. For instance, conductivity of UTHW (1.3 mS/m) is well below that of BLUT (3 mS/m), with the first being comparable to the data obtained by Kiatyongchai et al. (2014). This is probably due to the complexes that are formed

between WPI and EGCG and mentioned earlier. These complexes may lead to the neutralization of some protein charges. The low conductivity of the HW emulsions could bear out a restriction during the electrospraying process, as the application of electric field causes coalescence or breaking of an emulsion (Abu-Ali and Barringer, 2005; Lee et al., 2001).

By adding HO or LW in the emulsions, lower conductivity values of 2.1-2.7 mS/ m can be seen compared to the blank. Thus, it can be said that in these cases the mentioned interactions between the proteins and EGCG are evident, although they are not as strong as in the case of HW emulsions. It is observed earlier that any addition of LW or HO have a large effect on the emulsion. Similar values for the conductivity have been found previously for emulsions stabilized with WPI and containing lipophilic antioxidant (lycopene), were conductivity values between 1.5 and 2 mS/m were reported (Pérez-Masiá et al., 2014). The formulations with LO exhibited conductivity values that do not significantly vary (2.9mS/m) from the blank. These data suggest that there were no interactions between the L-EGCG and the WPI, as the catechin is efficiently incorporated in the oil phase of the emulsion.

As far as the surface tension is concerned, a drastic increase occurs when treating the emulsions with ultrasounds. Specifically, for UT emulsions the surface tension bears values of 28-40 mN/m, while for US emulsions the values go up to 31-43 mN/m. This significant increase of the surface tension could be attributed to the predominant effect that US have on the emulsions' ingredients. Specifically, it has already been reported that US induced a certain degree of molecular unfolding of the protein molecules leading to a more pronounced exposition of the hydrophobic groups and regions inside the molecules to the more polar surrounding environment (Arzeni et al., 2012; Gulseren et al., 2007). This increase in the hydrophobicity ultimately leads to an increase in surface tension values.

What is more, the contribution of the HW to the surface tension of the emulsions is typically high as the surface tension increases by its addition due to the formation of the mentioned complexes and has been reported on emulsions when a lipophilic compound was added (Pérez-Masiá et al., 2014). Moreover, the LW incorporation amounts to altering the surface tension; as a decrease in this value is observed. It was suggested that emulsions prepared by the complexes of WPI and EGCG exhibit higher interfacial accumulation of EGCG due to the fact that EGCG in the complexes binds to proteins through strong interactions and cannot be easily dispersed in the aqueous phase (von Staszewski et al., 2014; Wang et al., 2014). However, the HO and LO do not affect the surface tension of the emulsions, as their values (28-31 mN/m) are similar to the blank emulsions. These results confirm the previous droplet size measurements, which postulated the absence of interactions between WPI and EGCG.

As far as the ζ-potential is concerned, all the emulsions are negatively charged due to the fact that BC is also negatively charged. Specifically, a drastic increase occurs when treating the emulsions with ultrasounds. For UT emulsions the ζ-potential bears values of –3 up to -8.5 mV, while for US emulsions the values go to –4 to -10 mV. This phenomenon is attributable to the effect that ultrasonication has on the emulsion (Paximada et al., 2016a). The particles have a significant electrical charge, so electrostatic interactions may play an important role in determining their overall stability and physicochemical properties. Indeed, ζ-potential results are in accordance to the stability results.

9.4. Emulsions' viscosity

Viscosity is one of the crucial parameters in predicting the ability of one solution to be electrosprayed. The viscosity of the emulsions is presented in Fig. 9.4 A. All the emulsions exhibit a shear-thinning behavior as their viscosity is decreasing by the increase of shear rate, regardless of the type of EGCG and the addition phase. This shear thinning behavior is typical for emulsions stabilized with BC (Paximada et al., 2016b; Paximada et al., 2016c).

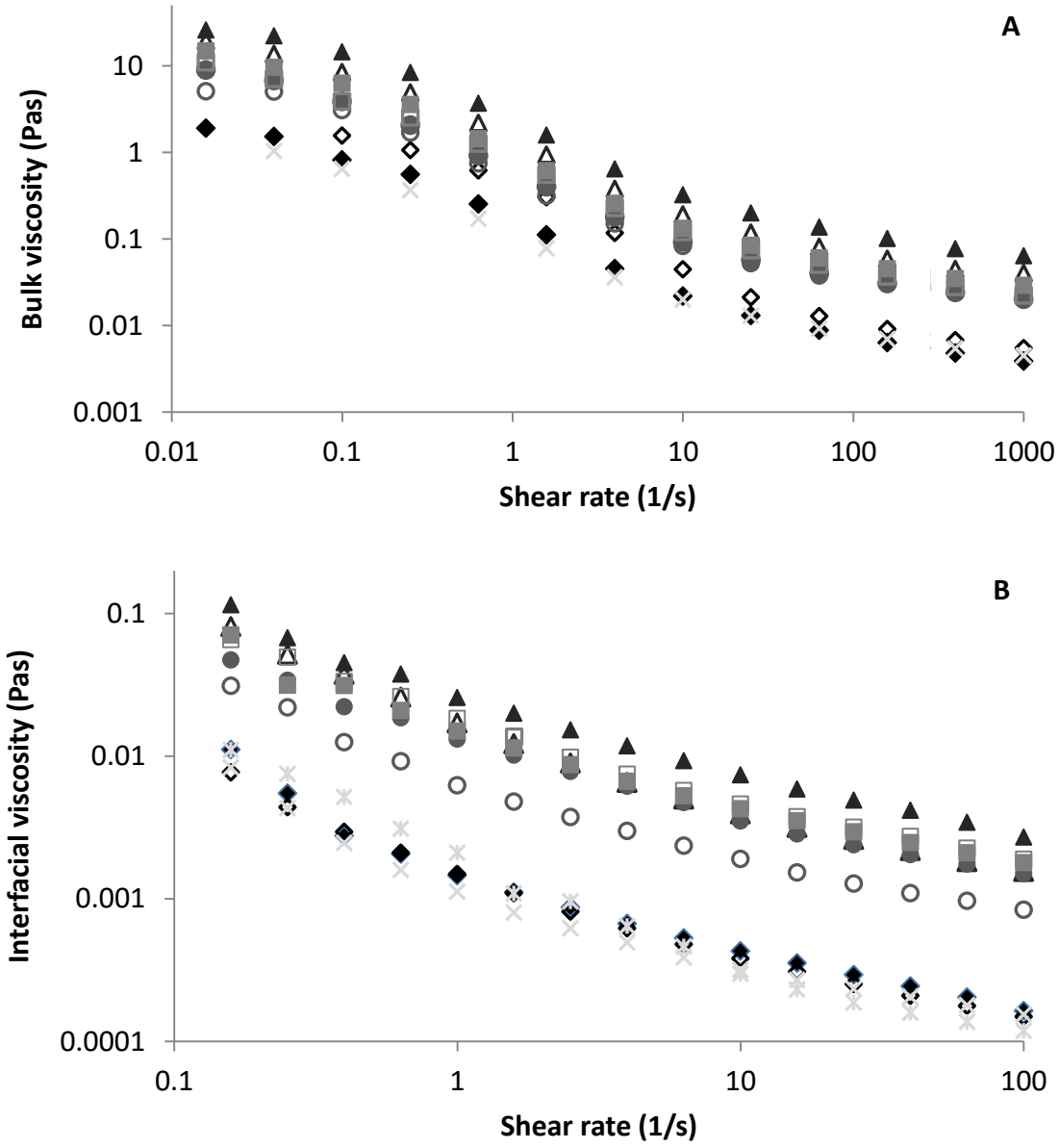

Fig. 9. 4 Bulk (A) and interfacial (B) viscosity curves of emulsions prepared by high shear homogenizer (closed symbols) or ultrasounds (open symbols) containing no EGCG (◆), HW (▲), LW (●), HO (■) and LO (✳) EGCG.

According to Fig. 9.4. A it is obvious that US has a negative effect on the viscosity of the emulsions, as their values decrease compared to the UT emulsions. Specifically, the US emulsions' viscosity decreases up to 0.5 -6 Pas, a decrease of 2 to 3 orders of magnitude compared to the UT emulsions. This behavior could be attributed to the predominant effect that US have on the viscosity of solutions and emulsions (Abismaïl et al., 1999; Canselier et al., 2002; Kaltsa et al., 2016).

As far as the HW and HO emulsions are concerned, their viscosity increases significantly up to 19 -26 Pas. The interaction between WPI and EGCG that was described earlier (3.1) could be related to the increase in viscosity. Studies showed similar tendency for emulsions containing lipophilic compounds (Pérez-Masiá et al., 2014). Such high viscosities may have a negative effect on the electrospraying process leading to the production of amorphous regions.

Interfacial rheology depicts the relationship between the deformation of an interface and the stresses exerted on it and the reorganization of the polymer molecules at the interface itself can be observed. Lately, numerous studies dealing with electrospraying depicted that the bulk rheological behavior is not efficient to predict the final particle structure (Pelipenko et al., 2012; Regev et al., 2010). Thus, interfacial viscosity of the emulsions as a function of different BC and WPI concentrations is evaluated and summarized in Fig. 9.4B.

The results of the interfacial viscosity measurements exhibit a similar trend to the bulk viscosity measurements (Fig. 9.4 A). However, the values of the interfacial viscosity are up to two orders of magnitude lower than those observed in the bulk, with the latter being comparable to data obtained by (Rošic et al., 2012). To sum up, the homogenization method, the EGCG type together with the addition phase play a key role to the physical properties of emulsions.

9.5. Electrosprayed particles properties

All the emulsions were processed with the electrospraying device and structures in the form of white powder were produced. However, there is a difference between the emulsions and the amount of the collected final product, which is evaluated with the aid of the productivity yield (Table 9.2).

Table 9. 2 Productivity yield and PDI of the particles obtained by electrospraying of the different emulsions.

Electrosprayed particles	Productivity yield (%)	PDI (-)
BLUT	49^{c} (1)	0.9^{c} (0.1)
BLUS	61^{f} (1)	0.7^{b} (0.0)
UTHW	21^{a} (1)	2.9^{g} (0.1)
USHW	25^{a} (1)	2.3^{f} (0.0)
UTLW	50^{c} (1)	0.9^{c} (0.0)
USLW	62^{f} (2)	0.7^{b} (0.1)
UTHO	45^{b} (2)	1.3^{e} (0.0)
USHO	57^{e} (2)	1.0^{d} (0.1)
UTLO	53^{d} (2)	0.6^{a} (0.0)
USLO	68^{g} (3)	0.5^{a} (0.1)

In parenthesis standard deviation values.

Mean values followed by the same letters in the same column are not significantly different ($P > 0.05$).

The productivity yield is affected by many parameters, namely the physical properties of the emulsions and the processing conditions. In general, ultrasonication of the emulsions, lead to higher productivities of the final particles, which is correlated to the enhanced physical properties of the emulsions produced by ultrasonication. The lowest productivities are observed at the HW formulations (21-25%), which could be attributed to the protein-catechin interactions, which apart from hindering proper encapsulation of catechin, lead to extensive dripping of the solution. The productivity yields the highest values at the LO and blank formulations (up to 68%). The productivity results are comparable or higher to other studies

producing electrosprayed particles for encapsulation prospects (5-65%) (Gomez-Mascaraque et al., 2016).

The properties of the emulsions that have been previously analyzed possess a major influence not only on the successful development of structures through electrospraying, but also on the morphology of the produced particles. Fig. 9.5 shows SEM images and the mean particles diameter (D_{50}) of the structures obtained after electrospraying of the different emulsions, while Table 9.2 summarizes the polydispersity index (PDI) of the produced materials.

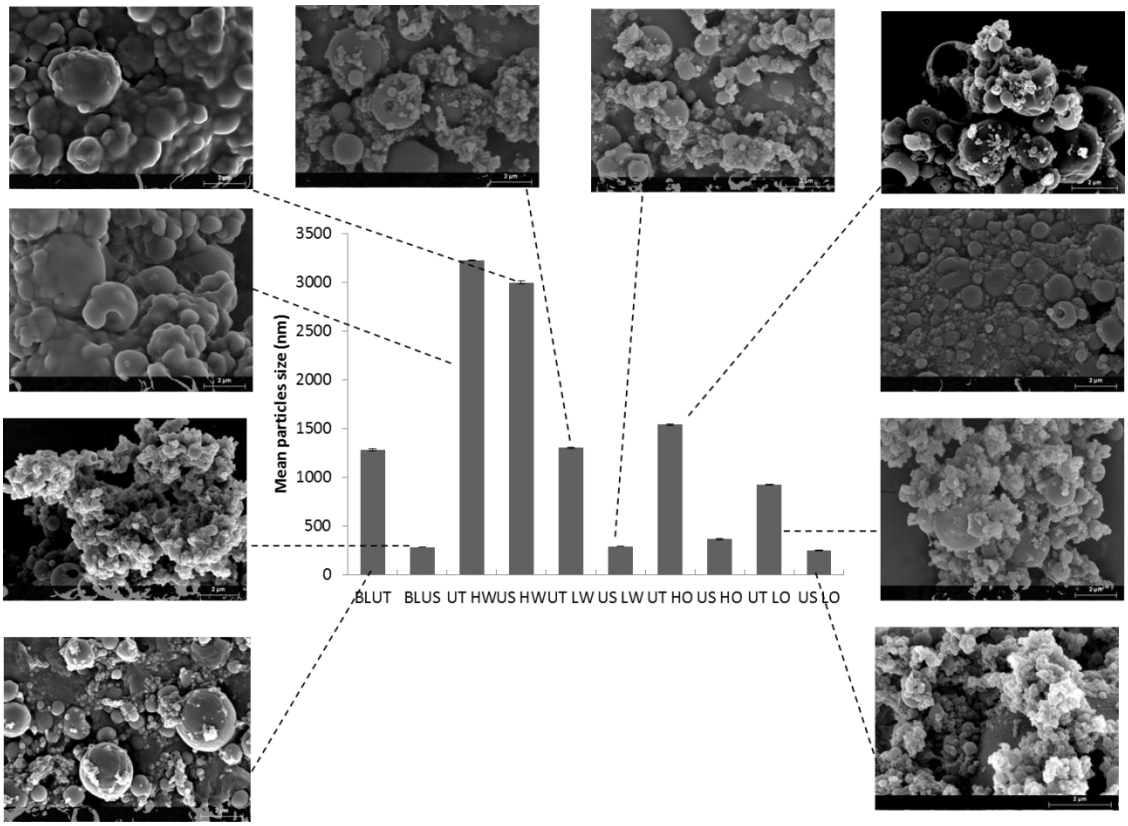

Fig. 9. 5 Average particle size and typical micrographs of BC-WPI particles obtained through emulsion electrospraying.

From Fig. 9.5 it can be seen that different material morphologies can be obtained through electro-hydrodynamic processing of emulsions depending on the homogenizing method, the type of EGCG and its addition phase. It was observed that spherical submicron and micron particles were obtained for the emulsions homogenized through both techniques.

Electrospraying of UT emulsions yield mixed heterogeneous structures combined with bigger average diameters and broader size distribution Table 9.2. On the other

hand, electrospraying of US emulsion yield proper microparticulate and homogeneous structures. For UT emulsions, their particles had the highest D_{50} (between 920 and 3200 nm), while the same emulsions produced by US, give rise to particles with smaller particle size (250 to 3000 nm, respectively). Also, the PDI follows the same trend. Small oil droplets can be enclosed and embedded more efficiently within the wall matrix of the particles. Thus, the resulted emulsion will be more stable during the electrospraying process achieving optimum structure. Therefore, it is expected that US emulsions lead to particles with the minimum particle size. In all cases, our data confirmed this trend (Fig. 9.5), which can be attributed to the lower stability of the UT emulsions as well. (Jafari et al., 2008a) reported similar results by spray drying emulsions with whey protein concentrate. They found that the particle size increased significantly with increasing emulsion size, due to instability of emulsions with bigger droplets. What is more, this difference in the D_{50} and the PDI of the particles might be explained by the greater conductivity of the US emulsions, which could destabilize the electrospraying jet, thus producing smaller particles. Finally, some other studies showed that the structure of the particles could be smoother after a heating process of the solution (Wang et al., 2016b). In our case, US emulsions have exhibited a small heating treatment with the ultrasonication, leading to smaller particle diameters.

As it can be seen from Table 9.2 and Fig. 9.5, the type of EGCG and the phase that is added play a key role on the properties of the electrosprayed particles. HW emulsions after electrospraying show signs of dripping and wetted particles. Specifically, they lead to amorphous structures combined with some particles with D_{50} up to 3.2 μm and a broad distribution (PDI = 2.3-2.9). This structure could be attributed either on the interactions between WPI and EGCG or on the properties that HW emulsions exhibit. For the first explanation, it was previously mentioned that interactions between WPI and EGCG lead to complex formation that remain in the aqueous phase. Since WPI is bounded to EGCG; there would be insufficient protein to fully cover the oil droplet surface. Thus, some of the adsorbed protein molecules on the oil droplets surfaces are likely to migrate to the air/water interface, which may lead to the coalescence of the inner oil droplets (Taneja et al., 2013) with a detrimental result in the structure of the produced particles (Wang et al., 2016b). On the other hand, for the second explanation, addition of HW leads to an increase in the viscosity of the emulsions (Fig 9.4 A). The increased viscosity subsequently increases the number of molecular entanglements in the emulsion which is reflected in the increase of the electrosprayed particle size (Neo et al., 2012). What is more, during the electrospraying process of an emulsion, in the electric field, the water droplets elongate (Opawale and Burgess, 1998) or chain along field lines, flocculate and ultimately, break (Wang and Wang, 2012). All these phenomena, increasing the conductivity so that sufficient charge builds up on the surface of the emulsion at the tip of the nozzle to produce good atomization (Wang et al., 2014). In our case, the

conductivity of the HW emulsions is low thus, resulting in amorphous electrosprayed matrices.

Regarding the particles that had been formed with LW emulsions; their structure is spherical with an average particle size in the range of 300-1300 nm. Also, some agglomeration causing the formation of bigger particles is evident in the SEM micrographs. Its particle size is insignificantly higher than the blank emulsions, indicating a good adsorption of EGCG onto the particles (Gómez-Estaca et al., 2015). The high stability, small droplet size and the high surface tension of the LW emulsions affects the structure of the LW particles.

HO emulsions give rise to particles with mean size of roughly 270-1300 nm and a PDI from 1 to 1.3. These values are similar to those of the blank emulsions. It is known that protein particles with similar sizes may differ in their morphology, flexibility, mechanical strength and other aspects (Maa et al., 1997). This observation bears an effect on the structure of the HO particles. Specifically, the surface of the particles is less smooth and some of the particles tend to partially collapse (Fig. 9.5). Particle collapse is mainly associated with the increase in the particle size with the flow rate (Gomez-Estaca et al., 2012). Taking into account the interactions between WPI and EGCG, the emulsion structure changes as more WPI molecules are adsorbed onto the oil/water interface. Consequently, the produced particles are neither smooth nor complete. What is more, the HO oil droplet size is too big to be encapsulated within the generated smaller particles, which is attributable to the particle collapse. Other studies have shown similar particle structure when they dealt with the production of gelatin-based particles containing curcumin (Gómez-Estaca et al., 2015).

When LO is added to the emulsions, the final electrosprayed particles show the smallest particle size (250-920 nm) combined with the smallest PDI values (0-5-0.6). The LO emulsions result in round and compact particles with a very smooth surface. This trend could be attributed to the properties of the emulsion. Specifically, LO emulsions showed the smallest droplet size, which therefore leads to the smallest particles. (Jafari et al., 2008a). What is more, the high stability of this emulsion indicate the presence of strong electrostatic repulsions along the oil droplets which hinder the formation of chain entanglements, thus, attaining small particles with this emulsion (Torres-Giner et al., 2008). In addition, WPI-EGCG interaction does not take place in LO samples; therefore, there are no changes in the morphology of the particles with or without EGCG (Gomez-Estaca et al., 2012). The results of the particle size of the LO emulsion are in agreement with other studies evaluating the production of particles containing WPC and lycopene (Pérez-Masiá et al., 2014).

The particle distribution of the final products is strongly influenced by the droplet size distribution of the emulsions. Fig. 9.6, the droplet and particle size distribution of selected emulsions and particles is depicted. Specifically, in Fig. 9.6 A the emulsion and their counterpart particles with the worst properties are summarized (UTHW),

while in Fig. 9.6 B the emulsion and their counterpart particles with the worst properties can be observed (USLO).

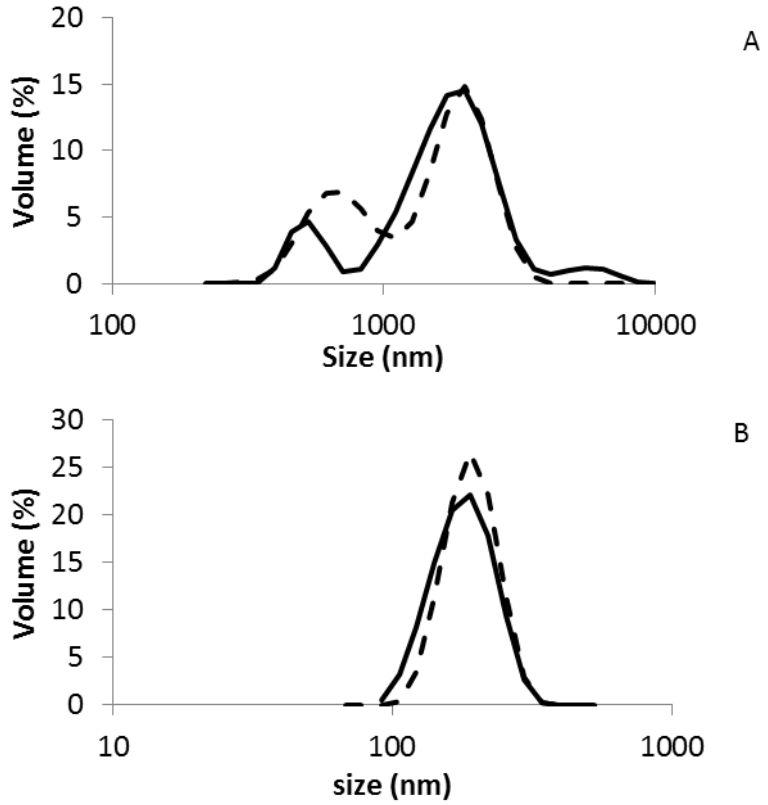

Fig. 9. 6 Droplet size distributions (solid lines) and particle size distribution (dotted lines) of the UTHW (A) and USLO (B) emulsions and particles respectively

The UTHW size distribution of the final particles is broader than the parent emulsion, indicating insufficient catechin encapsulation. A small peak around 800 nm is illustrated on the final particles distribution. It may be the result of agglomeration of some large oil droplets in the core of the particles forming a "core-sheath" structure, favored by the evaporation and jet stretching process during electrospraying (Yarin, 2011). On the other hand, the USLO size distribution of the final particles is almost identical to the parent emulsion, indicating that most of the catechin has been distributed together with the oil droplets (with similar size as in the parent emulsion) inside the particles. Other studies revealed that the final particle size incorporated into electrospinning structures is highly depended on the initial emulsion droplet size (García-Moreno et al., 2016).

Shrinkage factor (a) is also evaluated taking into account (Eq 8.1). The theoretical shrinkage factor (calculated considering the chemical composition of the dispersed phase) corresponds to 1.6, while the actual shrinkage factor varied from 0.9 to 2,

depending on the sample. These values are in agreement with other studies (Imbrogno et al., 2014; Piacentini et al., 2017).

Finally, viscosity and specifically interfacial viscosity are shown to have a key role on the structure of the particles. From Fig. 9.4B it is observed that emulsions can be divided in two groups based on their viscosity; one containing the BLUT, BLUS, UTLO and USLO emulsions and the other containing the rest (UTHW, USHW, UTLW, USLW, UTHO, USHO). This categorization is not obvious on the bulk viscosity results. Taking the interfacial viscosity groups into consideration, good correlation (Table 9.3) can be made between the interfacial viscosity values (Fig. 9.4B) and the produced particles' structure and size (Fig. 9.5).

Table 9. 3 Correlation factors from multiple variant analysis

	viscosity	interfacial viscosity	size	PDI
viscosity	-	**0.9347**	**0.8162**	**0.6843**
interfacial viscosity	**-**	**-**	**0.8325**	**0.9523**
size	**-**	**-**	**-**	**0.9237**

The pairs of variables with bold have $P < 0.05$.

Specifically, the emulsions belonging to the first group of low interfacial viscosity produce particles with small size and good uniformity. The emulsions falling into the second group of high interfacial viscosity produce either broken or amorphous particles. As a deduction, the interfacial viscosity is in better concurrence with the size and structure of the produced particles as it allows the determination of even slight variations between solutions (Palangetic et al., 2014; Pelipenko et al., 2012; Regev et al., 2010). A recent study made a correlation between the rheological properties of the chitosan-PEO blends and their electrospinability (Rošic et al., 2012). They correlated the viscosity regions with the ability of the blends to form fibers by electrospininning process. An interesting observation that they made was that interfacial viscosity gave better response in predicting the electrospinability of the solutions.

What is more, emulsions containing L-EGCG have been categorized in the group of low viscosity emulsions (Fig. 9.4B) accompanied with blank emulsions. Taking into account the results from Fig. 9.5 it can be seen that L-EGCG emulsions and blank emulsions exhibited the most homogeneous particles with the smallest sizes. This has been also reported by Pérez-Masiá et al. (2014) when dealing with electrospraying of WPC emulsions containing lycopene.

To sum up, parameters such as the size and distribution of emulsion and stability of emulsions during electrospraying influence not only the emulsion storability but also the electrospraying process. US emulsions gave rise to smooth, homogeneous particles with smaller size compared to the HO and blank sample.

9.6. Encapsulation efficiency

UV-Vis measurement was used to estimate the encapsulation efficiency (EE) of EGCG in the various electrosprayed particles and the results are summarized in Fig. 9.7.

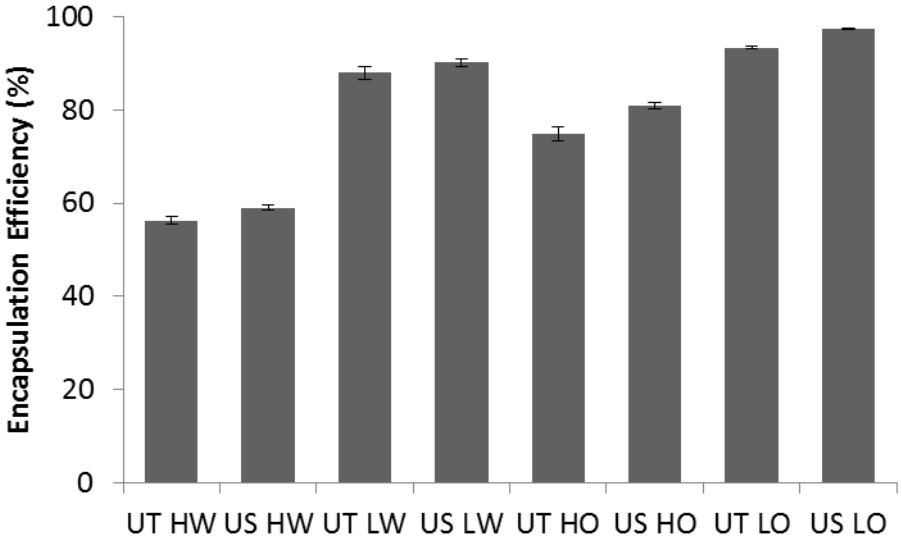

Fig. 9. 7 Encapsulation efficiency (EE) of the particles obtained by electrospraying of the different emulsions. Bars indicate standard deviation.

The EE show differences between UT and US particles, indicating that different emulsification processes affect the amount of encapsulated EGCG. Specifically, lower EE values can be seen in UT particles (56- 93%) compared to US particles (60– 97%). This could be directly related to the stability of the emulsions during the electrospraying process and to the particles diameter. In fact, UT emulsions are generally more unstable and with a more pronounced particle distribution than US, leading to particles with bigger diameters. Pérez-Masiá et al. (2014) have mentioned the decrease in EE of lycopene in emulsion-based particles when a fall of particles size was observed. It can be said that the initial structure, oil droplet size and stability of the emulsions before electrospraying have affected the EE of EGCG in a more pronounced way than the ultrasonication treatment.

What is more, the type of EGCG and the addition phase have seen to affect the EE of the produced BC-WPI particles. Concerning the EE of the HW particles, they yield the lowest values (56-59%) probably because of a great degradation of H-EGCG due to the structure of the particles and the interactions between WPI and EGCG.

Specifically, SEM micrographs (Fig. 9.5) confirm that HW emulsions after electrospraying process, lead to amorphous structures with some particles, which bears an effect on the EE of EGCG. When EGCG is extracted from HO particles, it presents an encapsulation yield around 88- 90%. It is observed that H-EGCG is poorly encapsulated in BC-WPI particles through emulsion electrospraying. This is attributed to the particle collapse, as shown in Fig. 9.5. The EE of LW particles vary from 75-81%, indicating that a higher amount of antioxidant has been encapsulated in these structures compared to HO and HW particles. Finally, the EE of LO particles is 93-97%, indicating that almost all the antioxidant was loaded within the BC-WPI particles. The EE values mentioned in this study are within the range of the results reported by studies producing structures through electrospraying or electrospinning (Aceituno-Medina et al., 2015; García-Moreno et al., 2016; Li et al., 2009; Neo et al., 2013). However, these values are considerably higher than those reported for structures obtained with other techniques (Baek et al., 2014; Edris et al., 2016; Wang et al., 2016a; Wang et al., 2016b). This could be explained taking into account the absence of thermal treatment or partitioning effects when using electrospraying as an encapsulation technique.

9.7. Catechin stability during various storage conditions

Dissolution in aqueous solutions with different pH, thermal treatments as well as storage in different humidities are commonly employed in the food processing industry to study the stability of the product and its properties. Hence, the stability of EGCG-encapsulated matrices under the various conditions is crucial to assess their stability. In this study, the stability of EGCG in all the produced particles combined with the raw H- or L-EGCG is studied after storing the samples under different conditions (Fig 9.8). In Fig 9.8A the stability of EGCG in the particles that showed the best EE (USLO) is depicted, expressed as the percentage of the initial amount of EGCG found in the particles, during 30 days of storage. In Fig. 9.8.B the stability of pure L-EGCG is shown, expressed as the percentage of the initial amount of EGCG found in the particles, during 30 days of storage.

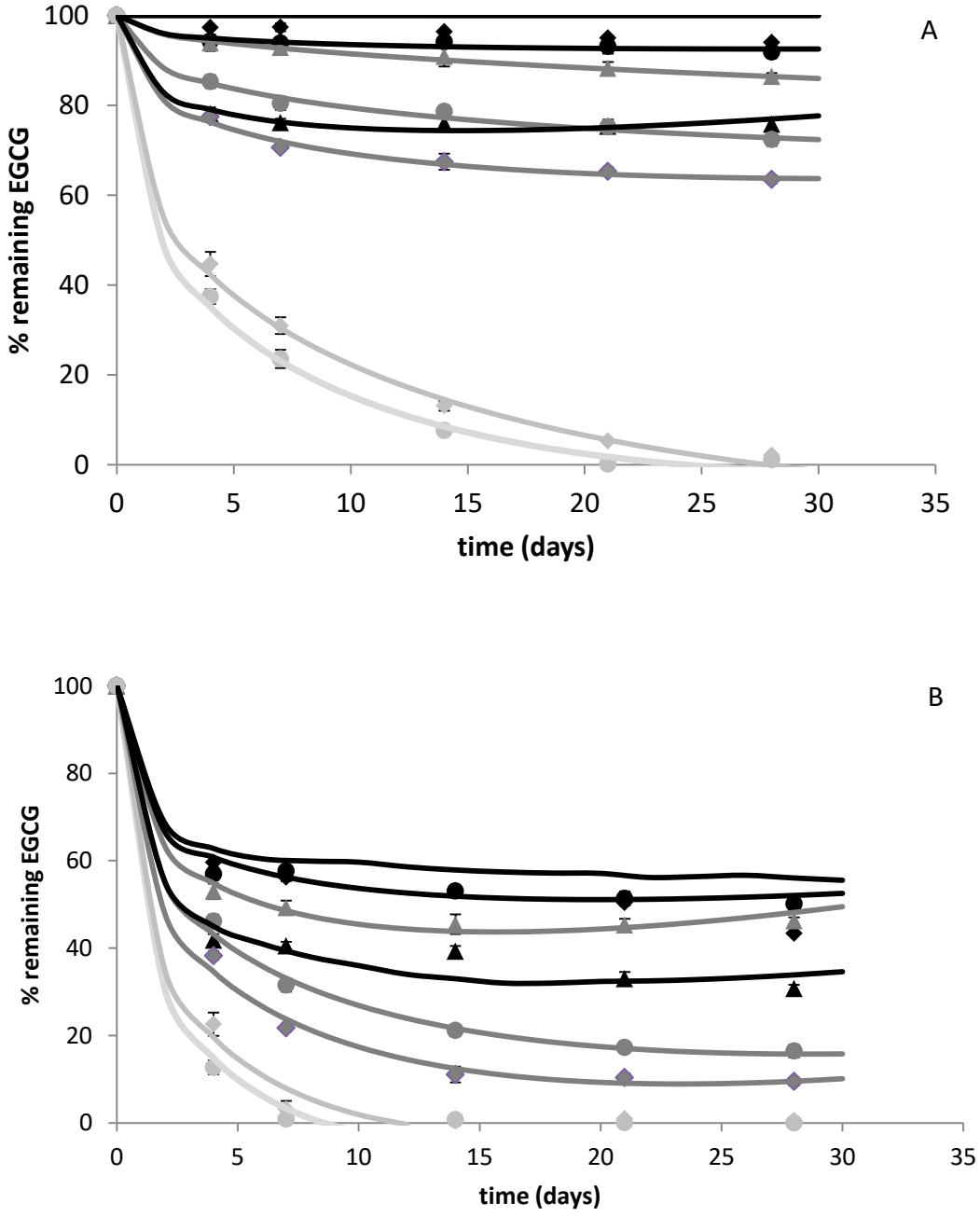

Fig. 9. 8 Stability of L-EGCG after being encapsulated in USLO (A) and pure L-EGCG (B) stored at various conditions; RH=26% (◆), RH=53% (●), RH=75% (▲),pH 3 (◆), pH 6 (●), pH 9 (▲), T=37 °C (◆) and T=60 °C (●). Bars indicate standard deviation.

From Fig. 9.8 it can be summarized that the stability of EGCG within the particles shows a different behavior depending on the storage conditions. As far as the storage in different humidities is concerned, by increasing the RH, a decrease in the stability of EGCG occurred. Specifically, an increase in RH from 26 to 53 up to 75%, result in a decrease in the remaining EGCG in the USLO particles from 94 to 92 to

roughly 76%. Therefore, in all cases, EGCG deteriorates faster under high RH and is more stable under low humidity content (RH=23%). For other lipophilic bioactives (orange oil), it has also been indicated that the optimum storage conditions are at low RH (Anker and Reineccius, 1988). When the particles are exposed to higher RH, they tend to collapse probably due to high solubility of BC in water (Aceituno-Medina et al., 2013). This easily diffusion of water into the particles, enhances the hydrolysis or other degradation reactions, thereby decreasing the stability of the encapsulated compounds. In addition, EGCG is known to exhibit higher stability in lower RH (Li et al., 2011).

It was seen that for particles dissolved in solutions, the pH played a significant role on the stability of the catechin after 30 days of storage. Specifically, acidic conditions (pH=3) showed the lowest remaining EGCG in the particles (63%). On the other side, encapsulation provide a great EGCG stability during storage time under neutral and basic conditions, reaching to values of remaining EGCG up to 72% for pH=6 and 86% for pH=9. Recent studies also found greater extent of degradation in ω-3-containing oleosomes at acidic pH than at neutral pH, supporting our results (Kapchie et al., 2013). These data could lead to the assumption that the produced particles could be effectively incorporated into food products with neutral pH, such as dairy products.

Regarding the EGCG stability upon high temperature exposure, it is seen that non-encapsulated EGCG is completely degraded after 7 days at 37^{o} C or 4 days at 60^{o} C. In contrast, the electrosprayed particles are able to significantly reduce the EGCG degradation, as in this case the bioactive is completely degraded after 25 days at 37^{o} C or 20 days at 60^{o} C. It is known that thermal treatment amounts to decrease the raw EGCG (Li et al., 2013). What is more, increasing the storage temperature from 37 to 60^{o} C, lead to faster degradation kinetics for the EGCG, as expected. It is well documented that EGCG is epimerized when exposed at high temperature, leading to the conversion to its corresponding isomers (GCG) and, ultimately, to the particle degradation (Ananingsih et al., 2013; Wang et al., 2008b). These results are in agreement with studies evaluating the stability of omega-3 fatty acid on electrosprayed zein particles (Torres-Giner et al., 2010). It is worth noting that all the other particles, exhibited the same trend, regarding the EGCG stability, as the presenting particles.

Table 9.4 depicts the EGCG kinetic constants for the Peppas- Sahlin equations at the different storage conditions for selected representative particles. The first observation is that k_1 constant show higher values than k_2 in all the electrosprayed particles, which is attributable to the diffusion which is the dominant mechanism on the particles. Similar behavior has been reported for other spherical carriers (Siepmann and Peppas, 2001). When the particles are stored at low humidity contents, the kinetic constants are almost zero. Specifically, the catechin degradation

is well fitted to a zero-order degradation model, assuming that the degradation is almost independent of the concentration.

Higher values of the kinetic constants indicate a much faster release of the antioxidant. Specifically, kinetic constants for the different particles seem to have the same trend as the EE results. For instance, UTLO particles stored at 26% RH show EE= 93%, k_1= 0.04 and k_2= -0.0036, while the USLO particles stored at the same conditions show EE=97%, k_1= 0.014 and k_2= 0.000012. This phenomenon is in accordance with studies modelling the kinetics of antioxidants (Gómez-Mascaraque et al., 2016; Spizzirri et al., 2013). If comparing the k_1, k_2 values of the same particles in different storage conditions, it is clear that the higher the values of the constants, the faster the release in the different conditions. For instance, USLO particles stored at 26% RH show k_1= 0.014 and k_2= 0.000012, while when the same particles are stored at 75% RH show k_1= 161 and k_2= -25. The Peppas- Sahlin model also confirms the faster EGCG release kinetics from the UT particles rather than US particles, which could partially be attributed to their larger particle size, besides the poorer properties of their parent emulsion. For instance, USLO particles stored at 53% RH show k_1= 35 and k_2= -4, while UTLO particles stored at the same conditions show k_1= 456 and k_2= -6.

One more point to add is the fact that k_1 values decrease with the increase of pH, indicating that the Fickian contribution also decreases. Especially, USLO particles stored at pH =3 show k_1= 164, while when the same particles stored at pH=9 show k_1= 30. Consequently, the contribution of Fickian diffusion to EGCG release is small, while both Fickian diffusion and relaxation controlled transport contribute to EGCG release from BC-WPI particles. This trend is consistent with other studies dealing with particles as encapsulants (Soares et al. 2002).

Table 9. 4 Release kinetic parameters (k_1, k_2) of the different electrosprayed particles.

Storage conditions	Kinetic parameters	H-EGCG	L-EGCG	UTHW	USHW	UTLW	USLW	UTHO	USHO	UTLO	USLO
RH= 26%	k_1	0.078 (0.003)	0.119 (0.004)	0.455 (0.008)	0.425 (0.009)	0.073 (0.001)	0.067 (0.001)	0.167 (0.036)	0.142 (0.013)	0.038 (0.006)	0.013 (0.006)
	k_2	-0.0015 (0.0001)	-0.0086 (0.0001)	-0.0736 (0.0021)	-0.0671 (0.0037)	-0.0093 (0.0002)	-0.0098 (0.0001)	-0.0235 (0.0011)	-0.0176 (0.0047)	-0.0035 (0.0004)	0.0001 (0.0000)
RH= 53%.	k_1	168 (2)	214 (5)	468 (11)	456 (8)	112 (14)	80 (3)	215 (17)	191 (4)	456 (8)	35 (5)
	k_2	-2 (0)	-29 (2)	-70 (3)	-72 (3)	-16 (4)	-10 (1)	-30 (2)	-29 (1)	-6 (0)	-4 (0)
RH= 75%	k_1	321 (6)	319 (8)	564 (10)	540 (19)	181 (3)	210 (4)	300 (5)	264 (6)	170 (4)	161 (2)
	k_2	-50 (2)	-44 (3)	-88 (3)	-85 (3)	-23 (1)	-30 (1)	--45 (2)	-42 (3)	-24 (3)	-25 (1)
pH= 3	k_1	395 (14)	470 (4)	556 (10)	546[c] (8)	201 (3)	242 (3)	362 (30)	330 (10)	192 (3)	164 (9)
	k_2	-42 (1)	-60(4)	-78 (3)	-75 (2)	-20 (1)	-30 (1)	-44 (1)	-41 (2)	-23 (1)	-18 (1)
pH= 6	k_1	346 (12)	398 (34)	502 (11)	502 (37)	212 (22)	171 (25)	340 (5)	287 (6)	148 (16)	96 (2)
	k_2	-35 (1)	-47 (2)	-76 (4)	-79 (2)	-30 (1)	-22 (1)	-44 (2)	-36 (2)	-17 (1)	-8 (1)
pH= 9	k_1	339 (7)	344 (3)	503 (9)	478 (9)	118 (2)	132 (3)	300 (4)	220 (2)	77 (2)	30 (1)
	k_2	-48 (2)	-52 (1)	-78 (3)	-76 (5)	-11 (0)	-20 (1)	-41 (1)	-27 (1)	-8 (0)	0.5 (0)
T= 37° C	k_1	578 (6)	605 (7)	638 (6)	594 (4)	477 (4)	459 (3)	521 (8)	540 (10)	434 (3)	377 (8)
	k_2	-82 (3)	-89 (2)	-98(2)	-87(1)	-58(2)	-53 (1)	-68 (1)	-73 (2)	-46 (3)	-33 (1)

T= 60^{o} C	k_1	613 (7)	654 (8)	634 (8)	600(8)	510 (3)	493 (1)	580 (5)	534 (3)	470 (2)	455 (4)
	k_2	-91 (2)	-102 (2)	-97 (3)	-88 (2)	-65 (1)	-61 (1)	-83 (2)	-71 (1)	-55 (1)	-48 (1)

In parenthesis standard deviation values.

R^2 varied between 0.9801-0.997).

9.8. Conclusions

Emulsions containing whey protein isolate (WPI), bacterial cellulose (BC) and extra virgin olive oil were developed either by ultraturrax (UT) or ultrasounds (US) and processed by the emulsion electrospraying technique. Two different catechins: hydrophilic (H-EGCG) or lipophilized (L-EGCG) were incorporated in the aqueous or the oil phase of the emulsions. All the emulsions produced particles with mean sizes in the submicron range, except HW that resulted in an amorphous matrix probably due to the complex formation between WPI and EGCG. Emulsion electrospraying showed promising results for EGCG encapsulation, especially when using US as an homogenization method, as it produced more stable emulsions with smaller oil droplet sizes and lower viscosity. The EE showed differences between samples (56-97%), indicating that nature of EGCG, the addition phase and the emulsifying method could induce variability of the results in the amount of encapsulated EGCG. The homogenization method (UT or US) had a significant influence on the properties of the particles and on the stability of the bioactive. L-EGCG showed the best encapsulation efficiencies and stability during storage. All in all, WPI-BC sub-micron particles protected EGCG from moisture, heating, and dissolution conditions, leading to the potential use of them as a substitute in order to enhance EGCG shelf life when incorporated within various food products.

Chapter 10. Conclusions and further work

In this thesis the production of emulsions and nanostructures for the encapsulation of catechins was explored. The main thickener in emulsions or encapsulation used was Bacterial Cellulose (BC). The key objectives are summarized below:

- Design a processing method as a pre-treatment in order to improve the physical properties of BC fibrils (Chapter 4).
- Evaluate the homogenizing method that results in the production of o/w emulsions with enhanced physical properties (Chapter 5 and 6).
- Study the role of BC as a stabilizer and as a thickener in o/w emulsions and the potential substitution of commercial thickeners (Chapter 5 and 6).
- Encapsulation of catechins in i) emulsions, ii) nanoparticles derived from biopolymer solution, and iii) nanoparticles derived from emulsion (Chapter 7, 8, and 9).

The main results and conclusion of this study are addressed below:

Physical properties of BC aqueous suspensions

- Ultrasonic processing or acid hydrolysis treatment was applied into BC aqueous suspensions in various processing conditions.
- Ultrasound treatment (1 min/ 15 kJ) reduces the dimensions of BC fibrils and the viscosity while improves stability.
- Acid hydrolysis with H_2SO_4 at 60^{o} C for 72 h decreases more the dimensions of BC fibrils while improves stability.
- Acid hydrolysis with H_2SO_4 at 60^{o} C for 72 h results in suspensions with lower viscosity and stability compared to the suspensions treated by ultrasounds.

Selection of the most suitable homogenization method

- Whey protein isolate (WPI) - BC emulsions were successfully produced.
- Homogenization with high shear mixer results in emulsions with lower stability and higher droplet sizes compared to the ultrasounds.
- US homogenization has greater efficiency as compared to the high pressure homogenization in obtaining stable emulsions.

BC as a stabilizer or thickener

- BC shows better emulsifying capability compared to commercial celluloses (HPMC, CMC).

- BC contributes towards the production of stable to coalescence o/w emulsions for long periods of time.
- BC acts as a particle stabilizer, like Pickering emulsions, on the oil/water interface.
- BC has the ability to thicken the aqueous phase of the emulsions.
- The viscosity profile of the BC emulsions showed three regions, including two shear thinning regions separated by a constant viscosity plateau (Newtonian).
- BC can act as alternative thickener as it has the ability to increase the yield stress compared to commercially-used thickeners (Xanthan gum, locust bean gum).

Encapsulation of catechins

- Two different catechins: hydrophilic (H-EGCG) or lipophilized (L-EGCG) were encapsulated in the aqueous or the oil phase of the emulsions or in the biopolymer solution.
- WPI-BC emulsions with EGCG were successfully produced.
- At optimized EGCG concentrations the highest encapsulation efficiency values of 85 ± 2% with reasonable droplet diameter of 680 ± 10 nm and 0% serum index can be achieved for the emulsions incorporating L-EGCGC in the oil phase.
- EGCG forms complexes with WPI hindering the stability of the emulsions.
- L-EGCG is more efficient in obtaining emulsions with enhanced oxidative stability as compared to the H-EGCG.
- WPI-BC solutions with EGCG were processed with electrospraying technique and successfully resulted in EGCG-loaded nanoparticles.
- The encapsulation efficiency of EGCG yields low values.
- WPI-BC emulsions with EGCG were processed with electrospraying technique and successfully resulted in EGCG-loaded nanoparticles.
- The encapsulation efficiency of EGCG using emulsions yields high values.
- Particles produced through emulsion electrospraying are protecting EGCG from pH, temperature and relative humidity.

To sum up, Table 10.1 summarizes the optimal carriers for hydrophilic EGCGC (H-EGCG).

Table 10. 1 Comparison of H-EGCG carriers.

	WPI-BC emulsion	**Particles from solution**	**Particles from emulsion**
Composition	5% wt WPI 1% wt BC 10% wt olive oil (US)	20% wt WPI 8% wt BC 5% wt Tween	20% wt WPI 8% wt BC 10% wt olive oil (US)
H-EGCG	Oil phase	Aqueous phase	Oil phase
D_{50}(nm)	560	-	270
SI (%)	0.8	-	0
Surface tension (mN/m)	-	32	32
El. conductivity (mS/m)	-	3.3	2.2
Viscosity (mPas for 1,5 s^{-1} shear rate)	6.2	0.7	0.55
Particle size (nm)	-	202	368
EE (%)	60	51	81
EE after 1 month of storage (%)	30	40	69

The WPI-BC emulsion homogenized by ultrasounds results in encapsulation efficiencies up to 60%, while the WPI-BC solution after electrospraying yields lower values (51%). The emulsion after electrospraying yields not only the highest efficiencies up to 81% but also the optimum physical properties.

Table 10.2 summarizes the optimal carriers independent from the type of EGCG.

Table 10. 2 Comparison of optimal carriers.

	WPI-BC emulsion	**Particles from solution**	**Particles from emulsion**
Composition	5% wt WPI 1% wt BC 10% wt olive oil (US)	20% wt WPI 8% wt BC 5% wt Tween	20% wt WPI 8% wt BC 10% wt olive oil (US)
EGCG	L-EGCG/ Oil phase	H-EGCG/ queous phase	L-EGCG/ Oil phase
D_{50}(nm)	531	-	206
SI (%)	0.8	-	0
Surface tension (mN/m)	-	32	39.8
El. conductivity (mS/m)	-	3.3	2.9
Viscosity (mPas for 1,5 s^{-1} shear rate)	5.9	0.7	0.08
Particle size (nm)	-	202	253
EE (%)	80	51	97
EE after 1 month of storage (%)	67	40	91

The WPI-BC emulsion homogenized by ultrasounds results in encapsulation efficiencies up to 80%, while the WPI-BC solution after electrospraying yields lower values (51%). The emulsion after electrospraying yields not only the highest efficiencies up to 97% but also the optimum physical properties.

This section aims to highlight areas which justify further potential research based on the conclusions developed from this study.

- BC is an innovative thickener and in this study it was shown that it can replace commercial thickeners in emulsions and dressings. It would be interesting to incorporate BC in other food products, such as yogurt, cheese, sausages, mix for soups, ect.
- In this study, the complexes that are formed between EGCG and protein have hindered the encapsulation efficiency of EGCG in the emulsions. Research towards the minimization of this effect is of utmost importance.
- Electrospinning is an emerging technology not widely used in the food industry. It is beneficial to know the ability of other food grade polysaccharides and other sensitive compounds (colorants, bioactives, and vitamins) to be electrosprayed.

References

Abismaïl, B., Canselier, J.P., Wilhelm, A.M., Delmas, H., Gourdon, C., (1999). Emulsification by ultrasound: drop size distribution and stability. Ultrasonics Sonochemistry 6(1–2), 75-83.

Abu-Ali, J., Barringer, S.A., (2005). Method for electrostatic atomization of emulsions in an EHD system. Journal of Electrostatics 63(5), 361-369.

Aceituno-Medina, M., Mendoza, S., Lagaron, J.M., López-Rubio, A., (2013). Development and characterization of food-grade electrospun fibers from amaranth protein and pullulan blends. Food Research International 54(1), 667-674.

Aceituno-Medina, M., Mendoza, S., Rodríguez, B.A., Lagaron, J.M., López-Rubio, A., (2015). Improved antioxidant capacity of quercetin and ferulic acid during in-vitro digestion through encapsulation within food-grade electrospun fibers. Journal of Functional Foods 12, 332-341.

Adeyeye, C., J.A., M., G.M.K., J., R.W., (2002). Viscoelastic evaluation of topical creams containing microcrystalline cellulose/ sodium carboxymethyl cellulose as stabilizer. AAPS PharmSciTech 3(2), 16-25.

Agoda-Tandjawa, G., Durand, S., Berot, S., Blassel, C., Gaillard, C., Garnier, C., Doublier, J.L., (2010). Rheological characterization of microfibrillated cellulose suspensions after freezing. Carbohydrate Polymers 80(3), 677-686.

Almajano, M.P., Carbo, R., Delgado, M.E., Gordon, M.H., (2007a). Effect of pH on the antimicrobial activity and oxidative stability of oil-in-water emulsions containing caffeic acid. J Food Sci 72(5), C258-263.

Almajano, M.P., Delgado, M.E., Gordon, M.H., (2007b). Changes in the antioxidant properties of protein solutions in the presence of epigallocatechin gallate. Food Chemistry 101(1), 126-130.

Ananingsih, V.K., Sharma, A., Zhou, W., (2013). Green tea catechins during food processing and storage: A review on stability and detection. Food Research International 50(2), 469-479.

Andresen, M., Stenius, P., (2007). Water-in-oil emulsions stabilized by hydrophobized microfibrillated cellulose. Journal of Dispersion Science and Technology 28(6), 837-844.

Angeles, M., Cheng, H.-L., Velankar, S.S., (2008). Emulsion electrospinning: composite fibers from drop breakup during electrospinning. Polymers for Advanced Technologies 19(7), 728-733.

Angellier, H., Putaux, J.-L., Molina-Boisseau, S., Dupeyre, D., Dufresne, A., (2005). Starch Nanocrystal Fillers in an Acrylic Polymer Matrix. Macromolecular Symposia 221(1), 95-104.

Anker, M.H., Reineccius, G.A., (1988). Encapsulated Orange Oil, *Flavor Encapsulation*. American Chemical Society, pp. 78-86.

Anton, F., (1934). Process and apparatus for preparing artificial threads. Google Patents.

Anu Bhushani, J., Anandharamakrishnan, C., (2014). Electrospinning and electrospraying techniques: Potential food based applications. Trends in Food Science and Technology 38(1), 21-33.

Araki, J., Wada, M., Kuga, S., Okano, T., (1998). Flow properties of microcrystalline cellulose suspension prepared by acid treatment of native cellulose. Colloids and Surfaces A: Physicochemical and Engineering Aspects 142(1), 75-82.

Arancibia, C., Bayarri, S., Costell, E., (2013). Comparing Carboxymethyl Cellulose and Starch as Thickeners in Oil/Water Emulsions. Implications on Rheological and Structural Properties. Food Biophysics 8(2), 122-136.

Arts, I.C., Hollman, P.C., (2005). Polyphenols and disease risk in epidemiologic studies. Am J Clin Nutr 81(1 Suppl), 317s-325s.

Aryee, A.N.A., Boye, J.I., (2014). Current and Emerging Trends in the Formulation and Manufacture of Nutraceuticals and Functional Food Products, *Nutraceutical and Functional Food Processing Technology*. John Wiley & Sons, Ltd, pp. 1-63.

Arzeni, C., Martínez, K., Zema, P., Arias, A., Pérez, O.E., Pilosof, A.M.R., (2012). Comparative study of high intensity ultrasound effects on food proteins functionality. Journal of Food Engineering 108(3), 463-472.

Augustin, M.A., Hemar, Y., (2009). Nano- and micro-structured assemblies for encapsulation of food ingredients. Chem Soc Rev 38(4), 902-912.

Azizi Samir, M.A.S., Alloin, F., Dufresne, A., (2005). Review of Recent Research into Cellulosic Whiskers, Their Properties and Their Application in Nanocomposite Field. Biomacromolecules 6(2), 612-626.

Baek, I.-h., Kim, J.-S., Ha, E.-S., Choo, G.-H., Cho, W., Hwang, S.-J., Kim, M.-S., (2014). Oral absorption of a valsartan-loaded spray-dried emulsion based on hydroxypropylmethyl cellulose. International Journal of Biological Macromolecules 69, 222-228.

Barhate, R.S., Loong, C.K., Ramakrishna, S., (2006). Preparation and characterization of nanofibrous filtering media. Journal of Membrane Science 283(1–2), 209-218.

Barnes, H.A., (1994). Rheology of emulsions — a review. Colloids and Surfaces A: Physicochemical and Engineering Aspects 91, 89-95.

Barnes, H.A., (1997). Thixotropy—a review. Journal of Non-Newtonian Fluid Mechanics 70(1–2), 1-33.

Barrero, A., Loscertales, I.G., (2007). Micro- and Nanoparticles via Capillary Flows. Annual Review of Fluid Mechanics 39(1), 89-106.

Baxter, S., Zivanovic, S., Weiss, J., (2005). Molecular weight and degree of acetylation of high-intensity ultrasonicated chitosan. Food Hydrocolloids 19(5), 821-830.

Bender, N., Portmann, M., Heg, Z., Hofmann, K., Zwahlen, M., Egger, M., (2014). Fish or n3-PUFA intake and body composition: a systematic review and meta-analysis. Obesity reviews 15(8), 657-665.

Bhardwaj, N., Kundu, S.C., (2010). Electrospinning: A fascinating fiber fabrication technique. Biotechnology Advances 28(3), 325-347.

Bock, N., Dargaville, T.R., Woodruff, M.A., (2012). Electrospraying of polymers with therapeutic molecules: State of the art. Progress in Polymer Science 37(11), 1510-1551.

Bodin, A., Bäckdahl, H., Petersen, N., Gatenholm, P., (2011). Bacterial Cellulose as Biomaterial, in: Ducheyne, P. (Ed.), *Comprehensive Biomaterials*. Elsevier, Oxford, pp. 405-410.

Bondeson, D., Mathew, A., Oksman, K., (2006). Optimization of the isolation of nanocrystals from microcrystalline celluloseby acid hydrolysis. Cellulose 13(2), 171.

Bouwmeester, H., Dekkers, S., Noordam, M.Y., Hagens, W.I., Bulder, A.S., de Heer, C., ten Voorde, S.E., Wijnhoven, S.W., Marvin, H.J., Sips, A.J., (2009). Review of health safety aspects of nanotechnologies in food production. Regul Toxicol Pharmacol 53(1), 52-62.

Buchko, C.J., Chen, L.C., Shen, Y., Martin, D.C., (1999). Processing and microstructural characterization of porous biocompatible protein polymer thin films. Polymer 40(26), 7397-7407.

Calligaris, S., Plazzotta, S., Bot, F., Grasselli, S., Malchiodi, A., Anese, M., (2016). Nanoemulsion preparation by combining high pressure homogenization and high power ultrasound at low energy densities. Food Research International 83, 25-30.

Camerlo, A., Bühlmann-Popa, A.-M., Vebert-Nardin, C., Rossi, R.M., Fortunato, G., (2014). Environmentally controlled emulsion electrospinning for the encapsulation of temperature-sensitive compounds. Journal of Materials Science 49(23), 8154-8162.

Camino, N.A., Pilosof, A.M.R., (2011). Hydroxypropylmethylcellulose at the oil–water interface. Part II. Submicron-emulsions as affected by pH. Food Hydrocolloids 25(5), 1051-1062.

Camino, N.A., Sanchez, C.C., Rodríguez Patino, J.M., Pilosof, A.M.R., (2012). Hydroxypropylmethylcellulose–β-lactoglobulin mixtures at the oil–water interface. Bulk, interfacial and emulsification behavior as affected by pH. Food Hydrocolloids 27(2), 464-474.

Camino, N.A., Sánchez, C.C., Rodríguez Patino, J.M., Pilosof, A.M.R., (2011). Hydroxypropylmethylcellulose at the oil–water interface. Part I. Bulk behaviour and dynamic adsorption as affected by pH. Food Hydrocolloids 25(1), 1-11.

Canselier, J.P., Delmas, H., Wilhelm, A.M., Abismaïl, B., (2002). Ultrasound Emulsification—An Overview. Journal of Dispersion Science and Technology 23(1-3), 333-349.

Cao, L., Luo, J., Tu, K., Wang, L.Q., Jiang, H., (2014). Generation of nano-sized core-shell particles using a coaxial tri-capillary electrospray-template removal method. Colloids Surf B Biointerfaces 115, 212-218.

Carlson, C., Hussain, S.M., Schrand, A.M., K. Braydich-Stolle, L., Hess, K.L., Jones, R.L., Schlager, J.J., (2008). Unique Cellular Interaction of Silver Nanoparticles: Size-Dependent Generation of Reactive Oxygen Species. The Journal of Physical Chemistry B 112(43), 13608-13619.

Casper, C.L., Stephens, J.S., Tassi, N.G., Chase, D.B., Rabolt, J.F., (2004). Controlling Surface Morphology of Electrospun Polystyrene Fibers: Effect of Humidity and Molecular Weight in the Electrospinning Process. Macromolecules 37(2), 573-578.

Chakraborty, S., Liao, I.C., Adler, A., Leong, K.W., (2009). Electrohydrodynamics: A facile technique to fabricate drug delivery systems. Advanced Drug Delivery Reviews 61(12), 1043-1054.

Chan, P.T., Fong, W.P., Cheung, Y.L., Huang, Y., Ho, W.K., Chen, Z.Y., (1999). Jasmine green tea epicatechins are hypolipidemic in hamsters (Mesocricetus auratus) fed a high fat diet. J Nutr 129(6), 1094-1101.

Chanamai, R., McClements, D.J., (2000). Creaming Stability of Flocculated Monodisperse Oil-in-Water Emulsions. J Colloid Interface Sci 225(1), 214-218.

Chaobo, H., Shuiliang, C., Chuilin, L., Darrell , H.R., Haiyan, Q., Ying, Y., Haoqing, H., (2006). Electrospun polymer nanofibres with small diameters. Nanotechnology 17(6), 1558.

Charernsriwilaiwat, N., Opanasopit, P., Rojanarata, T., Ngawhirunpat, T., Supaphol, P., (2010). Preparation and characterization of chitosan-hydroxybenzotriazole/polyvinyl alcohol blend nanofibers by the electrospinning technique. Carbohydrate Polymers 81(3), 675-680.

Charlton, A.J., Baxter, N.J., Khan, M.L., Moir, A.J., Haslam, E., Davies, A.P., Williamson, M.P., (2002). Polyphenol/peptide binding and precipitation. J Agric Food Chem 50(6), 1593-1601.

Chau, C.-F., Wu, S.-H., Yen, G.-C., (2007). The development of regulations for food nanotechnology. Trends in Food Science & Technology 18(5), 269-280.

Chaudhry, Q., Scotter, M., Blackburn, J., Ross, B., Boxall, A., Castle, L., Aitken, R., Watkins, R., (2008). Applications and implications of nanotechnologies for the food sector. Food Addit Contam Part A Chem Anal Control Expo Risk Assess 25(3), 241-258.

Chellaram, C., Murugaboopathi, G., John, A.A., Sivakumar, R., Ganesan, S., Krithika, S., Priya, G., (2014). Significance of Nanotechnology in Food Industry. APCBEE Procedia 8, 109-113.

Chemat, F., Zill e, H., Khan, M.K., (2011). Applications of ultrasound in food technology: Processing, preservation and extraction. Ultrasonics Sonochemistry 18(4), 813-835.

Chen, H.-M., Yu, D.-G., (2010). An elevated temperature electrospinning process for preparing acyclovir-loaded PAN ultrafine fibers. Journal of Materials Processing Technology 210(12), 1551-1555.

Chen, Z.P., Schell, J.B., Ho, C.T., Chen, K.Y., (1998). Green tea epigallocatechin gallate shows a pronounced growth inhibitory effect on cancerous cells but not on their normal counterparts. Cancer Lett 129(2), 173-179.

Chevalier, Y., Bolzinger, M.-A., (2013). Emulsions stabilized with solid nanoparticles: Pickering emulsions. Colloids and Surfaces A: Physicochemical and Engineering Aspects 439(0), 23-34.

Chime, S.A., Kenechukwu, F.C., Attama, A.A., (2014). *Nanoemulsions — Advances in Formulation, Characterization and Applications in Drug Delivery, Application of Nanotechnology in Drug Delivery*. InTech, Croatia.

Cho, S.S., Almeida, N., (2012). *Dietary fiber and health*. CRC Press.

Cobb, M.D., Macoubrie, J., (2004). Public perceptions about nanotechnology: Risks, benefits and trust. Journal of Nanoparticle Research 6(4), 395-405.

Cooley, J.F., (1902). Apparatus for electrically dispersing fluids. Google Patents.

Corley, E.A., Scheufele, D.A., Hu, Q., (2009). Of risks and regulations: how leading U.S. nanoscientists form policy stances about nanotechnology. Journal of Nanoparticle Research 11(7), 1573-1585.

Cushen, M., Kerry, J., Morris, M., Cruz-Romero, M., Cummins, E., (2012). Nanotechnologies in the food industry – Recent developments, risks and regulation. Trends in Food Science & Technology 24(1), 30-46.

Dai, J., Mumper, R.J., (2010). Plant phenolics: extraction, analysis and their antioxidant and anticancer properties. Molecules 15(10), 7313-7352.

Date, A.A., Desai, N., Dixit, R., Nagarsenker, M., (2010). Self-nanoemulsifying drug delivery systems: formulation insights, applications and advances. Nanomedicine (Lond) 5(10), 1595-1616.

de Freitas Zompero, R.H., Lopez-Rubio, A., de Pinho, S.C., Lagaron, J.M., de la Torre, L.G., (2015). Hybrid encapsulation structures based on beta-carotene-loaded nanoliposomes within electrospun fibers. Colloids Surf B Biointerfaces 134, 475-482.

de Lima, R., Feitosa, L.O., Maruyama, C.R., Barga, M.A., Yamawaki, P.C., Vieira, I.J., Teixeira, E.M., Corrêa, A.C., Mattoso, L.H.C., Fraceto, L.F., (2012). Evaluation of the genotoxicity of cellulose nanofibers. International Journal of Nanomedicine 7, 3555-3565.

Dehnad, D., Emam-Djomeh, Z., Mirzaei, H., Jafari, S.-M., Dadashi, S., (2014). Optimization of physical and mechanical properties for chitosan–nanocellulose biocomposites. Carbohydrate Polymers 105, 222-228.

Deitzel, J.M., Kleinmeyer, J., Harris, D., Beck Tan, N.C., (2001). The effect of processing variables on the morphology of electrospun nanofibers and textiles. Polymer 42(1), 261-272.

Deladino, L., Anbinder, P.S., Navarro, A.S., Martino, M.N., (2008). Encapsulation of natural antioxidants extracted from Ilex paraguariensis. Carbohydrate Polymers 71(1), 126-134.

Demir, M.M., Yilgor, I., Yilgor, E., Erman, B., (2002). Electrospinning of polyurethane fibers. Polymer 43(11), 3303-3309

Desai, K.G.H., Jin Park, H., (2005). Recent Developments in Microencapsulation of Food Ingredients. Drying Technology 23(7), 1361-1394.

Dewettinck, K., Deroo, L., Messens, W., Huyghebaert, A., (1998). Agglomeration Tendency during Top-Spray Fluidized Bed Coating with Gums. LWT - Food Science and Technology 31(6), 576-584.

Di Mattia, C.D., Sacchetti, G., Mastrocola, D., Pittia, P., (2009). Effect of phenolic antioxidants on the dispersion state and chemical stability of olive oil O/W emulsions. Food Research International 42(8), 1163-1170.

Dickinson, E., (1992). An Introduction to Food Colloids. . 36(5), 514-514.

Dickinson, E., (2009). Hydrocolloids as emulsifiers and emulsion stabilizers. Food Hydrocolloids 23(6), 1473-1482.

Dickinson, E., (2011). Mixed biopolymers at interfaces: Competitive adsorption and multilayer structures. Food Hydrocolloids 25(8), 1966-1983.

Dickinson, E., Ritzoulis, C., (2000). Creaming and Rheology of Oil-in-Water Emulsions Containing Sodium Dodecyl Sulfate and Sodium Caseinate. J Colloid Interface Sci 224(1), 148-154.

Doshi, J., Reneker, D.H., (1995). Electrospinning process and applications of electrospun fibers. Journal of Electrostatics 35(2), 151-160.

Drosou, C.G., Krokida, M.K., Biliaderis, C.G., (2017). Encapsulation of bioactive compounds through electrospinning/electrospraying and spray drying: A comparative assessment of food-related applications. Drying Technology 35(2), 139-162.

Dubeau, S., Samson, G., Tajmir-Riahi, H.-A., (2010). Dual effect of milk on the antioxidant capacity of green, Darjeeling, and English breakfast teas. Food Chemistry 122(3), 539-545.

Dumay, E., Chevalier-Lucia, D., Picart-Palmade, L., Benzaria, A., Gràcia-Julià, A., Blayo, C., (2013). Technological aspects and potential applications of (ultra) high-pressure homogenisation. Trends in Food Science & Technology 31(1), 13-26.

Edge, R., McGarvey, D., Truscott, T., (1997). The carotenoids as anti-oxidants—a review. Journal of Photochemistry and Photobiology B: Biology 41(3), 189-200.

Edris, A.E., Kalemba, D., Adamiec, J., Piatkowski, M., (2016). Microencapsulation of Nigella sativa oleoresin by spray drying for food and nutraceutical applications. Food Chem 204, 326-333.

Efsa Panel on Dietetic Products, N., Allergies, (2011). Guidance on the scientific requirements for health claims related to antioxidants, oxidative damage and cardiovascular health. EFSA Journal 9(12), 2474-n/a.

Eltayeb, M., Bakhshi, P.K., Stride, E., Edirisinghe, M., (2013). Preparation of solid lipid nanoparticles containing active compound by electrohydrodynamic spraying. Food Research International 53(1), 88-95.

Esfanjani, A.F., Jafari, S.M., Assadpoor, E., Mohammadi, A., (2015). Nano-encapsulation of saffron extract through double-layered multiple emulsions of pectin and whey protein concentrate. Journal of Food Engineering 165, 149-155.

Everett, D.W., McLeod, R.E., (2005). Interactions of polysaccharide stabilisers with casein aggregates in stirred skim-milk yoghurt. International Dairy Journal 15(11), 1175-1183.

Fang, Z., Bhandari, B., (2010). Encapsulation of polyphenols – a review. Trends in Food Science & Technology 21(10), 510-523.

Floury, J., Desrumaux, A., Legrand, J., (2002). Effect of Ultra-high-pressure Homogenization on Structure and on Rheological Properties of Soy Protein-stabilized Emulsions. Journal of Food Science 67(9), 3388-3395.

Foegeding, E.A., Davis, J.P., Doucet, D., McGuffey, M.K., (2002). Advances in modifying and understanding whey protein functionality. Trends in Food Science & Technology 13(5), 151-159.

Freeman, J., (1996). Rheological Methods in Food Process Engineering. Freeman Press, 418.

Freitas, S., Hielscher, G., Merkle, H.P., Gander, B., (2006). Continuous contact- and contamination-free ultrasonic emulsification—a useful tool for pharmaceutical development and production. Ultrasonics Sonochemistry 13(1), 76-85.

Fu, L., Zhang, J., Yang, G., (2013). Present status and applications of bacterial cellulose-based materials for skin tissue repair. Carbohydrate Polymers 92(2), 1432-1442.

Fu, N., Zhou, Z., Jones, T.B., Tan, T.T.Y., Wu, W.D., Lin, S.X., Chen, X.D., Chan, P.P.Y., (2011). Production of monodisperse epigallocatechin gallate (EGCG) microparticles by spray drying for high antioxidant activity retention. Int J Pharm 413(1–2), 155-166.

Futamura, T., Kawaguchi, M., (2012). Characterization of paraffin oil emulsions stabilized by hydroxypropyl methylcellulose. Journal of Colloid and Interface Science 367(1), 55-60.

Gadkari, P.V., Balaraman, M., (2015a). Catechins: Sources, extraction and encapsulation: A review. Food and Bioproducts Processing 93, 122-138.

Gadkari, P.V., Balaraman, M., (2015b). Extraction of catechins from decaffeinated green tea for development of nanoemulsion using palm oil and sunflower oil based lipid carrier systems. Journal of Food Engineering 147(C), 14-23.

García-Moreno, P.J., Stephansen, K., van der Kruijs, J., Guadix, A., Guadix, E.M., Chronakis, I.S., Jacobsen, C., (2016). Encapsulation of fish oil in nanofibers by emulsion electrospinning: Physical characterization and oxidative stability. Journal of Food Engineering 183, 39-49.

Gaskell, G., Eyck, T.T., Jackson, J., Veltri, G., (2005). Imagining nanotechnology: cultural support for technological innovation in Europe and the United States. Public Understanding of Science 14(1), 81-90.

Genser, B., Silbernagel, G., De Backer, G., Bruckert, E., Carmena, R., Chapman, M.J., Deanfield, J., Descamps, O.S., Rietzschel, E.R., Dias, K.C., (2012). Plant sterols and cardiovascular disease: a systematic review and meta-analysis. European heart journal 33(4), 444-451.

Gharsallaoui, A., Roudaut, G., Chambin, O., Voilley, A., Saurel, R., (2007). Applications of spray-drying in microencapsulation of food ingredients: An overview. Food Research International 40(9), 1107-1121.

Ghorani, B., Tucker, N., (2015). Fundamentals of electrospinning as a novel delivery vehicle for bioactive compounds in food nanotechnology. Food Hydrocolloids 51, 227-240.

Gomez-Estaca, J., Balaguer, M.P., Gavara, R., Hernandez-Munoz, P., (2012). Formation of zein nanoparticles by electrohydrodynamic atomization: Effect of the main processing variables and suitability for encapsulating the food coloring and active ingredient curcumin. Food Hydrocolloids 28(1), 82-91.

Gómez-Estaca, J., Gavara, R., Hernández-Muñoz, P., (2015). Encapsulation of curcumin in electrosprayed gelatin microspheres enhances its bioaccessibility and widens its uses in food applications. Innovative Food Science & Emerging Technologies 29, 302-307.

Gómez-Mascaraque, L.G., Lagarón, J.M., López-Rubio, A., (2015). Electrosprayed gelatin submicroparticles as edible carriers for the encapsulation of polyphenols of interest in functional foods. Food Hydrocolloids 49, 42-52.

Gomez-Mascaraque, L.G., Lopez-Rubio, A., (2016). Protein-based emulsion electrosprayed micro- and submicroparticles for the encapsulation and stabilization of thermosensitive hydrophobic bioactives. J Colloid Interface Sci 465, 259-270.

Gomez-Mascaraque, L.G., Morfin, R.C., Pérez-Masiá, R., Sanchez, G., Lopez-Rubio, A., (2016). Optimization of electrospraying conditions for the microencapsulation of probiotics and evaluation of their resistance during storage and in-vitro digestion. LWT - Food Science and Technology 69, 438-446.

Gómez-Mascaraque, L.G., Soler, C., Lopez-Rubio, A., (2016). Stability and bioaccessibility of EGCG within edible micro-hydrogels. Chitosan vs. gelatin, a comparative study. Food Hydrocolloids 61, 128-138.

Gordon, V., Marom, G., Magdassi, S., (2015). Formation of hydrophilic nanofibers from nanoemulsions through electrospinning. Int J Pharm 478(1), 172-179.

Gouin, S., (2004). Microencapsulation: industrial appraisal of existing technologies and trends. Trends in Food Science & Technology 15(7–8), 330-347.

Gulseren, I., Guzey, D., Bruce, B.D., Weiss, J., (2007). Structural and functional changes in ultrasonicated bovine serum albumin solutions. Ultrason Sonochem 14(2), 173-183.

Guo, J., Catchmark, J.M., (2012). Surface area and porosity of acid hydrolyzed cellulose nanowhiskers and cellulose produced by Gluconacetobacter xylinus. Carbohydrate Polymers 87(2), 1026-1037.

Gupta, P., Elkins, C., Long, T.E., Wilkes, G.L., (2005). Electrospinning of linear homopolymers of poly(methyl methacrylate): exploring relationships between fiber

formation, viscosity, molecular weight and concentration in a good solvent. Polymer 46(13), 4799-4810.

Guzey, D., McClements, D.J., (2006). Characterization of β-lactoglobulin–chitosan interactions in aqueous solutions: A calorimetry, light scattering, electrophoretic mobility and solubility study. Food Hydrocolloids 20(1), 124-131.

Habibi, Y., Lucia, L.A., Rojas, O.J., (2010). Cellulose Nanocrystals: Chemistry, Self-Assembly, and Applications. Chemical Reviews 110(6), 3479-3500.

Haghi, A.K., Akbari, M., (2007). Trends in electrospinning of natural nanofibers. physica status solidi (a) 204(6), 1830-1834.

Håkansson, A., Fuchs, L., Innings, F., Revstedt, J., Trägårdh, C., Bergenståhl, B., (2011). High resolution experimental measurement of turbulent flow field in a high pressure homogenizer model and its implications on turbulent drop fragmentation. Chemical Engineering Science 66(8), 1790-1801.

Han, J., Britten, M., St-Gelais, D., Champagne, C.P., Fustier, P., Salmieri, S., Lacroix, M., (2011). Polyphenolic compounds as functional ingredients in cheese. Food Chemistry 124(4), 1589-1594.

Hart, E.J., Henglein, A., (1985). Free radical and free atom reactions in the sonolysis of aqueous iodide and formate solutions. The Journal of Physical Chemistry 89(20), 4342-4347.

Haslam, E., (1996). Natural Polyphenols (Vegetable Tannins) as Drugs: Possible Modes of Action. Journal of Natural Products 59(2), 205-215.

Hayati, I., Man, Y.B.C., Tan, C.P., Aini, N., (2009). Droplet characterization and stability of soybean oil/ palm kernel olein o/w emulsions with the presence of selected polysaccharides. Food Hydrocolloids 23, 233-243.

Henry, J.V.L., Fryer, P.J., Frith, W.J., Norton, I.T., (2009). Emulsification mechanism and storage instabilities of hydrocarbon-in-water sub-micron emulsions stabilised with Tweens (20 and 80), Brij 96v and sucrose monoesters. Journal of Colloid and Interface Science 338(1), 201-206.

Henry, J.V.L., Fryer, P.J., Frith, W.J., Norton, I.T., (2010). The influence of phospholipids and food proteins on the size and stability of model sub-micron emulsions. Food Hydrocolloids 24(1), 66-71.

Hestrin, S., Schramm, M., (1954). Synthesis of cellulose by Acetobacter xylinum. II. Preparation of freeze-dried cells capable of polymerizing glucose to cellulose. Biochemical Journal 58(2), 345-352.

Higuchi, T., (1961). Rate of release of medicaments from ointment bases containing drugs in suspension. Journal of Pharmaceutical Sciences 50(10), 874-875.

Hirai, A., Inui, O., Horii, F., Tsuji, M., (2009). Phase Separation Behavior in Aqueous Suspensions of Bacterial Cellulose Nanocrystals Prepared by Sulfuric Acid Treatment. Langmuir 25(1), 497-502.

Hong, Y., Li, Y., Yin, Y., Li, D., Zou, G., (2008). Electrohydrodynamic atomization of quasi-monodisperse drug-loaded spherical/wrinkled microparticles. Journal of Aerosol Science 39(6), 525-536.

Hoshiyama, Y., Kawaguchi, T., Miura, Y., Mizoue, T., Tokui, N., Yatsuya, H., Sakata, K., Kondo, T., Kikuchi, S., Toyoshima, H., Hayakawa, N., Tamakoshi, A., Ohno, Y., Yoshimura, T., (2004). A nested case-control study of stomach cancer in relation to green tea consumption in Japan. Br J Cancer 90(1), 135-138.

Hsu, C.H., Tsai, T.H., Kao, Y.H., Hwang, K.C., Tseng, T.Y., Chou, P., (2008). Effect of green tea extract on obese women: a randomized, double-blind, placebo-controlled clinical trial. Clin Nutr 27(3), 363-370.

Huang, X., Kakuda, Y., Cui, W., (2001). Hydrocolloids in emulsions: particle size distribution and interfacial activity. Food Hydrocolloids 15(4–6), 533-542.

Huang, Z.-M., Zhang, Y.Z., Kotaki, M., Ramakrishna, S., (2003). A review on polymer nanofibers by electrospinning and their applications in nanocomposites. Composites Science and Technology 63(15), 2223-2253.

Ide, R., Fujino, Y., Hoshiyama, Y., Mizoue, T., Kubo, T., Pham, T.M., Shirane, K., Tokui, N., Sakata, K., Tamakoshi, A., Yoshimura, T., (2007). A prospective study of green tea consumption and oral cancer incidence in Japan. Ann Epidemiol 17(10), 821-826.

Iguchi, Yamanaka, Budhiono, (2000). Bacterial cellulose — A masterpiece of nature's arts. Journal of Materials Science 35, 261-270.

Imbrogno, A., Piacentini, E., Drioli, E., Giorno, L., (2014). Micro and nano polycaprolactone particles preparation by pulsed back-and-forward cross-flow batch membrane emulsification for parenteral administration. Int J Pharm 477(1-2), 344-350.

Innings, F., Trägårdh, C., (2007). Analysis of the flow field in a high-pressure homogenizer. Experimental Thermal and Fluid Science 32(2), 345-354.

Iotti, M., Gregersen, O.W., Moe, S., Lenes, M., (2011). Rheological Studies of Microfibrillar Cellulose Water Dispersions. Journal of Polymers and the Environment 19(1), 137-145.

IUPAC, (1997). *Compendium of Chemical Terminology*. Blackwell Scientific Publications, Oxford.

Jafari, S., He, Y., Bhandari, B., (2006). Nano-Emulsion Production by Sonication and Microfluidization—A Comparison. International Journal of Food Properties 9(3), 475-485.

Jafari, S.M., Assadpoor, E., Bhandari, B., He, Y., (2008a). Nano-particle encapsulation of fish oil by spray drying. Food Research International 41(2), 172-183.

Jafari, S.M., Assadpoor, E., He, Y., Bhandari, B., (2008b). Re-coalescence of emulsion droplets during high-energy emulsification. Food Hydrocolloids 22(7), 1191-1202.

Jafari, S.M., He, Y., Bhandari, B., (2007). Production of sub-micron emulsions by ultrasound and microfluidization techniques. Journal of Food Engineering 82(4), 478-488.

Jambrak, A.R., Lelas, V., Mason, T.J., Krešić, G., Badanjak, M., (2009). Physical properties of ultrasound treated soy proteins. Journal of Food Engineering 93(4), 386-393.

Jambrak, A.R., Mason, T.J., Lelas, V., Herceg, Z., Herceg, I.L., (2008). Effect of ultrasound treatment on solubility and foaming properties of whey protein suspensions. Journal of Food Engineering 86(2), 281-287.

Jaworek, A., Krupa, A., (1999). CLASSIFICATION OF THE MODES OF EHD SPRAYING. Journal of Aerosol Science 30(7), 873-893.

Jaworek, A., Sobczyk, A.T., (2008). Electrospraying route to nanotechnology: An overview. Journal of Electrostatics 66(3–4), 197-219.

Jayasinghe, S.N., Edirisinghe, M.J., (2004). Electrostatic atomisation of a ceramic suspension. Journal of the European Ceramic Society 24(8), 2203-2213.

Jia, X., Xu, R., Shen, W., Xie, M., Abid, M., Jabbar, S., Wang, P., Zeng, X., Wu, T., (2015). Stabilizing oil-in-water emulsion with amorphous cellulose. Food Hydrocolloids 43(0), 275-282.

Jia, Z., Dumont, M.-J., Orsat, V., (2016). Encapsulation of phenolic compounds present in plants using protein matrices. Food Bioscience 15, 87-104.

Jo, C., Son, J.H., Son, C.B., Byun, M.W., (2003). Functional properties of raw and cooked pork patties with added irradiated, freeze-dried green tea leaf extract powder during storage at 4 °C. Meat Science 64(1), 13-17.

Jo, Y.-J., Kwon, Y.-J., (2014). Characterization of β-carotene nanoemulsions prepared by microfluidization technique. Food Science and Biotechnology 23(1), 107-113.

Johnell, O., Gullberg, B., Kanis, J.A., Allander, E., Elffors, L., Dequeker, J., Dilsen, G., Gennari, C., Lopes Vaz, A., Lyritis, G., et al., (1995). Risk factors for hip fracture in European women: the MEDOS Study. Mediterranean Osteoporosis Study. J Bone Miner Res 10(11), 1802-1815.

Joye, I.J., McClements, D.J., (2014). Biopolymer-based nanoparticles and microparticles: Fabrication, characterization, and application. Current Opinion in Colloid & Interface Science 19(5), 417-427.

Kalashnikova, I., Bizot, H., Cathala, B., Capron, I., (2011). New Pickering Emulsions Stabilized by Bacterial Cellulose Nanocrystals. Langmuir 27(12), 7471-7479.

Kalra, E.K., (2003). Nutraceutical--definition and introduction. AAPS PharmSci 5(3), E25.

Kaltsa, O., Gatsi, I., Yanniotis, S., Mandala, I., (2014a). Influence of Ultrasonication Parameters on Physical Characteristics of Olive Oil Model Emulsions Containing Xanthan. Food and Bioprocess Technology 7(7), 2038-2049.

Kaltsa, O., Michon, C., Yanniotis, S., Mandala, I., (2013). Ultrasonic energy input influence on the production of sub-micron o/w emulsions containing whey protein and common stabilizers. Ultrasonics Sonochemistry 20(3), 881-891.

Kaltsa, O., Paximada, P., Mandala, I., Scholten, E., (2014b). Physical characteristics of submicron emulsions upon partial displacement of whey protein by a small molecular weight surfactant and pectin addition. Food Research International 66(0), 401-408.

Kaltsa, O., Yanniotis, S., Mandala, I., (2016). Stability properties of different fenugreek galactomannans in emulsions prepared by high-shear and ultrasonic method. Food Hydrocolloids 52, 487-496.

Kamogawa, K., Okudaira, G., Matsumoto, M., Sakai, T., Sakai, H., Abe, M., (2004). Preparation of Oleic Acid/Water Emulsions in Surfactant-Free Condition by

Sequential Processing Using Midsonic–Megasonic Waves. Langmuir 20(6), 2043-2047.

Kanakis, C.D., Hasni, I., Bourassa, P., Tarantilis, P.A., Polissiou, M.G., Tajmir-Riahi, H.A., (2011). Milk beta-lactoglobulin complexes with tea polyphenols. Food Chem 127(3), 1046-1055.

Kanis, J., Johnell, O., Gullberg, B., Allander, E., Elffors, L., Ranstam, J., Dequeker, J., Dilsen, G., Gennari, C., Vaz, A.L., Lyritis, G., Mazzuoli, G., Miravet, L., Passeri, M., Perez Cano, R., Rapado, A., Ribot, C., (1999). Risk factors for hip fracture in men from southern Europe: the MEDOS study. Mediterranean Osteoporosis Study. Osteoporos Int 9(1), 45-54.

Kapchie, V.N., Yao, L., Hauck, C.C., Wang, T., Murphy, P.A., (2013). Oxidative stability of soybean oil in oleosomes as affected by pH and iron. Food Chemistry 141(3), 2286-2293.

Karaosmanoglu, H., Kilmartin, P.A., (2015). 9 - Tea extracts as antioxidants for food preservation A2 - Shahidi, Fereidoon, *Handbook of Antioxidants for Food Preservation*. Woodhead Publishing, pp. 219-233.

Karbstein, H., Schubert, H., (1995). Developments in the continuous mechanical production of oil-in-water macro-emulsions. Chemical Engineering and Processing: Process Intensification 34(3), 205-211.

Karppinen, A., Saarinen, T., Salmela, J., Laukkanen, A., Nuopponen, M., Seppala, J., (2012). Flocculation of microfibrillated cellulose in shear flow. Cellulose 19(6), 1807-1819.

Kayaci, F., Uyar, T., (2012). Encapsulation of vanillin/cyclodextrin inclusion complex in electrospun polyvinyl alcohol (PVA) nanowebs: Prolonged shelf-life and high temperature stability of vanillin. Food Chemistry 133(3), 641-649.

Kentish, S., Wooster, T.J., Ashokkumar, M., Balachandran, S., Mawson, R., Simons, L., (2008). The use of ultrasonics for nanoemulsion preparation. Innovative Food Science & Emerging Technologies 9(2), 170-175.

Khan, M.K.I., Maan, A.A., Schutyser, M., Schroën, K., Boom, R., (2013). Electrospraying of water in oil emulsions for thin film coating. Journal of Food Engineering 119(4), 776-780.

Khan, N., Mukhtar, H., (2007). Tea polyphenols for health promotion. Life sciences 81(7), 519-533.

Khouryieh, H., Puli, G., Williams, K., Aramouni, F., (2015). Effects of xanthan–locust bean gum mixtures on the physicochemical properties and oxidative stability of whey protein stabilised oil-in-water emulsions. Food Chemistry 167(0), 340-348.

Kiatyongchai, T., Wongsasulak, S., Yoovidhya, T., (2014). Coaxial electrospinning and release characteristics of cellulose acetate–gelatin blend encapsulating a model drug. Journal of Applied Polymer Science 131(8), n/a-n/a.

Kim, Y.J., Park, J.H., Kim, M.H., Kim, S.B., Hwang, S.H., Lee, Y.M., (2012). Sweetener composition for preventing and improving obesity, containing glycolysis inhibitor ingredient. Google Patents.

Klemm, D., Heublein, B., Fink, H.P., Bohn, A., (2005). Cellulose: fascinating biopolymer and sustainable raw material. Angew Chem Int Ed Engl 44(22), 3358-3393.

Koo, S.Y., Cha, K.H., Song, D.-G., Chung, D., Pan, C.-H., (2014). Microencapsulation of peppermint oil in an alginate–pectin matrix using a coaxial electrospray system. International Journal of Food Science & Technology 49(3), 733-739.

Kriegel, C., Kit, K.M., McClements, D.J., Weiss, J., (2009). Electrospinning of chitosan–poly(ethylene oxide) blend nanofibers in the presence of micellar surfactant solutions. Polymer 50(1), 189-200.

Kroll, J., uuml, rgen, Rawel, H.M., Rohn, S., (2003). Reactions of Plant Phenolics with Food Proteins and Enzymes under Special Consideration of Covalent Bonds. Food Science and Technology Research 9(3), 205-218.

Kuijk, A., Koppert, R., Versluis, P., van Dalen, G., Remijn, C., Hazekamp, J., Nijsse, J., Velikov, K.P., (2013). Dispersions of Attractive Semiflexible Fiberlike Colloidal Particles from Bacterial Cellulose Microfibrils. Langmuir 29(47), 14356-14360.

Kunzek, H., Opel, H., Senge, B., (1997). Rheological examination of material with cellular structure II. Creep and oscillation measurements of apple material with cellular structure. Zeitschrift für Lebensmitteluntersuchung und -Forschung A 205(3), 193-203.

Kuriyama, S., (2008). The relation between green tea consumption and cardiovascular disease as evidenced by epidemiological studies. J Nutr 138(8), 1548s-1553s.

Labuckas, D.O., Maestri, D.M., Perelló, M., Martínez, M.L., Lamarque, A.L., (2008). Phenolics from walnut (Juglans regia L.) kernels: Antioxidant activity and interactions with proteins. Food Chemistry 107(2), 607-612.

Laine, P., Kylli, P., Heinonen, M., Jouppila, K., (2008). Storage stability of microencapsulated cloudberry (Rubus chamaemorus) phenolics. J Agric Food Chem 56(23), 11251-11261.

Lakenbrink, C., Lapczynski, S., Maiwald, B., Engelhardt, U.H., (2000). Flavonoids and other polyphenols in consumer brews of tea and other caffeinated beverages. J Agric Food Chem 48(7), 2848-2852.

Lavelli, V., Vantaggi, C., Corey, M., Kerr, W., (2010). Formulation of a dry green tea-apple product: study on antioxidant and color stability. J Food Sci 75(2), C184-190.

Lee, C.M., Sams, G.W., Wagner, J.P., (2001). Power consumption measurements for ac and pulsed dc for electrostatic coalescence of water-in-oil emulsions. Journal of Electrostatics 53(1), 1-24.

Lee, L., Hancocks, R., Noble, I., Norton, I.T., (2014). Production of water-in-oil nanoemulsions using high pressure homogenisation: A study on droplet break-up. Journal of Food Engineering 131, 33-37.

Lee, L., Norton, I.T., (2013). Comparing droplet breakup for a high-pressure valve homogeniser and a Microfluidizer for the potential production of food-grade nanoemulsions. Journal of Food Engineering 114(2), 158-163.

Lefebvre, J., (1982). Viscosity of concentrated protein solutions. Rheologica Acta 21(4), 620-625.

Leong, T.S., Wooster, T.J., Kentish, S.E., Ashokkumar, M., (2009). Minimising oil droplet size using ultrasonic emulsification. Ultrason Sonochem 16(6), 721-727.

Li, M.K., Fogler, H.S., (2006). Acoustic emulsification. Part 1. The instability of the oil-water interface to form the initial droplets. Journal of Fluid Mechanics 88(3), 499-511.

Li, N., Taylor, L.S., Ferruzzi, M.G., Mauer, L.J., (2013). Color and chemical stability of tea polyphenol (−)-epigallocatechin-3-gallate in solution and solid states. Food Research International 53(2), 909-921.

Li, N., Taylor, L.S., Mauer, L.J., (2011). Degradation kinetics of catechins in green tea powder: effects of temperature and relative humidity. J Agric Food Chem 59(11), 6082-6090.

Li, Y., Lim, L.T., Kakuda, Y., (2009). Electrospun zein fibers as carriers to stabilize (-)-epigallocatechin gallate. J Food Sci 74(3), C233-240.

Lian, W.-C., Hsiao, H.-C., Chou, C.-C., (2002). Survival of bifidobacteria after spray-drying. International Journal of Food Microbiology 74(1–2), 79-86.

Liedtke, S., Wissing, S., Muller, R.H., Mader, K., (2000). Influence of high pressure homogenisation equipment on nanodispersions characteristics. Int J Pharm 196(2), 183-185.

Lin, D., Li, R., Lopez-Sanchez, P., Li, Z., (2015a). Physical properties of bacterial cellulose aqueous suspensions treated by high pressure homogenizer. Food Hydrocolloids(0).

Lin, D., Li, R., Lopez-Sanchez, P., Li, Z., (2015b). Physical properties of bacterial cellulose aqueous suspensions treated by high pressure homogenizer. Food Hydrocolloids 44, 435-442.

Lin, Y., Yao, Y., Yang, X., Wei, N., Li, X., Gong, P., Li, R., Wu, D., (2008). Preparation of poly(ether sulfone) nanofibers by gas-jet/electrospinning. Journal of Applied Polymer Science 107(2), 909-917.

Liu, F., Antoniou, J., Li, Y., Majeed, H., Liang, R., Ma, Y., Ma, J., Zhong, F., (2016). Chitosan/sulfobutylether-β-cyclodextrin nanoparticles as a potential approach for tea polyphenol encapsulation. Food Hydrocolloids 57, 291-300.

Liu, L., Zhao, Q., Liu, T., Kong, J., Long, Z., Zhao, M., (2012). Sodium caseinate/carboxymethylcellulose interactions at oil–water interface: Relationship to emulsion stability. Food Chemistry 132(4), 1822-1829.

Liu, T.T., Yang, T.S., (2008). Effects of water-soluble natural antioxidants on photosensitized oxidation of conjugated linoleic acid in an oil-in-water emulsion system. J Food Sci 73(4), C256-261.

Long, Z., Zhao, Q., Liu, T., Kuang, W., Xu, J., Zhao, M., (2013). Influence of xanthan gum on physical characteristics of sodium caseinate solutions and emulsions. Food Hydrocolloids 32(1), 123-129.

López-Rubio, A., Lagaron, J.M., (2012). Whey protein capsules obtained through electrospraying for the encapsulation of bioactives. Innovative Food Science & Emerging Technologies 13, 200-206.

López-Rubio, A., Sanchez, E., Wilkanowicz, S., Sanz, Y., Lagaron, J.M., (2012). Electrospinning as a useful technique for the encapsulation of living bifidobacteria in food hydrocolloids. Food Hydrocolloids 28(1), 159-167.

Lu, D., Yang, Y., Li, Y., Sun, C., (2015). Analysis of tocopherols and tocotrienols in pharmaceuticals and foods: a critical review. Current Pharmaceutical Analysis 11(1), 66-78.

Lu, T.-M., Lee, C.-C., Mau, J.-L., Lin, S.-D., (2010). Quality and antioxidant property of green tea sponge cake. Food Chemistry 119(3), 1090-1095.

Luo, C.J., Loh, S., Stride, E., Edirisinghe, M., (2012). Electrospraying and Electrospinning of Chocolate Suspensions. Food and Bioprocess Technology 5(6), 2285-2300.

Maa, Y.-F., Costantino, H.R., Nguyen, P.-A., Hsu, C.C., (1997). The Effect of Operating and Formulation Variables on the Morphology of Spray-Dried Protein Particles. Pharmaceutical Development and Technology 2(3), 213-223.

Madene, A., Jacquot, M., Scher, J., Desobry, S., (2006). Flavour encapsulation and controlled release – a review. International Journal of Food Science & Technology 41(1), 1-21.

Makino, K., Mossoba, M.M., Riesz, P., (1983). Chemical effects of ultrasound on aqueous solutions. Formation of hydroxyl radicals and hydrogen atoms. The Journal of Physical Chemistry 87(8), 1369-1377.

Mandala, I.G., Savvas, T.P., Kostaropoulos, A.E., (2004). Xanthan and locust bean gum influence on the rheology and structure of a white model-sauce. Journal of Food Engineering 64(3), 335-342.

Martinez-Sanz, M., Lopez-Rubio, A., Lagaron, J.M., (2011). Optimization of the nanofabrication by acid hydrolysis of bacterial cellulose nanowhiskers. Carbohydrate Polymers 85(1), 228-236.

Matos, M., Gutiérrez, G., Iglesias, O., Coca, J., Pazos, C., (2015). Enhancing encapsulation efficiency of food-grade double emulsions containing resveratrol or vitamin B12 by membrane emulsification. Journal of Food Engineering 166, 212-220.

McClements, D.J., (2004). Protein-stabilized emulsions. Current Opinion in Colloid & Interface Science 9(5), 305-313.

McClements, D.J., (2005). Food Emulsions: Principles, Practice and Techniques. Boca Raton, CRC Press.

McClements, D.J., (2006). Non-covalent interactions between proteins and polysaccharides. Biotechnology Advances 24(6), 621-625.

McClements, D.J., (2011). Edible nanoemulsions: fabrication, properties, and functional performance. Soft Matter 7(6), 2297-2316.

McClements, D.J., Decker, E.A., Weiss, J., (2007). Emulsion-based delivery systems for lipophilic bioactive components. J Food Sci 72(8), R109-124.

Meftahi, R., K., A., R., M., S., E., Y.M., M., T., (2010). The effects of cotton gauze coating with microbial cellulose. Cellulose 17(1), 199-204.

Megelski, S., Stephens, J.S., Chase, D.B., Rabolt, J.F., (2002). Micro- and Nanostructured Surface Morphology on Electrospun Polymer Fibers. Macromolecules 35(22), 8456-8466.

Mehnert, W., Mäder, K., (2001). Solid lipid nanoparticles: Production, characterization and applications. Advanced Drug Delivery Reviews 47(2–3), 165-196.

Mei, L., McClements, D.J., Wu, J., Decker, E.A., (1998). Iron-catalyzed lipid oxidation in emulsion as affected by surfactant, pH and NaCl. Food Chemistry 61(3), 307-312.

Miura, Y., Chiba, T., Miura, S., Tomita, I., Umegaki, K., Ikeda, M., Tomita, T., (2000). Green tea polyphenols (flavan 3-ols) prevent oxidative modification of low density lipoproteins: an ex vivo study in humans. The Journal of Nutritional Biochemistry 11(4), 216-222.

Moon, R.J., Martini, A., Nairn, J., Simonsen, J., Youngblood, J., (2011). Cellulose nanomaterials review: structure, properties and nanocomposites. Chemical Society Reviews 40(7), 3941-3994.

Moschakis, T., Murray, B.S., Dickinson, E., (2005). Microstructural evolution of viscoelastic emulsions stabilised by sodium caseinate and xanthan gum. Journal of Colloid Interface Science 284(2), 714-728.

Mulaudzi, R.B., Ndhlala, A.R., Kulkarni, M.G., Van Staden, J., (2012). Pharmacological properties and protein binding capacity of phenolic extracts of some Venda medicinal plants used against cough and fever. J Ethnopharmacol 143(1), 185-193.

Munir, M.M., Suryamas, A.B., Iskandar, F., Okuyama, K., (2009). Scaling law on particle-to-fiber formation during electrospinning. Polymer 50(20), 4935-4943.

Munro, I.C., Haighton, L.A., Lynch, B.S., Tafazoli, S., (2009). Technological challenges of addressing new and more complex migrating products from novel food packaging materials. Food Addit Contam Part A Chem Anal Control Expo Risk Assess 26(12), 1534-1546.

Muraki, S., Yamamoto, S., Ishibashi, H., Oka, H., Yoshimura, N., Kawaguchi, H., Nakamura, K., (2007). Diet and lifestyle associated with increased bone mineral density: cross-sectional study of Japanese elderly women at an osteoporosis outpatient clinic. J Orthop Sci 12(4), 317-320.

Naczk, M., Oickle, D., Pink, D., Shahidi, F., (1996). Protein Precipitating Capacity of Crude Canola Tannins: Effect of pH, Tannin, and Protein Concentrations. Journal of Agricultural and Food Chemistry 44(8), 2144-2148.

Naderi, A., Lindstrom, T., Sundstrom, J., (2014). Carboxymethylated nanofibrillated cellulose: rheological studies. Cellulose 21(3), 1561-1571.

Nagao, T., Hase, T., Tokimitsu, I., (2007). A green tea extract high in catechins reduces body fat and cardiovascular risks in humans. Obesity (Silver Spring) 15(6),

1473-1483.

Neethirajan, S., Jayas, D.S., (2011). Nanotechnology for the Food and Bioprocessing Industries. Food and Bioprocess Technology 4(1), 39-47.

Neo, Y.P., Ray, S., Easteal, A.J., Nikolaidis, M.G., Quek, S.Y., (2012). Influence of solution and processing parameters towards the fabrication of electrospun zein fibers with sub-micron diameter. Journal of Food Engineering 109(4), 645-651.

Neo, Y.P., Ray, S., Jin, J., Gizdavic-Nikolaidis, M., Nieuwoudt, M.K., Liu, D., Quek, S.Y., (2013). Encapsulation of food grade antioxidant in natural biopolymer by electrospinning technique: a physicochemical study based on zein-gallic acid system. Food Chem 136(2), 1013-1021.

Nieuwland, M., Geerdink, P., Brier, P., van den Eijnden, P., Henket, J.T.M.M., Langelaan, M.L.P., Stroeks, N., van Deventer, H.C., Martin, A.H., (2013). Food-grade electrospinning of proteins. Innovative Food Science & Emerging Technologies 20, 269-275.

Nishiyama, Y., (2009). Structure and properties of the cellulose microfibril. Journal of Wood Science 55(4), 241-249.

O'Sullivan, J., Murray, B., Flynn, C., Norton, I., (2016). The effect of ultrasound treatment on the structural, physical and emulsifying properties of animal and vegetable proteins. Food Hydrocolloids 53, 141-154.

Okiyama, A., Motoki, M., Yamanaka, S., (1992a). Bacterial Cellulose II. Processing of the gelatinous cellulose for food materials. Food Hydrocolloids 6(5), 479-487.

Okiyama, A., Motoki, M., Yamanaka, S., (1993). Bacterial Cellulose III. Development of a new form of cellulose. Food Hydrocolloids 6(6), 493-501.

Okiyama, A., Shirae, H., Kano, H., Yamanaka, S., (1992b). Bacterial Cellulose I. 2-stage fermentation process for cellulose production Acetobacter Aceti. Food Hydrocolloids 6(5), 471-477.

Okutan, N., Terzi, P., Altay, F., (2014). Affecting parameters on electrospinning process and characterization of electrospun gelatin nanofibers. Food Hydrocolloids 39, 19-26.

Olsson, R.T., Kraemer, R., Lopez-Rubio, A., Torres-Giner, S., Jose Ocio, M., Maria Lagaron, J., (2010). Extraction of Microfibrils from Bacterial Cellulose Networks for Electrospinning of Anisotropic Biohybrid Fiber Yarns. Macromolecules 43(9), 4201-4209.

Opawale, F.O., Burgess, D.J., (1998). Influence of Interfacial Rheological Properties of Mixed Emulsifier Films on the Stability of Water-in-Oil-in-Water Emulsions. Journal of Pharmacy and Pharmacology 50(9), 965-973.

Oshima, T., Taguchi, S., Ohe, K., Baba, Y., (2011). Phosphorylated bacterial cellulose for adsorption of proteins. Carbohydrate Polymers 83(2), 953-958.

Ostwald, W., (1910). Beiträge zur Kenntnis der Emulsionen. Zeitschrift für Chemie und Industrie der Kolloide 6(2), 103-109.

Ougiya, H., Hioki, N., Watanabe, K., Morinaga, Y., Yoshinaga, F., Samejima, M., (1998). Relationship between the Physical Properties and Surface Area of Cellulose Derived from Adsorbates of Various Molecular Sizes. Bioscience, Biotechnology, and Biochemistry 62(10), 1880-1884.

Ougiya, H., Watanabe, K., Morinaga, Y., Yoshinaga, F., (1997). Emulsion-stabilizing effect of bacterial cellulose. Bioscience Biotechnology and Biochemistry 61(9), 1541-1545.

Ozdal, T., Capanoglu, E., Altay, F., (2013). A review on protein–phenolic interactions and associated changes. Food Research International 51(2), 954-970.

Paakko, M., Ankerfors, M., Kosonen, H., Nykanen, A., Ahola, S., Osterberg, M., Ruokolainen, J., Laine, J., Larsson, P.T., Ikkala, O., Lindstrom, T., (2007). Enzymatic hydrolysis combined with mechanical shearing and high-pressure homogenization for nanoscale cellulose fibrils and strong gels. Biomacromolecules 8(6), 1934-1941.

Pae, M., Ren, Z., Meydani, M., Shang, F., Smith, D., Meydani, S.N., Wu, D., (2012). Dietary supplementation with high dose of epigallocatechin-3-gallate promotes inflammatory response in mice. J Nutr Biochem 23(6), 526-531.

Palangetic, L., Reddy, N.K., Srinivasan, S., Cohen, R.E., McKinley, G.H., Clasen, C., (2014). Dispersity and spinnability: Why highly polydisperse polymer solutions are desirable for electrospinning. Polymer 55(19), 4920-4931.

Panagopoulou, E., Tsouko, E., Kopsahelis, N., Koutinas, A., Mandala, I., Evageliou, V., (2015). Olive oil emulsions formed by catastrophic phase inversion using bacterial cellulose and whey protein isolate. Colloids and Surfaces A: Physicochemical and Engineering Aspects 486, 203-210.

Panaras, G., Moatsou, G., Yanniotis, S., Mandala, I., (2011). The influence of functional properties of different whey protein concentrates on the rheological and emulsification capacity of blends with xanthan gum. Carbohydrate Polymers 86(2), 433-440.

Pancholi, K., Ahras, N., Stride, E., Edirisinghe, M., (2009a). Novel electrohydrodynamic preparation of porous chitosan particles for drug delivery. J Mater Sci Mater Med 20(4), 917-923.

Pancholi, K., Ahras, N., Stride, E., Edirisinghe, M., (2009b). Novel electrohydrodynamic preparation of porous chitosan particles for drug delivery. Journal of Materials Science: Materials in Medicine 20(4), 917-923.

Panusa, A., Zuorro, A., Lavecchia, R., Marrosu, G., Petrucci, R., (2013). Recovery of natural antioxidants from spent coffee grounds. Journal of Agricultural and Food Chemistry 61(17), 4162-4168.

Parvez, S., Malik, K.A., Ah Kang, S., Kim, H.Y., (2006). Probiotics and their fermented food products are beneficial for health. J Appl Microbiol 100(6), 1171-1185.

Pascual-Pineda, L.A., Flores-Andrade, E., Jiménez-Fernández, M., Beristain, C.I., (2015). Kinetic and thermodynamic stability of paprika nanoemulsions. International Journal of Food Science & Technology 50(5), 1174-1181.

Paximada, P., Dimitrakopoulou, E.A., Tsouko, E., Koutinas, A.A., Fasseas, C., Mandala, I.G., (2016a). Structural modification of Bacterial Cellulose fibrils under ultrasonic irradiation. Carbohydrate Polymers.

Paximada, P., Koutinas, A.A., Scholten, E., Mandala, I.G., (2016b). Effect of bacterial cellulose addition on physical properties of WPI emulsions. Comparison with common thickeners. Food Hydrocolloids 54, Part B, 245-254.

Paximada, P., Tsouko, E., Kopsahelis, N., Koutinas, A.A., Mandala, I., (2014). Bacterial Cellulose as stabilizer of o/w emulsions. Food Hydrocolloids(0).

Paximada, P., Tsouko, E., Kopsahelis, N., Koutinas, A.A., Mandala, I., (2016c). Bacterial cellulose as stabilizer of o/w emulsions. Food Hydrocolloids 53, 225-232.

Pelipenko, J., Kristl, J., Rosic, R., Baumgartner, S., Kocbek, P., (2012). Interfacial rheology: an overview of measuring techniques and its role in dispersions and electrospinning. Acta Pharm 62(2), 123-140.

Peppas, N.A., Sahlin, J.J., (1989). A simple equation for the description of solute release. III. Coupling of diffusion and relaxation. Int J Pharm 57(2), 169-172.

Pérez-Masiá, R., Lagaron, J.M., Lopez-Rubio, A., (2014). Morphology and Stability of Edible Lycopene-Containing Micro- and Nanocapsules Produced Through Electrospraying and Spray Drying. Food and Bioprocess Technology 8(2), 459-470.

Pérez-Masiá, R., López-Nicolás, R., Periago, M.J., Ros, G., Lagaron, J.M., López-Rubio, A., (2015). Encapsulation of folic acid in food hydrocolloids through nanospray drying and electrospraying for nutraceutical applications. Food Chemistry 168, 124-133.

Perrechil, F.A., Cunha, R.L., (2012). Development of multiple emulsions based on the repulsive interaction between sodium caseinate and LBG. Food Hydrocolloids 26(1), 126-134.

Peshkovsky, A.S., Peshkovsky, S.L., Bystryak, S., (2013). Scalable high-power ultrasonic technology for the production of translucent nanoemulsions. Chemical Engineering and Processing: Process Intensification 69, 77-82.

Petrier, C., Jeunet, A., Luche, J.L., Reverdy, G., (1992). Unexpected frequency effects on the rate of oxidative processes induced by ultrasound. Journal of the American Chemical Society 114(8), 3148-3150.

Piacentini, E., Yan, M., Giorno, L., (2017). Development of enzyme-loaded PVA microspheres by membrane emulsification. Journal of Membrane Science 524, 79-86.

Pickering, S.U., (1907). Emulsions. Journal of the Chemical Society, Transactions 91(0), 2001-2021.

Poiana, M.A., (2012). Enhancing oxidative stability of sunflower oil during convective and microwave heating using grape seed extract. Int J Mol Sci 13(7), 9240-9259.

Pool, H., Mendoza, S., Xiao, H., McClements, D.J., (2013). Encapsulation and release of hydrophobic bioactive components in nanoemulsion-based delivery systems: impact of physical form on quercetin bioaccessibility. Food Function 4(1), 162-174.

Price, G.J., West, P.J., Smith, P.F., (1994). Control of polymer structure using power ultrasound. Ultrasonics Sonochemistry 1(1), S51-S57.

Puglia, C., Blasi, P., Rizza, L., Schoubben, A., Bonina, F., Rossi, C., Ricci, M., (2008). Lipid nanoparticles for prolonged topical delivery: An in vitro and in vivo investigation. Int J Pharm 357(1–2), 295-304.

Qian, C., McClements, D.J., (2011). Formation of nanoemulsions stabilized by model food-grade emulsifiers using high-pressure homogenization: Factors affecting particle size. Food Hydrocolloids 25(5), 1000-1008.

R., C.P., B., B.I., A., S.S., S., S.R., (2009). Microbial Cellulose: Fermentative Production and Applications. Food Technology and Biotechnology 47(2), 107-124.

Raso, J., Mañas, P., Pagán, R., Sala, F.J., (1999). Influence of different factors on the output power transferred into medium by ultrasound. Ultrasonics Sonochemistry 5(4), 157-162.

Rawel, H.M., Meidtner, K., Kroll, J., (2005). Binding of Selected Phenolic Compounds to Proteins. Journal of Agricultural and Food Chemistry 53(10), 4228-4235.

Ray, S., Raychaudhuri, U., Chakraborty, R., (2016). An overview of encapsulation of active compounds used in food products by drying technology. Food Bioscience 13, 76-83.

Regev, O., Vandebril, S., Zussman, E., Clasen, C., (2010). The role of interfacial viscoelasticity in the stabilization of an electrospun jet. Polymer 51(12), 2611-2620.

Reithmeier, H., Herrmann, J., Göpferich, A., (2001). Development and characterization of lipid microparticles as a drug carrier for somatostatin. Int J Pharm 218(1–2), 133-143.

Relkin, P., Yung, J.-M., Kalnin, D., Ollivon, M., (2008). Structural Behaviour of Lipid Droplets in Protein-stabilized Nano-emulsions and Stability of α-Tocopherol. Food Biophysics 3(2), 163-168.

Reneker, D.H., Yarin, A.L., Zussman, E., Xu, H., (2007). Electrospinning of Nanofibers from Polymer Solutions and Melts, in: Hassan, A., Erik van der, G. (Eds.), *Advances in Applied Mechanics*. Elsevier, pp. 43-346.

Renou, F., Petibon, O., Malhiac, C., Grisel, M., (2013). Effect of xanthan structure on its interaction with locust bean gum: Toward prediction of rheological properties. Food Hydrocolloids 32(2), 331-340.

Rezaei, A., Nasirpour, A., Fathi, M., (2015). Application of Cellulosic Nanofibers in Food Science Using Electrospinning and Its Potential Risk. Comprehensive Reviews in Food Science and Food Safety 14(3), 269-284.

Rezayati Charani, P., Dehghani-Firouzabadi, M., Afra, E., Shakeri, A., (2013). Rheological characterization of high concentrated MFC gel from kenaf unbleached pulp. Cellulose 20(2), 727-740.

Richard, T., Lefeuvre, D., Descendit, A., Quideau, S., Monti, J.P., (2006). Recognition characters in peptide–polyphenol complex formation. Biochimica et Biophysica Acta (BBA) - General Subjects 1760(6), 951-958.

Ritger, P.L., Peppas, N.A., (1987). A simple equation for description of solute release II. Fickian and anomalous release from swellable devices. Journal of Controlled Release 5(1), 37-42.

Rocha, S., Generalov, R., Pereira Mdo, C., Peres, I., Juzenas, P., Coelho, M.A., (2011). Epigallocatechin gallate-loaded polysaccharide nanoparticles for prostate cancer chemoprevention. Nanomedicine (Lond) 6(1), 79-87.

Roman, M., Winter, W.T., (2004). Effect of Sulfate Groups from Sulfuric Acid Hydrolysis on the Thermal Degradation Behavior of Bacterial Cellulose. Biomacromolecules 5(5), 1671-1677.

Ronsse, F., Pieters, J.G., Dewettinck, K., (2009). Modelling heat and mass transfer in batch, top-spray fluidised bed coating processes. Powder Technology 190(1–2), 170-175.

Roosen, J., Bieberstein, A., Blanchemanche, S., Goddard, E., Marette, S., Vandermoere, F., (2015). Trust and willingness to pay for nanotechnology food. Food Policy 52, 75-83.

Rošic, R., Pelipenko, J., Kocbek, P., Baumgartner, S., Bešter-Rogač, M., Kristl, J., (2012). The role of rheology of polymer solutions in predicting nanofiber formation by electrospinning. European Polymer Journal 48(8), 1374-1384.

Ru, Q., Yu, H., Huang, Q., (2010). Encapsulation of epigallocatechin-3-gallate (EGCG) using oil-in-water (O/W) submicrometer emulsions stabilized by iota-carrageenan and beta-lactoglobulin. J Agric Food Chem 58(19), 10373-10381.

S, P., Anandharamakrishnan, C., (2016). Enhancement of oral bioavailability of vitamin E by spray-freeze drying of whey protein microcapsules. Food and Bioproducts Processing 100, Part A, 469-476.

Saito, T., Nishiyama, Y., Putaux, J.-L., Vignon, M., Isogai, A., (2006). Homogeneous Suspensions of Individualized Microfibrils from TEMPO-Catalyzed Oxidation of Native Cellulose. Biomacromolecules 7(6), 1687-1691.

Saldaña, M.D.A., dos Reis Coimbra, J.S., Cardozo-Filho, L., (2015). Recovery, encapsulation and stabilization of bioactives from food residues using high pressure techniques. Current Opinion in Food Science 5, 76-85.

Salvia-Trujillo, L., Rojas-Graü, A., Soliva-Fortuny, R., Martín-Belloso, O., (2015). Physicochemical characterization and antimicrobial activity of food-grade emulsions and nanoemulsions incorporating essential oils. Food Hydrocolloids 43, 547-556.

Salvia-Trujillo, L., Rojas-Graü, M.A., Soliva-Fortuny, R., Martín-Belloso, O., (2013). Effect of processing parameters on physicochemical characteristics of microfluidized lemongrass essential oil-alginate nanoemulsions. Food Hydrocolloids 30(1), 401-407.

Samtlebe, M., Ergin, F., Wagner, N., Neve, H., Küçükçetin, A., Franz, C.M.A.P., Heller, K.J., Hinrichs, J., Atamer, Z., (2016). Carrier systems for bacteriophages to supplement food systems: Encapsulation and controlled release to modulate the human gut microbiota. LWT - Food Science and Technology 68, 334-340.

Santiago, L.G., Castro, G.R., (2016). Novel technologies for the encapsulation of bioactive food compounds. Current Opinion in Food Science 7, 78-85.

Sarhan, W.A., Azzazy, H.M.E., (2015). High concentration honey chitosan electrospun nanofibers: Biocompatibility and antibacterial effects. Carbohydrate Polymers 122, 135-143.

Sasazuki, S., Inoue, M., Hanaoka, T., Yamamoto, S., Sobue, T., Tsugane, S., (2004). Green tea consumption and subsequent risk of gastric cancer by subsite: the JPHC Study. Cancer Causes Control 15(5), 483-491.

Schrecker, S.T., Gostomski, P.A., (2005). Determining the Water Holding Capacity of Microbial Cellulose. Biotechnology Letters 27(19), 1435-1438.

Schubert, H., Ax, K., Behrend, O., (2003). Product engineering of dispersed systems. Trends in Food Science & Technology 14(1–2), 9-16.

Selvamuthukumar, S., Velmurugan, R., (2012). Nanostructured Lipid Carriers: A potential drug carrier for cancer chemotherapy. Lipids in Health and Disease 11, 159-159.

Sencadas, V., Correia, D.M., Areias, A., Botelho, G., Fonseca, A.M., Neves, I.C., Gomez Ribelles, J.L., Lanceros Mendez, S., (2012). Determination of the parameters affecting electrospun chitosan fiber size distribution and morphology. Carbohydrate Polymers 87(2), 1295-1301.

Shahidi, F., Alexander, D.M., (1998). Green tea catechins as inhibitors of oxidation of meat lipids. Journal of Food Lipids 5(2), 125-133.

Shenoy, S.L., Bates, W.D., Frisch, H.L., Wnek, G.E., (2005). Role of chain entanglements on fiber formation during electrospinning of polymer solutions: good solvent, non-specific polymer–polymer interaction limit. Polymer 46(10), 3372-3384.

Shi, Z., Zhang, Y., Phillips, G.O., Yang, G., (2014). Utilization of bacterial cellulose in food. Food Hydrocolloids 35, 539-545.

Shutov, A.A., (2008). Production of superfine fibers by the electrospinning method. Fluid Dynamics 43(4), 533-546.

Siebert, K.J., (2006). Haze formation in beverages. LWT - Food Science and Technology 39(9), 987-994.

Siegrist, M., Cousin, M.-E., Kastenholz, H., Wiek, A., (2007). Public acceptance of nanotechnology foods and food packaging: The influence of affect and trust. Appetite 49(2), 459-466.

Siepmann, J., Peppas, N.A., (2001). Modeling of drug release from delivery systems based on hydroxypropyl methylcellulose (HPMC). Advanced Drug Delivery Reviews 48(2–3), 139-157.

Sjöström, B., Bergenståhl, B., (1992). Preparation of submicron drug particles in lecithin-stabilized o/w emulsions I. Model studies of the precipitation of cholesteryl acetate. Int J Pharm 88(1), 53-62.

Soares, P.I.P., Sousa, A.I., Silva, J.C., Ferreira, I.M.M., Novo, C.M.M., Borges, J.P., Chitosan-based nanoparticles as drug delivery systems for doxorubicin: optimization and modelling. Carbohydrate Polymers.

Spizzirri, U.G., Hampel, S., Cirillo, G., Nicoletta, F.P., Hassan, A., Vittorio, O., Picci, N., Iemma, F., (2013). Spherical gelatin/CNTs hybrid microgels as electro-responsive drug delivery systems. Int J Pharm 448(1), 115-122.

Stang, M., Schuchmann, H., Schubert, H., (2001). Emulsification in High-Pressure Homogenizers. Engineering in Life Sciences 1(4), 151-157.

Stern, J.L., Hagerman, A.E., Steinberg, P.D., Mason, P.K., (1996). Phlorotannin-protein interactions. Journal of Chemical Ecology 22(10), 1877-1899.

Sukigara, S., Gandhi, M., Ayutsede, J., Micklus, M., Ko, F., (2003). Regeneration of Bombyx mori silk by electrospinning—part 1: processing parameters and geometric properties. Polymer 44(19), 5721-5727.

Sun, C., Gunasekaran, S., (2009). Effects of protein concentration and oil-phase volume fraction on the stability and rheology of menhaden oil-in-water emulsions stabilized by whey protein isolate with xanthan gum. Food Hydrocolloids 23(1), 165-174.

Sun, C., Gunasekaran, S., Richards, M.P., (2007). Effect of xanthan gum on physicochemical properties of whey protein isolate stabilized oil-in-water emulsions. Food Hydrocolloids 21(4), 555-564.

Sun, T., Ho, C.-T., (2001). Antiradical efficiency of tea components. Journal of Food Lipids 8(3), 231-238.

Suslick, K.S., (2003). 1.41 - Sonochemistry, in: Meyer, J.A.M.J. (Ed.), *Comprehensive Coordination Chemistry II*. Pergamon, Oxford, pp. 731-739.

Türünç, O., Meier, M.A.R., (2012). Biopolymers, *Food and Industrial Bioproducts and Bioprocessing*, pp. 267-292.

Tabuchi, M., (2007). Nanobiotech versus synthetic nanotech? Nat Biotechnol 25(4), 389-390.

Tadros, T., Izquierdo, P., Esquena, J., Solans, C., (2004). Formation and stability of nano-emulsions. Advances in Colloid and Interface Science 108–109, 303-318.

Tadros, T.F., (1994). Fundamental principles of emulsion rheology and their applications. Colloids and Surfaces A: Physicochemical and Engineering Aspects 91, 39-55.

Tan, H.L., McGrath, K.M., (2012). Na-caseinate/oil/water systems: Emulsion morphology diagrams. Journal of Colloid and Interface Science 381(1), 48-58.

Tan, S.H., Inai, R., Kotaki, M., Ramakrishna, S., (2005). Systematic parameter study for ultra-fine fiber fabrication via electrospinning process. Polymer 46(16), 6128-6134.

Taneja, A., Ye, A., Jones, J.R., Archer, R., Singh, H., (2013). Behaviour of oil droplets during spray drying of milk-protein-stabilised oil-in-water emulsions. International Dairy Journal 28(1), 15-23.

Tang, S.Y., Shridharan, P., Sivakumar, M., (2013). Impact of process parameters in the generation of novel aspirin nanoemulsions--comparative studies between ultrasound cavitation and microfluidizer. Ultrason Sonochem 20(1), 485-497.

Tavares, G.M., Croguennec, T., Carvalho, A.F., Bouhallab, S., (2014). Milk proteins as encapsulation devices and delivery vehicles: Applications and trends. Trends in Food Science & Technology 37(1), 5-20.

Taylor, G., (1964). Disintegration of Water Drops in an Electric Field. Proceedings of the Royal Society of London A: Mathematical, Physical and Engineering Sciences 280(1382), 383-397.

Tcholakova, S., Denkov, N.D., Sidzhakova, D., Ivanov, I.B., Campbell, B., (2003). Interrelation between Drop Size and Protein Adsorption at Various Emulsification Conditions. Langmuir 19(14), 5640-5649.

Teixeira, A., Baenas, N., Dominguez-Perles, R., Barros, A., Rosa, E., Moreno, D.A., Garcia-Viguera, C., (2014). Natural Bioactive Compounds from Winery By-Products as Health Promoters: A Review. International Journal of Molecular Sciences 15(9), 15638-15678.

Tischer, P.C.S.F., Sierakowski, M.R., Westfahl, H., Tischer, C.A., (2010). Nanostructural Reorganization of Bacterial Cellulose by Ultrasonic Treatment. Biomacromolecules 11(5), 1217-1224.

Torres-Giner, S., Martinez-Abad, A., Ocio, M.J., Lagaron, J.M., (2010). Stabilization of a nutraceutical omega-3 fatty acid by encapsulation in ultrathin electrosprayed zein prolamine. J Food Sci 75(6), N69-79.

Torres-Giner, S., Ocio, M.J., Lagaron, J.M., (2008). Development of Active Antimicrobial Fiber-Based Chitosan Polysaccharide Nanostructures using Electrospinning. Engineering in Life Sciences 8(3), 303-314.

Toschi, T.G., Bordoni, A., Hrelia, S., Bendini, A., Lercker, G., Biagi, P.L., (2000). The Protective Role of Different Green Tea Extracts after Oxidative Damage Is Related to Their Catechin Composition. Journal of Agricultural and Food Chemistry 48(9), 3973-3978.

Trotta, M., Debernardi, F., Caputo, O., (2003). Preparation of solid lipid nanoparticles by a solvent emulsification–diffusion technique. Int J Pharm 257(1–2), 153-160.

Trzciński, S., Staszewska, D.U., (2004). Kinetics of ultrasonic degradation and polymerisation degree distribution of sonochemically degraded chitosans. Carbohydrate Polymers 56(4), 489-498.

Tsatsaragkou, K., Paximada, P., Protonotariou, S., Mandala, I., (2016). 17 Functional Foods.

Tsouko, E., Kourmentza, C., Ladakis, D., Kopsahelis, N., Mandala, I., Papanikolaou, S., Paloukis, F., Alves, V., Koutinas, A., (2015). Bacterial Cellulose Production from Industrial Waste and by-Product Streams. International Journal of Molecular Sciences 16(7), 14832.

Tubesha, Z., Bakar, Z.A., Ismail, M., (2013). Characterization and stability evaluation of thymoquinone nanoemulsions prepared by high-pressure homogenization. J. Nanomaterials 2013, 126-126.

Vilkhu, K., Mawson, R., Simons, L., Bates, D., (2008). Applications and opportunities for ultrasound assisted extraction in the food industry — A review. Innovative Food Science & Emerging Technologies 9(2), 161-169.

Vladić, J., Ambrus, R., Szabó-Révész, P., Vasić, A., Cvejin, A., Pavlić, B., Vidović, S., (2016). Recycling of filter tea industry by-products: Production of A. millefolium powder using spray drying technique. Industrial Crops and Products 80, 197-206.

von Staszewski, M., Pizones Ruiz-Henestrosa, V.M., Pilosof, A.M.R., (2014). Green tea polyphenols-β-lactoglobulin nanocomplexes: Interfacial behavior, emulsification and oxidation stability of fish oil. Food Hydrocolloids 35, 505-511.

Walker, R., Decker, E.A., McClements, D.J., (2015). Development of food-grade nanoemulsions and emulsions for delivery of omega-3 fatty acids: opportunities and obstacles in the food industry. Food Funct 6(1), 42-55.

Walstra, P., van Vliet, T., (2003). Chapter II Functional properties, in: W.Y. Aalbersberg, R.J.H.P.J.H.H.J.d.J.C.G.d.K.P.W., Wolf, F.A.d. (Eds.), *Progress in Biotechnology*. Elsevier, pp. 9-30.

Wang, C., Wang, L., Wang, M., (2014). Evolution of core–shell structure: From emulsions to ultrafine emulsion electrospun fibers. Materials Letters 124, 192-196.

Wang, C., Wang, M., (2012). Dual-source dual-power electrospinning and characteristics of multifunctional scaffolds for bone tissue engineering. Journal of Materials Science: Materials in Medicine 23(10), 2381-2397.

Wang, L., Gao, Y., Li, J., Subirade, M., Song, Y., Liang, L., (2016a). Effect of resveratrol or ascorbic acid on the stability of α-tocopherol in O/W emulsions stabilized by whey protein isolate: Simultaneous encapsulation of the vitamin and the protective antioxidant. Food Chemistry 196, 466-474.

Wang, R., Zhou, W., Jiang, X., (2008a). Mathematical modeling of the stability of green tea catechin epigallocatechin gallate (EGCG) during bread baking. Journal of Food Engineering 87(4), 505-513.

Wang, R., Zhou, W., Jiang, X., (2008b). Reaction Kinetics of Degradation and Epimerization of Epigallocatechin Gallate (EGCG) in Aqueous System over a Wide Temperature Range. Journal of Agricultural and Food Chemistry 56(8), 2694-2701.

Wang, S.-Q., He, J.-H., Xu, L., (2008c). Non-ionic surfactants for enhancing electrospinability and for the preparation of electrospun nanofibers. Polymer International 57(9), 1079-1082.

Wang, S., Cheng, Q., (2009). A novel process to isolate fibrils from cellulose fibers by high-intensity ultrasonication, Part 1: Process optimization. Journal of Applied Polymer Science 113(2), 1270-1275.

Wang, Y., Liu, W., Chen, X.D., Selomulya, C., (2016b). Micro-encapsulation and stabilization of DHA containing fish oil in protein-based emulsion through mono-disperse droplet spray dryer. Journal of Food Engineering 175, 74-84.

Watanabe, K., Tabuchi, M., Morinaga, Y., Yoshinaga, F., (1998). Structural Features and Properties of Bacterial Cellulose Produced in Agitated Culture. Cellulose 5(3), 187-200.

Wei, Z., Yang, W., Fan, R., Yuan, F., Gao, Y., (2015). Evaluation of structural and functional properties of protein–EGCG complexes and their ability of stabilizing a model β-carotene emulsion. Food Hydrocolloids 45, 337-350.

Whelan, (1994). Polymer technology dictionary,Chapman & Hall. Acta Polymerica 45(5), 398-398.

Williams, P.A., Phillips, G.O., (2003). 11 - The use of hydrocolloids to improve food texture, in: McKenna, B.M. (Ed.), *Texture in Food*. Woodhead Publishing, pp. 251-274.

Winuprasith, T., Suphantharika, M., (2013). Microfibrillated cellulose from mangosteen (Garcinia mangostana L.) rind: Preparation, characterization, and evaluation as an emulsion stabilizer. Food Hydrocolloids 32(2), 383-394.

Winuprasith, T., Suphantharika, M., (2015). Properties and stability of oil-in-water emulsions stabilized by microfibrillated cellulose from mangosteen rind. Food Hydrocolloids 43(0), 690-699.

Wissing, S.A., Kayser, O., Müller, R.H., (2004). Solid lipid nanoparticles for parenteral drug delivery. Advanced Drug Delivery Reviews 56(9), 1257-1272.

Wongsasulak, S., Kit, K.M., McClements, D.J., Yoovidhya, T., Weiss, J., (2007). The effect of solution properties on the morphology of ultrafine electrospun egg albumen–PEO composite fibers. Polymer 48(2), 448-457.

Wooster, T.J., Golding, M., Sanguansri, P., (2008). Impact of oil type on nanoemulsion formation and Ostwald ripening stability. Langmuir 24(22), 12758-12765.

Xhanari, K., Syverud, K., Stenius, P., (2011). Emulsions Stabilized by Microfibrillated Cellulose: The Effect of Hydrophobization, Concentration and O/W Ratio. Journal of Dispersion Science and Technology 32(3), 447-452.

Xu, J.Z., Yeung, S.Y., Chang, Q., Huang, Y., Chen, Z.Y., (2004). Comparison of antioxidant activity and bioavailability of tea epicatechins with their epimers. Br J Nutr 91(6), 873-881.

Xu, M., Dumont, M.-J., (2015). Evaluation of the stability of pea and canola protein-based hydrogels in simulated gastrointestinal fluids. Journal of Food Engineering 165, 52-59.

Xu, R., (2015). Light scattering: A review of particle characterization applications. Particuology 18, 11-21.

Yanjun, S., Jianhang, C., Shuwen, Z., Hongjuan, L., Jing, L., Lu, L., Uluko, H., Yanling, S., Wenming, C., Wupeng, G., Jiaping, L., (2014). Effect of power ultrasound pre-treatment on the physical and functional properties of reconstituted milk protein concentrate. Journal of Food Engineering 124, 11-18.

Yarin, A.L., (2011). Coaxial electrospinning and emulsion electrospinning of core–shell fibers. Polymers for Advanced Technologies 22(3), 310-317.

Yu, D.-G., Branford-White, C., Williams, G.R., Bligh, S.W.A., White, K., Zhu, L.-M., Chatterton, N.P., (2011). Self-assembled liposomes from amphiphilic electrospun nanofibers. Soft Matter 7(18), 8239-8247.

Yuan, Y., Gao, Y., Zhao, J., Mao, L., (2008). Characterization and stability evaluation of β-carotene nanoemulsions prepared by high pressure homogenization under various emulsifying conditions. Food Research International 41(1), 61-68.

Zeleny, J., (1914). The Electrical Discharge from Liquid Points, and a Hydrostatic Method of Measuring the Electric Intensity at Their Surfaces. Physical Review 3(2), 69-91.

Zhang, N., Mutilangi, W., (2011). Zero calorie polyphenol aqueous dispersions. Google Patents.

Zhong, Y., Shahidi, F., (2012). Lipophilised epigallocatechin gallate (EGCG) derivatives and their antioxidant potential in food and biological systems. Food Chemistry 131(1), 22-30.

Zhou, L., Elias, R.J., (2013). Antioxidant and pro-oxidant activity of (−)-epigallocatechin-3-gallate in food emulsions: Influence of pH and phenolic concentration. Food Chemistry 138(2–3), 1503-1509.

Zhu, N., Sang, S., Huang, T.-C., Bai, N., Yang, C.S., Ho, C.-T., (2000). Antioxidant chemistry of green tea catechins: oxidation products of (-)-epigallocatechin gallate and (-)-epigallocatechin with peroxidase. Journal of Food Lipids 7(4), 275-282.

Zinoviadou, K.G., Scholten, E., Moschakis, T., Biliaderis, C.G., (2012). Properties of emulsions stabilised by sodium caseinate–chitosan complexes. International Dairy Journal 26(1), 94-101.

Zong, X., Kim, K., Fang, D., Ran, S., Hsiao, B.S., Chu, B., (2002). Structure and process relationship of electrospun bioabsorbable nanofiber membranes. Polymer 43(16), 4403-4412.

Zorilla, R., Liang, L., Remondetto, G., Subirade, M., (2011). Interaction of epigallocatechin-3-gallate with β-lactoglobulin: molecular characterization and biological implication. Dairy Science & Technology 91(5), 629.